Oklahoma Geological Survey Guidebook 24

The Slick Hills of Southwestern Oklahoma—Fragments of an Aulacogen?

1986

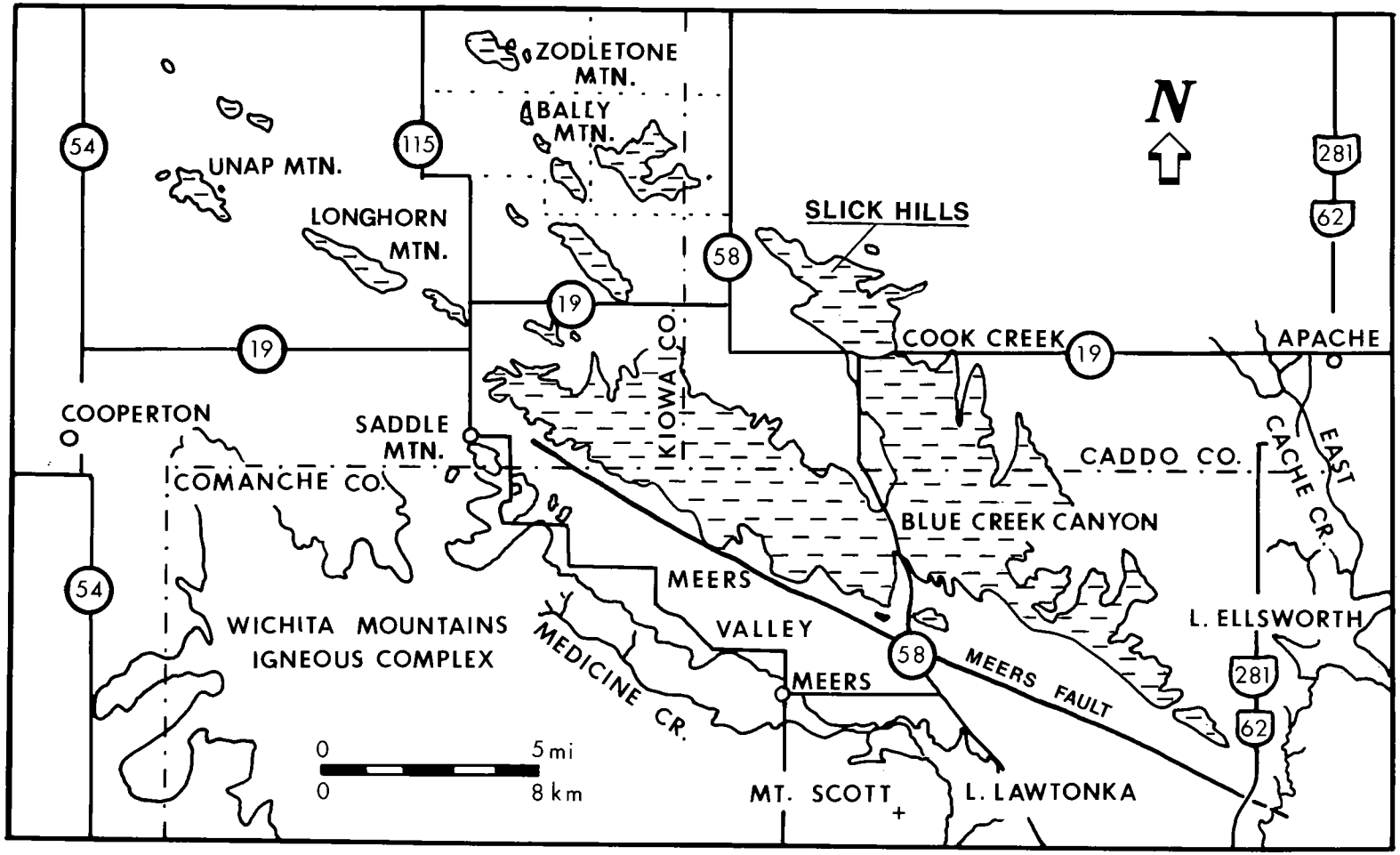

Field-Trip Location Map

OKLAHOMA GEOLOGICAL SURVEY
Charles J. Mankin, *Director*
Guidebook 24

ISSN 0078-4400

THE SLICK HILLS OF SOUTHWESTERN OKLAHOMA—FRAGMENTS OF AN AULACOGEN?

R. Nowell Donovan, *Editor*
Department of Geology
Oklahoma State University
Stillwater, Oklahoma

Contributors:

Weldon Beauchamp, Sun Co., Dallas
Steve Bridges, Oklahoma State University
Kelly Cloyd, State University of New York, Binghamton
Kathy Collins, Plains Resources, Oklahoma City
Anthony J. Crone, United States Geological Survey, Denver
R. E. (Tim) Denison, Mobil Research and Development, Dallas
Curtis Ditzell, Conoco, Houston
R. Nowell Donovan, Oklahoma State University
Arthur W. Hounslow, Oklahoma State University
Lois Jones, Conoco Research, Ponca City
Kenneth V. Luza, Oklahoma Geological Survey
Richard F. Madole, United States Geological Survey
David (Max) Marchini, Queen's University of Belfast, Northern Ireland
David McConnell, Texas A&M University
Angus M. McCoss, Queen's University of Belfast, Northern Ireland
Ken M. Morgan, Texas Christian University
Mary B. Rafalowski, Conoco, Lafayette
Deborah A. Ragland, Oklahoma State University
Alan R. Ramelli, University of Nevada, Reno
David J. Sanderson, Queen's University of Belfast, Northern Ireland
Diana Schaefer, Oklahoma State University
D. Burton Slemmons, University of Nevada, Reno
Tekleab Tsegay, Oklahoma State University
Steven J. Wilhelm, Texas Christian University
Paul Younger, University of Newcastle-upon-Tyne, England

Guidebook for Field Trip 12, November 7–9, 1986, preceding the 99th annual national meeting of The Geological Society of America, November 10–13, 1986, San Antonio, Texas

The University of Oklahoma
Norman, Oklahoma
1986

Field-Trip Leaders

R. Nowell Donovan
Department of Geology
Oklahoma State University

Deborah A. Ragland
Department of Environmental Sciences
Oklahoma State University

Diana Schaefer
Department of Geology
Oklahoma State University

Front Cover

"Leopard-skin" texture in a zone of partial dolomitization, Kindblade Formation. (See Stop 4, this volume.)

Back Cover

Zoned barite from Zodletone Spring. (See Younger and others, this volume.)

This publication, printed by the University of Oklahoma Printing Services, Norman, Oklahoma, is issued by the Oklahoma Geological Survey as authorized by Title 70, Oklahoma Statutes, 1981, Section 3310, and Title 74, Oklahoma Statutes, 1981, Sections 231–238. 1,000 copies have been prepared for distribution at a cost of $6,135.00 to the taxpayers of the State of Oklahoma. Copies have been deposited with the Publications Clearinghouse of the Oklahoma Department of Libraries.

PREFACE

In 1982 Gilbert and Donovan edited Oklahoma Geological Survey Guidebook 21, entitled *Geology of the Eastern Wichita Mountains, Southwestern Oklahoma.* At that time we recognized that the Wichita Mountains area was attracting an increasing amount of interest among the geologic community. Our original plan was to issue a similar guidebook for the 1986 annual meeting of the Geological Society of America in San Antonio. However, much of the research which was initiated in the early 1980s is coming (or has come) to fruition, and so we have had to split our efforts into companion volumes (OGS Guidebooks 23, 24) edited by Gilbert and Donovan respectively.

This guidebook discusses and describes aspects of the Slick Hills (sometimes referred to as the "Limestone Hills"), which are a low range of bald hills lying north of the igneous Wichitas. As presently exposed, the Slick Hills are fragments of the frontal fault zone between the Wichitas and the Anadarko basin. The hills are a potpourri of lower Paleozoic igneous and sedimentary rocks, comprehensively deformed by Pennsylvanian tectonism and subsequently overlapped by Permian strata. Within this relatively small area, it is possible to illustrate most of the significant facets related to the development of the southern Oklahoma aulacogen. The GSA field trip has been designed with this theme in mind.

The work herein presented clearly involves some considerable effort on the part of the various contributors. This work collectively has been spearheaded by the Oklahoma Geological Survey, who have been supportive of most of the studies presented here. One of the principal aims of the Survey is the production of a new and detailed map of the Slick Hills as a companion to a similar map of the Wichita Mountains. Many of the contributors join with me in thanking the Survey for their support; we are all grateful to Larry N. Stout, geologist/editor, and his staff for the meticulous and thoughtful care which they have brought to this volume.

Many of the landowners in the Slick Hills have willingly allowed us access to their land. We are grateful for their support—without it our studies would be a dim and dismal set of observations on road cuts. At Zodletone, Mr. Dan Trobe has supported our work with interest. Similarly, at Bally Mountain, Mr. W. Hodges and Mr. D. Leatherbury have been generous to us. In particular, Mr. and Mrs. David Kimbell of the Kimbell Ranch and his managing partnership Charlie Bob and Dixie Oliver have opened their home and land to us on every conceivable occasion. Charlie Bob and Dixie are the only couple I know who have ever allowed a seismograph to be installed in their house.

I would like to end this Preface on two personal notes. First, I would like to thank my wife, Jeanne, who typed most of this volume from scratch in a tiny cabin near Cañon City, Colorado, in temperatures that ranged from 30° to 100°F. Second, I have recently left Oklahoma State for Texas Christian University. During my time in Oklahoma I have had the privilege of teaching and advising a large body of students, many of whom have worked in the Slick Hills. Collectively we have had fun and discovered much of interest. Consequently, I would like to dedicate my contributions to this volume to the students of OSU—past, present, and future.

R. N. DONOVAN
August 1986

CONTENTS

Stop Descriptions

Oklahoma Geological Survey Guidebook 24, 1986

GEOLOGY OF THE SLICK HILLS

R. Nowell Donovan

INTRODUCTION

To the traveler crossing the plains of Oklahoma, the Wichita Mountains are an incongruity, providing welcome relief in a land dominated by gentle contours. To the geologist, the mountains are a compelling presence—a concatenation of deformed igneous and sedimentary rocks surrounded by an aura of Permian déjà vu (for these are ancient hills formed of ancient rocks, not modern hills formed of ancient rocks). The bulk of the hills is built by a variety of igneous rocks—gabbros, granites, and rhyolites (see Gilbert, 1986). These igneous rocks, particularly the granites, constitute the steepest relief in Oklahoma, displaying an often bizarre array of tors and exfoliation surfaces (Gilbert, 1982).

To the north of the igneous Wichitas lie the Slick Hills, a broken, treeless range of modest slopes built mostly from folded and fractured Cambrian–Ordovician limestones and surrounded by foothills of cemented Permian detritus (Fig. 1).

Since Schatski first introduced the hypothesis in 1946, the geological community has gradually come to accept that perhaps the geology of southern Oklahoma can best be explained by his concept of an aulacogen (redefined as "linear graben-like depressions of ancient platforms" by Milanovsky in 1981). However, as a recent Penrose Conference on the southern Oklahoma aulacogen demonstrated, we are still in ignorance with respect to some of the controls which are implicit in the concept of a failed rift system. Nevertheless, the hypothesis is not yet disproven and certainly forms a convenient framework for discussion. Let us therefore contemplate the Wichita Mountains and Slick Hills as fragments of an aulacogen.

TIMING OF THE AULACOGEN

The overall trend of the southern Oklahoma aulacogen, as reflected in numerous faults and by sediment isopachs, is WNW–ESE. The trend extends from southeastern Oklahoma to the Texas Panhandle, and perhaps as far as western Colorado, where it is marked by Cambrian–Ordovician dikes (Larson and others, 1985). Four stages can be recognized in the evolution of the aulacogen, and all are represented in the Slick Hills:

1) Initial heat flux, as recorded by the bimodal late Precambrian–Cambrian igneous suite;

2) An exponentially slowing rate of basin subsidence during the earlier parts of the Paleozoic, during which time great thicknesses of carbonates and lesser amounts of siliciclastics were deposited;

3) Dismemberment of the Paleozoic basin during Pennsylvanian and Early Permian time into a series of asymmetric basins (e.g., the Anadarko and Hollis basins) and uplifts (e.g., the Wichitas and Arbuckles);

4) Quiescence as the aulacogen stabilized within the craton from mid-Permian time until today; small quivers may still occur (e.g., the Recent movement of the Meers fault), but they are quantitatively minor.

The overall timing and patterns of stages 2–4 are echoed both within the adjacent craton and in the Ouachita orogene (Donovan and others, 1983). It is the coincidence between events in aulacogen and orogene which forms part of the evidence used to integrate southern Oklahoma into the Paleozoic plate-tectonic scenario.

INITIAL HEAT FLUX

The varieties of igneous rock, their relative ages, and their genetic relationships have been analyzed in a companion volume by Gilbert (1986) (see also Gilbert, 1982,1983b,1984; Powell and Phelps, 1977). Within the Slick Hills, only the topmost of the

Figure 1. Characteristic scenery in the Slick Hills. Rocks in the foreground are part of the Cool Creek Formation; the fold is the Oliver syncline.

igneous units is exposed—the Carlton Rhyolite Group (however, the rhyolite is cut by a few diabase dikes). Gilbert (1982) has concluded that the rhyolite magmas were near-liquidus, high-temperature outpourings with a minimum temperature of 950–1,000°C. Thus, it is a reasonable expectation that the aulacogen crust was subjected to considerable initial thermal expansion (which may account for the apparent near absence of rift-valley sediments). Approximately 10–20 m.y. after the end of lava extrusion, in Franconian time, the eroded rhyolite terrane, which had been sculpted into a series of low hills, was transgressed, in common with much of the adjacent craton, presumably as a result of contraction of the thermally expanded lithosphere.

LOWER PALEOZOIC RECORD

Factors Controlling Sedimentation

Chronostratigraphic subsidence-rate curves for the aulacogen (e.g., Fig. 2) all show a similar pattern: A rapid rate of sediment entrapment in Cambrian–Ordovician time gradually slowed exponentially until during the Silurian and Devonian Periods the time spans represented by unconformities exceeded those of the tangible rock record. More-detailed analyses (Feinstein, 1981), based on studies of individual cores in the Ardmore area, suggest the following stages:

1) An initial period of slow subsidence, perhaps related to elastic flexure, during which the Timbered Hills Group and Fort Sill Formation were deposited. (Estimation of rates of subsidence for this time is somewhat vague, because there is little if any biostratigraphic control on the Reagan Sandstone.)

2) A short-lived, rapid increase in the rate of subsidence, which may have been due to unlocking of aulacogen boundary faults.

3) A long period of ~50 m.y. during which much of the Arbuckle and Simpson Groups was deposited in a relatively rapidly subsiding basin.

4) A second short-lived increase in the subsidence rate, perhaps as a result of compaction of the underlying sediment, during which the Sylvan Shale was deposited. Wickham and others (1976) mark this increase as an indication that the opening ocean to the southeast had begun to subduct.

5) A long period of ~100 m.y. of cratonic torpor, during which sediment entrapment slowed greatly. The six formations of the Hunton Group deposited at this time are punctuated by unconformities of great duration.

6) Finally, in Late Devonian and Mississippian time, increasing rates of sediment entrapment herald the dismemberment of the whole area.

In summary, the patterns of subsidence in the aulacogen are similar to those of young-ocean trailing (passive) margins and equate well with McKenzie's (1978) model of isostatic response to a cooling thermal anomaly.

Sedimentary Response to the Anomaly

Timbered Hills Group

By Franconian time, the surface of the aulacogen in the Slick Hills area consisted of a number of small hills as much as 350 ft (~100 m) high. Slopes on these hills were rarely steeper than 10°. Before the transgression, the rhyolite was tilted slightly (by no more than 5°), was cut by dikes, and bore the imprint of some N–S faulting. One of these faults, the Turtle Creek fault, which bears clear evidence of left-lateral strike-slip motion, is truncated by the Reagan Sandstone.

Prior to the marine transgression, the initial deposits on the hilly rhyolite terrain comprised alluvial talus and braided-river sediments of local origin (i.e., composed of rhyolite fragments). In fact, the rhyolite hills continued to shed diminishing amounts of detritus into the basin throughout Timbered Hills time (Donovan and Ragland, this volume), thus greatly complicating the lithostratigraphic architecture of this group (Fig. 3).

In addition to the detritus of local origin, substantial amounts of quartz were involved in the transgression. This quartz, which is associated with minor amounts of plagioclase and microcline, is an unstrained variety, perhaps sourced by the Proterozoic terrane of volcanic rocks and anorogenic granites which lies to the north of the aulacogen (Condie, 1982).

The third petrographic component of the initial transgression comprises a variety of ferroan minerals, as cements (hematite, iron-rich illite), replacements (ankerite, pyrite, glauconite, siderite), and intraformational grains (ferruginous ooids, glauconite peloids). Presumably the source of iron was the deeply weathered rhyolite terrane, and the resulting minerals record mobilization and reprecipitation under fluctuating pH and Eh controls (Cloyd and others, this volume).

Eventually a fourth component, carbonate grains, was added to the siliciclastic mix. These grains are dominantly coarse fragments of pelmatozoans with lesser amounts of robust-carapaced trilobites and brachiopods. Although a few grains appear toward the top of the Reagan Sandstone, the widespread incoming of bioclastic grainstones is taken as the base of the Honey Creek Limestone. When a fifth minor component—phosphate—is added to the picture, it is clear that the Timbered Hills rocks are petrographically complex both in terms of their original mineralogy and also in their perigenesis (Fig. 4).

The base of the Honey Creek marks the birth of the great Cambrian–Ordovician carbonate platform in this area. Slowly the siliciclastic "tap" was turned off; throughout the Honey Creek and up into the limestones of succeeding Fort Sill Formation, the amounts of glauconite and quartz diminish, as does the size of quartz grains (Rafalowski, 1984). Rhyolite detritus is increasingly restricted to the neighbor-

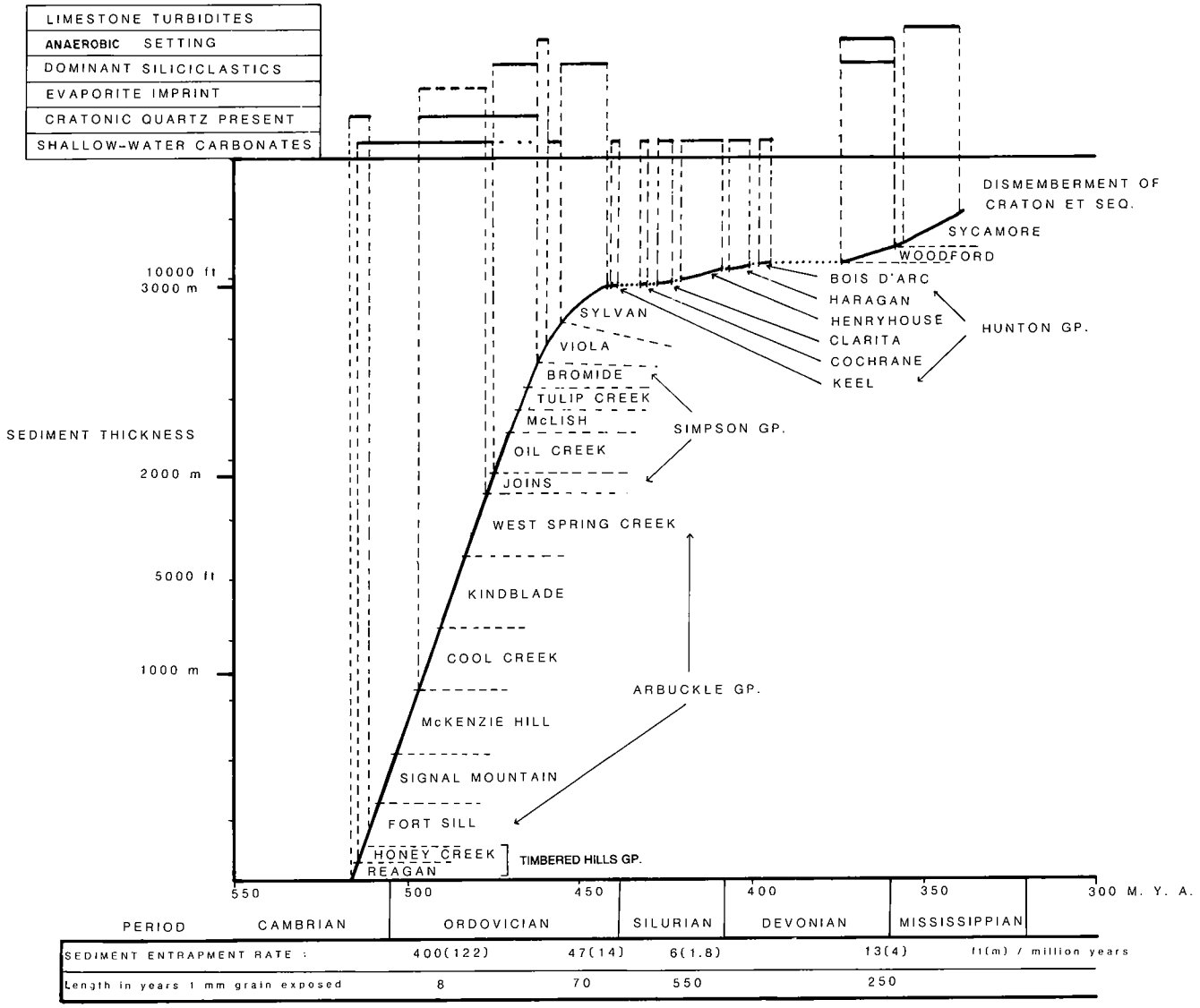

Figure 2. A generalized chronostratigraphic sediment-thickness graph for the aulacogen, illustrating the effects of a near-exponential rate of decay of subsidence. Sediment-entrapment rates are shown; in all cases the likely short-term rates of sediment production are much greater than permanent entrapment rates. Some significant environmental imprints are also listed.

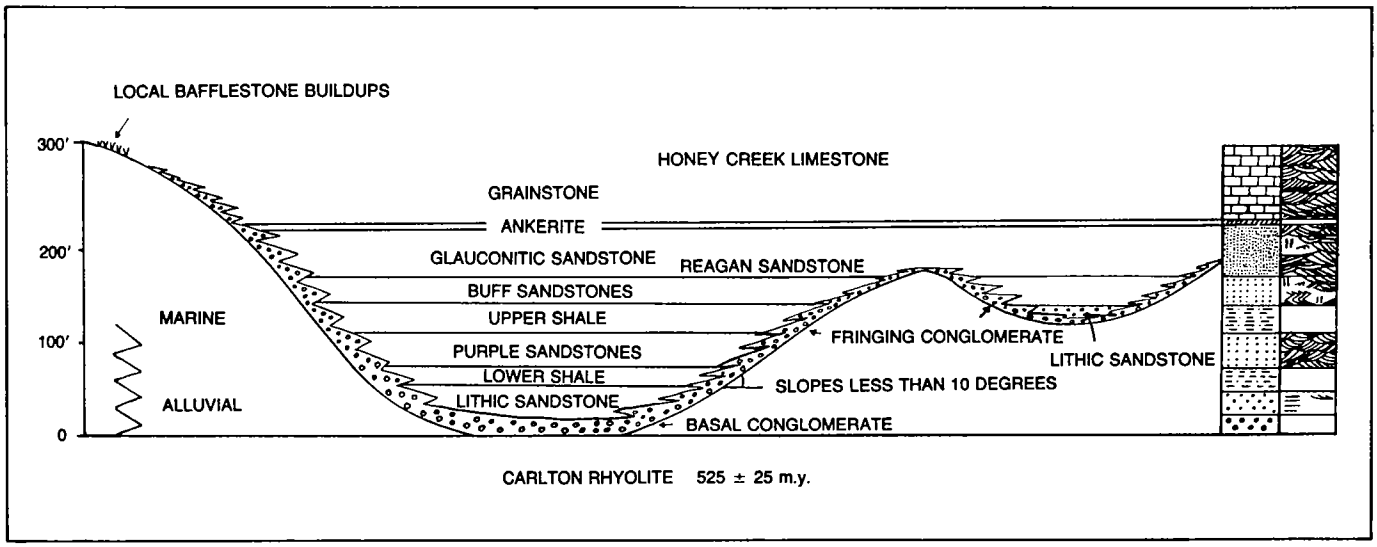

Figure 3. Schematic representation of lithostratigraphic architecture in the Timbered Hills Group (from Tsegay, 1983).

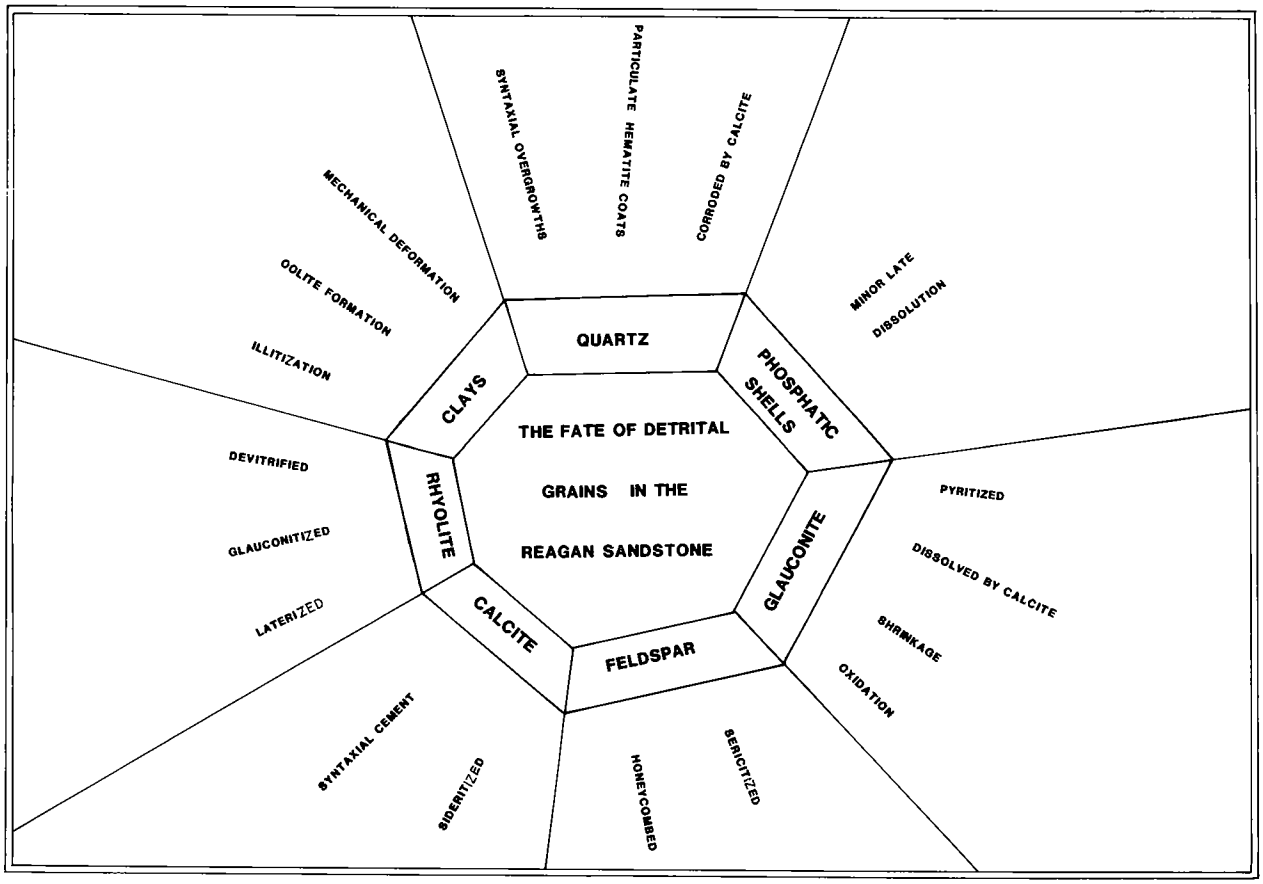

Figure 4. A representation of the diagenetic complexity of the Reagan Sandstone (from Tsegay, 1983).

hood of the gradually vanishing islands of the Timbered Hills archipelago.

In order to explain the complexities of the Timbered Hills Group, and in particular to account for the initiation of carbonate sedimentation, a fairly complex model is proposed (Fig. 5). Under the aegis of the elastic flexure of the lithosphere previously discussed, the marine transgression slowly inundated the irregular rhyolite surface from the opening ocean to the southeast. At the same time, quartz sand was transported by rivers flowing perpendicular to the subsiding craton margin, from sources which (on the evidence of paleocurrents) lay to the northwest. In the area of the Slick Hills, this quartz was mixed with variable amounts of rhyolite detritus shed from the adjacent hills. The initial deposits around the hills were alluvium (including channel sands), much of which was incorporated into the advancing seas. Iron produced by weathering of the rhyolite was mobilized and redistributed as the transgression progressed. In quantitative terms, iron in the lower (alluvial) Reagan is mostly represented by hematite cements, whereas in the upper (marine) Reagan, glauconite is the principal residence for iron (as Fe^{3+} and Fe^{2+}). Ferruginous ooids occur in limited quantities in the middle part of the Reagan; they appear to have been reworked from coastal-margin settings, perhaps lakes (Tsegay, 1983).

Within the marine Reagan, the quartz and rhyolite fragments were mixed with variable amounts of glauconite peloids, forming buff-colored sand bodies characterized by lenticular geometry, abundant medium-scale cross-bedding, and the *Skolithos* trace-fossil assemblage. Paleocurrents within the larger sand bodies tend to be unimodal and record transport to the southeast. On the other hand, thinner sandstones exhibit bimodal cross-bedding distribution. Some of these distributions are bipolar and feature herringbone cross-bedding, suggesting tidal control. Where not bipolar, bimodal distributions may reflect deflected tidal pathways around rhyolite islands. Thus, in summary, the sandstones of the Reagan are characterized by complex paleocurrent patterns showing some tidal influence, but in the case of the larger bodies also suggesting movement by storm tracks moving to the southeast.

The uppermost unit of the Reagan (Fig. 3) is a spectacular greensand, up to half of which is characterized by glauconite peloids. Several lines of evidence suggest that this facies was deposited slowly in water less-agitated than that which had existed earlier in the transgression. For example, pebble conglomerates in the greensand, which are composed of phosphatic nodules and both glauconitized and unglauconitized rhyolite pebbles, clearly record both substantial reworking and the importance of slow-

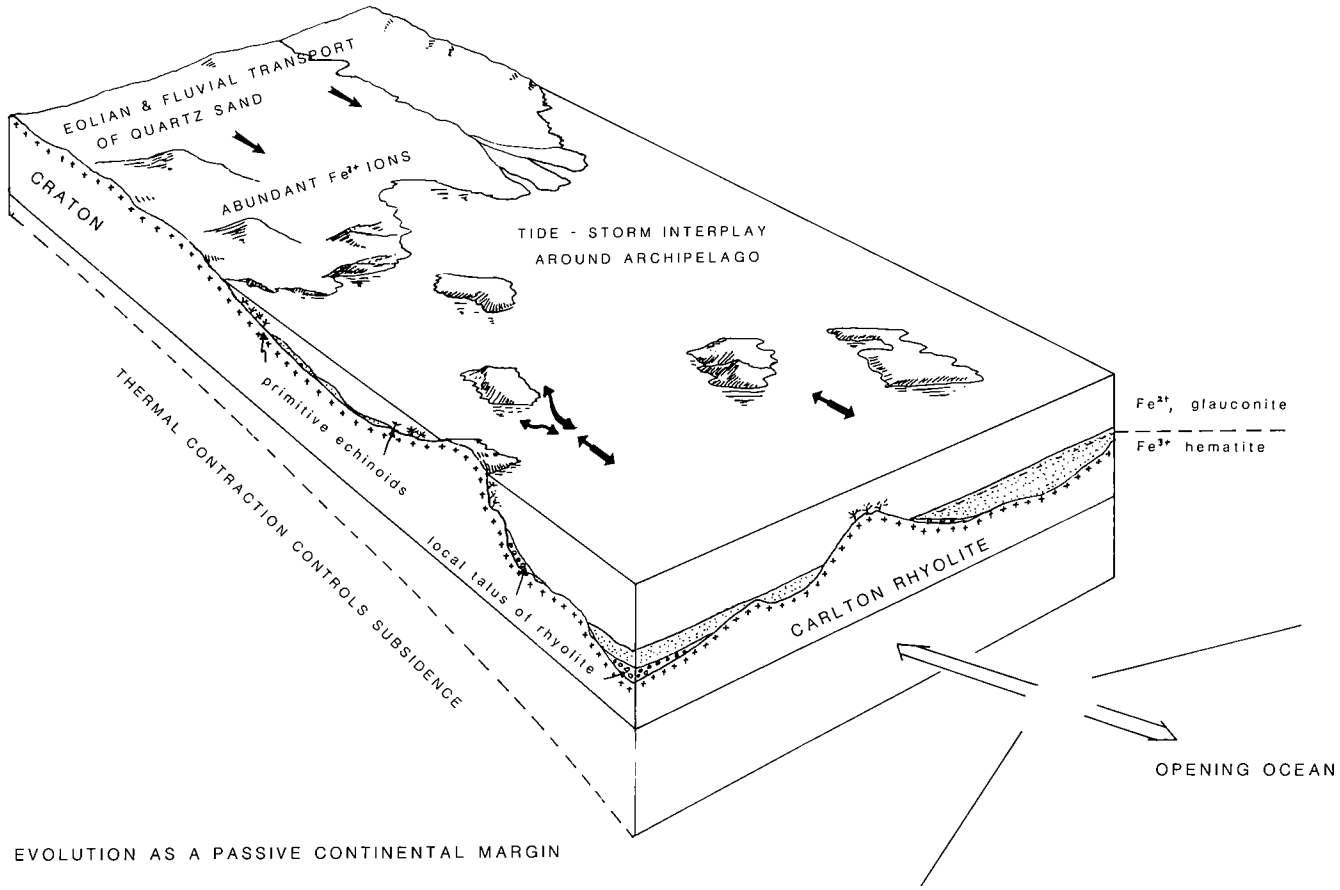

Figure 5. A model of the Franconian transgression across the Slick Hills area (see discussion in text).

acting chemical sedimentary processes (the latter also suggested by the great abundance of glauconite peloids). Furthermore, some cross-beds exhibit evidence of very slow development (in the form of abundant reactivation surfaces; Stop 3, this volume). In addition, an inverse relationship between glauconite content and the *Skolithos* assemblage suggests that at least some of the greensand bodies either initially formed in or were subsequently covered by water less-agitated than that which had existed earlier.

A likely environmental scenario for formation of the greensand is one in which the transgressive shoreline was by then located far to the northwest (except locally around islands), and as a result the input of cratonic quartz had diminished (this is suggested by the smaller size and lesser amount of quartz in the greensand). The slowed depositional rate gave the nascent seas time to redistribute the iron inherited from the basement. This explanation of glauconite formation involves a non-uniformitarian element which can be supported by the fact that glauconite formed at the unconformity between rhyolite and (Honey Creek) limestone around islands in the archipelago (Rafalowski, 1984).

As discussed previously, the Honey Creek grainstones contain a simple faunal assemblage of shallow-water invertebrates dominated by pelmatozoans of probably sessile habit. Their appearance could reflect either a decreasing amount of fluvially transported siliciclastics in the area and/or a decrease in the iron content of the sea. An appealing reconstruction is to have the relatively clear water around the islands of the archipelago colonized by invertebrates first, while less-amiable conditions still existed in the deeper straits between. Subsequently the broken pelomatozoans were redistributed across the entire area by waves and tides. The dominant bed form in the lower part of the Honey Creek is medium-scale cross-bedding which shows a bipolar distribution oriented NW–SE (as in the Reagan). The carbonate sandstones are not lenticular (as in the Reagan), but appear to have formed as a result of migration of numerous small (no larger than 12 in. [30 cm]) lunate dunes. These dunes presumably clogged the deeper waters of the straits, recording an increased rate of sedimentation as the carbonate-producing system became more and more effective.

Arbuckle Group

The Arbuckle Group is one of the world's great sequences of platform carbonates, representing part of the colossal Cambrian–Ordovician carbonate platform which extended over much of the western seaboard of the Iapetus Ocean. In the Arbuckle Mountains, the group is perhaps 6,000 ft (1,800 m) thick,

whereas in the Slick Hills the group is about 10–15% thinner (the top of the West Spring Creek Formation is nowhere exposed). It is possible that this decrease in thickness is due to the relative position of the two areas within the aulacogen (the Wichita Mountains are ~100 mi (160 km) farther from the presumed triple-junction point than the Arbuckle Mountains).

In the Slick Hills, Stitt (1978) has defined the base of the group in paleostratigraphic terms; in lithostratigraphic terms the principal change is the incoming of vast amounts of lime mud (Donovan and Ragland, this volume). The pelmatozoan-rich, cross-bedded grainstones of the Honey Creek gradually disappear from the section, giving way to the visually monotonous, homotaxially difficult sequence of thinly bedded limestones which form the familiar tombstone topography. The biota becomes more diversified: Pelmatozoan fragments are still common, but thin-and thick-shelled trilobites, gastropods, brachiopods, sponges, and a diversity of algal boundstones are very important. Oolitic grainstones are significant at some levels, and peloids are found throughout, but quantitatively the most important allochems are intraclasts of various sizes as much as 6 in. (15 cm) in length. These help to form a textural spectrum of clastic carbonates ranging from intraformational conglomerates (which may be either cemented by sparite or consolidated by a lime-mud matrix), through grainstones, packstones, and wackestones, to mudstones. The percentage of the sequence built of intraformational conglomerates is remarkable (14% in the Kindblade Formation at the Cook Creek road cut; Stop 4, this volume). Individual bed thicknesses are rarely >24 in. (~60 cm), and often considerably less. Hardgrounds (some multiple) are abundant. The rapid vertical contrasts seen in the sequence are amplified to some extent by the large numbers of bedding-parallel stylolites which cut the section. The latter can be regarded as a mechanism by which the rapidly lithified sequence responded to compaction (i.e., back-stripped).

In essence, most of the Arbuckle sequence appears to have been deposited in either the intertidal or shallow subtidal zones. Only in the Cool Creek and West Spring Creek Formations are substantial imprints of the supratidal zone discernible (Ragland and Donovan, 1985b, this volume; Cloyd and others, this volume). These imprints include several evidences of evaporite precipitation and dolomite formation in an environment similar to modern coastal sabkhas.

In analyzing the intertidal and subtidal facies, it is important to recognize that tidal energy on the shallow platform would have been significantly dampened by frictional diffusion. Although the algal boundstones clearly show a morphological response to varying water depths, exposure duration, and turbulence (Ragland, 1983; Ragland and Donovan, 1985b, this volume), it is probable that fair-weather waves and periodic storms were more effective in molding the final character of the sediments. In this respect the concept of the "platform triangle" is an easy way of visualizing the dominant motif found throughout the group (Figs. 6,7). In essence, the triangle relates (1) the destructive effect of storms; (2) fair-weather sedimentation, and (3) contemporaneous lithification. In tangible terms, this relationship is expressed as (1) poorly sorted intraformational conglomerates and other intraclastic limestones; (2) lime mudstones, algal boundstones, oolitic grainstones, and other well-washed sediments; and (3) hardgrounds. Clearly the triangle does not account for all the textural relationships seen (for example, many grainstones probably were converted into packstone-like textures by infiltration of lime mud). Nevertheless, it does emphasize the importance of the fair-weather wave base as a control on sediment packing and sorting.

For the most part, the Arbuckle Group is a sequence bedeviled by homotaxis; most formational boundaries are difficult to determine. There are, however, two emphatic contacts within the group. The first of these is the Fort Sill–Signal Mountain junction (Fig. 8). Feinstein (1981) has suggested that the abrupt lithologic change at this point records reactivation of aulacogen-margin faults which had been "locked" during the previous stage of elastic flexure. In the field, the change is seen as the passage from massive algal boundstones (the most commonly observed stromatolite form consists of distinctive, laterally linked hemispheroids 6 in. (15 cm) in diameter) into thinly bedded clastic carbonates devoid of boundstones (Rafalowski, 1984; Ditzell, 1984). The

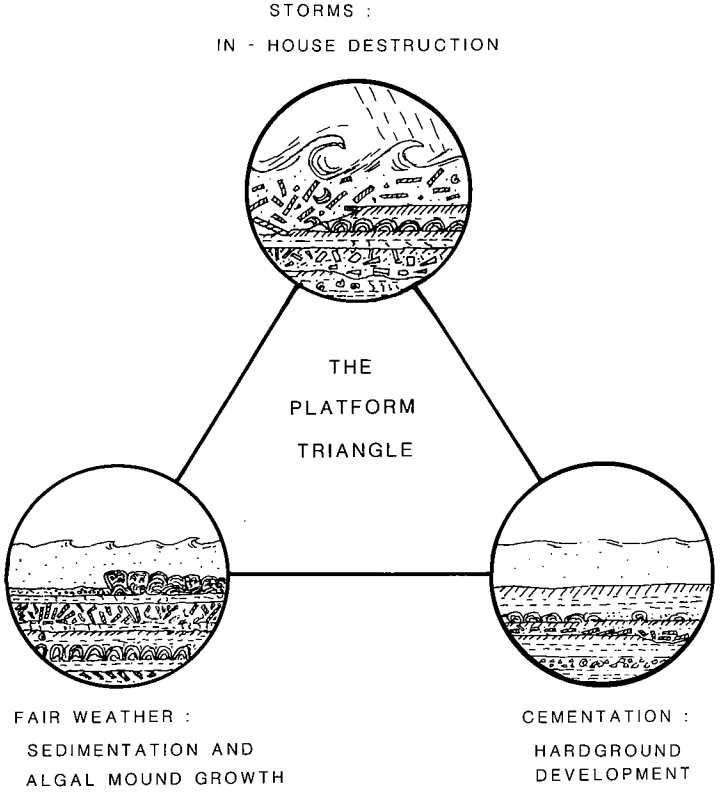

Figure 6. Platform-triangle concept (see discussion in text).

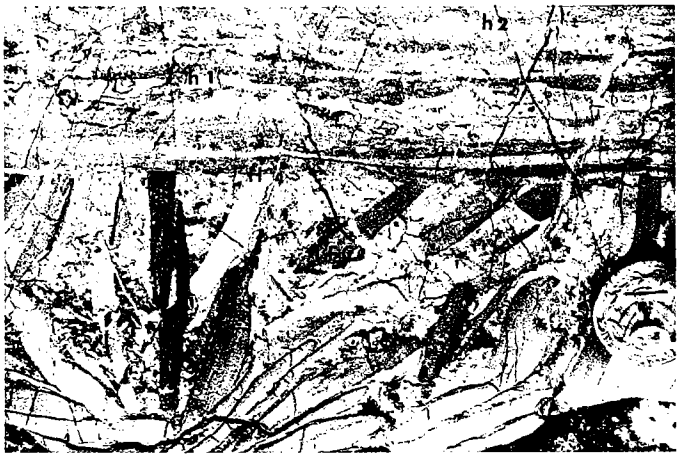

Figure 7. An example of a short section which illustrates the platform-triangle concept. The lower part of the rock is an intraformational conglomerate (IFC) in which wave-sorted, vertically packed mud clasts have acted as a mechanical baffle stone, trapping much mud and intraclastic detritus. It was cemented as a hardground (H) and subsequently planed by erosion. Overlying the hardground is a sequence of laminated mudstones and wackestones, lightly bioturbated and containing several hardgrounds (h1, h2, etc.).

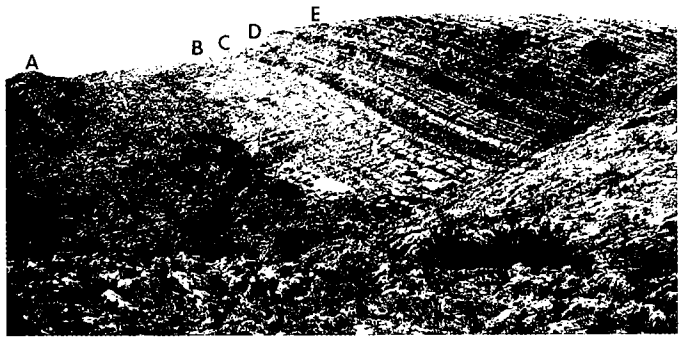

Figure 8. View of part of the Bally Mountain range, showing (A) the Royer (Bally) Dolomite, (B) the uppermost Fort Sill Limestone, (C) the contact between the Fort Sill and Signal Mountain Formations (see discussion in text), (D) a single boundstone horizon in the Signal Mountain Formation (this dies out across the mountain), and (E) typical thinly bedded Signal Mountain lithology.

boundstone-free zone extends throughout the Signal Mountain Formation to the upper part of the McKenzie Hill Formation. If the change is indeed related to tectonic activity, then it is interesting that the sedimentary response is expressed entirely as shallow-water carbonates. An environmental comparison does suggest that more of the Signal Mountain Formation may have been deposited below fair-weather wave base than is the case in the Fort Sill Formation. Nevertheless, it is clear both from the evidence of multiple hardgrounds and from simple subsidence-rate calculations (Fig. 2) that short-term sedimentation rates operating on the platform were more than sufficient to keep pace with subsidence within the aulacogen at this time.

The second emphatic boundary within the group is the appearance of large quantities of quartz grains at the base of the Cool Creek Formation (the Thatcher Creek lithology of Ragland and Donovan, 1985a) and subsequently throughout the group. The petrographic character of the siliciclastic grains associated with this "second coming" is virtually identical with that of the "first coming" in the Reagan Sandstone, i.e., mostly unstrained, monocrystalline quartz, with minor amounts of plagioclase and microcline. A similar source can be inferred (i.e., high-level non-orogenic plutonic complexes); the relative absence of feldspar in both "comings" of quartz (and indeed in the incredibly pure quartz arenites of the overlying Simpson Group) may reflect alkaline weathering of granitoid rocks similar to that reported by Russell and Allison (1985) beneath the Cambrian quartz arenites of northern Scotland. These authors record the widespread development of a paleosaprolite in which mafic minerals and feldspars have been altered to green muscovite (agalmatolite). They envisage the riverine transport of the remaining quartz-rich soil (plus the agalmatolitic clay) into adjacent marine basins to form the great basal quartzites so characteristic of the Scottish section.

While it is perhaps possible to explain the petrographic character of the lower Paleozoic siliciclastic grain population, the mechanism which led to the "second coming" is more enigmatic. Clearly, a peripheral uplift of some sort is required, possibly to the north (Ragland and Donovan, 1985a).

In addition to the interplay of (rapidly cemented) limestone lithotypes within the group, two quantitatively significant diagenetic imprints are apparent: chert and dolomite. Ragland (1983) has documented a considerable variety of secondary-silica textures in the Cool Creek Formation, which she relates to various types of primary precipitation, cement, and replacement (see also Cloyd and others, this volume). Some cherts are found in the lower part of the Fort Sill Limestone (Rafalowski, 1984), but most are found from the middle part of the McKenzie Hill Formation to the top of the group (Donovan and Ragland, this volume). The source of silica is not always apparent, but it could be related to siliceous sponges (particularly in the McKenzie Hill Formation), or to corrosion of quartz in higher formations. The penecontemporaneous character of most, if not all, of the secondary-silica occurrences evidences variable alkalinities during eodiagenesis. The widespread occurrence of chert in the upper McKenzie Hill Formation suggests that a chemical signature related to the "second coming" of siliciclastics presaged the tangible record as expressed by the Thatcher Creek Member.

Dolomite textures have been reviewed elsewhere in this volume (Cloyd and others). In general these dolomites are either stratigraphically more or less concordant and apparently of early diagenetic origin, or they are discordant and late—probably post- or syn-dismemberment. Some of the early dolomites have evaporite affinities; most are probably a record

of ground-water mixing, i.e., they formed in a schizohaline environment. Interestingly, some cherts associated with the evaporative dolomites are length-slow colloform varieties ("cauliflower cherts"), while some cherts associated with schizohaline dolomites are length-fast nodules, as might be expected from Folk and Pittman's hypothesis (1971).

Post-Arbuckle Group Rocks

The top of the West Spring Creek Formation is not exposed in the Slick Hills, as it is covered by Permian deposits. Younger Paleozoic rocks are found only in the conical knolls that constitute the Sugar Hills. In each of these hills, the upper Simpson and lower Viola Groups are found, although in only one case is the contact between the Bromide Formation and the Viola clearly seen. Otherwise, no tangible record of sedimentation is exposed in the area until the conglomerates and shales of the Permian. Nevertheless, the full Paleozoic section is known in the subsurface (Fig. 2).

THE DISMEMBERMENT

From Late Mississippian until Early Permian time, the geology of southern Oklahoma was greatly modified: In the southeast of the state, the Ouachita orogene formed, while in the south and southwest the old Paleozoic carbonate sequences were dismembered into a series of linear basins and uplifts oriented parallel to the aulacogen trend.

The Slick Hills constitute the only exposed part of the frontal fault zone, a 15-mi- (24-km) -wide zone which constitutes the interface between the Anadarko basin to the north and the igneous Wichitas. The zone is bounded on the north by the Mountain View fault and on the south by the Meers fault; maximum stratigraphic separation of ~8 mi (13 km) occurs across the zone. The major bounding faults have been interpreted to dip SSW in the subsurface (Brewer and others, 1982). The dip on the Mountain View fault is less than that given to the Meers.

As was evident at the recent Penrose Conference on the southern Oklahoma aulacogen (Gilbert and others, in press), there is a healthy debate on the style of Pennsylvanian deformation within the aulacogen. Evidence suggestive of components of both compression and left-lateral wrench exists. Most cross sections across the axis of the aulacogen (see, for example, Riggs, 1957; Brewer and others, 1982; Brown, 1984) show convincing evidence of crustal shortening in the form of reverse faulting and tight folding. Evidence in support of left-lateral strike-slip motion is more problematic, partly because no vertical markers which would permit "jigsaw fits" cross the aulacogen, and also because surface exposures are relatively scanty. The importance of the Slick Hills is that they constitute the best-exposed terrane in the whole aulacogen where structural styles can be analyzed by detailed surface mapping. Mapping was initiated by Harlton (1951,1963,1972), by Ham and others (1964), and more recently by a joint research program conducted by Oklahoma State University and the Queen's University, Belfast, Northern Ireland (see, for example, Babaei, 1980; Donovan, 1982; Donovan and others, 1982; Beauchamp, 1983; McConnell, 1983; Marchini, 1986).

Two principal structural terranes are exposed in the Slick Hills (Fig. 9). To the north and east lies a homoclinally tilted area ("Blue Creek horst" of Harlton, 1963), characterized by relatively simple structure (as presently exposed). To the north and east, the horst is bounded by the Mountain View fault, which is known only in the subsurface. The southwest boundary of the horst, the Blue Creek Canyon fault, is exposed for a short distance within Blue Creek Canyon. Across the fault lies the "Lawtonka graben," a terrane of enormous structural complexity, which at the present level of exposure consists of folded, sheared, and faulted Arbuckle Group limestones. The southwest boundary of the graben is formed by the Meers fault.

Clearly, the principal exposed structural feature in the area is the Blue Creek Canyon fault (in reality a braided complex of faults), which constitutes the boundary between two distinct structural blocks. The stratigraphic effect of this pre-Permian fault is to juxtapose the Carlton Rhyolite Group and overlying Cambrian formations with Ordovician strata of the Arbuckle Group (Fig. 10). Within the canyon area, the fault shows evidence of left-lateral oblique (transpressive), high-angle reverse movement. However, the segment of the fault exposed in the canyon has an anomalous trend (N–S, as opposed to a more general N. 50° W.). Within the Lawtonka graben, adjacent to the N–S fault segment, axes of folds are more northerly than elsewhere in the graben (Fig. 10), folds plunge consistently northward at ~20°, and the rocks generally bear the imprint of an E–W compression which has locally tightened folds and produced considerable pressure-solution cleavage. This suggests that the anomalous fault segment is a compressive bend in an otherwise left-lateral fault system.

Within the graben, the principal structural features are the following:

1) An en echelon array of folds trending between N. 55° W. (close to the Meers fault) and N. 35° W. Some folds are locally slightly overturned (facing northeast).

2) Reverse faults of trend similar to that of the folds. The most important of these faults is the Stumbling Bear thrust, which recently has been interpreted by Marchini (1986) as a transpressive thrust (characterized more by ramps than flats), steepening downward.

3) Small-scale, left-lateral, en echelon solution arrays characterized by intense pressure solution and commonly cut by Riedel fractures (McCoss and Donovan, this volume).

Clearly the deformation in the Lawtonka graben shows evidence of both intense compression and left-lateral wrench motion. One appropriate reconcilia-

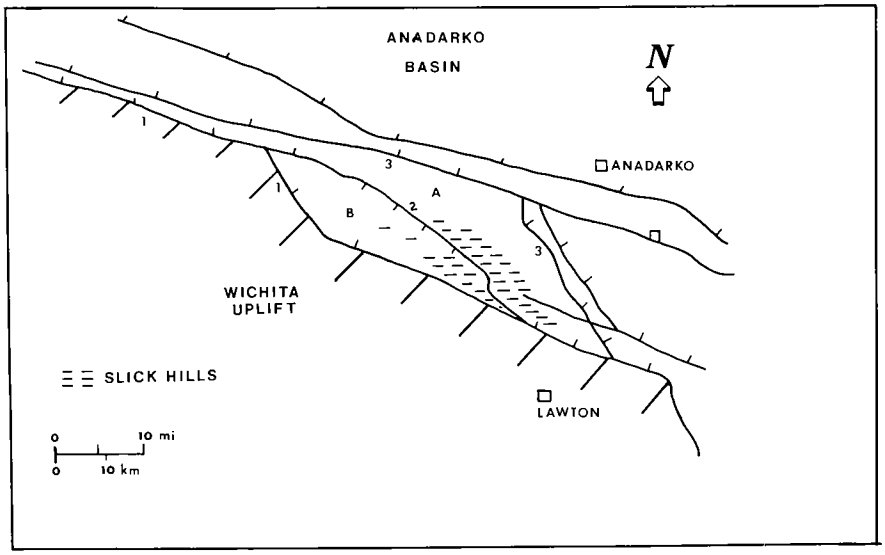

Figure 9. Sketch map illustrating the general setting of the Slick Hills in relation to the Anadarko basin and Wichita uplift. A = Blue Creek horst; B = Lawtonka graben; 1 = Meers fault; 2 = Blue Creek Canyon fault; 3 = Mountain View fault. Simplified from Harlton (1963).

tion of this apparent contradiction of styles is to recognize that the area has been subject to left-lateral transpression. Sanderson and Marchini (1984) have described pertinent effects of transpression, including (1) steep cleavage and a stretching lineation that may be either vertical or horizontal; (2) folds and thrusts at small angles to the zone boundary; (3) normal faults, veins, and other extensional structures at a high angle to the zone boundary; and (4) crustal thickening and vertical uplift. All these effects relate well to observations made by the Stillwater–Belfast group. McCoss and Donovan (this volume) have examined fold- and shear-array data, using a technique developed by McCoss (in press); they have been able to determine consistent transpression vectors within the graben.

PERMIAN–RECENT QUIESCENCE

Permian Sedimentation Patterns

In essence, the deformation related to the Pennsylvanian dismemberment ceased by Early Permian time (although a small caveat must be made concerning the Recent movements on the Meers fault). During the Permian, the Slick Hills, together with the Wichita Mountains, were slowly buried beneath their own detritus (Fig. 11). This detritus can be conceptualized either as syntectonic or as post-tectonic. At the present level of exposure, as recorded by the Post Oak Conglomerate, most of the detritus is post-tectonic and simply records the denudation of the final relief of the uplift. However, in the Meers Valley a limestone-boulder breccia, containing blocks the size of a small house, is interbedded with pebble conglomerates more typical of the Post Oak. This breccia and the great extent of limestone-pebble Post Oak in the Meers Valley (implying relief inversion) may well record localized downthrow of the Meers fault to the south and corresponding uplift of the Slick Hills to the north (Donovan, 1984; Collins, 1985; Bridges, 1985). If so, then it follows that in Early Permian time the relative motion of the Meers fault was reversed, perhaps as a result of stress relaxation.

During late Paleozoic time, the climate of southwestern Oklahoma became progressively more arid. One of the evidences of a semi-arid climate in Early Permian time is the occurrence of calcrete (caliche). Not only are these indurated pedocals climatic indicators, they also require geomorphological stability during their formation. The latter factor indicates that they are of use as chronostratigraphic as well as lithostratigraphic markers (Donovan, 1982). In the present context, this property is important because (1) Oklahoma Permian red beds are difficult to date properly, and (2) there are dramatic differences in subsidence rates from basin to uplift. For example, because the Meers Valley was an area of minimal subsidence by comparison with adjacent basins, the calcretes are more closely spaced ("condensed") within the available host sediments.

Sub-Permian Unconformity

The Post Oak Conglomerate, which is a facies equivalent of the Hennessey Group and Wellington Formation, oversteps all older rocks in the Slick Hills. The unconformity is extremely irregular; it is clear that the present topography is a lightly modified Permian inheritance. Beneath the unconformity, lower Paleozoic limestones show karst features, including small cave systems (Donovan, 1982). Within these caves a substantial fossil vertebrate fauna occurs (Simpson, 1979), and a variety of phreatic and vadose carbonate deposits were precipitated. At one

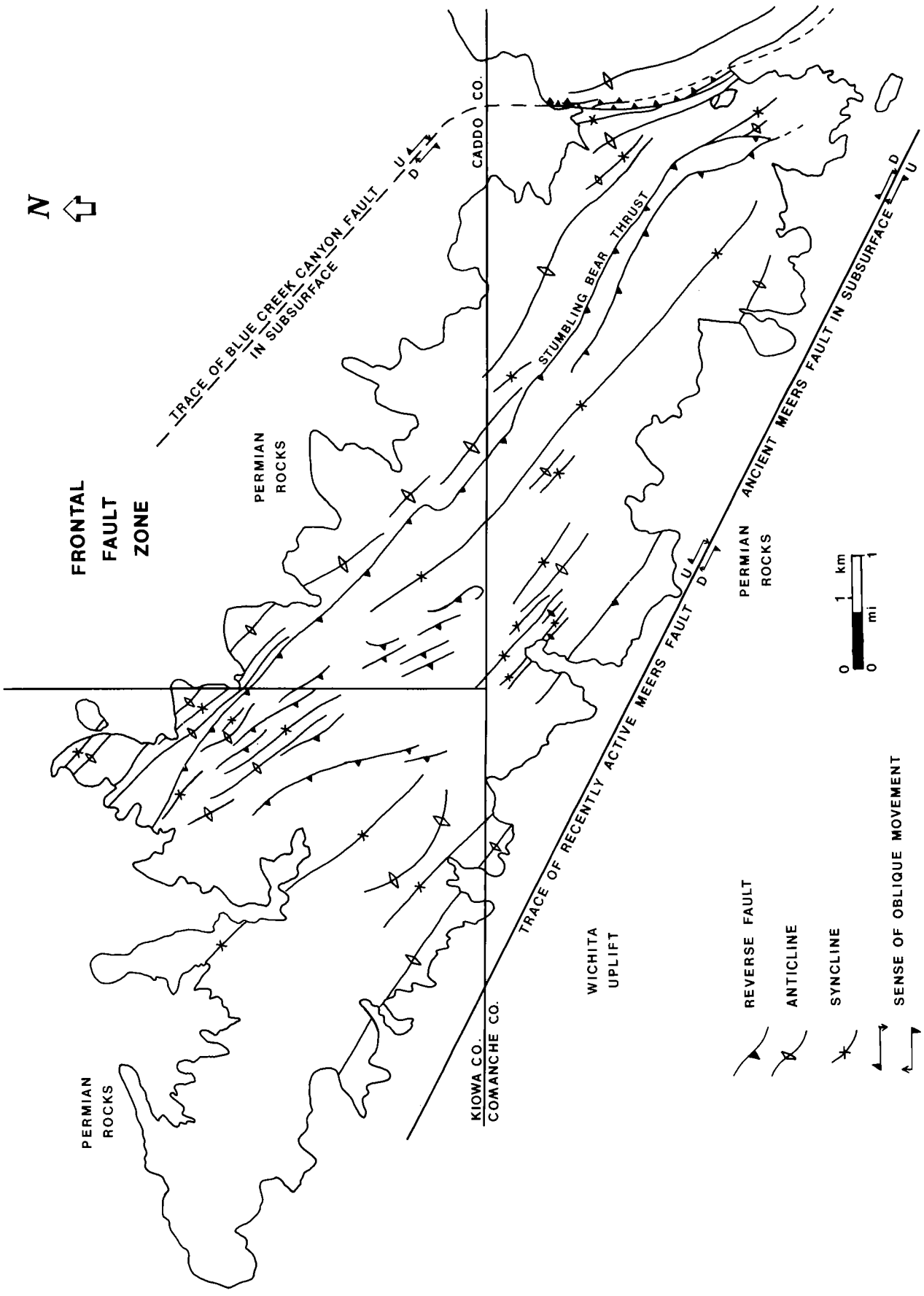

Figure 10. Principal folds and thrusts in the Lawtonka graben. Modified from Donovan (1982), Beauchamp (1983), McConnell (1983), and Marchini (1986).

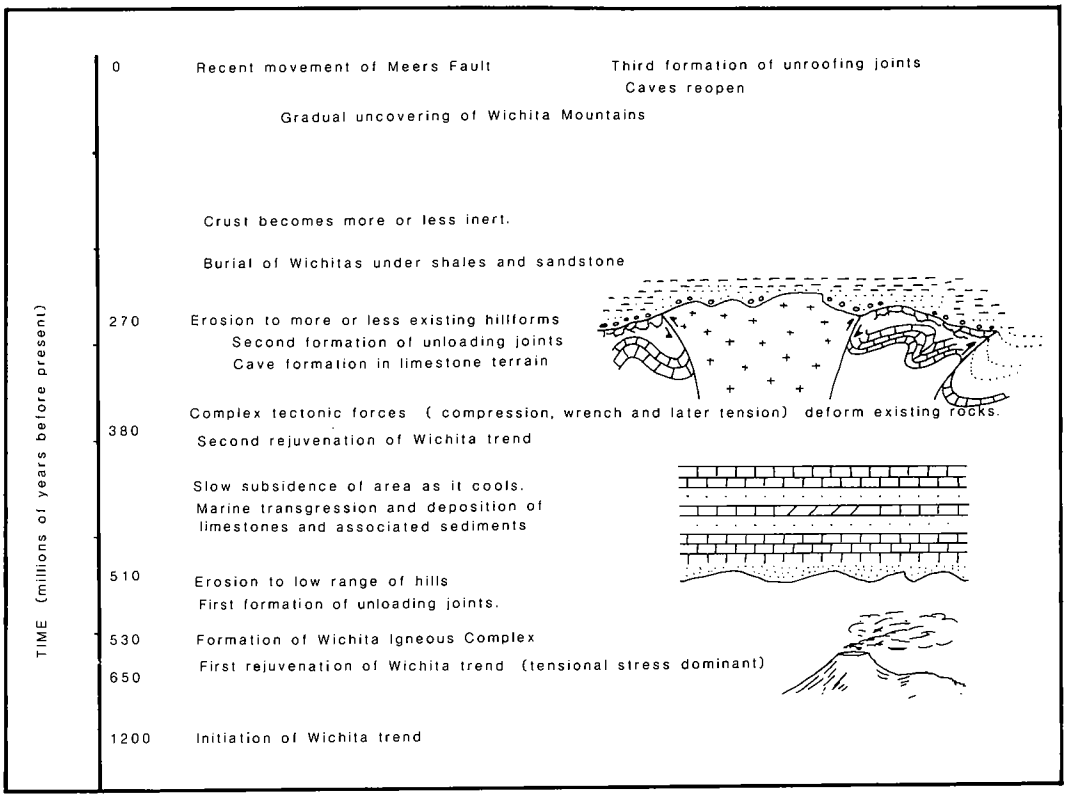

Figure 11. Summary of the history of the Slick Hills.

cave on Bally Mountain, the cave deposits were precipitated contemporaneously with fluid hydrocarbons.

Diagenetic Pathways for Hydrocarbons, Dolomite, and Barite

As noted above, the cave systems of the Slick Hills contain a small but convincing record of the passage of hydrocarbons during Early Permian (perhaps Late Pennsylvanian) time. These hydrocarbons probably did not form as a result of maturation of rocks presently exposed in the Slick Hills themselves, because local occurrences of the principal potential source rocks (Viola and Woodford; Fig. 2) were never buried deeply enough (Cardott and Lambert, 1985). The timing of hydrocarbon entry (by vertebrate biostratigraphy) into rocks at or near the surface suggests that maturation took place at depth during late Paleozoic dismemberment of the lower Paleozoic terrane. Subsequent upward migration from the more deeply buried and maturing parts of this terrane through fractures in the deformed Slick Hills appears to have been widespread, especially through the northern overhang above the Mountain View fault (Fig. 12).

A similar upward motion of late, "warm" dolomitizing fluids (producing discordant replacements characterized by xenotopic and baroque textures) has apparently taken place (Cloyd and others, this volume). These fluids may have been derived from formation brines trapped and overpressured (by both sedimentary and tectonic load) in the Anadarko basin. These fluids are still "escaping" today (in a modified form) from a barite-depositing spring at Zodletone Mountain, the most northerly of the Slick Hills (Younger and others, this volume).

ACKNOWLEDGMENTS

It is a pleasure to acknowledge helpful discussion with a number of colleagues, including Charlie Gilbert, Dave Sanderson, Ken Johnson, Tim Denison, Brian Cardott, John Wickham, Carol Simpson, and Jim Granath. I am grateful for the field support given to me by the Oklahoma Geological Survey and Sun Co. Many landowners have freely admitted me to their property: Doyle Leatherbury, Bill Hodges, Don Trobe, the Dietrich family, the Woods family, and, in particular, the Olivers and Kimbells of Blue Creek Canyon (to whom I must have seemed a permanent resident at times). However, my greatest appreciation is to the following graduate students, who have stormed into these Slick Hills, seeking out the hidden places and unsolved problems: Weldon Beauchamp, Steve Bridges, Kelly Cloyd, Kathy Collins, Curtis Ditzell, Kit Hester, Max Marchini, Dave McConnell, Deborah Ragland, Mary Rafalowski, Diana Schaeffer, Milton Stubbs, and Tekleab Tsegay.

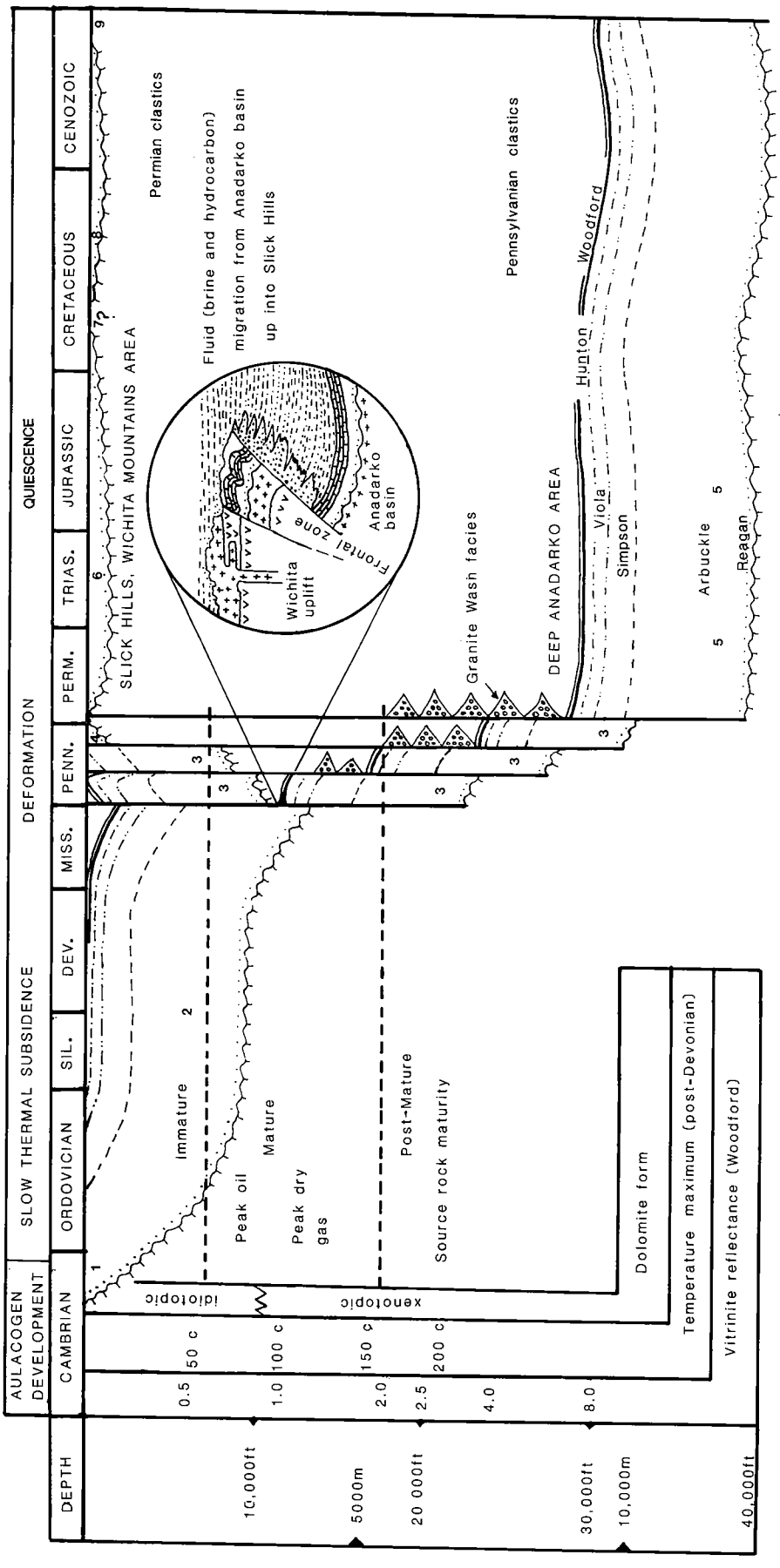

Diagenetic stage of Arbuckle Group

1 Eodiagenesis
2 Mesodiagenesis (shallow burial submarine)
3 Mesodiagenesis (tectonic)
4 Telodiagenesis (karst)
5 Mesodiagenesis (deep burial submarine)
6 Mesodiagenesis (2nd imprint shallow burial subcontinental)
7 Telodiagenesis (karst?)
8 Mesodiagenesis (2nd imprint shallow burial submarine)
9 Telodiagenesis (karst)

Figure 12. Tactical comparison of the histories of the Slick Hills and the Anadarko basin. Vitrinite-reflectance and temperature data derived from Cardott and Lambert (1985). Hydrocarbon source maturity is based on the Woodford Shale; given the relationship between source-rock maturity and time, the oil and gas windows will have been gradually rising through the Anadarko section from Pennsylvanian time until today.

Oklahoma Geological Survey Guidebook 24, 1986

PALEOZOIC STRATIGRAPHY OF THE SLICK HILLS, SOUTHWESTERN OKLAHOMA

R. Nowell Donovan and Deborah A. Ragland

INTRODUCTION

Within the confines of the southern Oklahoma aulacogen, the lower Paleozoic section is more familiar in the Arbuckle Mountains than it is in the Wichita Mountains. In part this is a function of accessibility, and in part it is because the top of the lower Paleozoic section is truncated by Permian erosion in the Wichitas. Nevertheless, the Timbered Hills and Arbuckle Groups are almost completely exposed in the Slick Hills, immediately north of the Wichitas (only the top of the West Spring Creek Formation is missing). Furthermore, in the slightly drier climate of the Wichitas these groups have an appealing completeness of exposure somewhat superior to that in the Arbuckles. In this communication we outline a descriptive analysis of the stratigraphy of the Slick Hills (Fig. 1). Our analysis is essentially a field geologist's guide tested by stratigraphic and structural workers in the region (Beauchamp, 1983; Ditzell, 1984; Donovan, 1982; Marchini, 1986; McConnell, 1983; Rafalowski, 1984; Ragland, 1983; Tsegay, 1983). We have utilized the paleontological and stratigraphic work of Ham and others (1964) and Stitt (1977,1983).

THE TIMBERED HILLS GROUP

The Timbered Hills Group records an initial Franconian transgression across an irregular land surface sculpted from the Carlton Rhyolite Group. Small hills of rhyolite as much as 350 ft (106 m) high were gradually buried beneath Cambrian sediments. In one case, a hill existed until Fort Sill time (Rafalowski, 1984). Clearly, given the available relief, the architecture of the group is complex, and stratigraphic overlap is a dominant theme. Furthermore, each of the individual rhyolite hills contributed wedge-shaped deposits of rhyolite detritus into the sequence until it was buried. Nevertheless, several mappable units are developed in both the Reagan and overlying Honey Creek Formations (Tsegay, 1983; Donovan, 1984; Rafalowski, 1984).

The Reagan Sandstone is the only formation in the area dominated by siliciclastics. Biostratigraphic control is very poor; the only body fossils found are phosphatic inarticulate brachiopods, although trace fossils referable to the *Skolithos* assemblage are commonly seen in many sandstone units. In general, the formation consists of interbedded sandstones and shales. The latter are very rarely exposed; the former are mappable as lenticular units as much as 35 ft (10 m) thick. Petrographically the sandstones are dominated by quartz (an unstrained variety), lesser amounts of rhyolite clasts, and, toward the top, glauconite peloids and phosphatic shell debris. The sandstones classify, a little awkwardly, as quartz arenites and lithic arenites. In general the lowest sandstones form fine-grained, red-brown beds cemented by quartz and hematite. They are succeeded by coarse-grained, purple-brown sandstones with ubiquitous medium-scale trough cross-bedding and quartz and hematite cement. Although *Skolithos* is seen in some of the purple sandstones, this trace-fossil assemblage is best developed in the overlying tan and light-brown sandstones. The latter are firmly cemented by quartz and contain some glauconite peloids. These peloids are the dominant sediment grains in the topmost unit of the Reagan, a conspicuous greensand, characterized by large cross-beds in sets 1–4 ft (~1 m) thick, which is developed across the entire area. This greensand consists of as much as 55% fine-sand-sized glauconite peloids mixed with quartz and minor amounts of rhyolite. The unit is fairly soft, as it is cemented by iron-rich illite (Tsegay, 1983), except toward the top, where increasing amounts of calcite-spar cement herald the beginning of carbonate sedimentation.

The base of the Honey Creek Limestone is taken as the first incoming of carbonate grains. A diagenetic reaction between carbonate and glauconite has resulted in the formation of a distinctive orange-weathering zone rich in ankerite at the formational contact (see Cloyd and others, this volume). The limestones of the Honey Creek are well-washed, cross-bedded, bioclastic grainstones dominated by pelmatozoans, together with lesser amounts of thick-shelled trilobites and orthid brachiopods. The limestones are contaminated by varying amounts of quartz, glauconite, rhyolite, and phosphatic shell grains. Stratigraphically, the Honey Creek can be

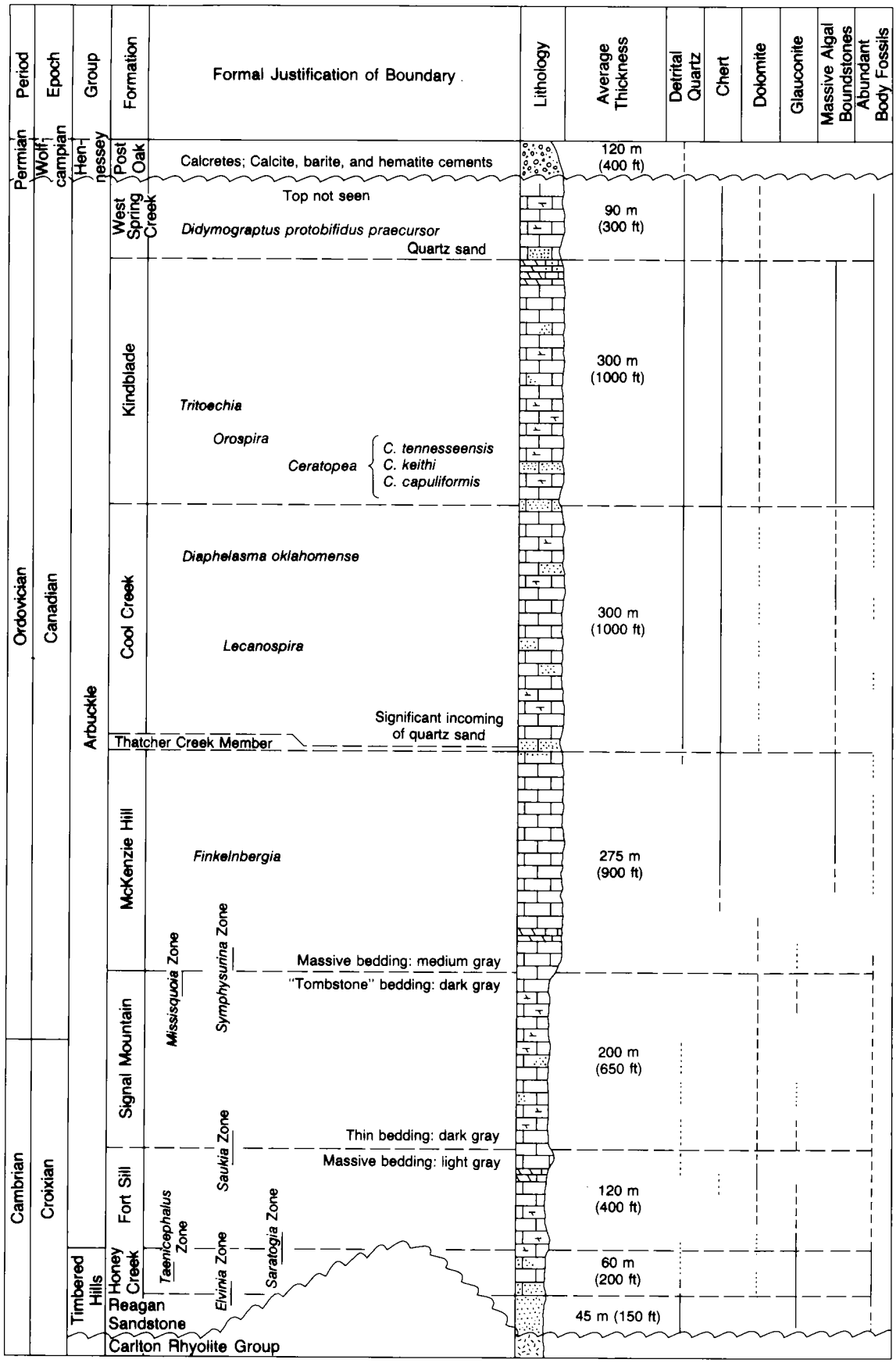

Figure 1. Resume of the stratigraphy of the Slick Hills. Lithologic symbols standard; sources as quoted in text. M. B. Rafalowski amended the Fort Sill–Carlton Rhyolite boundary. Thicknesses averaged from several measured sections.

divided into three informal units (Rafalowski, 1984): Lower and upper carbonate members sandwich a fine-grained, calcareous quartz arenite as much as 40 ft (12 m) thick. The latter is resistant to weathering, forming a ledge characterized by a curious honeycomb weathering which is due to the dissolution of lenticles of carbonate shell hash. These lenticles are in part a remnant of more-extensive carbonate sands which were partially removed during diagenesis (Donovan, 1982).

THE ARBUCKLE GROUP

Siliciclastic detritus gradually diminishes in both grain size and amount toward the top of the Honey Creek. The base of the succeeding Arbuckle Group (specifically the Fort Sill Formation) is demarcated lithostratigraphically by the incoming of major amounts of lime mud (micrite) into the section. Grainstones still occur, but they are rarely cross-bedded. It is apparent that simple gravity settling played an important role in sedimentation throughout Arbuckle Group time. Thus, in general, sediments were poorly washed, and as a result packstone, wackestone, and mudstone textures are common. Hardgrounds are frequently seen, although many bed boundaries have been obfuscated by stylolitization. A variety of algal boundstones is found at some levels, while cherts occur in abundance in the upper parts of the group. Intraformational conglomerates are found throughout. Unless dolomitized, the rocks are essentially nonporous.

In the field, Arbuckle Group exposures are characterized by the development of "tombstone topography." Vertical elements in this topography are joint-controlled, whereas "tombstone" thickness is a function of bed thickness and stylolite frequency, not lithology. In detail, variations in the weathering profile can be recognized and often prove to be stratigraphically significant.

Throughout the Slick Hills, three informal members can be recognized in the Fort Sill Formation: (1) a basal thin-bedded-limestone sequence dominated by mudstones, but with important packstones and grainstones; (2) a middle sequence consisting of alternations of lime mudstones with very thin-bedded dolomitic siltstones; and (3) a topmost sequence of more-massive limestones, containing abundant algal boundstones. On Bally Mountain and adjacent Zodletone Mountain (but not elsewhere in the Slick Hills), the central part of the upper member has been comprehensively dolomitized to a coarsely crystalline texture. A similar dolomite, the Royer, occupies a close but not identical stratigraphic position in the Arbuckle Mountains. We propose that in the Slick Hills this dolomite be referred to as the "Bally dolomite." It is one of a number of thick strata-bound dolomites of somewhat enigmatic origin which characterize the Arbuckle Group (e.g., the Royer, Butterly, Strange, and Kindblade "brown zone").

The contact between the Fort Sill and Signal Mountain Formations is lithostratigraphically distinct, as the latter is the most consistently thin-bedded formation in the Arbuckle Group. As a result, it weathers to form the weakest topographic expression. The distinctness of the contact may be related to accelerated subsidence within the aulacogen (Feinstein, 1981). In the Signal Mountain, the dominant lithologies are a textural spectrum of clastic limestones, from intraformational conglomerates through grainstones and packstones to wackestones and mudstones (many of the finer lithologies are bioturbated). Some glauconite peloids are found, particularly toward the base of the formation.

The boundary between the Cambrian and Ordovician is within the Signal Mountain Formation; it is lithologically undistinguished. The formation is particularly fossiliferous and contains an abundant fauna of trilobites, gastropods, and brachiopods (Stitt, 1977,1983). In fact, the whole Arbuckle Group is highly fossiliferous, with the exception of the Cool Creek Formation, where fossils are scarcer. In general, the younger formations show a greater faunal diversity. However, it should be noted that the strata are well indurated, and that many bed boundaries throughout the group have been stylolitized; as a practical result, fossils are not easy to spot. On the other hand, particularly in the Kindblade and upper Cool Creek Formations, some fossils are highly conspicuous because they have been silicified.

Whereas the lower boundary of the Signal Mountain is clear-cut, the upper boundary is the most difficult to place in the entire group. In general, the incoming of the McKenzie Hill Formation is heralded by rather massively bedded micrites, forming distinctively thick "tombstones." Unfortunately "McKenzie Hill" and "Signal Mountain" lithologies overlap through a thickness of ~200 ft (~60 m) (Ditzell, 1984). The McKenzie Hill is informally separated into two units: a lower, non-cherty member and an upper, cherty member. The first appearance of secondary silica represents the oldest conspicuous cherts in the Arbuckle Group. In the McKenzie Hill, the chert takes the form of burrow-filling textures and small nodule beds. The source of some of the silica may have been siliceous sponges, which are common in the upper part of the formation.

The Cool Creek Formation is the most varied unit of the Arbuckle Group (Ragland, 1983). The formation is composed of a spectacular variety of algal boundstones, interbedded with intraformational conglomerates and breccias, oolitic limestones, micrites and pelmicrites, evaporite-pseudomorph-bearing dolostones, and quartz-rich sandstones. The basal quartz sand, the Thatcher Creek Member, represents the first significant quartz-detritus input in the Arbuckle Group and has been invaluable in mapping the structural features of the Slick Hills (Beauchamp, 1983; McConnell, 1983; Marchini, 1986).

Detrital quartz is a component of the Fort Sill Formation, but is largely absent from the Signal Mountain and McKenzie Hill Formations. As noted above, detrital quartz occurs conspicuously at the base of the Cool Creek Formation (the Thatcher

Creek Member of Ragland and Donovan, 1985) and at several higher horizons throughout the remainder of the group. All these quartz-rich units are similar in that they consist of cross-bedded, mixed carbonate-quartz sandstones which appear to have formed in small erosive-based channels. The quartz is consistently unstrained and is mixed with a small percentage of microcline.

The contact of the Cool Creek Formation with the Kindblade Formation is taken as the first incoming of the gastropod genus *Ceratopea*. In practice this boundary is somewhat unsatisfactory, because these fossils are not common, and the boundary is readily visible only when silicified (i.e., the formation boundary depends on a diagenetic imprint for its integrity during mapping). In general, the Kindblade is similar to the Cool Creek in character, except that (1) shelled invertebrates form a significant percentage of the limestone; (2) bed thickness is greater (in part because of boundstone production), and as a result Kindblade "tombstones" are thicker; and (3) evaporative dolomites are uncommon.

The contact between the Kindblade and West Spring Creek Formations is taken as the base of a thick and persistent quartz-bearing unit (of "Thatcher Creek" type). The West Spring Creek is not found in complete stratigraphic section in the Slick Hills. The exposed part of the section continues the pattern templated in the Kindblade and Cool Creek. The formation is paleontologically distinctive in that it is the only formation in the Arbuckle Group to yield graptolites.

Boundstones in the Arbuckle Group

The Arbuckle Group contains a spectacular assemblage of algal boundstones, particularly in (1) the topmost member of the Fort Sill Formation, (2) the upper part of the McKenzie Hill Formation, and (3) throughout the Cool Creek, Kindblade, and West Spring Creek Formations. No algal boundstones have been observed in the Signal Mountain Formation. The Kindblade boundstones include complex edifices which involve framework-builders other than blue-green algae (e.g., *Archaeoscyphia, Pulchrilamina*; Toomey and Nitecki, 1979). However, the greatest diversity of external form and internal construction in algal boundstones is seen in the Cool Creek Formation. External forms include encrustations, mats, mounds, and reefs; internal organization into varieties of stromatolite and thrombolite is apparent. The boundstone varieties in the Cool Creek Formation may have been controlled by fluctuations in water depth.

Diagenetic Imprints

The principal diagenetic imprints on the Arbuckle Group (apart from calcite cements) involve dolomitization and silicification. Stratabound dolomite "giants" (e.g., the Bally and Kindblade "brown zone") have already been noted; in addition, the Cool Creek and West Spring Creek Formations contain stratiform dolomites which are intimately associated with cherts of "cauliflower" type. These cherts contain inclusions of both anhydrite and celestite, suggesting an evaporative relationship.

A third type of dolomite is found in thin (~3-ft, or 1-m) beds in many parts of the section and is not associated with an evaporative imprint. This dolomite is rarely completely pervasive and frequently forms "leopard-skin" textures (Stop 4, this volume). This dolomite may record the imprint of groundwater mixing.

In addition to the "cauliflower" textures noted above, cherts of several external forms (nodules of various forms, and thinly laminated beds) are present from the upper part of the McKenzie Hill Formation to the top of the group. Some of the silicification is fabric-selective (e.g., in burrows), some is not, and some of the chert is a cement rather than a replacement. In addition, some of the cherts in the McKenzie Hill Formation are recognizable as siliceous sponges.

PERMIAN RELATIONSHIPS

The Slick Hills are essentially Permian landforms which are being slowly exhumed. Lower Paleozoic strata down to and including the Carlton Rhyolite Group were deeply dissected in Permian times. The detritus produced by this dissection formed small alluvial aprons around individual hills. Where exposed at the surface, this pebbly alluvium is referred to as the Post Oak Conglomerate—strictly speaking, an informal stratigraphic usage (Bridges, 1985). Beneath the conglomerate veneer, a karst imprint is often apparent. This karst is dated by vertebrate faunas washed into small cave systems (Simpson, 1979). Cementation of the Post Oak was a complex process involving both vadose and phreatic calcite cements, and many sequences are punctuated by calcareous soil profiles (calcretes) (Donovan, 1982; Collins, 1985; Bridges, 1985). In places, these calcretes extend right up to individual limestone hills. The Post Oak conglomerates interfinger with and pass basinward into red-brown sandstones and shales (Hennessey Group).

ACKNOWLEDGMENTS

We are grateful for the field support provided by the Oklahoma Geological Survey and Sun Co. Our studies would have been impossible without the cooperation of many landowners, especially D. Kimbell, C. B. Oliver, D. Leatherbury, and W. Hodges. We are grateful to them for their support.

ANKERITE AT THE CONTACT BETWEEN THE REAGAN SANDSTONE AND THE HONEY CREEK LIMESTONE (TIMBERED HILLS GROUP)

Kelly Cloyd, R. Nowell Donovan, and Mary B. Rafalowski

INTRODUCTION

In the area of the Slick Hills of southwestern Oklahoma, the initial Late Cambrian (Franconian) transgression is recorded by the Reagan Sandstone. The Reagan is a siliciclastic unit notable for its content of iron, manifest as hematite cement (often an intense impregnation forming as much as 30% of the rock), ferruginous ooids, iron-rich illite, pyrite, and, most illustriously, glauconite. The upper part of the Reagan is characterized by sandstones which are composed of as much as 55% fine, sand-sized glauconite peloids. This iron-rich siliciclastic milieu gradually gave way to a carbonate factory of unusual efficiency and duration. The lowest carbonate unit is the Honey Creek Limestone, consisting of pelmatozoan-rich grainstones intermixed and interbedded with siliciclastics similar (iron-rich) to those found in the underlying Reagan.

In diagenetic terms, the formational boundary is an interface of some interest, marking the transition from iron–silica to iron–silica–carbonate cementation pathways. One aspect of this transition is that ferrous iron was incorporated into carbonate lattices during perigenesis. As a result, the formational contact is marked by a significant development of coarsely crystalline ankerite, which has replaced some of the original grains and early cement textures.

FIELD RELATIONSHIPS

The upper Reagan Sandstone is a peloidal, glauconitic, fine- to coarse-grained quartzitic sandstone with abundant phosphatic shell fragments (*Lingula* sp.) and rhyolite clasts. By contrast, the Honey Creek Limestone is a bioclastic limestone, consisting largely of pelmatozoan, trilobite, and brachiopod fragments, with lesser amounts of peloidal glauconite, rhyolite clasts, phosphatic brachiopods, and detrital quartz (Figs. 1,2). The ankerite zone lies between these lithologies and marks the first incoming of carbonate.

The ankerite zone is easily recognized by its characteristic orange color, which is due to oxidation of iron in the ankerite during surficial weathering. This zone is 2–15 ft (0.5–5 m) thick and is laterally persistent throughout the Slick Hills area over an exposed distance of 30 mi (48 km). The contacts of the ankerite zone with overlying and underlying units are sharp, but do not always coincide with bedding. The slightly discordant nature of the zone and its variation in thickness is probably due to permeability differences that existed when diagenetic fluid passed through this unit, forming the ankerite.

Although the ankerite is a replacement, primary sedimentary structures are still clearly visible in the Honey Creek; these structures are mostly medium-scale trough cross-beds, but also include parallel lamination and some small-scale cross-lamination.

PETROGRAPHY

Both primary and diagenetic components of the Timbered Hills Group vary systematically through the section (Fig. 2). Within the Timbered Hills Group, the ankerite zone marks the first incoming of carbonate on a previously siliciclastic shelf (Fig. 3).

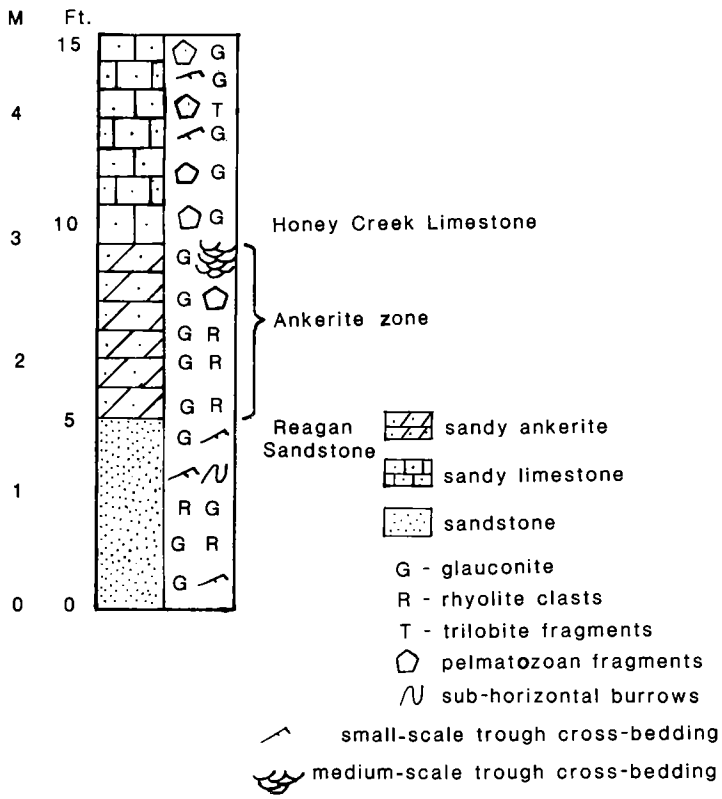

Figure 1. Stratigraphic log depicting the ankerite zone as it is developed on Bally Mountain.

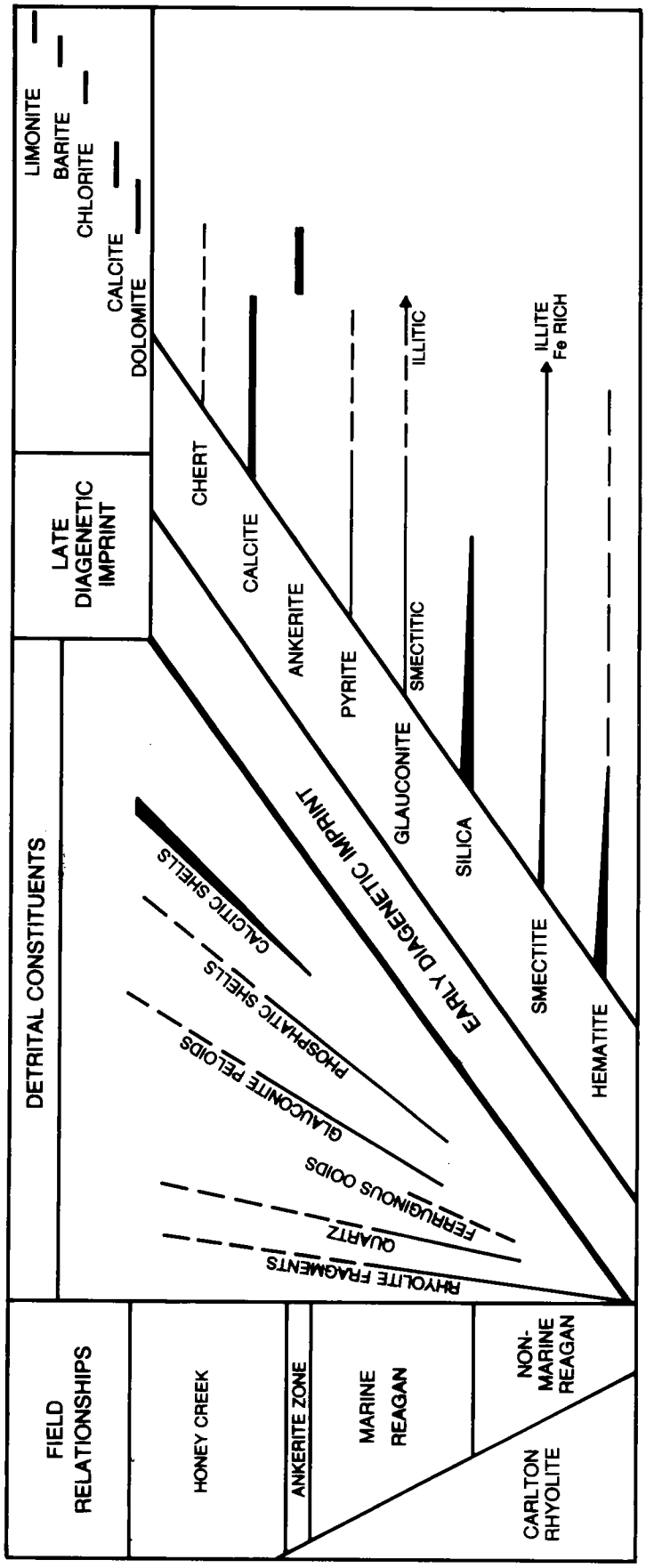

Figure 2. Generalized relationships in the Timbered Hills Group, showing complexity of field relationships, variety of detrital constituents, and early and late diagenetic imprints.

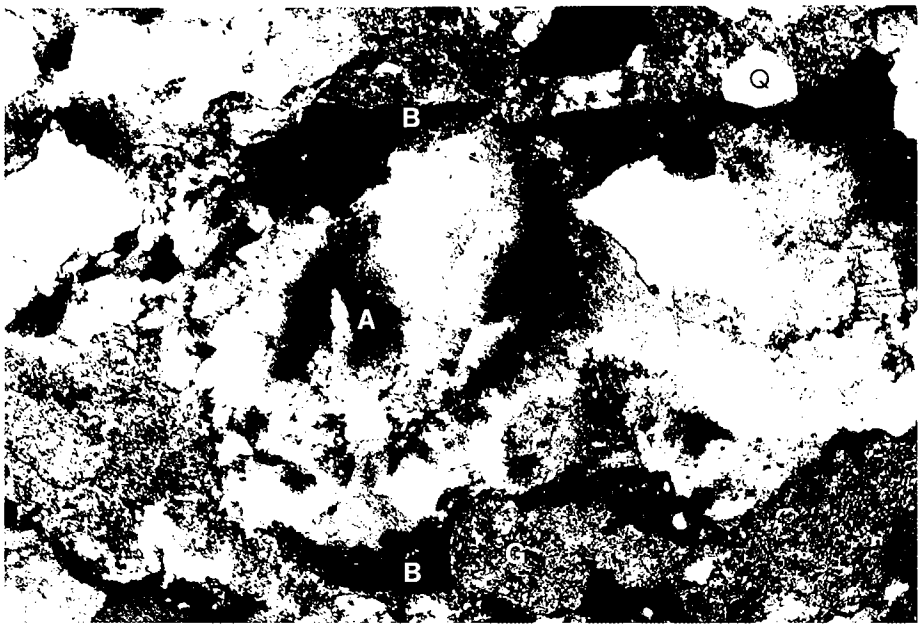

Figure 3. Photomicrograph showing typical occurrence of baroque ankerite with xenotopic-c texture (A). Also present are glauconite (G), phosphatic brachiopods (B), and quartz (Q). Cross-polarized light, 25×.

Ankerite of the lowermost Honey Creek Limestone exhibits idiotopic-e and -s (euhedral and subhedral) and xenotopic-c (cement) textures (nomenclature of Gregg and Sibley, 1984). The idiotopic ankerite is made up of large, euhedral to subhedral rhombs as much as 2 mm across. These rhombs have plane compromise boundaries and exhibit apparent pleochroism in plane-polarized light. Xenotopic-c ankerite is made up of large (as much as 3 mm in length) scimitar-shaped crystals characterized by strongly undulose extinction in cross-polarized light and apparent pleochroism in plane-polarized light. Both xenotopic and idiotopic ankerite can be seen replacing primary components (principally skeletal carbonate and glauconitic peloids). The replacement of glauconite was likely the source of iron for the formation of ankerite.

X-ray-diffraction data (Fig. 4) indicate that a nonferroan dolomite phase is a minor constituent of the ankerite zone. In thin section, this dolomite is a minor pore-filling cement with xenotopic-c textures.

WHAT WAS THE SOURCE OF IRON?

Iron has played an important role in the petrographic evolution of the Timbered Hills Group (Fig. 5). The ultimate source of this iron was the pre-Franconian land surface (Tsegay, 1983; Gilbert and Donovan, 1984). In the Slick Hills area, this surface was a weathered Carlton Rhyolite Group terrane forming hills as much as 300 ft (~90 m) high. The initial inundation of this terrane involved deposition of alluvium on low-lying ground. Subsequently, the entire terrane was blanketed by marine sediments; by Honey Creek time the old land surface was reduced to an archipelago of rocky rhyolite islands (Rafalowski, 1984; Gilbert and Dono-

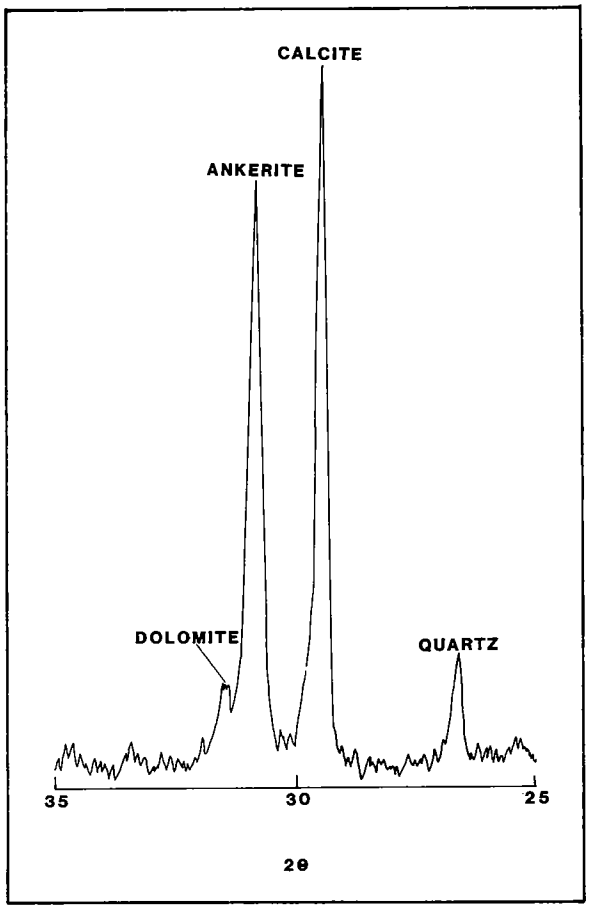

Figure 4. X-ray-diffraction spectrum of the carbonate fraction of the ankerite zone.

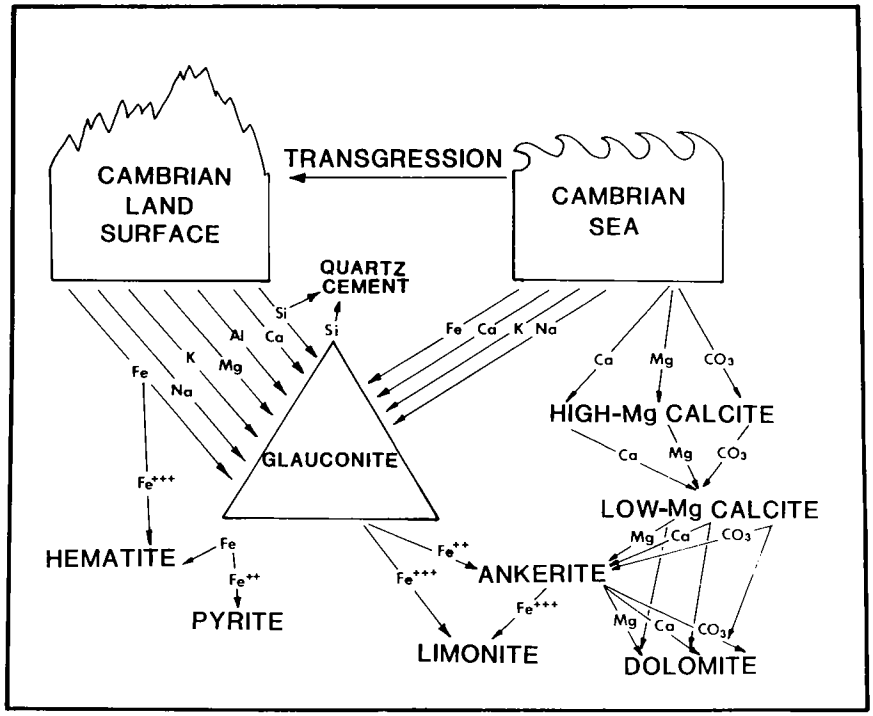

Figure 5. Suggested ion pathways which operated within the ankerite zone.

van, 1984). Within this geometrically complex scenario, iron found its way into a number of minerals (oxides, carbonates, silicates, and sulfides) in either of its oxidation states (Fig. 5). The quantitatively most significant of these minerals are hematite (as cement in the lower Reagan) and glauconite (mostly as peloids, but also as a replacement of rhyolite and as an infill of pelmatozoan pores).

ANKERITE DIAGENESIS

The ankerite of the Timbered Hills Group occurs at a transition from siliciclastic to carbonate sedimentation. This zone must have acted as a permeable conduit through which basinal fluids migrated. The fact that glauconite in these rocks is commonly replaced by ankerite indicates that iron was mobile (as Fe^{2+}). It follows that the solutions in which these reactions took place were reducing. The coarse crystal size and the baroque morphology of much of the ankerite suggests that these diagenetic solutions were relatively hot (~50°C) (Radke and Mathis, 1980; Gregg and Sibley, 1984).

Oklahoma Geological Survey Guidebook 24, 1986

AN ENVIRONMENTAL ANALYSIS OF THE LOWER ORDOVICIAN COOL CREEK FORMATION OF SOUTHWESTERN OKLAHOMA

Deborah A. Ragland and R. Nowell Donovan

INTRODUCTION

The Arbuckle Group as it is developed in the southern Oklahoma aulacogen is one of the world's great carbonate sequences, locally as much as 6,000 ft (1,800 m) thick. Lying athwart the Cambrian–Ordovician (Croixian–Canadian) boundary, the group is divided into six formations in the Wichita Mountains area, each of extraordinary thickness. Within the confines of the aulacogen, sediment-entrapment rates were relatively rapid: 220 ft (67 m)/m.y., as opposed to 48 ft (15 m)/m.y. on the adjacent craton (Donovan and others, 1983). Feinstein (1981) has suggested that this rate was not constant, but varied in response to aulacogen-margin fault movement.

The Cool Creek is fourth from the base among Arbuckle Group formations. It varies somewhat in thickness, but is usually >1,000 ft (300 m) thick. It is perhaps the most varied of the formations. The base is defined on a lithostratigraphic criterion: the first substantial incoming of quartz sand in the upper Arbuckle Group (Decker, 1939; Ham, 1956). This incoming is recorded by a distinctive sequence, the Thatcher Creek Member (Ragland and Donovan, 1985a). Significant faunal changes also mark the Thatcher Creek horizon (Stitt, 1983; R.L. Ethington, personal communication). The top of the formation usually is taken as the first incoming of the gastropod genus *Ceratopea*. This is an unsatisfactory field-mapping horizon, as we have pointed out elsewhere (Donovan and Ragland, this volume). Bed thickness is a little greater in the overlying Kindblade Formation, but in general homotaxial problems make this a difficult boundary to place.

General controls on the Cool Creek environment were a warm, arid to semiarid climate (in the southern hemisphere) and vast expanses of shallow epicontinental seas (St. John and Eby, 1978; Ragland and Donovan, 1985b). The "carbonate factory" (James, 1984) dominated the depositional system; siliciclastic input from the craton was quantitatively minor.

THE ESSENTIAL LITHOTYPES

Algal Boundstones

Algal boundstones are an important carbonate lithotype throughout the formation. The boundstones were classified by utilizing several of the well-established systems (Nelson and others, 1962; Logan and others, 1964; Hofmann, 1969; Wilson, 1975), with necessary modifications by the authors (Ragland and others, 1985). Four broad categories based on growth habits have been identified: encrusting algae, algal mat, algal mounds, and algal reefs (Fig. 1). Transitional forms link end members.

Encrusting algae initiated growth on any of several lithotypes, often a substratum with some minor relief. This crust either continued to grow as subparallel laminae for several millimeters or passed upward into other algal forms. Oncolites are rare in the formation, but some as long as 30 cm (long axis of an ellipsoid) have been identified.

Algal mats are composed of nearly flat to undulatory cryptalgal laminae. Wavelengths of the laminae undulations average 1 m, several times greater than the vertical extent of the mat. Most cross-profiles are smooth; some are crinkly.

Algal mounds and reefs contain the most-diverse forms of cryptalgae (Fig. 1). Mounds may consist of one large individual, a colony of smaller individuals, or several colonies grouped together. Reefs are composed of multiple colonies and individuals; they extend for considerable distances. Bioherms or miniherms may form the lateral termini of algal reefs. (An arbitrary limiting height established by the authors for a bioherm is 2 m; miniherms are defined to be <2 m.)

In the context used here, these reef ends terminate against some lithotype other than algal, usually mudstones or intraformational conglomerates. As an example, a bioherm located 100 m above the base of the formation in Blue Creek Canyon forms the end of an algal reef which can be traced laterally >1 km.

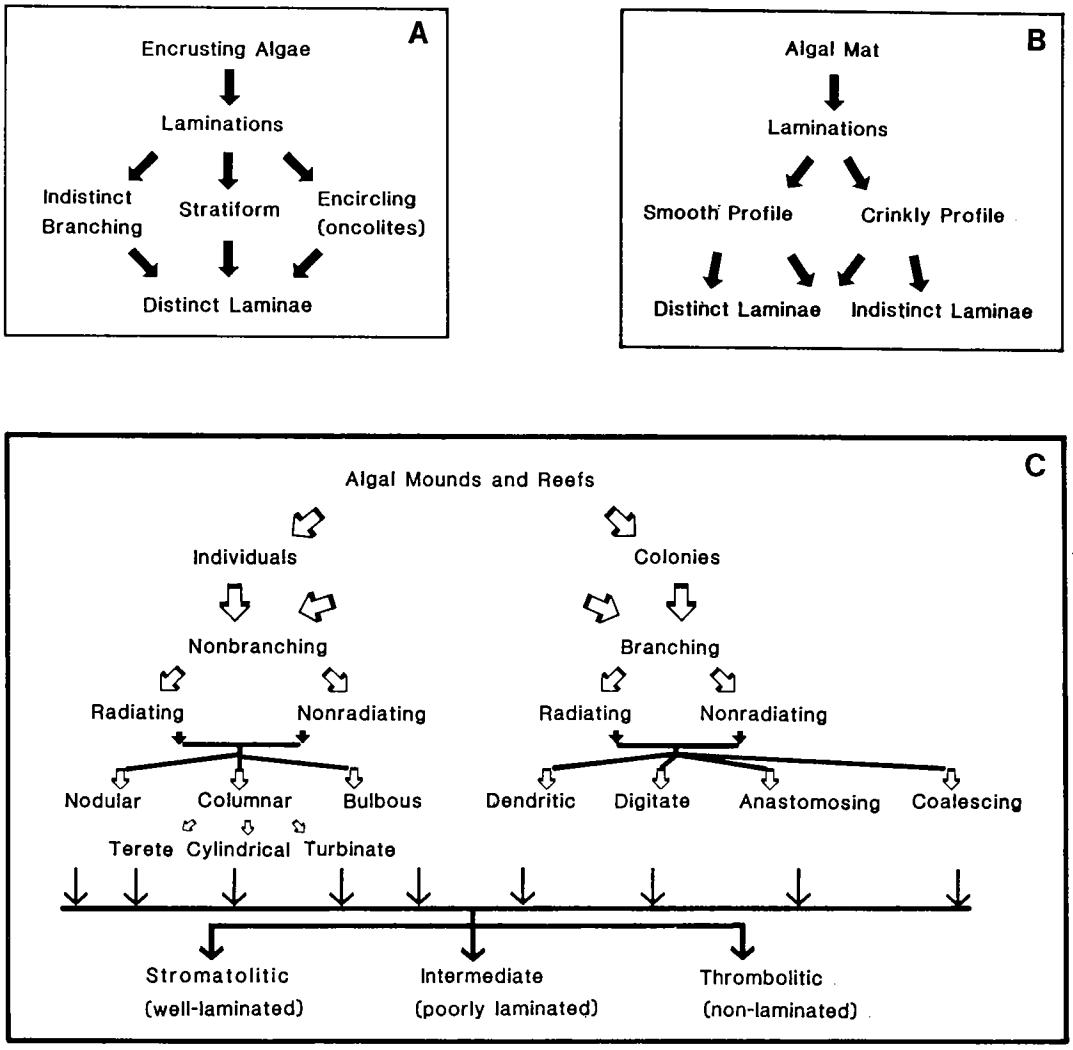

Figure 1. Typical cryptalgal morphologies of the boundstones found in the Cool Creek Formation. *A*, encrusting algae. *B*, algal mat. *C*, algal mounds and reefs. Note that the constituents of mounds and reefs are the most diverse.

The 6-m-high bioherm terminates abruptly against laminated mudstones and intraformational conglomerates, which show compactional draping around the end of the algal buildup (Fig. 2).

Typical constituents of the mounds and reefs in this formation—and indeed, the entire upper Arbuckle Group—are illustrated in Figure 3. Single columns are 12–200 mm in diameter, whereas branching forms are usually smaller (diameters <20 mm).

Internal textures of the algal members include well-laminated stromatolites, nonlaminated thrombolites, and all varieties intermediate between the two end members.

Intraformational Conglomerates

Intraformational conglomerates (IFCs), sometimes referred to as storm deposits or flat-pebble conglomerates, are found as discrete beds, as infill between individual algal members, and as channel fill. These deposits consist of elongate, disk- and blade-shaped pebbles as much as 15 cm in length, together with variable amounts of peloids, ooids, quartz sand and silt, and shell fragments. The detritus usually is embedded in a lime-mud matrix; occasionally, an open framework of pebbles (bafflestone) allowed later cementation by calcite spar.

Most clasts are micrite or quartz-sand micrite, but they can be composed of any lithotype present in the formation. The pebbles usually are packed with their long axes parallel to bedding, or in a random (mixed) fashion; less often, imbrication and vertical packing are seen.

Oolites

Ooids either form discrete beds or are found as admixtures with all other lithotypes. Discrete units often are cross-bedded (medium-scale, trough), and rarely display soft-sediment deformation structures, including overturned cross-bedding.

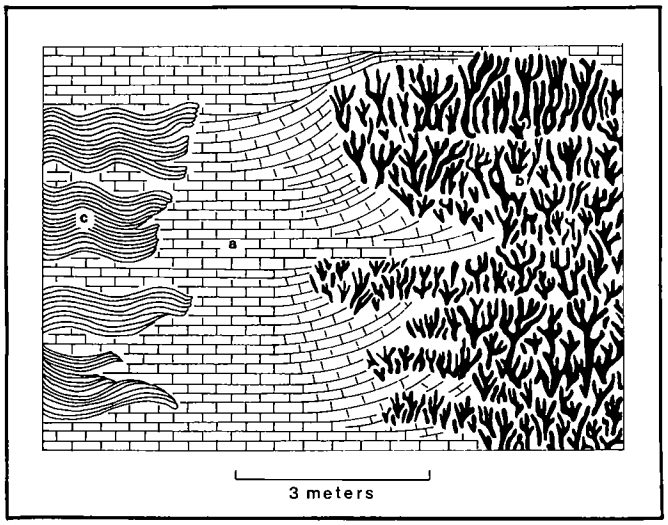

Figure 2. Compactional draping of laminated lime mudstones and intraformational conglomerates (a) against a bioherm (b); algal mat (c) interbedded with micrite and intraformational conglomerates.

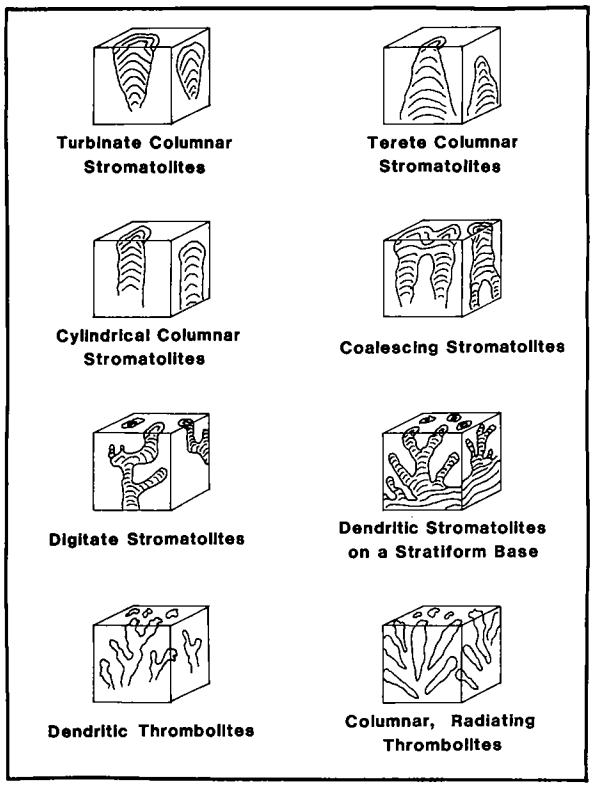

Figure 3. Stromatolite and thrombolite morphologies in mounds and reefs in the Cool Creek Formation. Terminology from Hofmann (1969).

Nuclei for the ooids consist of any available detritus found in the formation; both concentric and radial calcite cortices surround the nuclei. Composite and deformed ooids are found in minor percentages.

Micrite (Microcrystalline Limestone)

A spectrum of lime-mud-supported textures—from IFCs through packstones and wackestones to micrite—is found throughout the formation. The most common allochems are intraclasts of lime mud, with subordinate peloids, shell hash, and ooids. Lime-mud beds are either massive or laminated (both horizontal lamination and small-scale trough cross-lamination are developed). The lamination is highlighted by quartz silt in many cases. Pink coloration in some mud strata is due to finely disseminated hematite. Bedding may be disrupted by bioturbation, subaerial mudcracks, and incomplete (subaqueous) shrinkage cracks.

Quartz-Rich Sandstones

As noted earlier, the base of the formation is defined by the first substantial appearance of detrital quartz sand. Units similar to the Thatcher Creek Member are found higher in the formation and throughout the Kindblade and West Spring Creek Formations. These units often are cross-bedded (medium-scale, trough), and linguloid and symmetrical ripple marks are seen on bedding planes in a few locations. The quartz detritus is generally medium-grained, although small fining-upward and coarsening-upward sequences show a range in grain size from coarse sand to fine sand and silt. Syntaxial overgrowths are well developed in some sandstones, while evidence of intense corrosion is seen in others.

Chert

The majority of the chert is secondary (replacement or cement). A few areally limited units of interlaminated dark-gray primary chert and medium-gray calcite (with minor dolomite) have been identified.

Secondary chert nodules of widely varying sizes (<1 cm to >30 cm) may be randomly dispersed or, more commonly, concentrated along bedding planes. In places they are so abundant that they coalesce, forming anastomosing networks. The nodules usually are formed of replacement chert with minor amounts of silica cement. Both "flinty" and translucent chert (white, pink, or gray) can be identified megascopically.

All primary lithotypes have been subject to silicification, dependent on three main parameters: availability of silica, ground-water chemistry, and ground-water circulation. No siliceous biota such as sponges are found in the formation (although they are present in the underlying McKenzie Hill Formation), thus leaving only the abundant quartz sand as the silica source (St. John and Eby, 1978; Ragland, 1984). In most cases, replacement is partial, presum-

ably because favorable conditions rarely persisted long enough to completely silicify great masses of rock.

Most, if not all, of the silica replacement and cementation occurred very early in the diagenetic history of the formation—some even penecontemporaneously. Evidence supporting an early silicification includes the distortion of semi-lithified micrite laminae by nodule growth, entrapment of evaporite minerals (anhydrite, gypsum, celestite; Ragland, 1984), and redeposition of silica nodules in IFCs.

Dolomite

At least three types of dolomite have been recognized: penecontemporaneous (sabkha?) dolomite, early replacement dolomite, and late replacement and vug-filling dolomite (Cloyd and others, this volume). Some penecontemporaneous dolomites are found in local patches that do not persist either laterally or vertically. "Cauliflower" chert nodules (terminology of Chowns and Elkins, 1974) containing evaporite traces suggest a linkage of these dolomites to hot, arid conditions.

Early idiotopic dolomites are seen on outcrop as buff to orange irregular patches ("leopard-skin texture," Stop 4, this volume). Ground-water circulation of magnesium-rich fluids selectively dolomitized more-permeable zones (e.g., burrows).

During later diagenesis (post-burial?), magnesium-rich fluids percolated through the formation, gradually dolomitizing all lithotypes in a nonselective manner. These dark-gray-brown, vuggy dolomites are enigmatic. Small dolomitized zones extending a few meters laterally and vertically are found in Blue Creek Canyon in association with folds, and on Bally Mountain in association with faults, perhaps indicating that a tectonic parameter may be partly responsible for the dolomitization.

Vugs in all dolomitic lithotypes are often completely or partially filled with large (as much as 3 mm) baroque crystals. This last infill is presumed to have been relatively late (at least post-Pennsylvanian-deformation) and may have been caused by the upward migration of warm fluids from deeply buried sediments.

AN ENVIRONMENTAL SYNOPSIS

A Cautionary Note

Interpretation of past environments relies heavily on the Principle of Uniformitarianism; this becomes less useful farther back in time. Not only was the area that is now southwestern Oklahoma located in an arid, tropical climate (~25° S. lat; Habicht, 1979), but the chemical balance in the atmosphere and seas was far different from present conditions (Windley, 1977). Taking these factors into account, we hypothesize environmental conditions that may have existed 500 m.y. ago, when the formation was being deposited.

Justification for Environmental Assignment

Algal boundstones and their associated sediments and structures have been utilized as the primary indicators of the paleoenvironmental conditions that existed during early Canadian time in Oklahoma. By comparison with modern algal depositional settings (Gebelein, 1969; Shinn, 1983), we have used the differing internal and external morphologies to define paleoenvironments. From these data, maximum sea-level change during Cool Creek times was determined to encompass the supratidal zone to the upper subtidal zone (Table 1). We have been cautious in this interpretation, recognizing that on the immense Ordovician carbonate platform tidal energy likely has significantly damped. Nevertheless, the sequencing and arrangement of the various lithologies is compatible with modern analogs.

TABLE 1.—RELATIONSHIP OF ALGAL BOUNDSTONES TO VARIOUS PHYSICAL AND CHEMICAL PARAMETERS

Algal type	Depth of water	Water turbulence	Clastic input/ chemical PPT	Biological activity
Algal mat				
Smooth profile	Supratidal	Gentle overwash, aperiodic	Minor	Very minor
Crinkly profile	Supratidal	Gentle overwash	Minor; possible evaporites	None
Algal mound/reef/bioherm				
Stromatolitic	Intertidal	Moderate	Minor to moderate	Moderate
Intermediate	Lowest intertidal–upper subtidal	Moderate	Minor	Moderate
Thrombolitic	Subtidal	Moderate	Aperiodic	Moderate

Supratidal Zone

The modern semiarid supratidal zone is characterized by carbonate mud flats (often with subaerial mud cracks), evaporite minerals, and algal mat. Such a facies is developed in the Cool Creek. Jaanusson (1984) has speculated that, during the Ordovician, lack of continental relief caused detrital input to be infrequent and that only aperiodic overwashes and spray moistened the tidal flats.

Dolomitic sabkha sequences similar to those found in the Persian Gulf (Bathurst, 1975) formed in areas of the supratidal flats where there was sufficient input of magnesium to raise the Mg^{2+}/Ca^{2+} ratio high enough to overcome the Mg^{2+} barrier (with respect to the formation of dolomite). These areas were not necessarily conjunct to dry land; the geometry of some of the dolomite suggests that the areas formed as isolated patches elevated slightly above the level of the surrounding seas (perhaps following a slight fall in sea level). In some sequences, quartz-rich, sandy dolomites alternate with pseudomorphed anhydrite-gypsum layers and nodules (Ragland, 1984). Although penecontemporaneous dolomitization destroyed most original textures, some evaporite pseudomorphs and relict laths were preserved by early silicification.

When sufficient magnesium was not available, evaporites formed in calcium carbonate mud. As recorded in some sequences, drying of the sediment and evaporation of pore waters caused sulfates to grow in the carbonate layers on top of and, in some cases, below algal mat, causing the otherwise-smooth mat profile to be distorted. This "crinkly" profile has been observed in recent sabkha sediments in Abu Dhabi (Butler and others, 1983).

Intertidal Zone

The modern intertidal zone is a far more varied environment than the supratidal zone. In the Cool Creek Formation, the vast majority of the preserved sediments represent this shallow-water environment between high and low water level; a wide variety of lithotypes is developed.

Algal Boundstones in the Intertidal Zone

The gradual transition from the supratidal flat to the intertidal zone is marked by the change from smooth, continuous algal mats with little internal structure to boundstones with progressively more complex external and internal features. LLH-C (laterally linked hemispheroids—close; Logan and others, 1964) mounds formed as tidal waters established small channels on the algal surface, but water velocity was not so great as to disconnect the mounds (Fig. 4). Doming probably was enhanced by irregularities on the initial surfaces and by gas bubbles caused by algal decomposition and respiration. Upper-intertidal flats in bays and behind barrier bars may have provided the best environments for these mounds. Slightly more-turbulent water along open marine fronts led to development of the LLH-S (laterally linked hemispheroids—spaced; Logan and others, 1964) mound morphology (Fig. 4).

Discrete mounds (SH-V and SH-C of Logan and others) probably formed in the middle-intertidal zone. Occasionally the mounds were composed of a single large stromatolite, but more often they were aggregations of smaller, branching stromatolites separated by detritus.

The paleomorphology of what may have been a typical intertidal flat is provided by 25 algal mounds exposed 3 mi (5 km) west of Blue Creek Canyon in the Slick Hills (Fig. 5). The nearly horizontal attitude of the beds has allowed erosion of the intermound sediments, with resulting exhumation of the mounds. The mounds were measured and their eccentricities calculated in order to determine if channeling (i.e., tidal or wave current flow) could have had some effect on their shape (Table 2). The greater the eccentricity (e approaches 1), the more elliptical the mound and presumably the greater the probability that channeling had some effect on shaping the mounds. The eccentricities are > 0.5 in 72% of the mounds, indicating that channeling probably was a relatively important process in their formation. The orientation of the long axes indicates the probable direction of flow in the channels (approximately N–S).

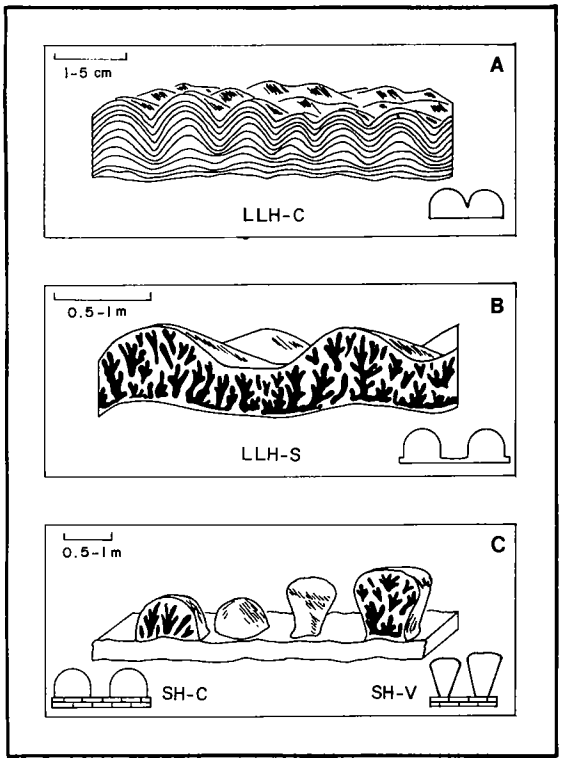

Figure 4. Algal-mound morphologies typical of the Cool Creek Formation (terminology from Logan and others, 1964). *A*, laterally linked hemispheroids—close (LLH-C). *B*, laterally linked hemispheroids—spaced (LLH-S). *C*, stacked hemispheroids—constant radius (SH-C) and stacked hemispheroids—variable radius (SH-V). Note that the stacked hemispheroids are not connected by algal growth.

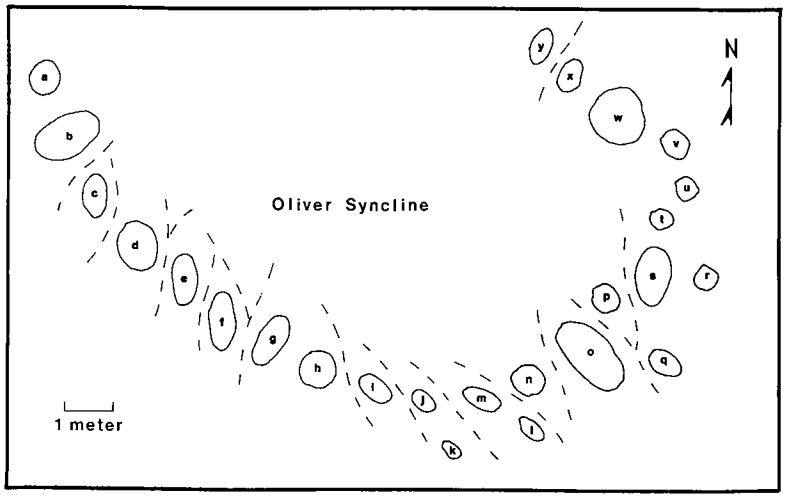

Figure 5. Diagrammatic plan view of algal mounds outcropping 3 mi (5 km) west of Blue Creek Canyon (sec. 10, T4N, R13W). Dashed lines represent possible tidal channels.

Algal reefs were formed in quiet areas where current flow was not great (e.g., intertidal and subtidal zones where the sea-floor gradient was very low). We speculate that continuous "forests" of columnar and branching algae formed laterally persistent, rigid framework structures on the sea floor (Cloud *in* Nelson and others, 1962; Pratt and James, 1982). Gently pulsing sheets of water caused branching and separation between individuals, but major channels rarely occurred, thus prohibiting the formation of mounds. Of course, reefs did not extend laterally indefinitely, but were terminated by major channels, entrances to embayments, and more-turbulent waters around headlands.

Intraformational Conglomerates in the Intertidal Zone

Intraformational conglomerates imply disturbances in the shallow water of the intertidal zone which ripped up clasts from partially lithified preexisting lithologies. IFCs are associated with all other primary lithotypes in the formation, probably because they could result from at least six processes. These six processes, summarized in Table 3, are (1) transgressions, (2) regressions, (3) storms, (4) tides, (5) channeling, and (6) waves (Ragland and Donovan, 1985b).

Transgressions, regressions, and major storms are the processes that were most likely to have resulted in the formation of discrete, areally extensive IFC beds. In such beds, clast lithologies are heterogeneous, including all types of micrite lithologies, algal fragments, chert pebbles, quartz sand, and minor amounts of fossil fragments, ooids, and peloids. Assuming that the carbonate platform was of low relief (Jaanussen, 1984), transgressions would have covered vast areas and consequently eroded many lithologies. The relatively long period of time associated with transgressions would have led to constant reworking and rounding of clasts. The fabric most likely to have resulted would have been a flat-packed arrangement due to gentle washing and reworking. Such IFC would have formed in the intertidal to upper-subtidal zones and eventually would have been buried under lime mud as the transgression continued. IFCs interpreted as transgressive deposits contain large clasts (as large as 5 cm); quartz sand

TABLE 2.—ECCENTRICITY CALCULATIONS FOR ALGAL MOUNDS

Mound*	$2a_1$	$2b_1$	a_1	b_1	$(a_1^2 - b_1^2)^{1/2} = c_1$	$c_1/a_1 = e$
a	24	20	12.0	10.0	6.63	0.5525
b	35	25	17.5	12.5	12.25	0.7000
c	25	16	12.5	8.0	9.60	0.7680
d	28	23	14.0	11.5	7.98	0.5700
e	27	17	13.5	8.5	10.49	0.7770
f	31	17	15.5	8.5	12.96	0.8361
g	30	16	15.0	8.0	12.69	0.8460
h	20	20	10.0	10.0	0.0	0.0
i	21	14	10.5	7.0	7.83	0.7457
j	15	12	7.5	6.0	4.50	0.6000
k	13	11	6.5	5.5	3.46	0.5323
l	16	11	8.0	5.5	5.81	0.7263
m	20	12	10.0	6.0	8.00	0.8000
n	14	14	7.0	7.0	0.0	0.0
o	40	24	20.0	12.0	16.00	0.8000
p	18	13	9.0	6.5	6.22	0.6911
q	17	14	8.5	7.0	4.82	0.5671
r	13	13	6.5	6.5	0.0	0.0
s	30	23	15.0	11.5	9.63	0.6420
t	13	11	6.5	5.5	3.46	0.5323
u	14	14	7.0	7.0	0.0	0.0
v	15	15	7.5	7.5	0.0	0.0
w	30	30	15.0	15.0	0.0	0.0
x	19	17	9.5	8.5	4.24	0.4463
y	18	14	9.0	7.0	5.66	0.6289

Location of mounds: 3 mi west of Blue Creek Canyon (sec. 10, T4N, R13W).
*See Figure 5.
a_1 = semi-major axis, measured in inches.
b_1 = semi-minor axis, measured in inches.
c_1 = half-distance between foci, measured in inches.
e = eccentricity, where $e = 0$ is a circle, $e = 1$ is a straight line.

TABLE 3.—INTRAFORMATIONAL CLASTS: A SUGGESTED GENETIC CLASSIFICATION

Process	Packing arrangement	Zone	Turbulence	Clastic input
Transgression/ regression	Flat-lying, vertical, imbricate, or random	Intertidal to lower subtidal	Low to moderate	High
Storms	Random	Supratidal to subtidal	High	Low to moderate
Tides	Flat-lying, random, imbricate	Intertidal	Moderate	Low
Channeling	Imbricate, flat-lying	Supratidal to subtidal	Moderate	Low to moderate
Waves	Vertical, flat-lying	Intertidal	Moderate	Low

is a common accessory particle. The abundance of quartz detritus reflects both the length of the transgressions and the increasing proximity to the presumed source area (landward). Inferred transgressive IFC beds are thicker than IFC beds formed by other processes.

Theoretically, regressive IFC would be expected to be thinner than transgressive IFCs, and as the seas receded they would have been subjected to other processes which altered their initial character. Although the clasts may have been as varied as those in transgressive IFC beds, regressive IFCs were exposed to very shallow-water and subaerial processes (e.g., desiccation). Erosion could have destroyed many of the clasts, removing them entirely from the record. record.

Major storms (equivalent to hurricanes or typhoons) could also have formed discrete layers of IFC clasts. Beds attributed to this mechanism are only a few centimeters thick, because storms are of much shorter duration than transgressions or regressions. Because of the limited time involved, the clast composition reflects only the lithotype sources which were locally available. Clasts are moderately rounded, but very poorly sorted and randomly packed, due to the short, but violent nature of the generating process. Most storm-generated IFCs have a high percentage of mud matrix, because the deposits were not cleanly worked over a relatively long period of time. This suggests that at least some IFCs may have been deposited below effective fair-weather wave base. It is pertinent to note that powerful storms could have produced IFCs in the subtidal zone.

Minor storms (equivalent to daily thunderstorms) probably produced thin layers of IFCs which draped over preexisting lithologies in a manner similar to that occurring in the intertidal areas of most modern algal environments (Logan, 1961; Logan and others, 1964; Shinn, 1983). Clasts inferred to have generated in this manner consist of local material and are randomly packed and poorly sorted. Accessory particles such as detrital quartz and ooids are uncommon. Lime-mud matrix forms a large part of the lithology, as it does in major-storm deposits.

The repetitive short-term processes of tides, channeling, and waves probably account for the majority of the IFCs seen in the Cool Creek Formation. These beds are neither laterally extensive nor >0.3 m thick. The movement of tides across the intertidal zone presumably picked up and redeposited pieces of lithologies that had dried and loosened during low-tide exposure. Tidal channels may have transported the clasts away from the immediate source area, but many clasts probably were deposited very close to their sources.

Packing arrangements due to the several processes resulted in random, imbricate, or flat-lying patterns, depending on supply, current velocity, and clast shape. Many clasts were deposited between algal structures, although a small percentage became trapped in the algal laminae.

An unusual form of clast arrangement is one in which flat clasts are packed into vertical or fan-shaped stacks (Ragland and Donovan, 1985b). Such arrangements are produced on modern beaches by waves of moderate energy (Sanderson and Donovan, 1974). Vertical arrangements are relatively stable and act as mechanical bafflestones, trapping mud and smaller particles. In the present context, they are an indication of reworking of clasts produced by other processes.

Oolites in the Intertidal Zone

Ooid-bearing beds are common throughout the formation. Oolitic grainstones are the most conspicuous of these deposits; they display ubiquitous cross-bedding, attesting to their probable mode of formation as mobile sand shoals in agitated shallow water. Two distinct textures are present in the ooids; cortices may be either tangential or radial, or both. If uniformitarian analogy holds, then the tangential ooids grew in high-energy environments (beaches and shoals), while the radial ooids formed in more-sheltered settings (Suess and Fulterer, 1972; Davies and others, 1978).

Lime Mud Deposits in the Intertidal Zone

It is a reasonable expectation that ephemeral ponds and lagoons, fed by intermittent streams and marine overwash, existed in shallow depressions on the high-intertidal flats, as they do today. Changes in water chemistry determined the composition of the sediment and, in some cases, created sedimentary structures. The sediment most often deposited was

calcium carbonate, with a minor admixture of quartz sand and silt. Seasonal changes and minor compositional changes may have led to the formation of laminated micrite sequences. Drying-up of ponds caused the formation of mudcracks, while changes in the salinity of the water led to formation of subaqueous shrinkage cracks (Donovan and Foster, 1972). Stacked layers of subaqueous shrinkage cracks indicate seasonal changes, as the "rainy" season (normal micrite deposition) alternated with the "dry" season (increased salinity of the brine and subsequent cracking of the carbonate mud).

In the deeper parts of the intertidal zone, lime mud formed the binding sediment matrix in poorly washed sediments. Also, minor relief on lime mud created topographic high points where encrusting algae could initiate growth; subsequently, chemically precipitated or recycled calcium carbonate constituted the non-organic layer in stromatolitic couplets.

Although the fossil content of the formation is sparse, and preserved body fossils are relatively rare, bioturbation and peloids (probably fecal pellets) are abundant in some units. Fossil fragments recognized in hand sample and thin section include gastropods (*Lecanospira*), brachiopods (*Diaphelasma*), trilobites, and echinoids (Ham, 1956).

Subtidal Zone

Within the subtidal zone, the imprint of storm becomes more pronounced, and the concept of "fair-weather wave base" is important in determining the degree of sorting to which sediments were subjected. Additionally, sedimentation processes operate in a more uniform manner than they do in the "swish-swash" of the intertidal zone.

Algal Boundstones in the Subtidal Zone

In increasingly deeper and more-permanent water cover, the diurnal lamination characteristic of stromatolites is gradually suppressed, leading to sequential development of thrombolitic stromatolites, stromatolitic thrombolites, and ultimately thrombolites (Aitken, 1967), which are the diagnostic boundstones of the subtidal facies. Thrombolites are recognized by their lack of internal laminae and by the clotted appearance of their colonies (Pratt and James, 1982). These colonies and their individual members generally are smaller than stromatolitic buildups; mounds and reefs usually are <1 m in height, and individuals almost always are <12 mm in diameter. In cross profile, thrombolite buildups often display a distinctive "sunburst" morphology produced by radiating, columnar individuals. If, as Hofmann (1969) suggested, branching can be attributed (Fig. 3) to accumulations of unbound detritus terminating vertical growth at certain points, then the minor amounts of detritus in the subtidal zone would have been conducive to single-axis structures. Once a colony was established, the individuals would have been able to continue upward growth unimpeded, except for lateral interference by adjacent colonies.

General Character of Subtidal Sediments

In general, subtidal sediments interbedded with thrombolites are of more-modest grain size than those found in the intertidal zone. Thus, quartz is found as silt-sized grains, and IFC clasts rarely are >5 mm across. Peloids (probably fecal pellets) appear to be more abundant in the subtidal zone, perhaps because of a larger invertebrate community (Pratt and James, 1982), or because they were not as quickly reworked and hence were preserved.

Laminated micrites formed sequences as much as 2 m thick in quiet areas of this zone. With the exception of parallel laminations and some bioturbation, sedimentary structures are almost nonexistent in such beds.

Introduction of Quartz into the Cool Creek Formation

The base of the Cool Creek Formation is defined by the first significant incoming of quartz sand, indicating that a mechanism existed that was capable of moving sand- and silt-sized grains from a source on land into the shallow-marine environment. Although the source for the quartz sand is not known, we hypothesize that cratonic regions of low relief may have existed to the north of Oklahoma. From this area, meandering rivers may have moved large quantities of terrigenous detritus, eventually depositing their loads in the vast tidal flats of the Early Ordovician seas. Some areal variability in this deposition did occur, as illustrated by the differences in lithology between the predominantly carbonate Cool Creek Formation and the quartz-rich Roubidoux Formation of northeastern Oklahoma and Missouri (McCracken, 1955).

In the area that is now southwestern Oklahoma, deposition of quartz-carbonate sand sheets as much as 2 m thick occurred on tidal flats or in channels meandering across the flats.

Once transported from the source area to the site of deposition, the quartz sands were subjected to reworking by local processes. Presumably tides and waves sorted the grains. Clearly, some grains falling into agitated waters became the nuclei of ooids, while others were washed into cross-bedded sand shoals. Distally, away from the shore, the overall size of the sand grains decreased and the fine sands and silts were either incorporated into lime muds or trapped in algal laminae. We speculate that this quartz, once it had arrived on the platform, was moved slowly from the margin of the platform by progradation of the platform sequence. Although difficult to quantify, there appears to be a cryptic coarsening-upward motif in quartz grain size, which culminates in each occurrence of "Thatcher" (i.e., upper-intertidal) facies. Thus, while the cratonic source of quartz may or may not have debouched sediment at a constant rate, processes operating on the platform itself were responsible for concentrating the quartz in particular facies.

ACKNOWLEDGMENTS

We are grateful to the Oklahoma Geological Survey, Sohio, and Sun Co. for the support of our field studies.

Oklahoma Geological Survey Guidebook 24, 1986

DOLOMITE WITH EVAPORITIC CONNECTIONS IN THE ORDOVICIAN COOL CREEK FORMATION, SOUTHWESTERN OKLAHOMA

Kelly Cloyd, Deborah A. Ragland, Lois Jones, and R. Nowell Donovan

INTRODUCTION

On the basis of field criteria, several types of dolomite can be recognized in the Cambrian–Ordovician Arbuckle Group (Ragland, 1983; Donovan and Ragland, this volume):

1) Fine-grained, stratabound dolomites associated with "cauliflower" chert and containing evidence of an evaporite association;
2) Fine-grained, stratabound dolomites occurring as incompletely altered, patchy mosaics ("leopard-skin" texture), with no apparent evaporite relationship;
3) Thick (>100 ft, or 30 m), stratabound, coarse-grained dolomites which have various degrees of intracrystalline porosity;
4) Irregular, discordant dolomites which are coarse-grained and baroque and appear to have a "parasitic" relationship with types 1–3 (i.e., in the field they are always intimately related to a stratabound occurrence);
5) Fracture-related, coarse-grained, baroque dolomites;
6) Minor late vug-filling cements.

To some extent, grain size in types 1–3 is dependent on the original grain size of the replaced limestone (in many cases, enough "ghosts" of the primary textures are visible to justify this conclusion).

In this paper, we describe occurrences of type 1 dolomite which are cut by types 4 and 5. The dolomite is in the upper part of the Cool Creek Formation on Bally Mountain (Stop 2, this volume).

FIELD RELATIONSHIPS

Dolomite of the upper Cool Creek Formation on Bally Mountain is in a sequence that is made up of 3- to 20-ft-thick (1- to 6-m-thick), shallowing-upward cycles (Fig. 1). These cycles comprise a basal oolitic or intraclastic grainstone and an overlying stromatolitic or thrombolitic boundstone (Fig. 2). This unit in turn is overlain by massive mudstones which grade upward into laminated mudstones. The latter typically display fenestral fabrics and are mud-cracked in the uppermost parts. Mud-cracked laminites are generally overlain by massive or laminated dolomitic mudstones (type 1) containing white colloform ("cauliflower") chert nodules that are interpreted as having replaced anhydrite. This anhydrite formed by displacive growth within the sediment, prior to compaction, since laminations are compacted around the nodules.

The fine-grained dolomite is present as either massive or finely laminated mudstones. Rarely, fine-grained dolomite is seen to have replaced intraclastic grainstones or packstones (in which case, dolomite grain size varies somewhat in response to primary textural variation). Fine-grained dolomite has also been observed in the form of cement between grains in calcitic grainstones.

Coarse-grained dolomites in the Cool Creek include those that are clearly associated with fractures and those that are not. Those that are associated with fractures (type 5) may occur as passive fracture fills, or they may replace either fine-grained dolomite or limestone adjacent to the fracture.

Irregularly shaped, discordant masses of coarse-grained dolomite (type 4) are common in the Cool Creek of Bally Mountain and elsewhere in the Slick Hills. These masses cut across bedding and replace both limestone and (syndepositional) fine-grained dolomite, obliterating all trace of previous textures (Fig. 3). Commonly, these irregular masses have no apparent relationship to fractures. This does not necessarily preclude the possibility that these coarse-grained masses may have formed through the movement of late-diagenetic fluids along fractures. These fractures, if they were present, may have been obliterated along with the sedimentary structures. Indeed, in a few cases the boundaries of the masses do follow joints trending N. 60° E. for short distances.

Coarse-grained dolomite cements in chert nodules and between grains (type 6) clearly are not directly related to fluid migration along fractures.

PETROGRAPHY

The dolomites can be divided into two petrographic types: (1) fine-grained, idiotopic dolomites, and (2) coarse-grained, xenotopic dolomites (nomenclature of Gregg and Sibley, 1984).

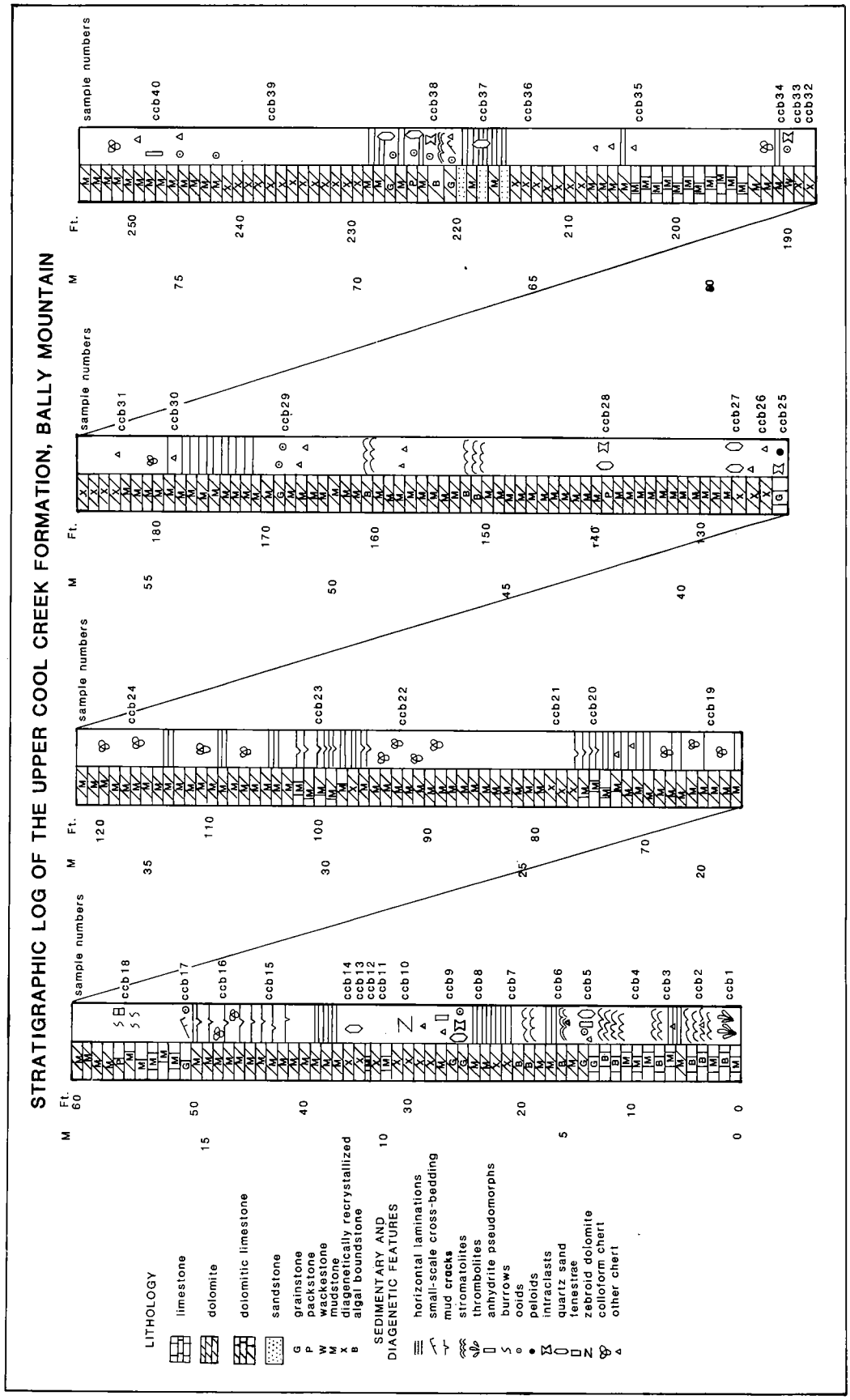

Figure 1. Stratigraphic log of part of the Cool Creek Formation on Bally Mountain.

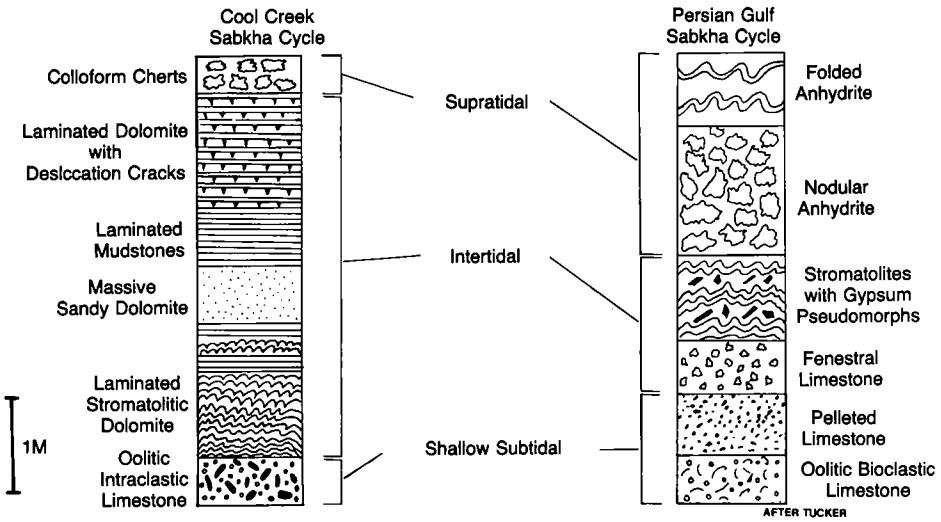

Figure 2. Comparison of a Cool Creek cycle with a Persian Gulf sabkha cycle.

Common textures observed in the fine-grained dolomite include idiotopic-c and -e. Dolomite exhibiting idiotopic-c textures occurs in a variety of relationships, most commonly in the form of equant void fillings in oolitic and intraclastic packstones. These void fillings consist of euhedral or subhedral rhombs 0.25–0.5 mm across. Idiotopic-dolomite cements also fill fenestrae in mudstones.

Idiotopic-e (euhedral) dolomite makes up considerable amounts of the upper Cool Creek Formation on Bally Mountain. This dolomite generally occurs as laminae several millimeters to 1 cm thick which are made up of small, euhedral rhombs (30–60 microns across). These layers may make up entire beds several tens of centimeters thick, or they may alternate with calcitic mudstones (Fig. 4).

Colloform chert nodules are intimately associated with the fine-grained dolomites. Within these nodules, a characteristic stratigraphy exists (Fig. 5). The outermost layer of a nodule consists of length-slow chalcedony which rests on randomly oriented, euhedral rhombs of idiotopic dolomite. The next layer inward is made up of baroque (xenotopic-c) dolomite. The innermost component is either open space or a coarse, blocky mosaic of equant calcite. In some samples, the boundary between chalcedony and baroque dolomite contains lath-shaped pseudomorphs (after anhydrite). The chert layer contains numerous small, lath-shaped anhydrite inclusions. More rarely, chert may pseudomorph what appear to be tiny gypsum and anhydrite crystals (Fig. 6).

Commonly associated with zones containing chert nodules are calcitized dolomite rhombs (dedolomite) in small amounts. Generally the outer rims of these rhombs have been replaced by fine-grained calcite mosaics, while their cores are irregularly shaped, single crystals (relics) of dolomite.

In addition to its occurrence within chert nodules, coarse-grained, xenotopic dolomite forms fracture fillings and irregular masses, and less commonly fills voids in grainstones. Fracture fillings (type 5) and void fillings (type 6) are made up of crystals exhibiting typical xenotopic-c (baroque) textures. The crystals are as much as 3 mm in length and have characteristic scimitar shapes. Undulose extinction in cross-polarized light is typical. Coarse-grained dolomites making up irregular masses (type 4) have slightly different textures, ranging from xenotopic-c to idiotopic-s. These crystals have slightly to strongly undulose extinction and slightly curved crystal boundaries (Fig. 7).

CARBON AND OXYGEN ISOTOPES

The Cool Creek carbonates (both limestones and dolomites) yield carbon isotopic ratios that are within the general range of those of modern marine carbonates (Fig. 8). The $\delta^{13}C$ values for the analyzed limestones are slightly heavier than those for the dolomites (-1.6 to -1.9 vs. -2.1 to -2.8 $\delta^{13}C$ PDB, ‰). The slight lightening effect in the dolomites might be due to meteoric influence, or it may be a result of oxidation of hydrocarbons. In either case, the lightening of the carbon isotopes has been very slight, probably because carbon in carbonates is strongly resistant to isotopic change.

Unlike the carbon isotopic composition, the oxygen isotopic composition of the Cool Creek carbonates deviates considerably from the values of modern marine carbonates, with $\delta^{18}O$ PDB (‰) values from -6.4 to -10.1 (Fig. 8). These unusually low negative values may be due to a combination of meteoric effects and recrystallization at elevated temperatures after burial.

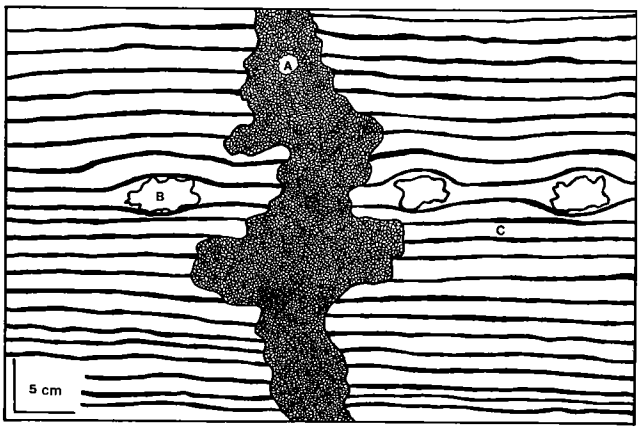

Figure 3. Generalized field relationships between dolomites: coarse-grained, xenotopic dolomites (A); colloform chert nodules (B); fine-grained, laminated, idiotopic dolomite (C).

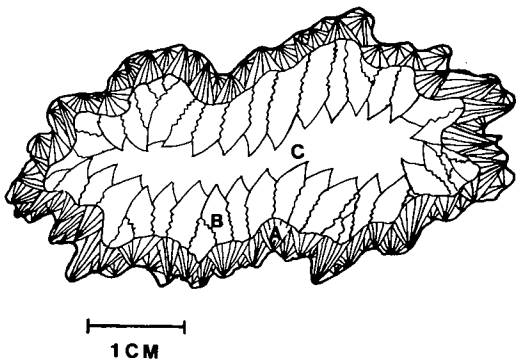

Figure 5. Cross-section of a colloform chert nodule: chalcedony (A); baroque dolomite (B); open space or sparry calcite (C).

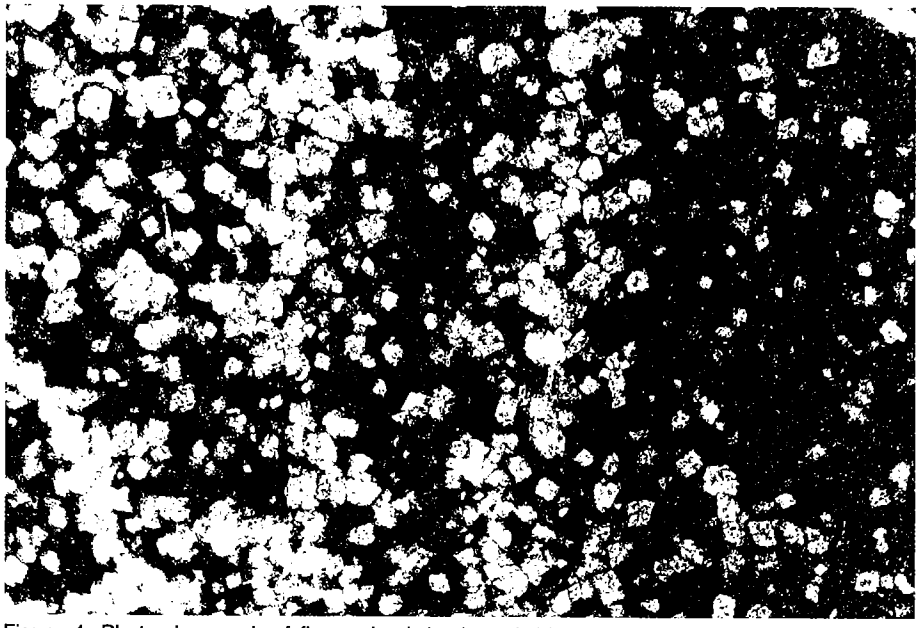

Figure 4. Photomicrograph of fine-grained, laminated, idiotopic-e dolomite in micrite (calcite). Plane-polarized light, 25×.

FORMATION OF THE DOLOMITES

A number of observed characteristics suggest that the fine-grained dolomites of the upper Cool Creek Formation formed in an arid setting similar to the sabkhas found along the margin of the modern Persian Gulf. The strongest piece of evidence to support this interpretation is the close association of these fine-grained dolomites with colloform chert nodules that mimic "chicken-wire" anhydrite and contain both anhydrite pseudomorphs and small, relict anhydrite inclusions. These nodules also contain length-slow chalcedony, a commonly reported replacement of sulfate minerals (Folk and Pittman, 1971; Siedlecka, 1972). In addition, pseudomorphs after gypsum are commonly found (Fig. 9).

The overall characteristics of the shallowing-upward cycles of the Cool Creek Formation are strikingly similar to those observed in the Persian Gulf (Fig. 2). The Persian Gulf sequence is capped with "chicken-wire" and folded anhydrite, whereas the Cool Creek sequences commonly are capped by colloform cherts. The near absence of fossils in this section of the Cool Creek also suggests a (hostile) sabkha environment.

Crystal size and morphology, and some association with fractures, suggest that the coarse-grained dolomites of the Cool Creek Formation formed by migration of hot (>50°C) (Radke and Mathis, 1980; Gregg and Sibley, 1984) dolomitizing fluids along fracture systems. Light oxygen-isotope values support the petrographic evidence that these fluids were hot (Fig. 8). These fluids probably originated as pore water, which was expelled by compaction in the Anadarko basin.

ACKNOWLEDGMENTS

We are grateful for the field support provided by the Oklahoma Geological Survey, Conoco, and Sun Co.

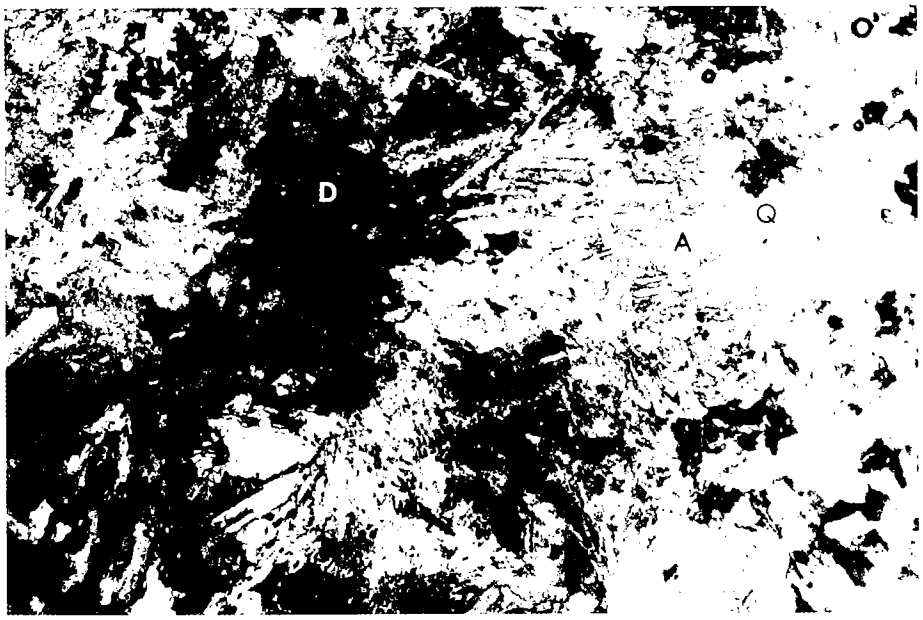

Figure 6. Photomicrograph of dolomite (D) and chert (Q) replacing anhydrite (A) in a colloform chert nodule. Cross-polarized light, 25×.

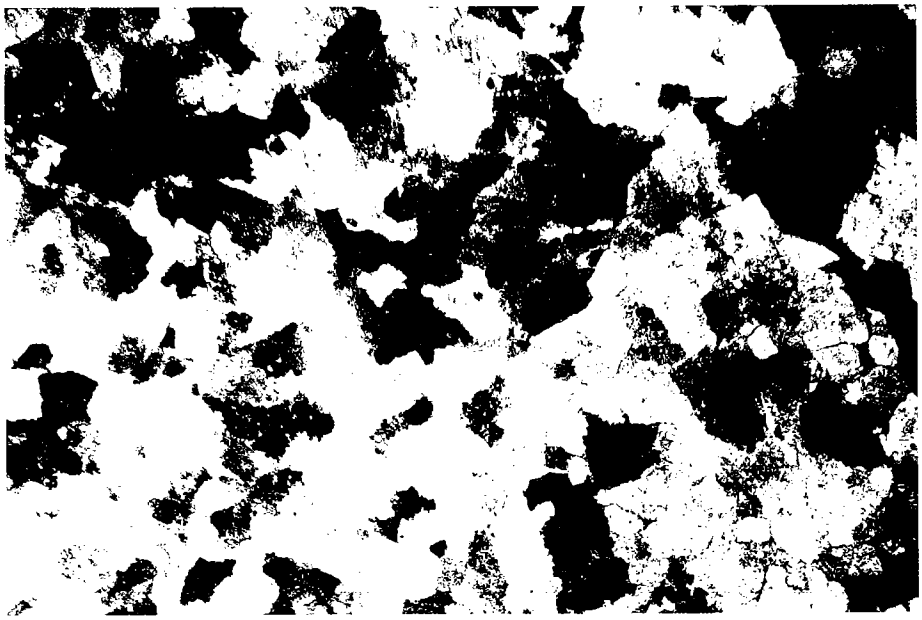

Figure 7. Photomicrograph of xenotopic-A dolomite. Cross-polarized light, 10×.

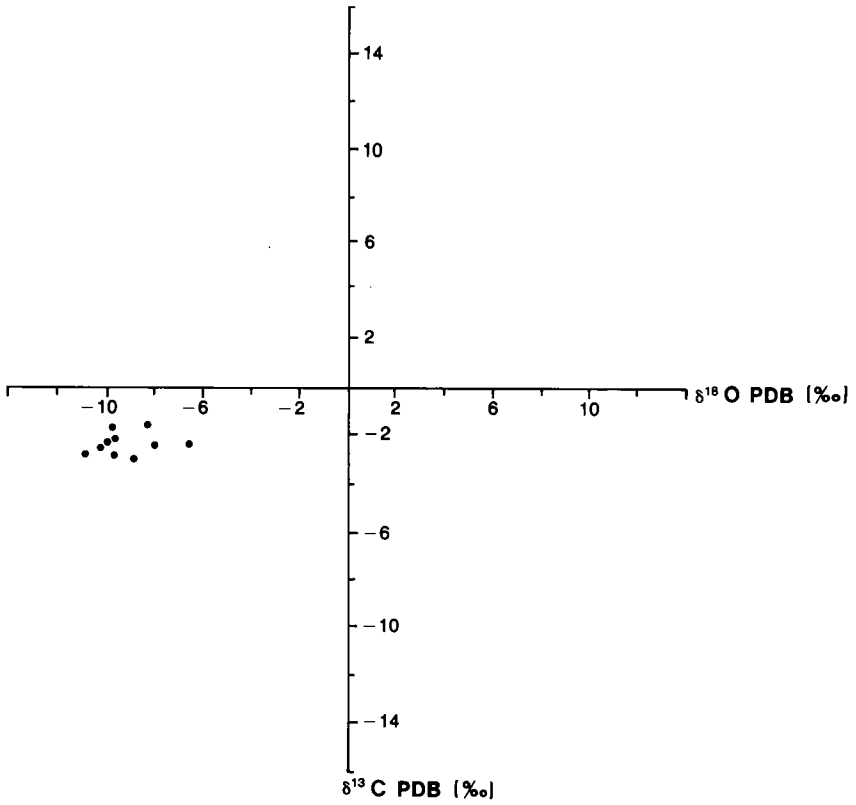

Figure 8. Carbon–oxygen-isotope plot for Cool Creek dolomites. See discussion in text.

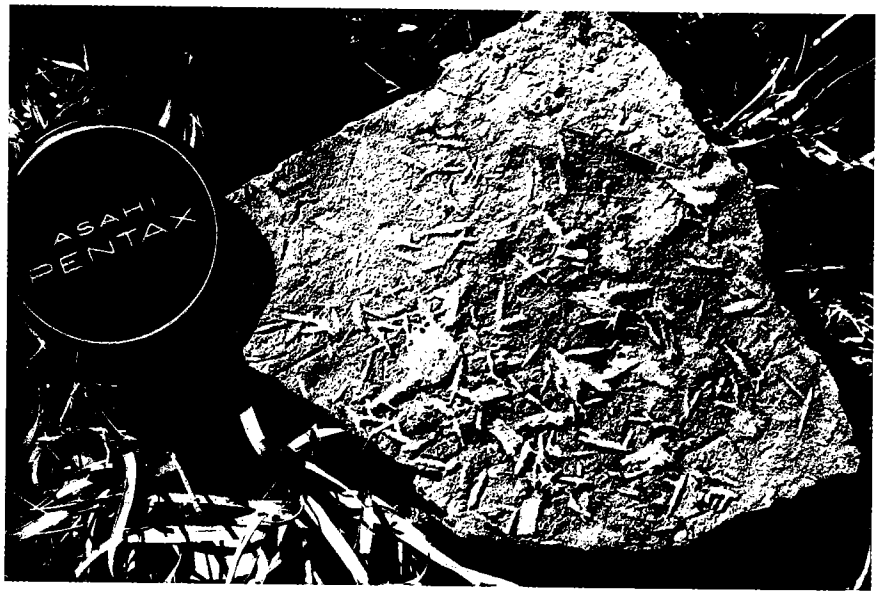

Figure 9. Dolomite pseudomorphs after gypsum(?). Cool Creek Formation on Bally Mountain.

UTILIZATION OF LANDSAT THEMATIC-MAPPER DATA FOR LINEAMENT ANALYSIS OF THE SLICK HILLS AREA

Steven J. Wilhelm and Ken M. Morgan

INTRODUCTION

Our study utilizes Landsat Thematic Mapper (TM) satellite data to map structural lineaments in the Slick Hills area in southwestern Oklahoma. The Slick (or Limestone) Hills occupy a part of the Wichita Mountains frontal fault system (Harlton, 1963) in Caddo, Comanche, and Kiowa Counties. This fault system separates the igneous basement rocks of the Wichita Mountains on the south from the sedimentary sequence in the deep Anadarko basin on the north. Three major NW-trending faults (Meers, Blue Creek Canyon, and Mountain View faults) divide the area into two large structural blocks (Fig. 1), the Lawtonka "graben" and the Blue Creek "horst" (Harlton, 1951). Of particular interest to this study are the Slick Hills and surrounding area, including Bally and Ragged Mountains, covering ~200 mi^2.

The Slick Hills are primarily Cambrian–Ordovician carbonates (upper Timbered Hills Group, Arbuckle Group) which were deposited on the Upper Cambrian Reagan Sandstone. These sedimentary rocks rest unconformably on the Cambrian Carlton Rhyolite Group (Gilbert and Donovan, 1984). Permian conglomerates and shales were deposited unconformably upon the preexisting lower Paleozoic carbonates. Subsequent erosion has exhumed the Slick Hills, leaving the Permian sediments in the valleys.

During the Pennsylvanian, rocks in this area were intensely deformed, creating numerous folds, faults, and fractures. The surface expression of these structural features has produced a regional pattern of lineaments. Previous lineament investigations in this area relied on localized field mapping and standard air-photo interpretation (Gilbert and Donovan, 1984; Gilbert, 1982; Harlton, 1951,1963). The purpose of our study is to identify and map the lineaments in the Slick Hills area using Landsat TM data, and to relate lineament orientations to a model of regional deformation.

LANDSAT TM AND IMAGE PROCESSING

The multispectral nature and digital character of Landsat satellite data have proven useful for regional geologic mapping (Sabins, 1978). In this study, we utilize the Landsat TM first launched 16 July 1982. As this satellite orbits the Earth, it collects 7 spectral bands of radiation reflected from the Earth's surface (Table 1) at a ground resolution of 30 m. The intensity of the reflected radiation from each 30- × 30-m picture element (pixel) is recorded on a gray scale of 0–255. This information is stored as digital data on computer-compatible tapes for image generation and quantitative analysis.

Landsat data offer substantial advantages over conventional air-photos for geologic mapping. The digital character of the satellite data allows computer processing to enhance the spectral nature of surface materials and structural features (Morgan and others, 1985). These data can also be manipulated by the computer to create numerous band combinations and generate new images of the study area for analysis and interpretation.

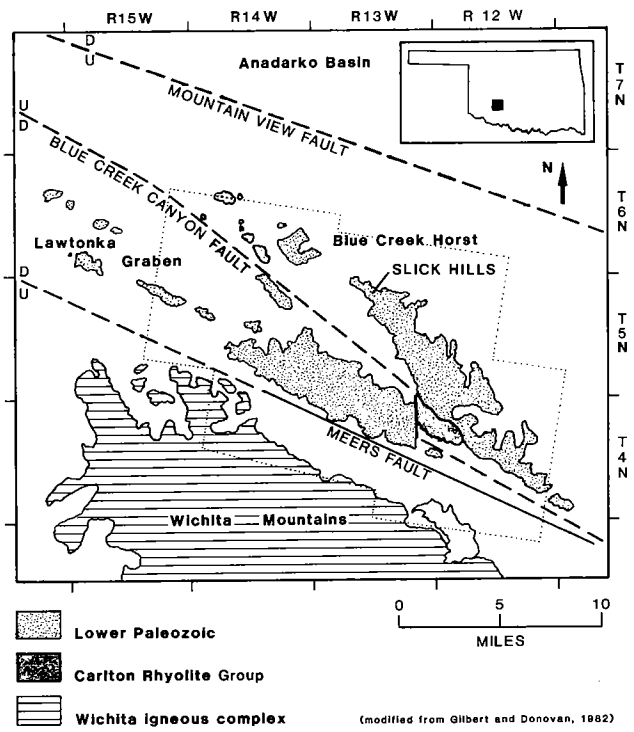

Figure 1. Simplified geologic map showing principal structural elements in the Slick Hills area. Study area enclosed by dotted lines.

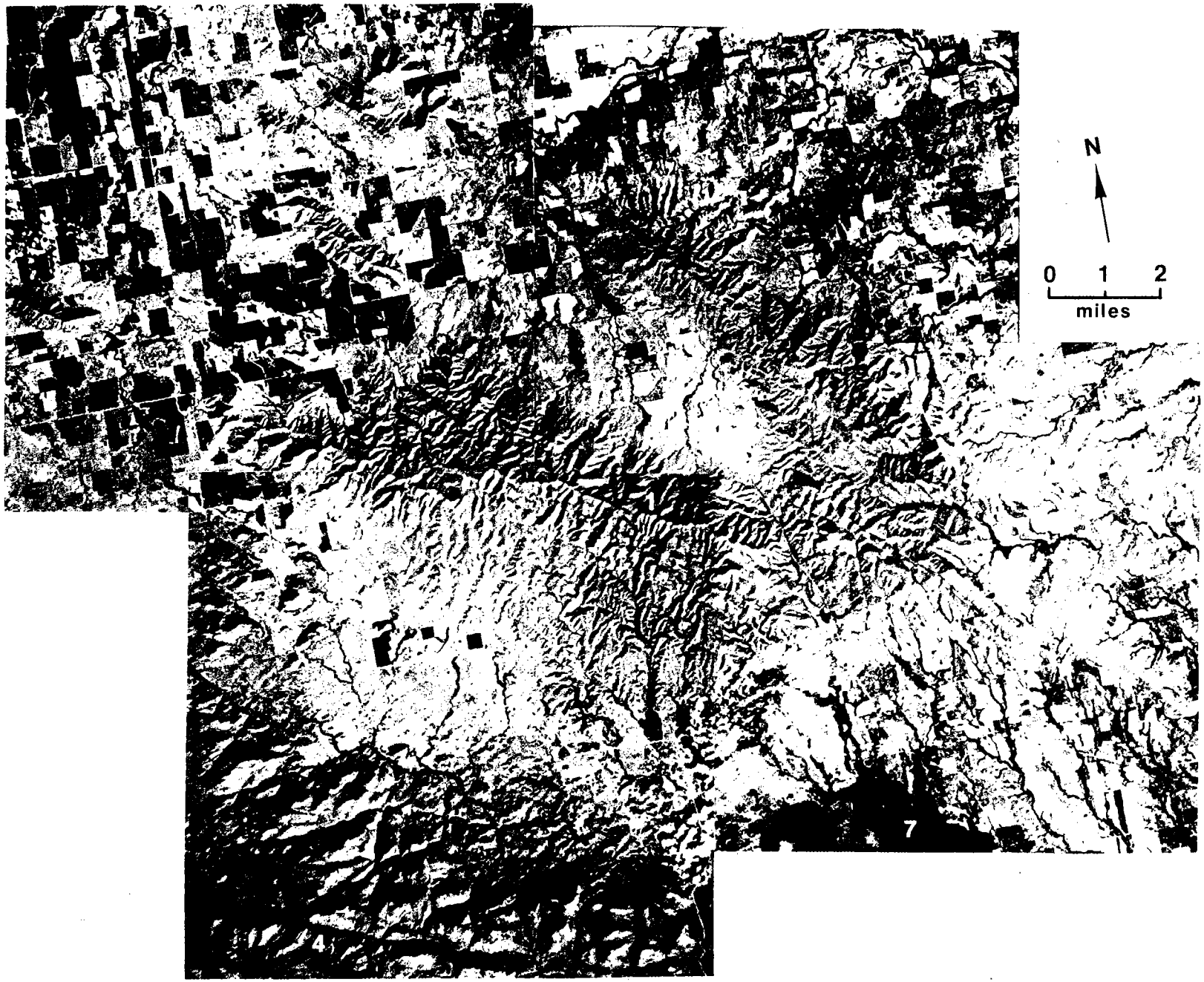

Figure 2. Landsat TM image mosaic of the Slick Hills area. 1 = Slick Hills; 2 = Bally Mountain; 3 = Ragged Mountain; 4 = Wichita Mountains; 5 = trace of Meers fault; 6 = Town of Meers; 7 = Lake Lawtonka.

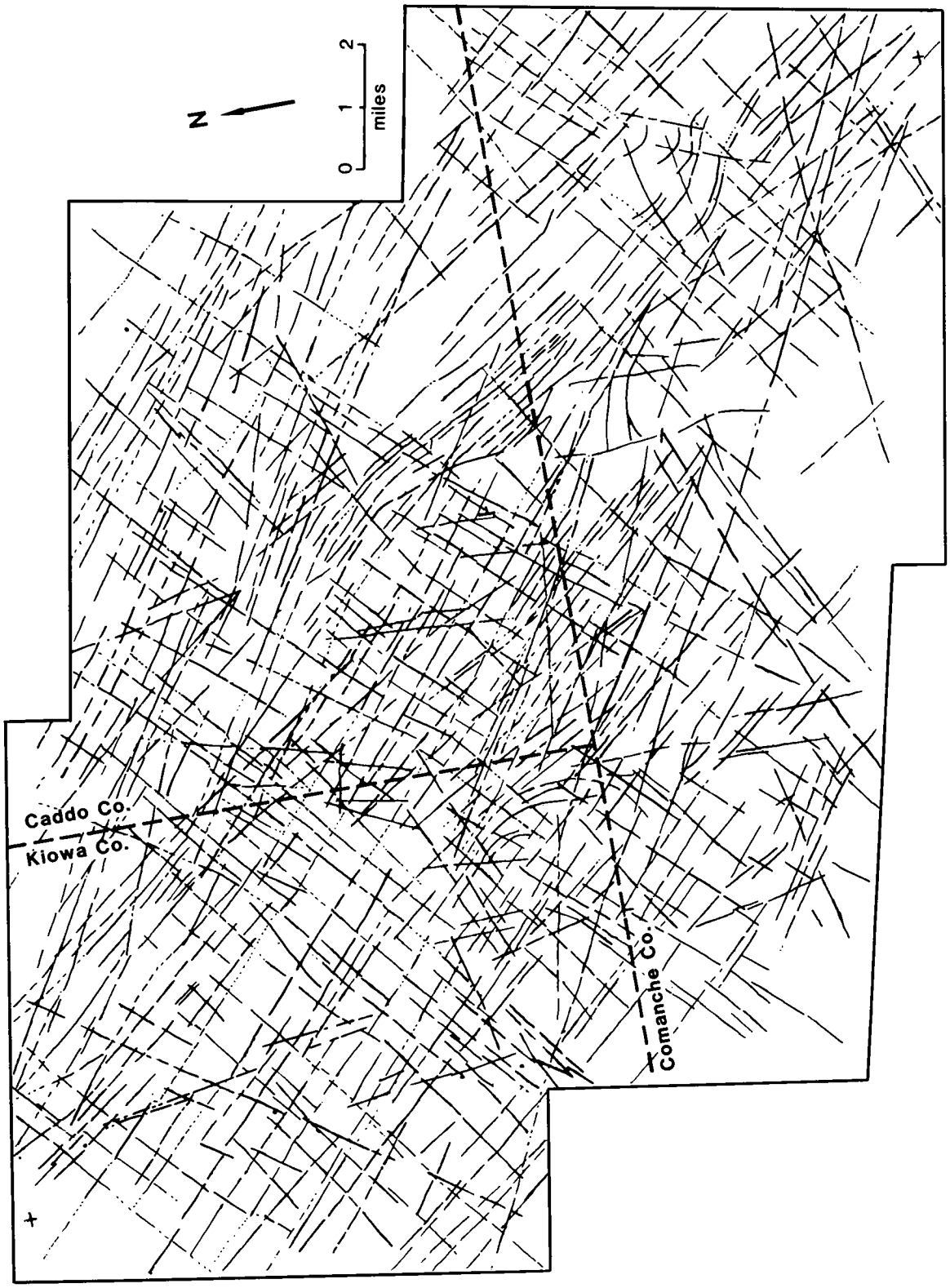

Figure 3. Lineaments interpreted from Landsat imagery (Fig.2). Lineaments within the igneous Wichita Mountains were not interpreted in this study.

TABLE 1.—SPECTRAL BANDS FOR LANDSAT TM

Bands	Spectral range (microns)	Characteristics
1	0.45–0.52	Some water penetration
2	0.52–0.60	Green wavelength for vegetation mapping
3	0.63–0.69	Red wavelength for soils, geology, vegetation, and urban mapping
4	0.76–0.90	Reflected IR, for mapping drainage, vegetation, and tonal patterns
5	1.55–1.75	Reflected IR for soil-moisture, geobotanical, and vegetation mapping; penetrates thin clouds
6	2.08–2.35	Reflected IR; used with band 5 for hydrothermal-alteration mapping; also for soils, geology, and tonal-pattern identification
7	10.4–12.5	Emitted thermal IR

Landsat TM data tapes (path 28, row 36) were obtained for 29 November 1982 and 21 July 1984. False-color composite images of TM bands 2, 3, and 4, weighted to infrared and sharpened to intensity, were generated on our computer system for both data sets at a scale of approximately 1:70,000. To cover the entire study area, two false-color-image mosaics were constructed from the July and the November data, respectively. Multitemporal data were employed in this study to provide contrasting sun angles and seasonal geobotanical variations which can emphasize lineaments for identification and mapping. Figure 2 is a black-and-white mosaic of the Slick Hills study area constructed from November band-4 and July band-5 data. This image has been computer-enhanced to emphasize the regional geology and lineament trends.

LINEAMENT ANALYSIS

Detailed mapping of lineaments was conducted by analyzing the two false-color-image mosaics. In this study, lineaments are defined as natural linear features visible on the imagery—such as stream, vegetation, and geomorphic alignments (O'Leary and others, 1976). Lineaments associated with cultural features were not mapped.

A total of 693 lineaments were identified using standard image-interpretation techniques (Fig. 3). We found that linear tonal anomalies associated with vegetation patterns and soil conditions accounted for most of the lineaments mapped on the imagery. These mapped features, along with confirmed fault and fracture patterns in the area, provided the basis of our interpretation.

Lineament lengths and orientations were measured, recorded, and then plotted on rose diagrams. Figure 4 is a rose diagram constructed from our data over the Slick Hills area, displaying the frequency and orientation of all the mapped lineaments. These lineaments are 0.25–12 mi long.

From our analysis of the area using Landsat TM, two distinct, major lineament orientations are observed; NW-trending lineaments predominate, followed by a NE-trending set (Fig. 4).

The dominant lineament set trends N. 30–60° W. throughout the area; this trend parallels the Wichita Mountains frontal fault system, which trends N. 50° W. (Gilbert and Donovan, 1984). Field observations indicate that many of these mapped lineaments are faults and fractures. Previous field investigations revealed left-lateral motion associated with most of these faults (McConnell, 1983; Beauchamp, 1983; Gilbert and Donovan, 1984). Other known structural features of similar trend include high-angle reverse faults, thrust faults, and fold axes, which may have also been mapped as lineaments.

Oriented perpendicular to the NW-trending lineaments is a second set of lineaments trending N. 40–55° E. Very little is found in the literature about NE-trending features within the sedimentary rocks in our study area. However, a field map by Ragland (1983) shows NE-trending faults in Ragged Mountain. Also, R. N. Donovan (personal communication, 1986) has stated that NE-trending faults do occur in the study area but have not been mapped in detail. The movement of the faults is confirmed to be right-lateral.

Determining these two major directions of faulting is very important to understanding the tectonic forces previously at work in this area. Our lineament analysis confirms the regional orientation of known left-lateral faults and also suggests the existence of numerous right-lateral faults in the Slick Hills area. A detailed study of the field relationships of these faults is needed to develop an accurate model of regional deformation.

RESULTS AND CONCLUSIONS

From our analysis of Landsat TM images over the Slick Hills area, we mapped 693 lineaments. Many of these lineaments are the result of tectonic stresses at work throughout the Pennsylvanian. Any model of regional deformation suggested for this area should incorporate the results of our study. Our findings include the following:

1) A regional lineament trend is associated with reverse faults and fold axes that reflect both left-lateral motion and elements of compression;

2) NE-trending lineaments, while not well documented in the literature, do exist throughout the area as right-lateral faults with minor displacement; and

3) The two major lineament trends intersect at ~90°.

While general models of regional deformation have been proposed for the Slick Hills area, left-lateral transpression seems most consistent with our findings. Elements of both left-lateral motion and com-

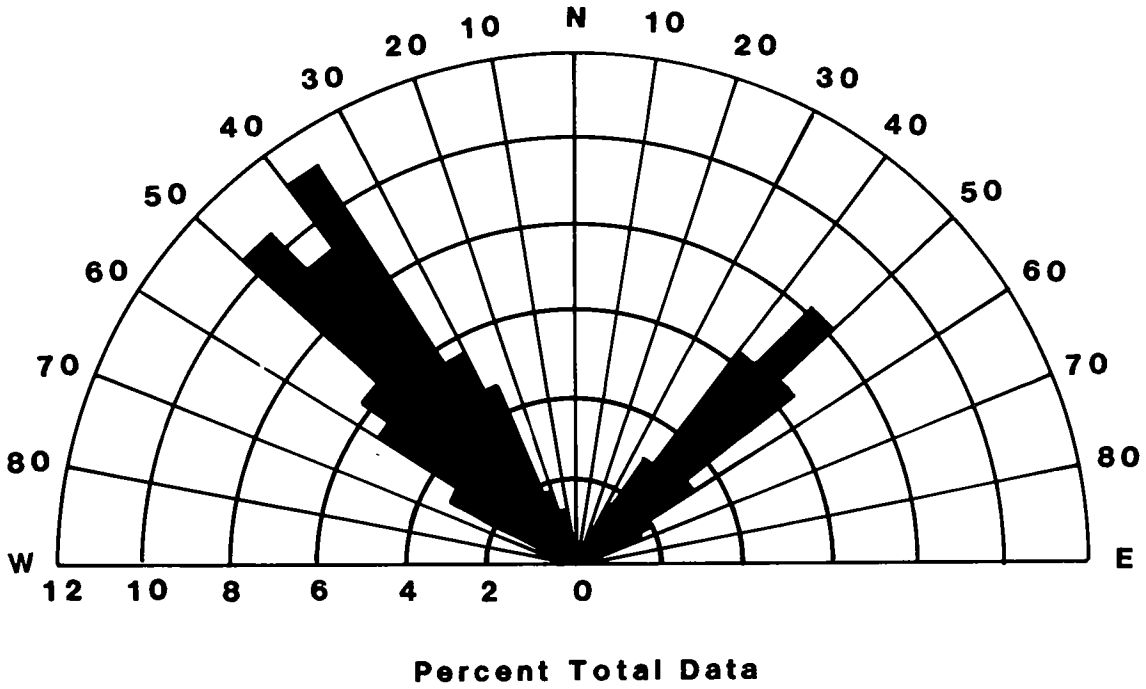

Figure 4. Frequency-weighted rose diagram illustrating the two major lineament orientations identified in this study.

pression would produce the major lineament trends, fault motions, and angular relationships found in our study.

However, from our analysis of satellite data we could not determine the amount of displacement or the relative timing of faulting in this area. Additional field observations and detailed mapping are still needed to answer these important questions.

ACKNOWLEDGMENTS

A special thanks is extended to David G. Koger for processing and generating the imagery used in this study. We would also like to thank Neta Hendrickson for typing the manuscript, and Texas Christian University for funding this project.

Oklahoma Geological Survey Guidebook 24, 1986

APPLICATION OF A CONSTRUCTION FOR DETERMINING DEFORMATION IN ZONES OF TRANSPRESSION TO THE SLICK HILLS IN SOUTHERN OKLAHOMA

Angus M. McCoss and R. Nowell Donovan

INTRODUCTION

The displacement direction of tectonic zone boundaries can be easily determined from first-increment structures using a construction for deformation in transpression/transtension zones demonstrated by McCoss (1986). This construction was developed from the transpression model of Sanderson and Marchini (1984). In this paper we apply the construction to structures present in the deformed lower Paleozoic rocks which form the Slick Hills of southwestern Oklahoma. We utilize data sets prepared by Donovan (1982), Beauchamp (1983), McConnell (1983), and Marchini (1986), plus some of our own observations. The analyzed structures are of Pennsylvanian age and formed during the "dismemberment" stage in the evolution of the southern Oklahoma aulacogen. Geographically, the analyzed area is part of the Lawtonka "graben" (terminology of Harlton, 1972). This "graben" is bounded on the south by the Meers fault and on the north by the Blue Creek Canyon fault. Regionally, the area is part of the frontal fault zone between the Wichita uplift and the Anadarko basin.

CONSTRUCTION TECHNIQUE

The theoretical basis for the construction is covered in Sanderson and Marchini (1984) and McCoss (1986). Here we simply present the construction technique.

The initial step is to draw a circle (or two circles if a symmetrical diagram is desired) which is (are) tangent to a line drawn parallel to the trend of the zone boundary (e.g., the Meers fault). Circle radius is not critical. However, for convenience, we recommend (1) that the chosen radius be equal to half that of an equatorial net, and (2) that tangents be constructed to coincide with the center of the net (Fig. 1).

In the second step, the trend of a selected first-increment compressional structure is followed until it intersects the circle(s). A tie line from the center of the circle to the intersection gives the orientation of the zone-boundary displacement vector. The movement sense of the vector is from the center to the intersection (Fig. 1).

APPLICATION TO THE SLICK HILLS

Two data bases are utilized (Fig. 1). The first comprises the trends of 108 major fold axes as identified by Donovan (1982), Beauchamp (1983), McConnell (1983), and Marchini (1986). These folds are generally of parallel style, have wavelengths of 100–750 yd (90–685 m), and generally have axial-plane dips >50°.

The second data base consists of decimetric-scale shear zones, which are a common feature in highly deformed areas of the "graben." These shear zones comprise en echelon, sigmoidal arrays of subvertical solution surfaces (Fig. 2).

In the analysis, the WNW-trending Meers fault is considered to be a controlling zone boundary. Not only is it a surface of major stratigraphic discontinuity (with an apparent vertical component of motion >2 mi (~3,200 m), but its trend coincides with the general Wichita-uplift trend of southwestern Oklahoma and the Texas Panhandle.

Analysis of Fold-Axis Data

A qualitative appraisal of fold trends in the Slick Hills (McConnell and others, in press) suggests that the deformation is markedly heterogeneous. For a mile to the northeast of the Meers fault, fold axes are subparallel to the fault. Folds in this region (the "Meers-fault domain") are considered separately from those in the rest of the Slick Hills (Fig. 3). Folds in the latter area have a general NW trend (Fig. 4).

Assuming that the fold axes have not been significantly rotated from parallelism with σ_2, then the displacement vectors determined for both areas suggest that the "graben" has undergone oblique left-lateral convergence (transpression). The Meers fault domainappears to have formed in a regime more-compressive than that which obtained for the rest of the area, as implied by the higher angle of displacement-vector incidence. Alternatively, the solution in this domain may reflect an increase in bulk rotation of the folds near the Meers fault during progressive transpression. A third interpretation, favored by the authors and suggested by Sanderson (personal communication), is that the subparallelism

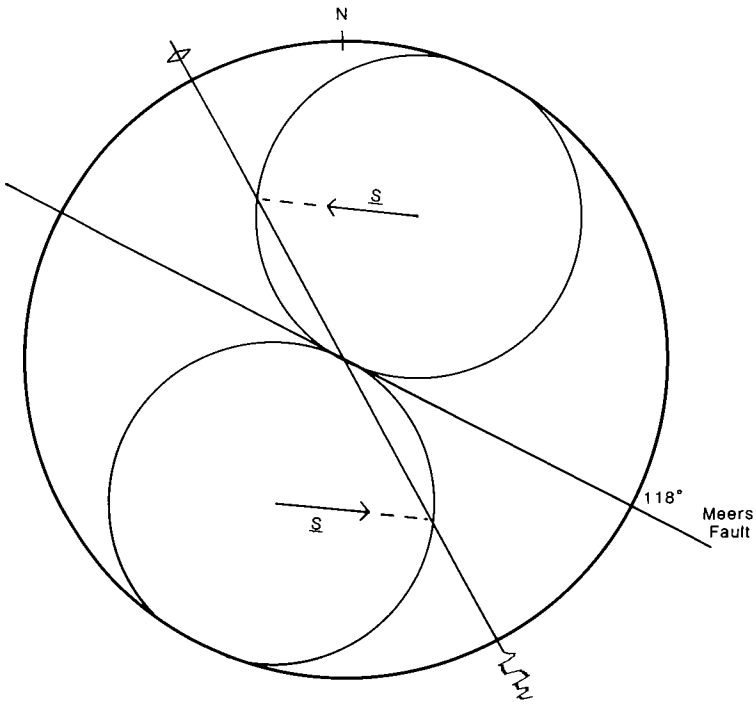

Figure 1. Construction for determining direction of the displacement vector *S*.

of the folds to the major fault is a complex boundary effect (forced folding, the quantitative description of which lies outside the scope of this paper).

Vector solutions for the rest of the Slick Hills suggest a higher component of shear (the mean angle of displacement-vector incidence is ~45° to the Meers fault). Furthermore, the solutions are only first-order approximations, relying on folds as paleostress indicators, and do not allow for significant bulk rotation of their axes during deformation. Thus, it is possible that the true solution would involve a yet greater component of shear.

Analysis of solution-array data

Although on a much smaller scale than the fold axes, all the en echelon, sigmoidal arrays of pressure-solution surfaces exhibit markedly heterogeneous deformation (Fig. 2). Because of their small scale, the arrays can conveniently be analyzed from photographs. We selected an array from the Stumbling Bear shear zone (McConnell and others, in press) for detailed analysis. A grid with 6- × 6-cm squares (at outcrop scale) placed on the photograph allowed 72 locally representative solution-surface trends to be obtained (Fig. 5). A systematic partitioning of the deformation is emphasized by differentiating between lines which subtend angles >22.5° to the zone boundary (trend N. 60° W.) from those which subtend angles <22.5°. Those with the higher angles lie in a band trending approximately N. 85° E.

Both the high- and low-angle trends generate left-lateral transpressive displacement vectors (Fig. 6). The low-angle trends may, as suggested above, reflect complex boundary effects. In the construction, the high-angle trends generate displacement vectors which have angles of incidence similar to those derived from the folds.

Comparison of the Two Analyses

The similarity in the angles between the two types of vector solutions and their respective boundaries may reflect a rheologically favored type of transpression at both orders of magnitude. In the type of transpression which may have operated, Riedel shears develop parallel to the displacement vector(s), allowing displacement of the Riedel-bounded block without generating further major fractures (perhaps a more energy-efficient type of deformation).

Interestingly, other than major reverse–wrench faults subparallel to the Meers fault, the only other significant faults in the "graben" trend subparallel to the predicted displacement vectors. These faults are best seen in the NE¼ sec. 6, T4N, R14W (Fig. 7), where en echelon folds are offset by left-lateral wrench faults (Beauchamp, 1983; Marchini, 1986; McConnell and others, in press). The orientation of these faults agrees favorably with the predicted orientation of left-lateral Riedel shears and folds when the displacement vector (*S*) is at 45° to the Meers trend and when the angle between a conjugate shear plane and σ_1 is 25° (Fig. 8).

A similar pattern of left-lateral Riedel fractures is developed in some of the en echelon solution arrays (Figs. 9,10). These fractures clearly have facilitated extension parallel to the length of the array zones.

CONCLUSIONS

The results of our study suggest three fruitful areas for further research: (1) a regional study of

Figure 2. View of a typical en echelon, sigmoidal array. Squatting observer is pointing to solution surfaces. This example is in the Stumbling Bear shear zone (McConnell and others, in press).

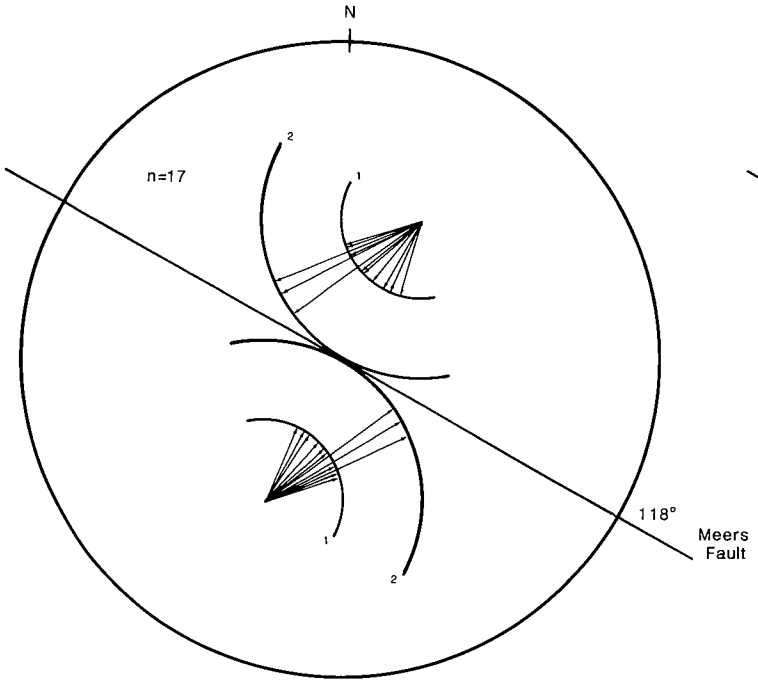

Figure 3. Analysis of displacement vectors for folds in the "Meers-fault domain." Data from Beauchamp (1983) and McConnell (1983); 17 folds are analyzed.

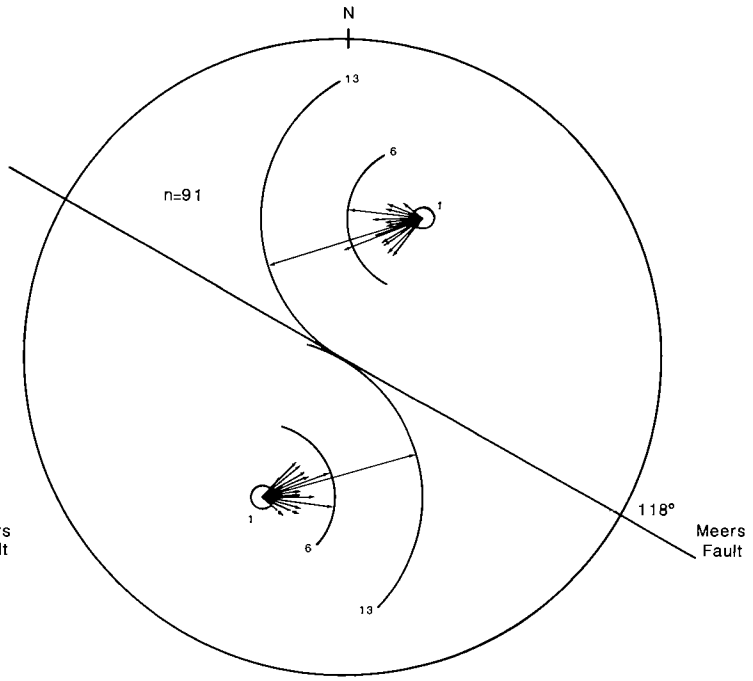

Figure 4. Analysis of displacement vectors for folds in the Slick Hills, excluding "Meers-fault domain." Data from Beauchamp (1983) and McConnell (1983); 91 folds are analyzed. The lengths of the displacement vectors in Figures 3, 4, and 6 depend on the number of folds or solution surfaces that imply that particular displacement direction. In Figure 4 the most common vector (n = 13) makes an angle of 43° to the Meers fault.

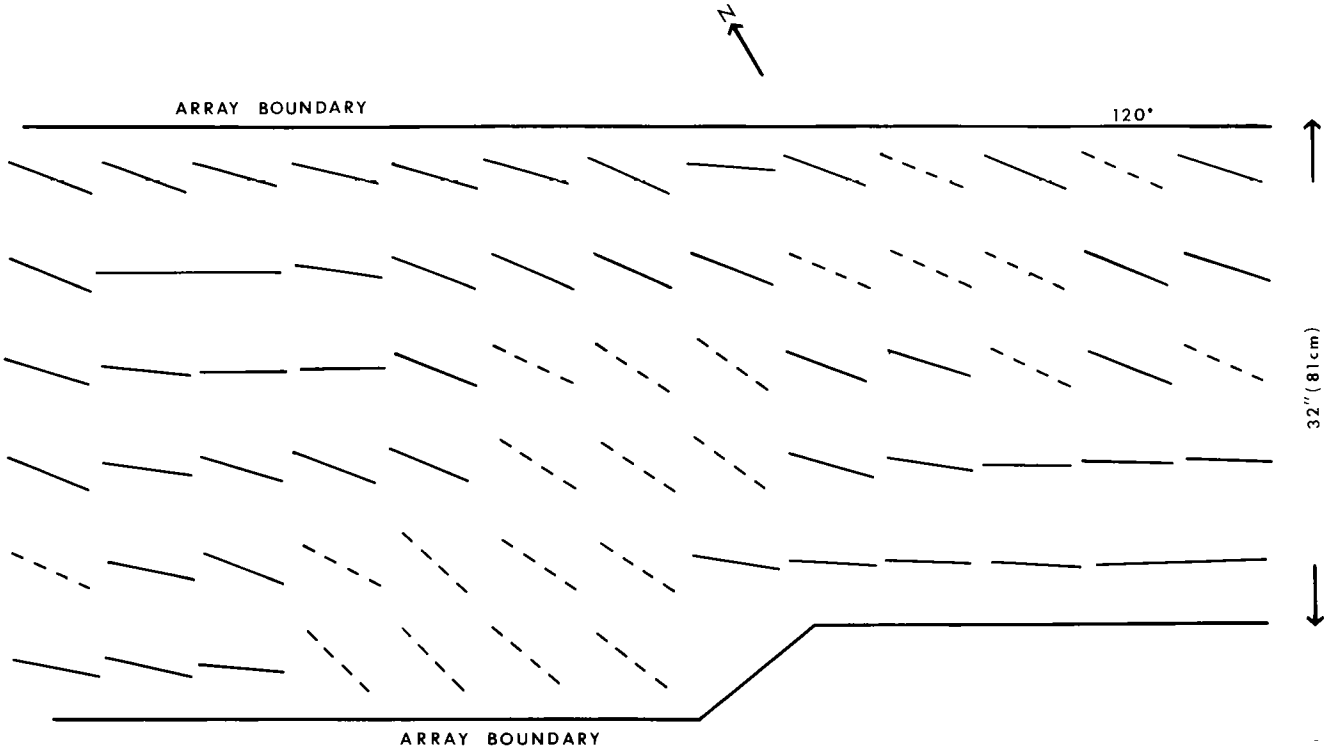

Figure 5. An example of the grid method used to determine displacement vectors on an en echelon, sigmoidal solution array.

displacement vectors from vein arrays, to supplement the fold- and solution-array data; (2) a study of the role of faults in partitioning domains of similar displacement vectors in anastomosing wrench zones; and (3) a study of boundary effects close to major faults.

ACKNOWLEDGMENTS

This work forms part of an ongoing study of the Slick Hills area by the Queen's University of Belfast, Oklahoma State University, and Texas Christian University, partly funded by the Oklahoma Geological Survey and Sun Co. Our work has benefited greatly from discussions with our colleagues Dave Sanderson, David McConnell, David Marchini, and Weldon Beauchamp. Diana Shaeffer expertly drafted the diagrams.

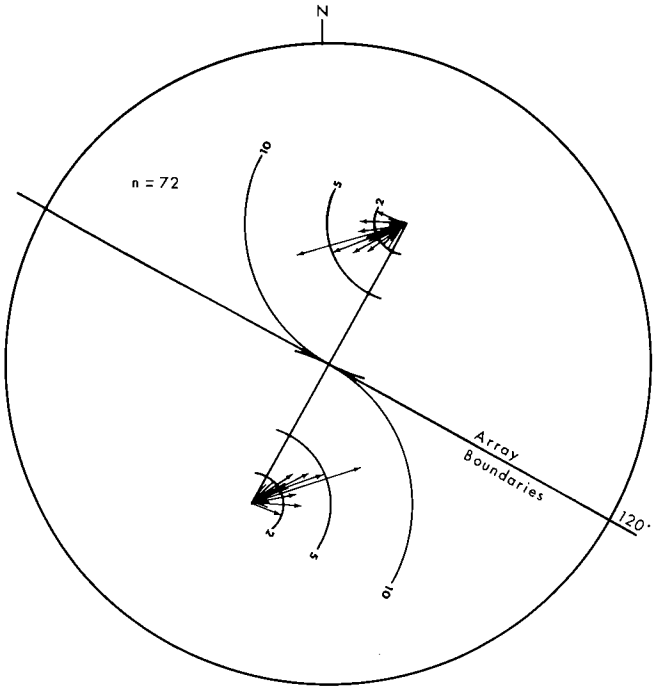

Figure 6. Displacement vectors calculated from the solution-surface trends in Figure 5. Left-lateral transpression is indicated: The most common vector (n = 7) makes an angle of 43° to the array boundaries.

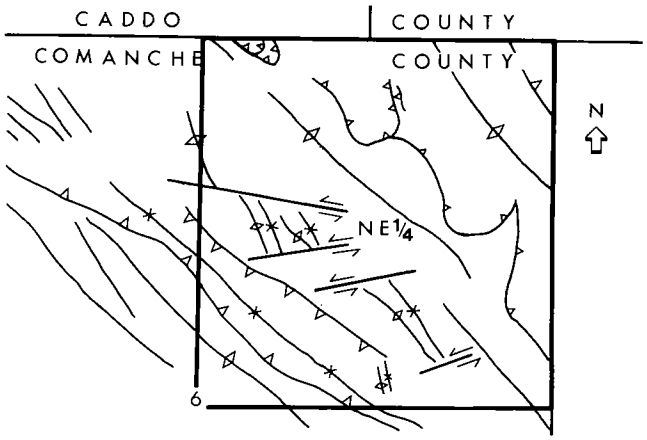

Figure 7. Map of a small part of the Slick Hills, showing an area where en echelon folds are offset by left-lateral wrench faults.

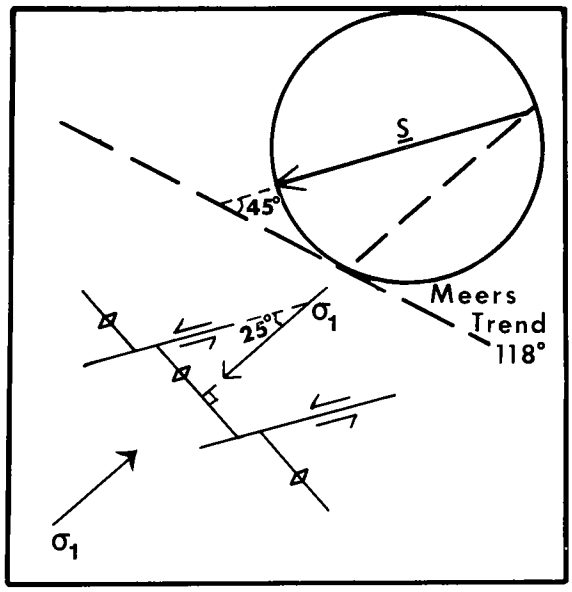

Figure 8. Interpretation of the faults shown in Figure 7 as left-lateral Riedel shears formed when the displacement vector is at 45° to the Meers trend and the angle between the conjugate shear plane and σ_1 is 25°.

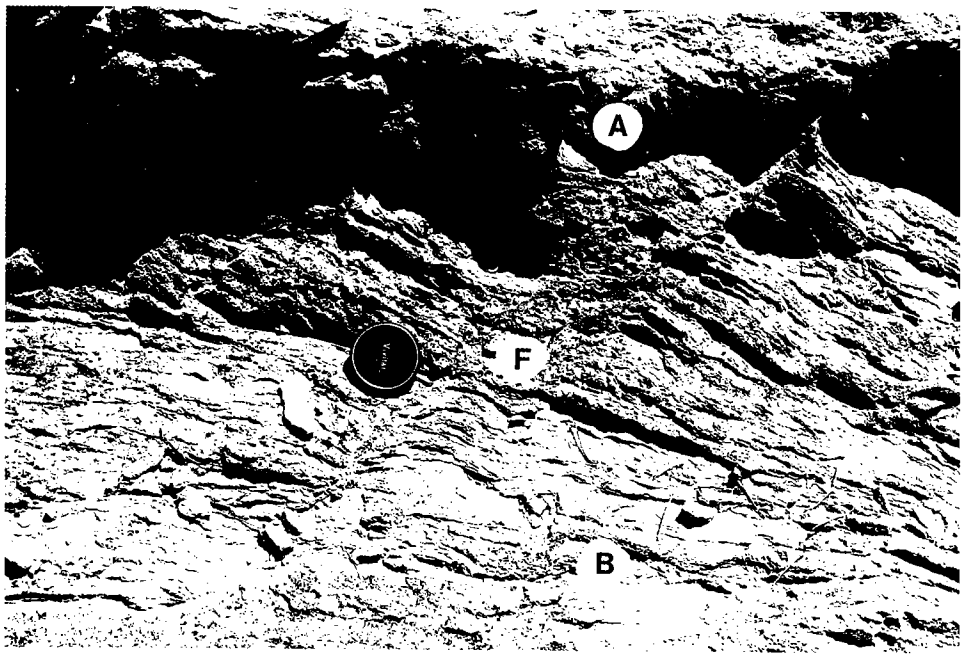

Figure 9. View of part of the en echelon array depicted in Figure 2. Array boundaries (AB) are visible at top and base of view. Note general sigmoidal shape of solution surfaces and also a throughgoing left-lateral fracture (F) located to right of camera cap.

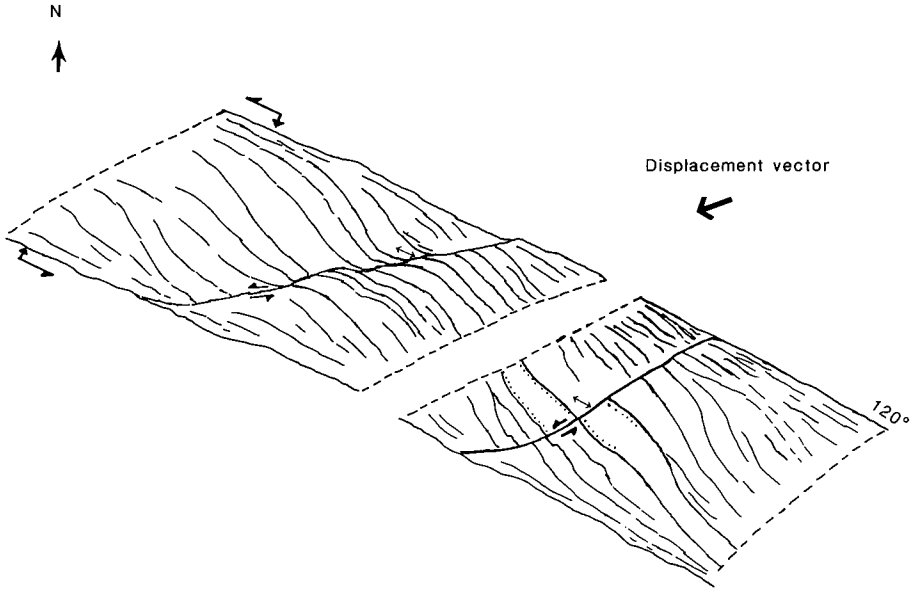

Figure 10. Sketch from photographs of two left-lateral fractures cutting the solution array analyzed in Figure 6. These fractures are interpreted as Riedel shears. Their relationship to the displacement vectors for the array as a whole is very similar to that shown on a much larger scale by the left-lateral faults depicted in Figure 7.

Oklahoma Geological Survey Guidebook 24, 1986

NEOTECTONIC ACTIVITY OF THE MEERS FAULT

Alan R. Ramelli and D. Burton Slemmons

INTRODUCTION

Tectonic Activity in Southwestern Oklahoma

The Meers fault in southwestern Oklahoma has recently been determined to be an active fault with the potential for causing large, damaging earthquakes (Seismological Society of America, 1985). This comes at a time when much effort is being given to the evaluation of seismic hazards in the eastern U.S. In this paper, "eastern U.S." indicates all of the U.S. east of the Rocky Mountains. In the past, potential for large-magnitude events (i.e., M >7) was assumed not to exist in the eastern U.S., with the exception of areas where large historical earthquakes have occurred (New Madrid, Missouri; Charleston, South Carolina; St. Lawrence Seaway). The recognition of activity on the Meers fault shows that additional large-magnitude-earthquake source areas likely exist in the eastern U.S., and that geological studies can greatly aid in identifying potential source areas.

The Meers fault has a very conspicuous surface expression (Fig. 1) resulting from late Holocene and Quaternary displacements. It owes this expression both to its recent movement and to its presence in a resistant rock unit, the Post Oak Conglomerate (Fig. 2). The two faulted units, the Post Oak and the Hennessey Group shale, have contrasting surface expressions due to their resistance to erosion. The fault has a much more subdued scarp in the Hennessey (Fig. 3). This is the best known surface expression of recent faulting in the eastern U.S. and well illustrates how active faults can escape recognition when they are unexpected. There likely are other faults with unrecognized surface expression elsewhere in the eastern U.S.

It is common to assume that active zones of deformation exhibit some level of historical seismicity, but the Meers fault shows that this is not always the case. This region has had very little historical seismicity, none of which has been specifically determined to be on the Meers fault. The record of felt earthquakes in southwestern Oklahoma dates back only ~85 yr, and the instrumental record only ~25 yr (Lawson and others, 1979). This demonstrates well that tectonically active areas can have temporal variations in seismicity which are greater than our historical records. Gordon and Dewey (1985) have interpreted a diffuse zone of seismicity (the "Wichita–Ouachita" zone) to indicate a higher seismic potential than the surrounding areas, but such interpretations do not necessarily define the potential for large-magnitude events. Seismicity data must be supplemented by geologic investigations, which should be concentrated along zones such as this, where fault orientations are favorable with respect to the stress field, and/or a definable concentration of seismicity exists.

Structural Interpretations of the Meers Fault

The Meers fault is considered to be an integral part of the Wichita Mountains frontal fault system, which was first mapped in detail by Harlton (1951, 1963,1972). His general relations remain accepted at the present, but many key questions remain about the structural nature of this fault system.

Harlton recognized that there is an extremely large vertical displacement across this zone: Uplift of the Wichita Mountains igneous complex and subsidence and sedimentation in the Anadarko basin amount to several miles of vertical deformation. He interpreted that this occurred along a vertical fault system, and he took the surface expression of the Meers fault to represent the southern bounding fault of this system. He originally described the Meers fault as having up-to-the-north displacement, based on the present scarp and the Permian sediments of the Meers Valley between the Wichita Mountains and the Slick Hills. Later, he realized that the proximity of the igneous rocks against the basin sediments required considerable up-to-the-south displacement, and he altered his interpretation of displacement on the Meers fault to accommodate this fact.

Detailed structural mapping of deformation in the Slick Hills and Wichita Mountains adjacent to the Meers fault (Donovan and others, 1982; Butler, 1980; McLean and Stearns, 1983) has demonstrated well that this area has a significant left-lateral strike-slip history. Evidence for this is shown by large- and small-scale features such as wrench folds, fault displacements, fracture patterns, slickensides, vein systems, and Riedel shears. These studies have taken the Meers fault to be the major strike-slip fault associated with this deformation. Features observed along the present exposure of the Meers fault (e.g., horizontal slickensides, linear fault trace, joint pattern, Riedel shears, proximity to the Post Oak Conglomerate–Arbuckle Group contact) strongly support this interpretation.

Recent seismic-survey interpretation (Brewer and others, 1983) has ascribed uplift of the Wichita

Figure 1. Low-sun-angle photograph of the Meers fault in Post Oak Conglomerate. Scale 1:6,000.

Mountains to thrusting of the igneous complex over the sedimentary rocks of the Anadarko basin along faults dipping moderately S. The Mountain View fault is seen to be the primary thrust fault of this system. This interpretation appears to be valid, but the Meers fault has also been postulated to be a S-dipping thrust fault. This does not appear to be the case. Recent displacement has occurred on an extremely linear fault dipping steeply (subvertical) N. This does not appear to be an overthrust fault dipping moderately S, although displacement might have been accomplished, at least in part, along a thrust fault rotated to, or even past, vertical. More likely, recent activity has occurred along a vertical fault zone created by Paleozoic strike-slip deformation. If so, the fact that linearity has been preserved is evidence that a lateral deformational phase either followed or slightly outlasted a thrusting phase.

Regional Extent of Activity: The Amarillo–Wichita–Arbuckle Uplift

Recent activity on a fault in a region with little historical seismicity indicates the possibility that this is only part of a larger active zone of deformation. This fault is part of a structural feature (Amarillo–Wichita–Arbuckle uplift) that extends for several hundreds of kilometers. Fault activity along a part of the zone may indicate that potential for activity exists along much if not all of the zone.

Stress conditions in this region have been constant over a long time. Activity apparently has resulted from combinations of stresses, fault orientation, and fault strength that have existed since long before "recent" time (i.e., late Quaternary). It seems possible that activity has continued over a long time, at very low rates, and at intermittent intervals. If so, the entire zone could potentially cause large earthquakes, but late-Quaternary activity would be expected only along parts of the zone. It thus becomes necessary to examine a longer period of geologic time.

For most of southern Oklahoma, including the area around the Meers fault, the post-Permian sedimentary record has been entirely eroded away, which makes examination of fault history extremely difficult. However, this problem does not exist in the Texas Panhandle, where various Mesozoic and Tertiary units are preserved. These units have been subjected to deformation at low rates along this zone over considerable geologic time (Budnick, 1983; McGookey and Budnik, 1983; Budnick, personal communication). An area near Amarillo, Texas, has had historical seismicity with several events of Modified Mercalli Intensity IV to VI—in particular, earthquake swarms in 1917 and 1925 (Stone and Webster Engineering Corp., 1983). Activity on a structural feature termed the "Whittenburg trough" is believed to be responsible for this seismicity, which is manifested by warping and tilting of sedimentary units at the surface.

Recent work by Roy Van Arsdale and Randy Cox of the University of Arkansas at Fayetteville has shown a possibility of recent activity on the Washita Valley fault in the Arbuckle Mountains southeast of the Meers fault. This is shown by ponding of alluvium against the fault and by surface expression in resistant carbonate rocks. This fault resembles the Meers fault in some features that they have observed closely, including fault trend, a steep to moderate N dip, exposure in resistant rock units, and up-to-the-north displacement.

Recent seismic activity near Enola, Arkansas, has occurred (Haar and others, 1984) along the northern

Figure 2. Meers fault scarp in Post Oak Conglomerate, a resistant carbonate unit. Downthrown block to the left (south-southwest).

Figure 3. Meers fault scarp in nonresistant Hennessey Group shale. Compare with Figure 2. Downthrown block to the left (south-southwest).

edge of the Ouachita fold and thrust belt, which truncates the Amarillo–Wichita–Arbuckle uplift. A composite focal mechanism derived from this activity is compatible with the observation of left-lateral displacement on the Meers fault.

Considering these various pieces of evidence, it appears likely that this zone does indeed have potential for activity along much if not all of its length, and it should be studied in detail. As a step in this direction, aerial photographs were taken under low-sun-angle conditions in conjunction with this study. The area of coverage extended 265 km (165 mi), from near Retrop, Oklahoma, to the Arbuckle Mountains. No obvious indications of tectonic activity were revealed. It appears either that conditions such as climate, surface materials, and recurrence intervals do not allow good preservation of geomorphic features indicative of neotectonic activity, or that activity is not evenly distributed along the zone, which may have only a few current "hot spots" of activity. Both possibilities likely are true to some extent. Much more study is needed to determine the extent and nature of neotectonic activity in this region.

QUATERNARY FAULT DISPLACEMENT

Rupture Length

Fault rupture during large-magnitude events (i.e., M >6) generally propagates to the surface, with the exception of subduction-zone events. The surface manifestation of faulting can tell us a great deal about size of the event, structural relations of the fault, style of faulting, and stresses in the crust. Detailed mapping of surface-rupture patterns should be done more often, both for historical and prehistorical events. Surface rupture on the Meers fault, according to present knowledge, is depicted in Figure 4.

Definition of surface-rupture length has evolved somewhat since the first recognition of activity on the Meers fault. The northwestern end can be well defined on standard aerial photography, and, whereas subsequent work has shown that rupture at this end is slightly more complex than originally believed, no significant extension has been found. However, to the southeast, the fault has a much less conspicuous scarp. This scarp can be traced on standard aerial photography within ~1 mi of Highway 281 near Richards Spur. Initial estimates (Gilbert, 1983) thus placed surface-rupture length at ~26 km (~16 mi). Field observations showed a probable subdued scarp at Highway 281, and a wide fracture zone with nondefinitive offsets on the east side of Interstate 44. No evidence of faulting could be seen along this line across the East Cache Creek flood plain, but this is a very active flood plain and small scarps could easily be erased in a short time. This evidence indicated that fault length was at least 3.5 km (2 mi) longer than originally recognized. The acquisition of low-sun-angle aerial photography has since shown that rupture extends eastward along a slightly different line onto the Fort Sill Military Reservation (Fig. 4). Rupture length now appears to be well defined at a minimum of 37 km (23 mi).

Sense of Displacement

The fault has a conspicuous surface expression, with the north side consistently up. This led to early

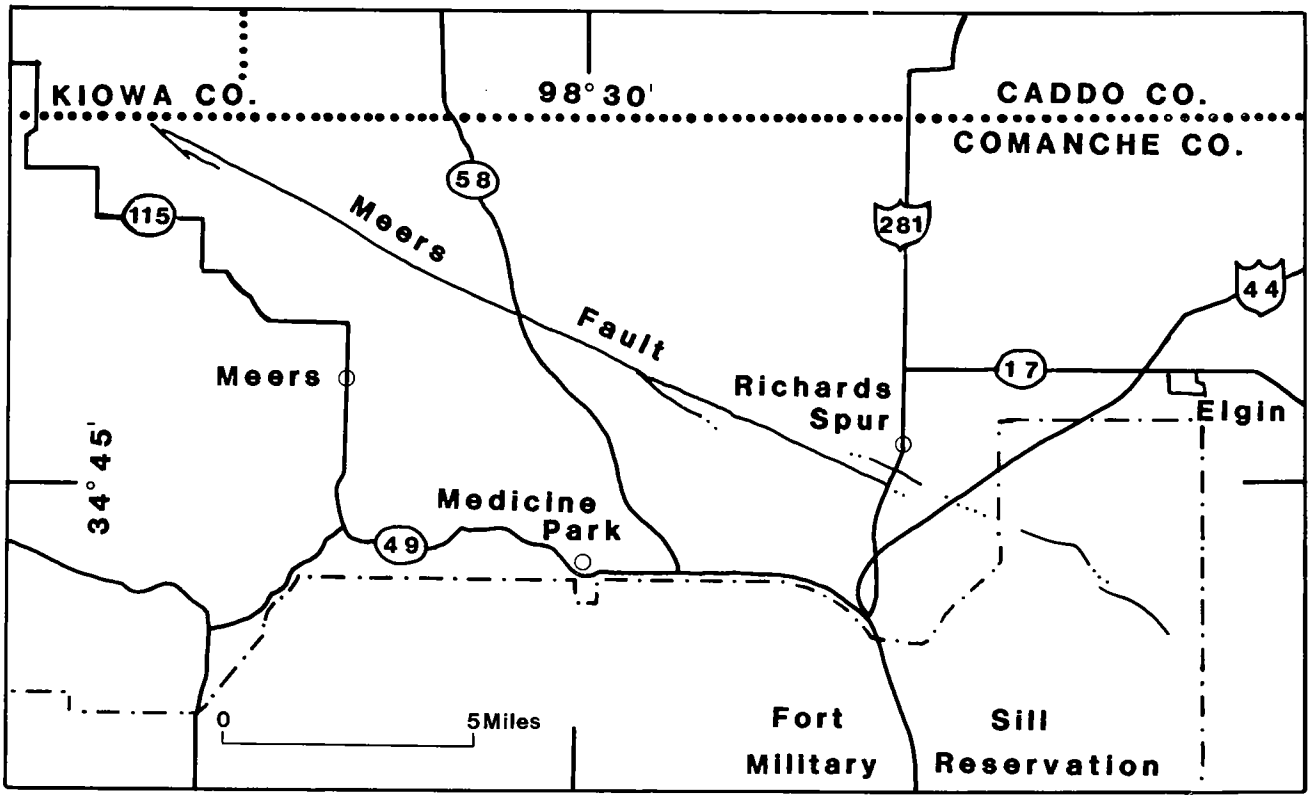

Figure 4. Surface-rupture map of Meers fault. Scale 1:250,000.

thought that displacement was normal, based on a S-dipping fault, as postulated by Brewer and others (1983). However, subsequent study has shown that, at least near the surface, the dip of the fault surface ranges from vertical to moderately N-dipping. This fault orientation and the determination that horizontal stresses are compressional, not tensional, seem to preclude normal faulting.

Two trenches dug by the Oklahoma Geological Survey showed a 20- to 50-cm-wide fault zone dipping moderately (55°) N, but this dip is probably a shallow, near-surface effect resulting from behavior of surficial alluvium, and the fault likely steepens within a few tens of meters of the ground surface. This phenomenon has been shown in experimental and theoretical work by Lade and Cole (1984).

Detailed offset measurements were made along the fault and are plotted in Figures 5 and 6. These offsets represent the displacement causing the presently observed fault scarp and are not due to older dis-

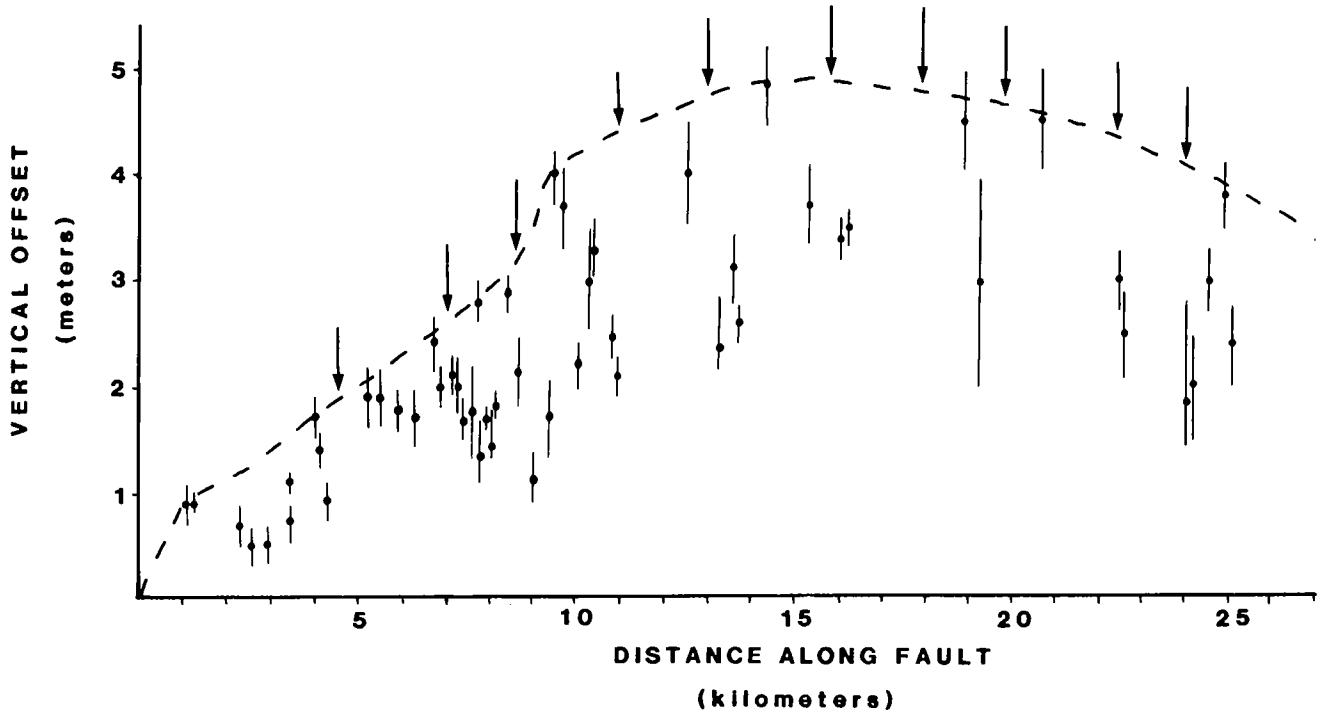

Figure 5. Graph of the vertical component of Quaternary displacement along the Meers fault, from the northwestern end of surface rupture to Highway 281. Major stream lines are indicated by arrows.

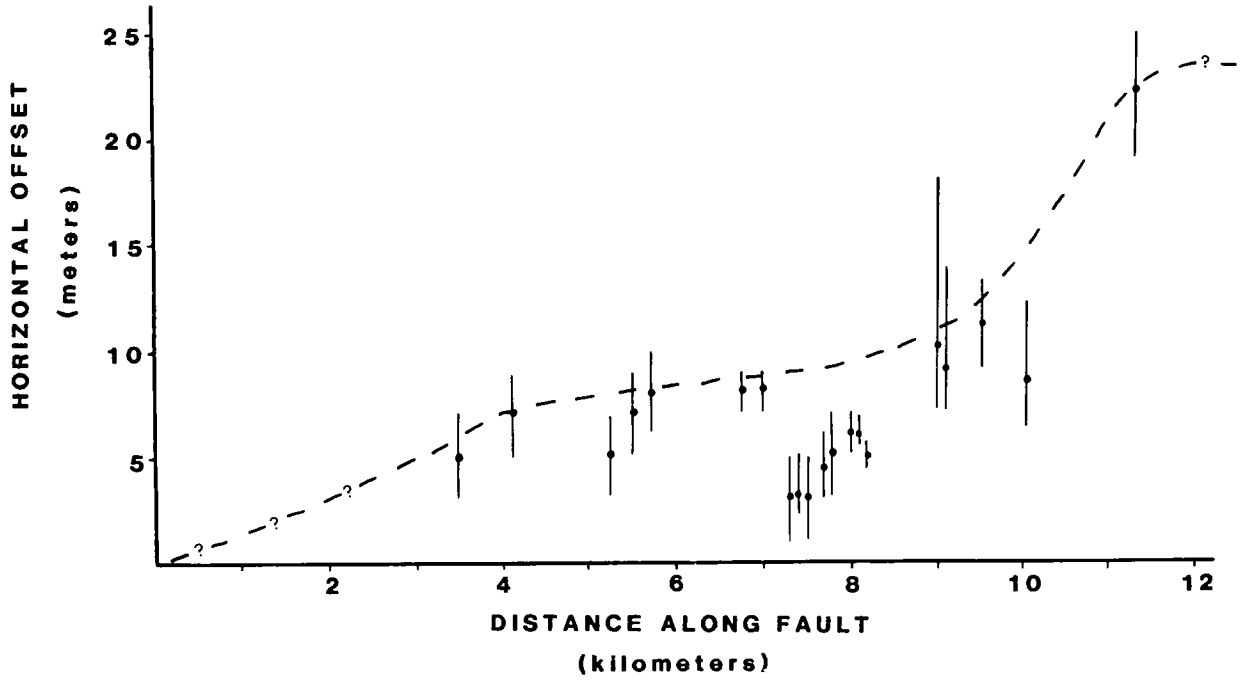

Figure 6. Graph of the lateral component of Quarternary displacement along the Meers fault (covering only the northwestern third of the fault, in Post Oak Conglomerate).

placements evident in an exhumed topographic surface, as has been suggested (Tilford and Westen, 1985). This work shows that displacements can be determined long after the occurrence of seismic events causing ground ruptures. Figure 5 shows vertical offset between the western end of the fault and the East Cache Creek flood plain. Rupture farther east is on the Fort Sill Military Reservation and has not been field-checked. Measurements of vertical offset (using the procedure depicted in Fig. 7) are easily obtained along this fault, due to the low topography, discrete fault zone, and subvertical fault orientation. Fifty-five screened data points representing the vertical separation of the original ground surface are plotted in Figure 5. Error bars are shown, indicating the intuitive upper and lower limits within which the actual displacement value could realistically lie. These plus-or-minus values are generally a few tenths of a meter or less for the western part of the fault in the Post Oak Conglomerate and a few to several tenths of a meter to the east in the Hennessey Shale.

An enveloping surface is shown enclosing the data points and is assumed to be an approximation of the cumulative offset across the zone represented by the existing scarp. A comparison of offset measurements and geodetic surveys for displacements during the 1906 San Francisco earthquake on the San Andreas fault shows that offset of discrete features taken for measurements generally approached or lay beneath the determined geodetic displacement (Fig. 8). One data point in this plot lies ~1 m above the geodetic measurement. This geodetic survey had a large plus-or-minus value and is an average for >50 km of the fault, so this may be misleading. Points that lie beneath the envelope may represent areas where either an older scarp was completely eroded (as will be discussed later) or additional deformation occurred by Riedel shears, warping, or other forms.

There is an apparent increase in offset ~9 km from the northwestern end of the surface rupture (Fig. 5). This approximately coincides with an area of the fault where a slight bend exists (Fig. 9), and roughly coincides with a possible increase in lateral displacement (Fig. 6). With left-lateral displacement, this would be a restraining bend which could be restricting offset of west-propagating rupture.

A left-lateral component of displacement was recognized by Donovan and others (1983). Offset measurements plotted in Figure 6 were taken from ridge lines and stream lines in the Post Oak Conglomerate. This unit is resistant enough to retain this evidence of lateral offset very well. However, the shale of the Hennessey Group apparently is too easily eroded and does not retain indicators of lateral offset very long.

Due to the normal lack of good markers of lateral offset, confidence levels in Figure 6 are on the order of several meters. This is small enough with respect to the amount of offset that measurements can be fairly well constrained. A check on measuring offset of ridges is afforded by scarp heights which are accentuated on the west sides of ridges and subdued on the east sides. By measuring scarp heights on both sides of the ridge and the side-slope angles, one can calculate trigonometrically the amount of required lateral offset. Results from this treatment agree remarkably well with direct measurements.

By constructing an enveloping surface for these data and comparing this to the vertical displacement, a ratio of the lateral to vertical components can be estimated. This shows that, at least in the Post Oak Conglomerate, the lateral component dominates the vertical by a ratio ranging from about 3:1 to 5:1.

A number of observable features clearly show that the fault has a definite strike-slip history, although to what extent the various evidence is a result of the recent activity or of more-ancient activity is not well known. Features probably resulting from ancient activity include the linear fault trace, horizontal slickensides, and a conjugate joint pattern dominated by the fault trace and consistent with E–W compression. Other features that could result from either ancient or recent activity include numerous Riedel shears that, even if preexisting, experienced slip during recent event(s), and tensional (dilational) features near the bend discussed previously. Although this is a restraining bend, tension would be expected on either side, as demonstrated in Figure 10.

Two separate studies based on information derived from areas in the Hennessey Group shale have argued against a dominant lateral component of displacement, at least for the most recent event. Two exploratory trenches were dug by the Oklahoma Geological Survey just east of the Hennessey–Post Oak contact. One of their trench logs shows good continuity of thin units across a zone of brittle failure, arguing against significant lateral offset along this plane. However, at that location, brittle failure accounts for only a small part (~30 cm, or 10%) of the total vertical deformation observed in the trench, monoclinal flexure having been the primary process. Lateral offset likewise could be largely accomplished through nonbrittle deformation and would not be

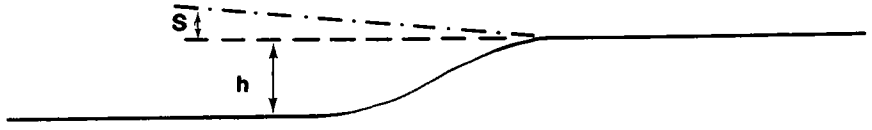

Figure 7. Method for determining vertical displacement; h = vertical displacement, s = original surface slope.

apparent in a two-dimensional plane afforded by a trench wall. An amount of lateral offset consistent with that observed to the west would call for only 1 m of brittle strike slip, assuming that the brittle failure was accomplished equally for the vertical and lateral components. The other trench showed more brittle failure and less continuity across the fault plane, but in much poorer stratigraphy. In a second study, conducted farther east (9.25 km, or 5.75 mi), by Diane Westen of Texas A&M University, samples of Hennessey shale recovered from the fault zone are reported to show near-vertical striations, but photographs of these samples indicate that this evidence is nondefinitive. Further work of this type is warranted.

Timing of Events

The fact that surface faulting was apparent in two such contrasting lithologies was recognized as evidence of recency (Donovan and others, 1983), and detailed studies of scarp morphology led to independent observations by the present authors and by Tilford and Westen (1985) that the observed faulting probably occurred within the last few thousand years. Dating of soil units (Madole and others, 1985) has shown that this very recent event probably occurred ~1,100 yr ago.

Comparison of vertical offset measurements and locations of major stream lines (Fig. 5) shows an apparent correlation. Near these streams, scarp heights are, in general, roughly half the total scarp height represented by the enveloping surface. This holds true more in the Hennessey shale than in the Post Oak Conglomerate. At the 13-km point, the Oklahoma Geological Survey dug two exploratory trenches. Stratigraphic units in these trenches showed 2.5–3 m of vertical displacement in one event. These units range in age up to ~12,000 yr and thus indicate a recurrence interval ≥10,000 yr. This is much longer than recurrence intervals determined for New Madrid or Charleston.

It thus appears that one or more faulting events occurred before 12,000 yr ago, creating a scarp that was completely eroded near stream lines, but at least partially retained where unaffected by streamflow. The climate at the end of the Pleistocene was much wetter, so there was probably sufficient streamflow to erode a scarp in the Hennessey shale. The Post Oak Conglomerate, being more resistant and having a surface higher above the water table, apparently was less affected. It is uncertain whether this represents

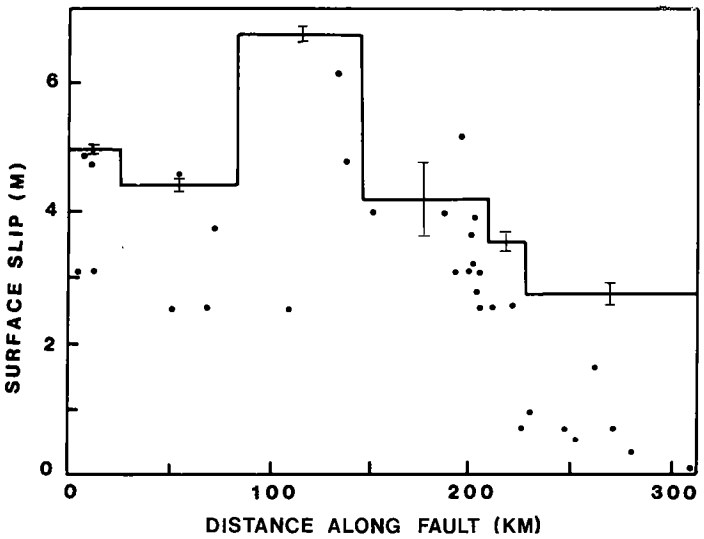

Figure 8. Offset measurements and geodetic surveys from the 1906 San Francisco earthquake on the San Andreas fault (adapted from Thatcher, 1975).

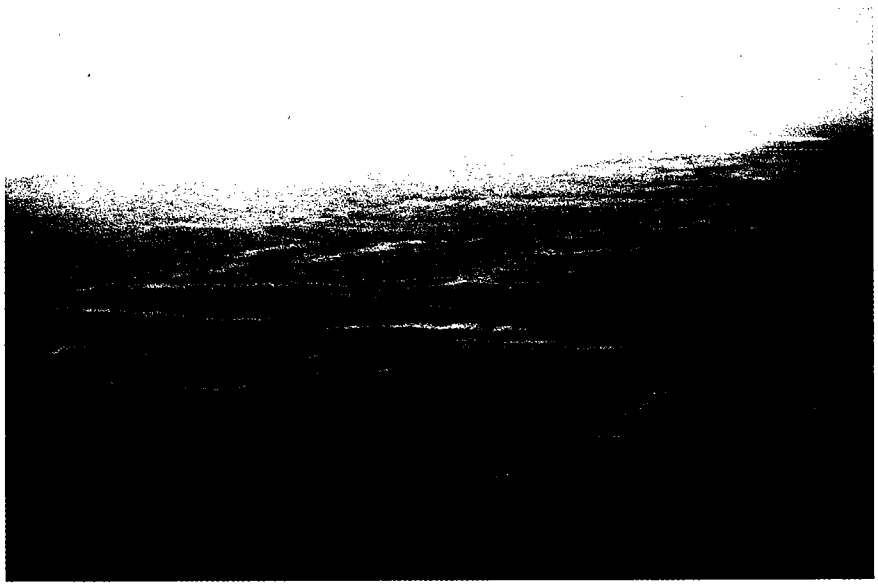

Figure 9. Photograph showing restraining bend in Post Oak Conglomerate along the Meers fault 7–10 km from the northwestern end of surface rupture (Fig. 5). View east-southeast.

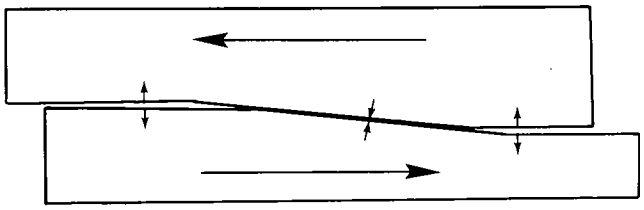

Figure 10. Model predicting dilation along a strike-slip fault on either side of a restraining bend.

two characteristic events or more than two noncharacteristic events.

DRIVING MECHANISMS

Historical earthquakes, such as the New Madrid series or the Charleston earthquake, and paleoearthquakes such as the Meers, serve to remind us that "mid-plate" areas are subjected to crustal stresses, and that—given the right combination of fault orientation and strength, time, and stress orientation—earthquakes just as devastating as those at plate boundaries can occur.

As methods of measuring stress in the crust have been refined and stress data have been amassed, it has become increasingly obvious that almost the entire central and eastern U.S. is subjected to a uniform, horizontal compressive stress oriented ENE–WSW to NE–SW (Zoback and Zoback, 1980). The region around the Meers fault has been determined to fit this pattern very well.

Fault-stress relationship models developed by various workers constrain the relative displacement that can be expected based on fault-plane orientation. The Meers fault and the Amarillo–Wichita uplift have WNW trends. Given this orientation and the existing ENE–WSW compression, left-lateral displacement would be predicted. This situation has been observed in geomorphic features on the Meers fault and is supported by a composite focal mechanism for an earthquake swarm near Enola, Arkansas (Haar and others, 1983).

The large component of vertical, up-to-the-north displacement indicates that the situation may be more complex than simple horizontal compression. While reverse faulting can occur under horizontal compression if the fault strikes at a great enough angle to the direction of greatest compression, this should occur along a moderately dipping surface. The Meers fault is oriented about 50–60° to the direction of compression. This angle may be large enough to induce a component of reverse displacement, but the fault dip is believed to be nearly vertical. Vertical stress may be caused by basinal effects, but these appear to play a subordinate role.

MAGNITUDES

Estimation of the maximum size of seismic events that could be expected for future rupture of the Meers or other faults of this zone is important for seismic-hazard evaluations of this and tectonically similar regions. Comparison of damage areas from large historical earthquakes in the U.S. (New Madrid and Charleston in the east, and San Francisco and San Fernando in the west) shows that events in the eastern U.S. cause damage over a much greater area (Fig. 11). Although this is largely due to lower attenuation of seismic waves, some studies indicate that the events are of greater magnitude.

The most common indicator used for quantification of earthquake size is magnitude. This is usually expressed in either Richter (ML, or local magnitude) or surface-wave (Ms) magnitude. Various magnitude scales are based on measurement of seismic waves with differing wavelengths. No scale can be used for all sizes of events. A good discussion on magnitude scales is given by Kanamori (1983).

Linear regressions have been developed from large historical earthquakes that relate surface-rupture length and maximum displacement to Ms (Slemmons, 1982; Bonilla and others, 1984). Magnitudes of prehistoric events can thus be estimated if rupture length and maximum displacement can be determined. Data sets of just over 50 screened values have been used in these studies and are grouped by fault type and region. A "mid-plate" fault such as the Meers fault is in a region without enough historical seismic activity to allow comparison with faults in similar regions. There are possibly significant differences between these faults and those used in the regression analyses, due to differences in crustal thicknesses, mantle structure, strain rates, and/or recurrence intervals. If these differences are ignored, regression analyses give an estimated magnitude for the Meers fault of 6.75–7.5.

Current ongoing studies on seismic risk in the eastern U.S. indicate that these relations may yield low magnitude estimations. The vast majority of historical earthquakes have occurred at or near tectonic plate margins. The few "intraplate" events have been shown to be different than their "interplate" counterparts in that they rupture with high stress drops, thus having greater displacements and larger magnitudes for a given rupture length. Scholz and others (1986) have indicated that displacements during intraplate events average 6× those of interplate events. The large displacements, with respect to surface-rupture length, evident for the Meers fault support this interpretation. The exact displacement is not well known, but it appears to be several meters. From Figure 12, it can be seen that this is a larger-than-normal displacement.

Kanamori and Allen (1985) believed that this greater displacement is due to the slip rate and recurrence interval. A fault with a low slip rate has a much greater chance to "heal" between events. A greater amount of stress accumulation and release is thus allowed, resulting in "high stress drop" when the fault ruptures. This relation of recurrence interval, rupture length, and magnitude shows definite correlation, although there is a large scatter of data.

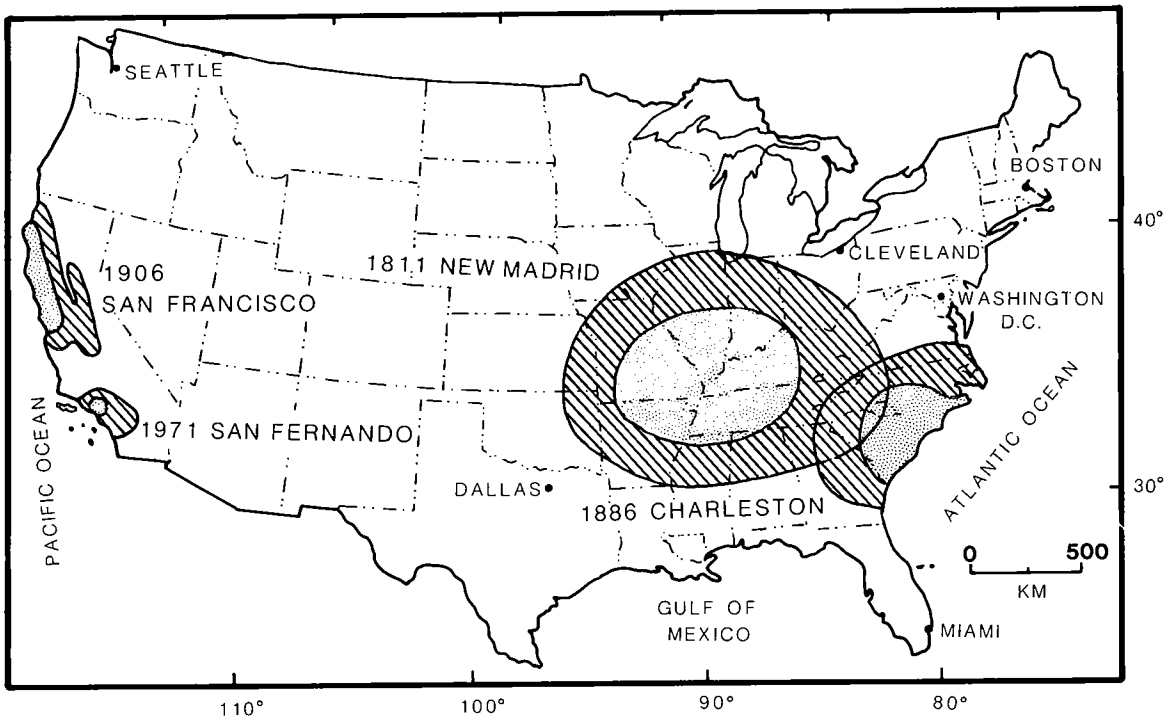

Figure 11. Comparison of damage areas for large historical earthquakes. Eastern earthquakes affect much larger areas. Lightly ruled areas correspond to Modified Mercalli Intensity VI to VII; densely ruled areas correspond to MMI VIII or greater (adapted from Nuttli, 1979).

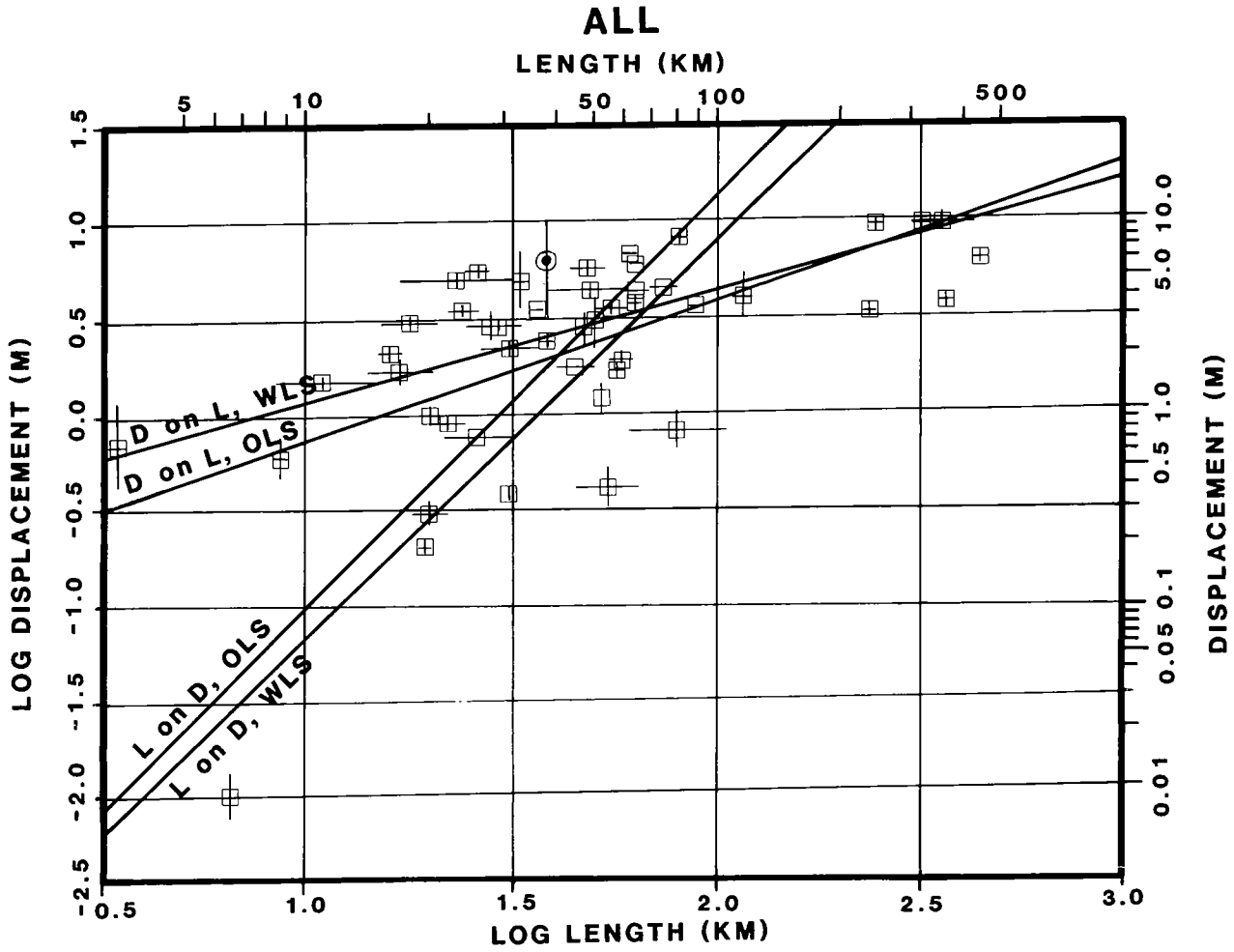

Figure 12. Length vs. displacement for historical earthquakes (from Bonilla and others, 1984). The Meers fault, shown by a circle, lies near the top of the data array. This relative position is believed to be characteristic of intraplate events (see text). Error bar ranges from pure dip-slip to 4:1 lateral displacement. Displacement is believed to be near the top of this range.

The Meers fault apparently has a recurrence interval ≥10,000 yr. By this treatment, a fault of 37-km length with a recurrence interval >2,000 yr would be expected to have earthquakes of magnitude ~7.5 or greater.

Relationships showing differences between intraplate and interplate earthquakes have been developed on the basis of "intraplate" events that are subject to plate-margin influences and are intermediate between those interplate events and mid-plate events such as that on the Meers fault (Scholz and others, 1986). There have been too few historical mid-plate events to determine the extent to which these differences hold true away from plate-margin influences. We would intuitively expect mid-plate events to bear these relations out even more strongly. Thus, an earthquake on the Meers fault of magnitude 7.5–8 is possible.

CONCLUSION

The Meers fault is very unusual in that it is one of only a few known active faults in a mid-continental region. Understanding of this fault could greatly aid in our comprehension of tectonic processes and seismic hazards in the eastern U.S. and other intraplate areas. Much remains to be learned about the Meers fault, but some aspects have been determined.

Recent displacement seems to have occurred along a reactivated Paleozoic strike-slip fault. This fault is subvertical, trends N. 60° W., and is part of the complex Wichita Mountains frontal fault system, which bounds the north side of the Wichita uplift. Information gathered along the Amarillo–Wichita–Arbuckle uplift indicates that this entire zone may have the potential to cause large-magnitude earthquakes.

Surface rupture on the Meers fault extends onto Fort Sill Military Reservation and has a length of 37 km (23 mi). Quaternary displacement apparently has a left-lateral component dominating an up-to-the-north component by about 3:1 to 5:1. Vertical displacement reaches a maximum of ~5 m, and lateral displacement reaches at least 12 m, and probably 20 m. This occurred during at least two events, the most recent accounting for roughly half of the vertical displacement and an undetermined amount of lateral displacement. The most recent event is very young and is estimated to have occurred ~1,100 yr ago. Previous events were apparently pre-Holocene, indicating a recurrence interval ≥10,000 yr.

The displacements observed at the surface require large-magnitude events. Comparison of surface rupture length to historical events causing surface rupture indicates a maximum expectable earthquake magnitude >6.75. Recent studies indicate that earthquake magnitudes are higher in mid-plate regions, and that magnitudes of 7.5–8 are possible on the Meers and other faults of this region.

Further work is needed for better understanding of age(s) of pre-Holocene event(s), relations of activity on the Meers fault to the Amarillo–Wichita–Arbuckle uplift, sense and amounts of individual displacements, and prehistoric earthquakes.

Oklahoma Geological Survey Guidebook 24, 1986

THE MEERS FAULT: QUATERNARY STRATIGRAPHY AND EVIDENCE FOR LATE HOLOCENE MOVEMENT

Richard F. Madole

INTRODUCTION

The Quaternary geology along the Meers fault was studied to determine whether or not movement had occurred on this feature during Quaternary time. Attention was focused on the southeast half of the area where a prominent scarp is associated with the Meers fault, because the valleys there have an alluvial stratigraphy that can be used to date movement on the fault. The scarp is more striking in the northwest half of the area, where the Meers fault offsets the resistant Post Oak Conglomerate, but the potential for dating fault movement is poor in that area, because Quaternary alluvial deposits are sparse. Relief is greater on the Post Oak Conglomerate, and streams flow in relatively steep, narrow valleys. On the upthrown (northeast) side of the fault, the streams have removed most of what little alluvium might have floored the valleys and have incised channels into bedrock. Downstream (southwest) from the fault, aggradation has dominated; cutbank exposures are shallow, and recent flood deposits conceal older alluvium over much of the area.

Two valleys that cross the southeast half of the Meers fault offer the greatest potential for study. These are the valley of Canyon Creek and the valley of an unnamed stream referred to informally in this report as "Browns Creek" (Fig. 1, areas 1 and 2). The valley of Canyon Creek is the largest intersected by the fault and has the most extensive sequence of alluvial deposits. The valley of Browns Creek is the second-largest intersected by the fault, and has the only exposure of the Meers fault displacing Quaternary deposits.

ALLUVIAL STRATIGRAPHY

Six fluvial allostratigraphic units were identified in the areas studied (Figs. 2,3). The units range in age from late Holocene to middle Pleistocene, and possibly even to early Pleistocene. Five units are believed to have regional distribution, but the sixth unit exists only in close proximity to the fault, to which it is genetically related. Because of the special nature of the fault-related deposits, they are discussed separately. The alluvial units are identified and correlated by (1) their position in the landscape, (2) superposition and crosscutting relations, and (3) differences in the soils formed in them (Fig. 4).

Allostratigraphic units (North American Commission on Stratigraphic Nomenclature, 1983) are defined by the discontinuities that bound them, rather than by differences in lithology. Lithologic characteristics may be useful for identifying units within a given drainage basin, but not between drainage basins, unless the basins are underlain by similar rock types and the streams are of similar size. A given unit differs lithologically from one drainage basin to another in much the same way as do present-day stream deposits. Therefore, detailed descriptions of lithology are not given for each unit in this report.

Differences in soil development, particularly depth of leaching and carbonate morphology (Gile and others, 1966), are useful for identifying and correlating units. The degree of soil development is also used to estimate the ages of the deposits and to check the reasonableness of ^{14}C ages. However, soil data must be interpreted carefully, because erosion has removed the upper part of the soil profile in many places, especially on the older Pleistocene deposits.

Lake Lawtonka Alluvium

The Lake Lawtonka alluvium is the oldest recognized unit in the area, and may include deposits of more than one age. Individual deposits of alluvium are difficult to relate to each other or to paleovalley systems, because they are poorly exposed and widely separated. The deposits are on the higher parts of interstream areas (Fig. 4) and clearly predate formation of the present-day valley system. Some deposits are near and approximately parallel to present-day streams, whereas others are remote from them. The topography has inverted since the Lake Lawtonka alluvium was deposited.

Stratigraphic information about the Lake Lawtonka alluvium is limited to observations in a few shallow road cuts. The distribution of Lake Lawtonka alluvium is inferred partly from the distribution of the Lawton soil series (Mobley and Brinlee, 1967), the principal soil developed in this alluvium. Most deposits of Lake Lawtonka alluvium are estimated to be 2–5 m thick and composed mainly of

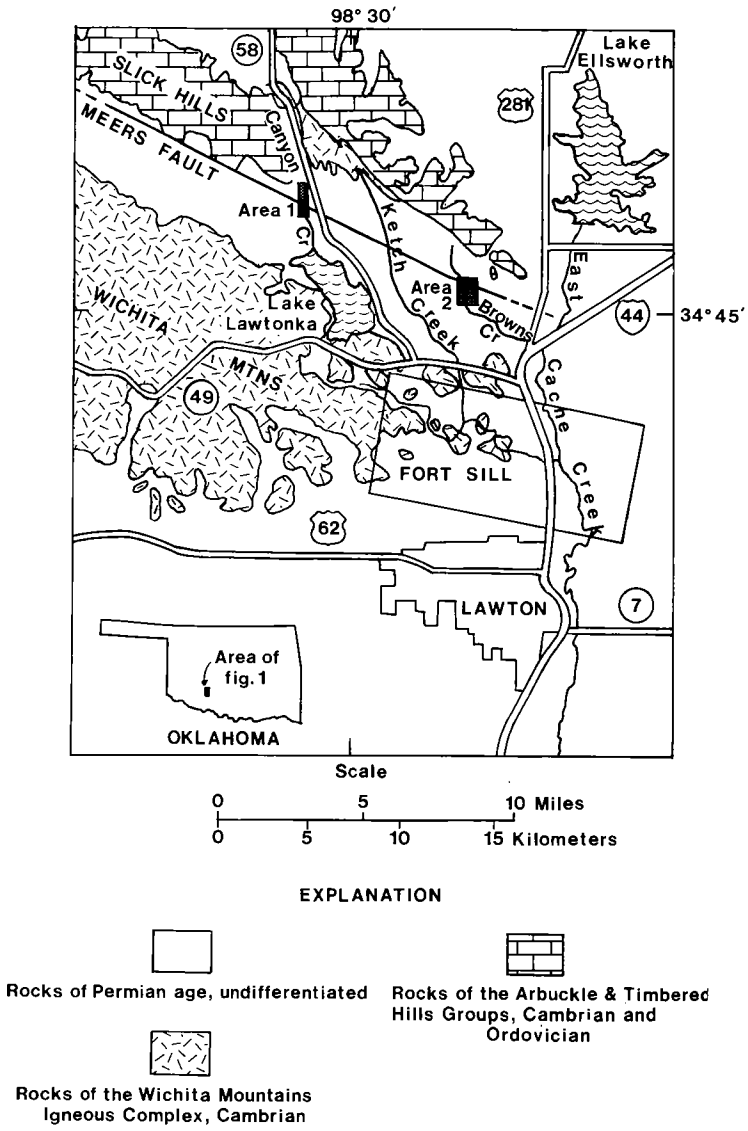

Figure 1. Generalized bedrock geologic map, showing the location of the Meers fault and the two study areas.

reddish-brown gravel overlain by thin-bedded fine sand, silt, and clay. Estimates of thickness and lithology are based in part on a presumed similarity to Porter Hill alluvium, which is better exposed.

The Lake Lawtonka alluvium is at least as old as middle Pleistocene (defined here as 790,000–130,000 yr), and is possibly as old as early Pleistocene (1.7 m.y. to 790,000 yr). The age of the unit is estimated on the basis of its position in the landscape and the strongly developed soil formed in it. The soil is thicker, redder, and more clayey than soils developed in the other units, and it appears, at least locally in two road cuts, to have a K horizon with stage-III carbonate morphology (Gile and others, 1966).

Stage-III carbonate morphology is characterized by essentially continuous coatings of carbonate that impart a white color to the soil. Stage-II carbonate morphology also is present in some soils in this area. Stage II differs from stage III in that carbonate coatings are not continuous. Stage II in non-gravelly parent materials is characterized by the development of nodules, and in gravelly materials it is characterized by carbonate coatings that are generally continuous on clasts, but discontinuous in the matrix.

Depth of leaching in the Lake Lawtonka alluvium is as much as 1.9 m. The Lawton soil series is defined as having been developed in non-calcareous alluvium. However, judging from the younger alluvial deposits, most alluvium in this area was initially calcareous. Therefore, the non-calcareous character of the Lawton soil in this area is attributed to leaching over a long time, rather than to derivation from non-calcareous sources.

Porter Hill Alluvium

The Porter Hill alluvium is a stream-terrace deposit that, unlike the Lake Lawtonka alluvium, is related to present-day valleys (Figs. 4–6). Only one terrace was found in the study areas. Along Browns Creek, the upper surface of the terrace is about 9–14 m above stream level, and along Canyon Creek, it is ~16 m above stream level.

The Porter Hill alluvium ranges in thickness from 2.3 m to 3.9 m at five localities. Gravel is a major component of the alluvium, and the deposits show color changes throughout due to oxidation; red hues (5YR and 7.5YR) dominate (color descriptions are based on the Munsell Soil Color Chart, Munsell Color Co., Inc., Baltimore). Along Browns Creek, the lower third (1.3–1.6 m) is pebble gravel, whereas the upper two-thirds (2.1–2.5 m) is mud and sand. Almost all of the upper part has 5YR hues, and the clayey strata are heavily mottled with iron oxide and contain mottles and 1-mm specks of manganese oxide. Along Canyon Creek, Porter Hill alluvium was studied in only two exposures, a trench excavated across the Meers fault (Crone and Luza, this volume) and a road cut just south of the trench. At these two sites, the alluvium is mostly gravel, 2.5 m and 2.3 m thick, respectively, capped by ~0.5 m of finer sediment. The gravel unit consists of 25–40% clasts, predominantly pebbles, but including abundant small and large cobbles, and a few small boulders. The matrix is sticky, red, clayey sand.

The age of the Porter Hill alluvium is not known; however, its position in the landscape and the soil developed in it suggest that it is significantly older than 30,000 yr. It probably was deposited during middle Pleistocene time (790,000–130,000 yr). A detailed study was not made of the soil developed in this unit, because it is difficult to find natural exposures where a complete soil profile can be observed. In most places, erosion has stripped part or all of the relict soil. A weak stage-III carbonate morphology is developed locally in gravelly parent material.

Kimbell Ranch Alluvium

The Kimbell Ranch alluvium was observed only in the Canyon Creek area. It is similar in color and

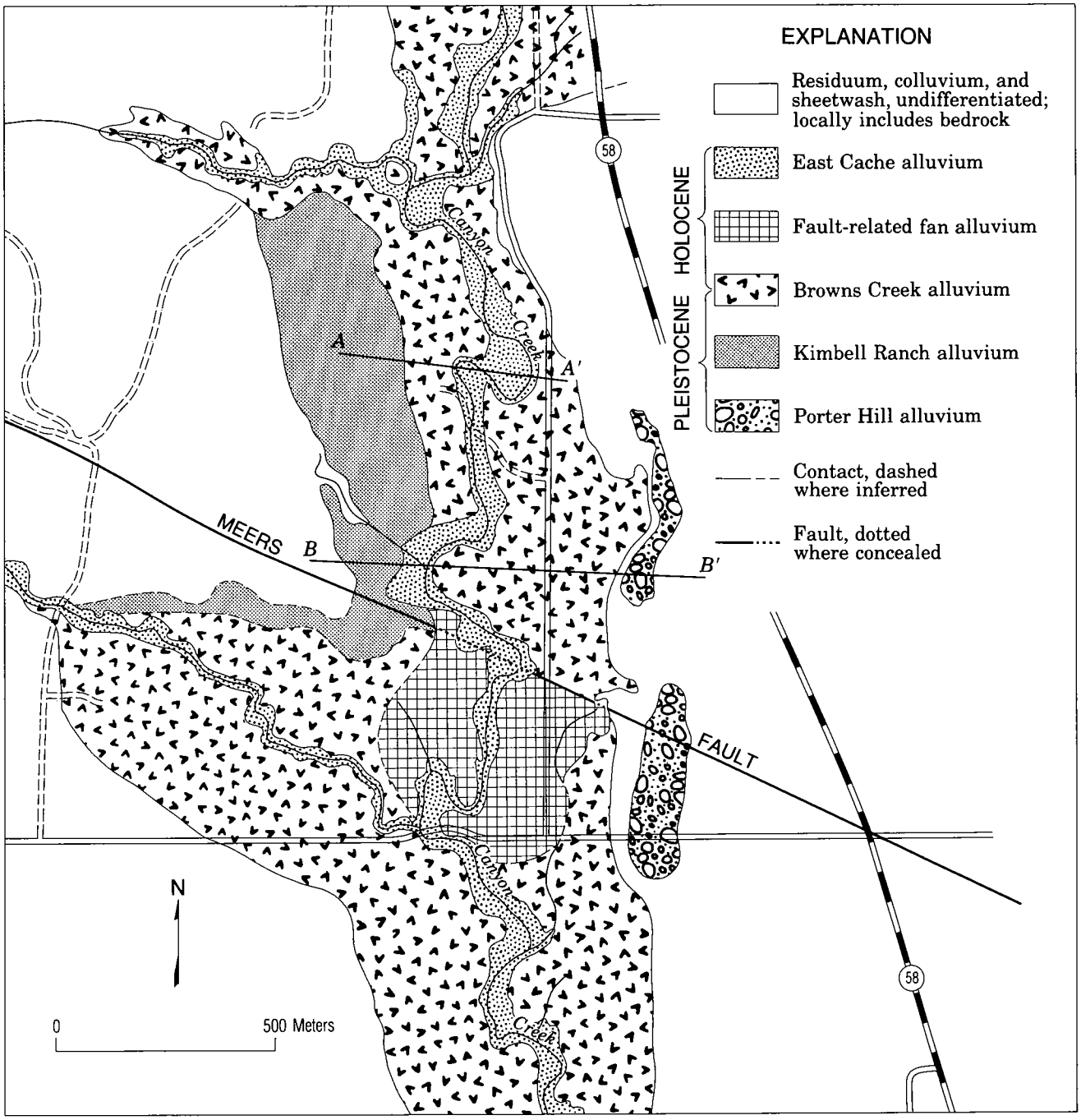

Figure 2. Map of surficial deposits along Canyon Creek (Fig. 1, area 1). Cross sections A–A′ and B–B′ are shown in Figure 5.

texture to the Porter Hill alluvium in this valley, but occupies the valley floor, rather than a terrace. The Kimbell Ranch alluvium is exposed in numerous stream cuts and gully banks along the valley axis, but is overlain by Browns Creek alluvium over much of the valley floor (Figs. 4,5). The Kimbell Ranch alluvium is easy to distinguish from the younger valley-floor alluvial deposits, because it is red and contains gravel, whereas the younger deposits are brown and are predominantly silt and clay.

The Kimbell Ranch alluvium is clast-supported pebble and cobble gravel interbedded with subordinate amounts of red, muddy sand. The coarser gravel is mostly in discontinuous beds 20–30 cm thick. Much of the Kimbell Ranch alluvium was eroded prior to deposition of the Browns Creek alluvium. The axis of the valley cut into Kimbell Ranch alluvium is now filled with the thickest sections of Browns Creek alluvium. Along this axis, only 1.4–1.5 m of Kimbell Ranch alluvium remains. The max-

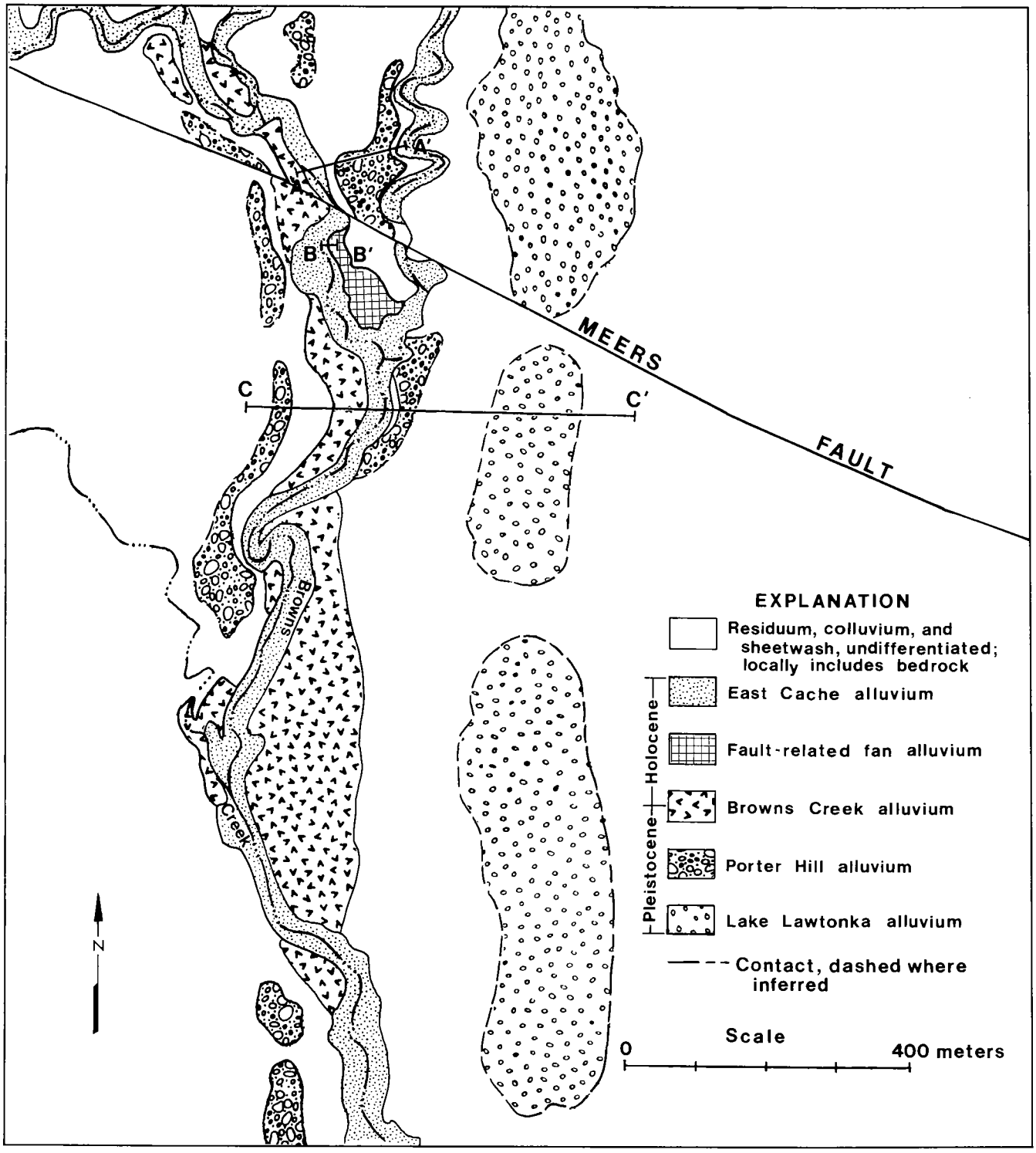

Figure 3. Map of surficial deposits along Browns Creek (Fig. 1, area 2). Cross sections A–A′, B–B′, and C–C′ are shown in Figure 6.

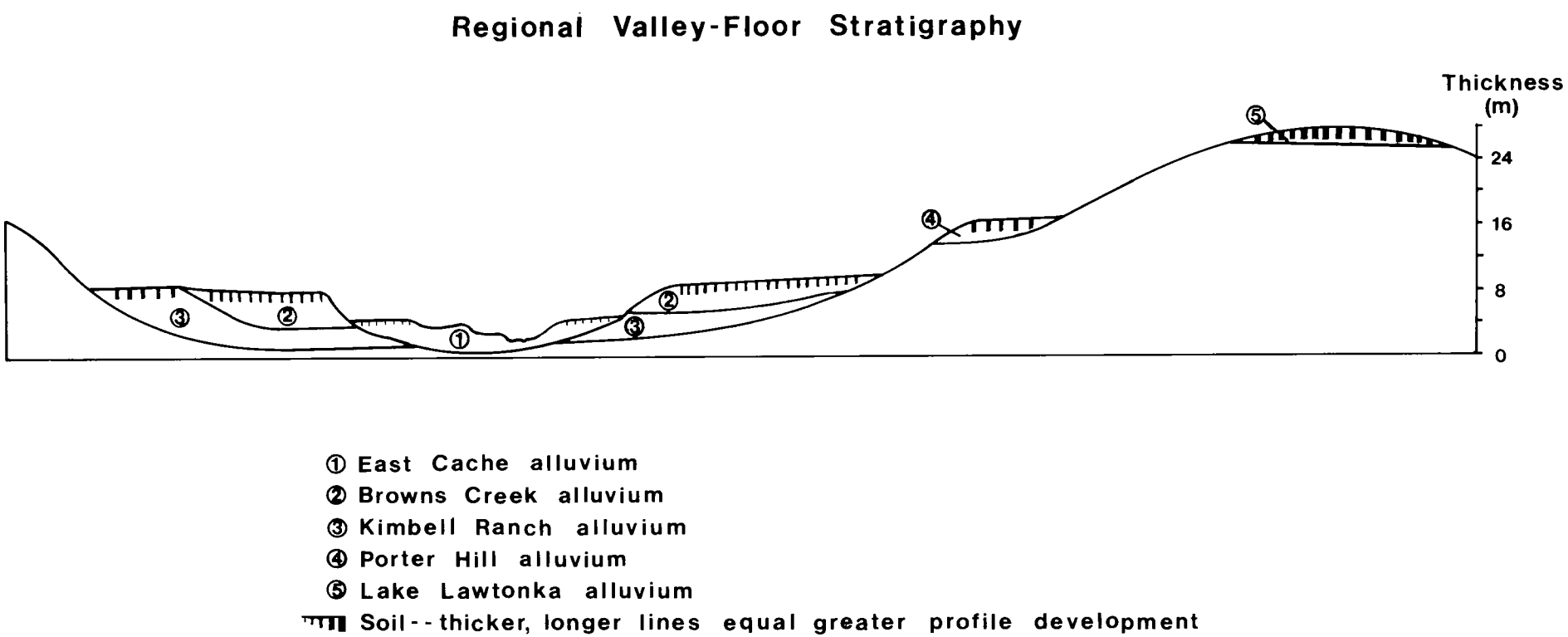

Figure 4. Schematic diagram showing stratigraphic relationships of five allostratigraphic units present along the larger streams of the area.

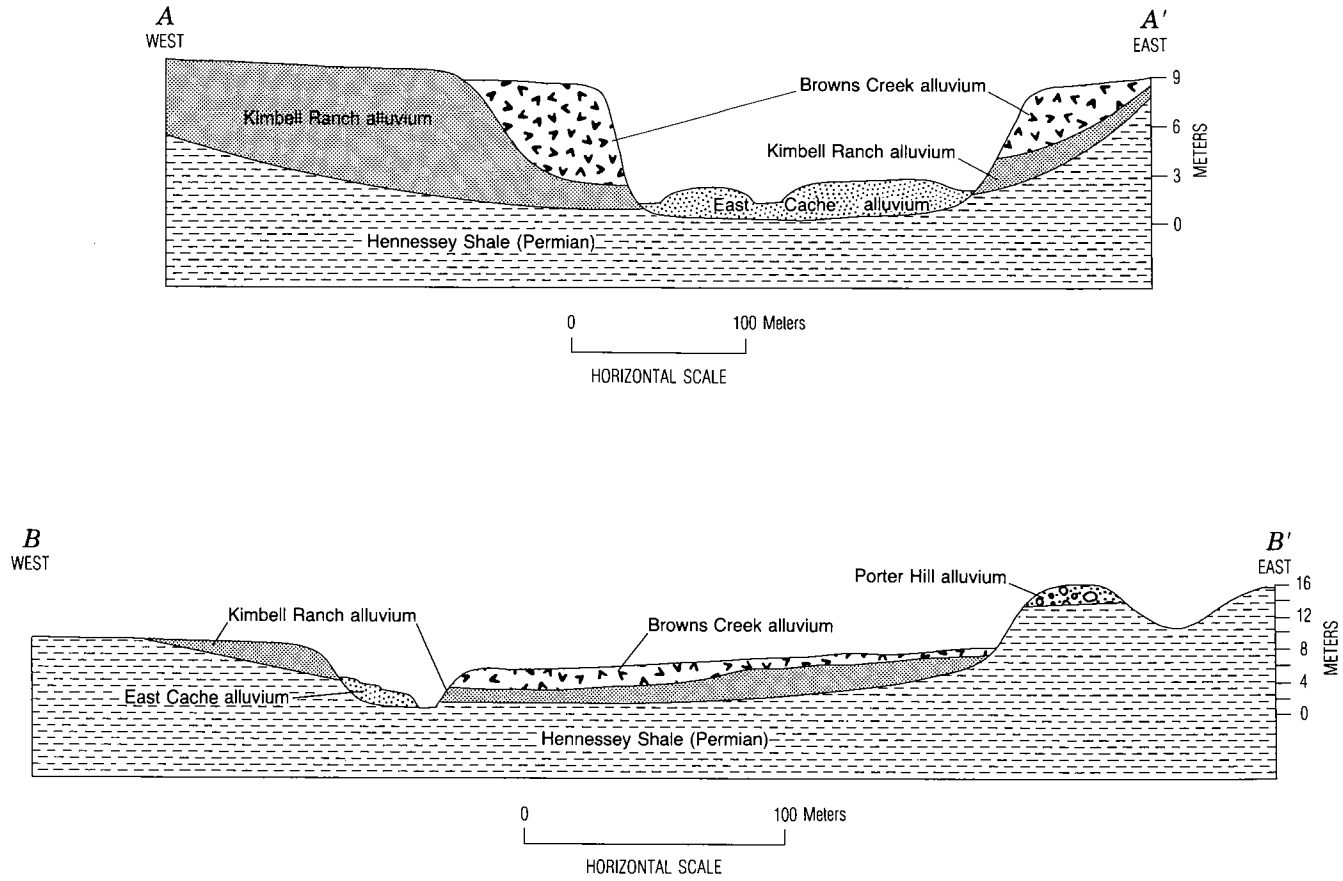

Figure 5. Cross sections showing stratigraphic relations of alluvial units along Canyon Creek. Cross-section locations are shown in Figure 2.

imum thickness of Kimbell Ranch alluvium is unknown because of poor exposure, but it is estimated to be 7–9 m.

The age of the Kimbell Ranch alluvium is not known precisely. It is older than 14,000 yr, the age of the basal part of the Browns Creek alluvium, and is judged to be significantly younger than the Porter Hill alluvium on the basis of the amount of valley deepening that occurred between deposition of these two units. Conceivably, the Kimbell Ranch alluvium could be as old as 150,000–130,000 yr.

Browns Creek Alluvium

Browns Creek alluvium underlies the modern valley floors of the area and locally forms a terrace on the upthrown side of the Meers fault because of postfaulting stream incision (Figs. 4–6). The alluvium is composed mainly of mud and sand, and is generally more drab in color than the older alluvial deposits. The color of a given alluvial unit varies more between valleys than does texture. In the valley of Browns Creek, the Browns Creek alluvium is predominantly browns of 10YR hue, whereas the older alluvial deposits are redder, mostly 7.5YR and 5YR hues. In the valley of Canyon Creek, Browns Creek alluvium is predominantly of 5YR hue, whereas the older alluvial deposits are even redder (2.5YR).

Browns Creek alluvium is 5–6 m thick in the Browns Creek area, and 6–7 m thick in the Canyon Creek area. Along Browns Creek, it is mostly thin-bedded and clayey. Stratification is weakly expressed, and most strata, except a few sandy beds, are mottled with iron oxide and minor manganese oxide. Along Canyon Creek, the contact between Browns Creek alluvium and Kimbell Ranch alluvium rises toward the valley sides, and in places the two units exist side by side at the surface (Figs. 4,5). In such places, their upper surfaces may or may not be separated by slight topographic breaks; thus, the contact between them is not easily located. The two units can be differentiated, however, on the basis of the soils developed in them.

Three ^{14}C ages of samples from the Browns Creek alluvium indicate that it began to be deposited ~14,000 yr ago (Table 1). Snails from the base of the Browns Creek alluvium along Browns Creek ~80 m upstream from the fault yielded a ^{14}C age of 13,670 ± 120 yr (sample DIC-3166). At two localities along Canyon Creek, lenses of clayey sediment contained enough colloidal-sized organic matter for radiocarbon dating. At one locality ~1 km downstream from

the fault, an organic-rich lens of clayey sediment at the base of the Browns Creek alluvium where it unconformably overlies red gravel of the Kimbell Ranch alluvium had an age of 12,240 ± 240 yr (sample DIC-3170). At a locality ~50 m upstream from the fault, a less-clayey and less-organic-rich lens of sediment, 70–90 cm above the contact with the Kimbell Ranch alluvium, provided a ^{14}C age of 9,880 ± 160 yr (sample DIC-3179).

Differences in the soils formed in Browns Creek alluvium suggest that it probably includes deposits of two ages. Most of the unit is of late Pleistocene age, but over large areas the uppermost 1–1.5 m may be Holocene. The soil profile in Browns Creek alluvium upstream from the fault on Browns Creek consists of A/Bt/Bk/C horizons. Collectively, the A and Bt horizons are ~75 cm thick. Soil structure is strongly developed, and clay films are present in the Bt horizon, largely because of the high percentage of clay in the strata in which this soil formed. Clay content is 28% in the A horizon, 31% in the Bt horizon, and 40% in the Bk horizon. Carbonate has been leached to a

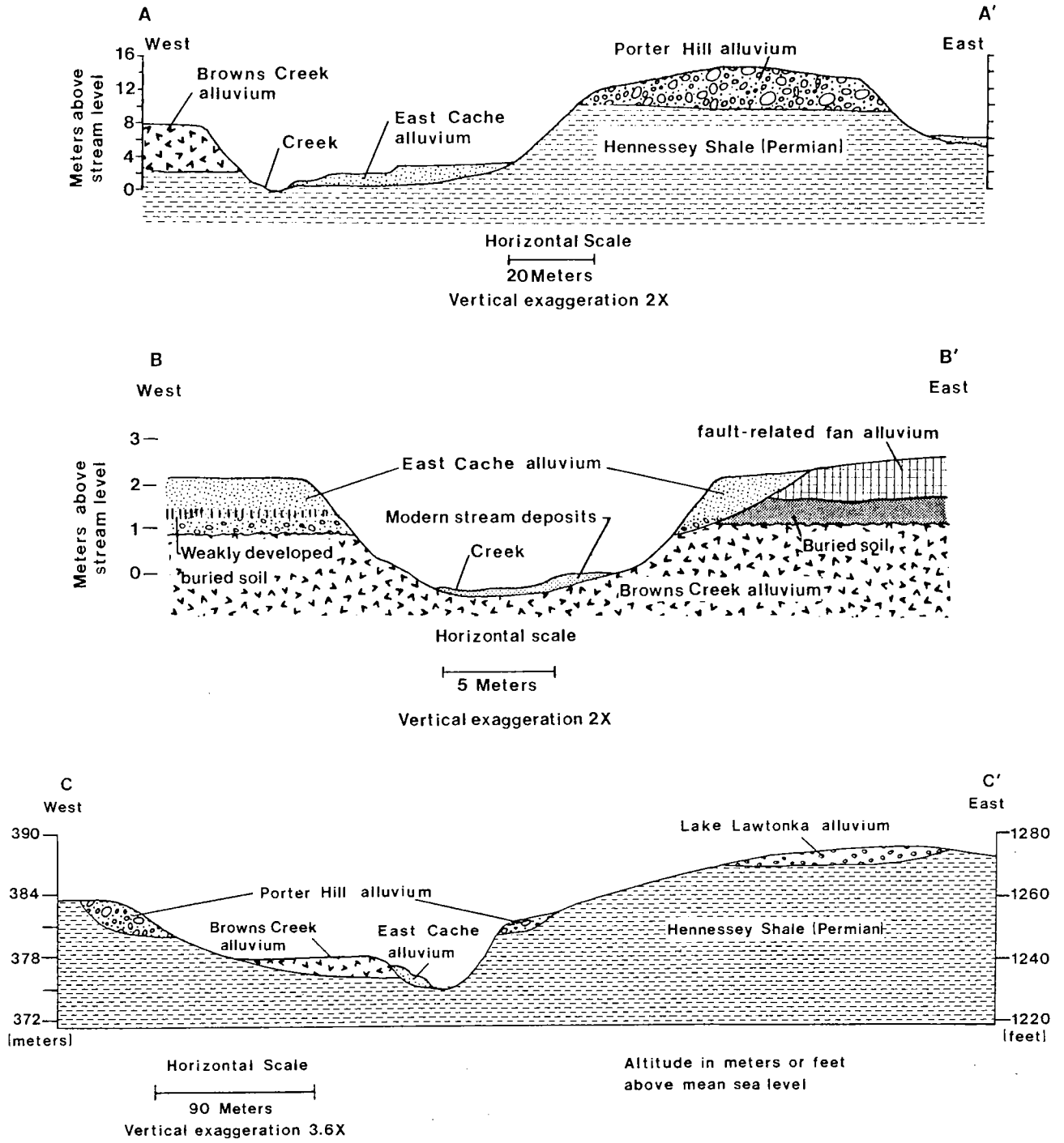

Figure 6. Cross sections showing stratigraphic relations of alluvial units along Browns Creek. Cross-section locations are shown in Figure 3.

TABLE 1.—RADIOCARBON AGES OF ALLUVIAL DEPOSITS USED TO DATE MOVEMENT ON THE MEERS FAULT

Stratigraphic unit	^{14}C age	Laboratory no.	Stratigraphic position	Material
East Cache alluvium	70 ± 150	DIC-3165	Near floor of present stream channel	Charcoal and carbonized wood
	310 ± 150	W-5533	Same interval as above	Clay–humus
	470 ± 150	W-5540	35–55 cm above bottom contact	Soil humus
	600 ± 50	DIC-3161	1.6 m above bottom contact	Charcoal
Fault-related alluvium	1,280 ± 140	DIC-3167	Beneath bottom contact	Charcoal
	1,360 ± 100	DIC-3169	"	Soil humus
	1,740 ± 200	W-5543	"	Soil humus
Browns Creek alluvium	9,880 ± 160	DIC-3179	70–90 cm above bottom contact*	Clay–humus
	12,240 ± 240	DIC-3170	25–30 cm above bottom contact	Clay–humus
	13,670 ± 120	DIC-3166	5–30 cm above bottom contact	Snails

*This sample is at least 1–1.5 m higher stratigraphically than the other two samples from this unit.

depth of ~75 cm, but below this depth, secondary carbonate is prominent over a zone a little more than 1 m thick (Bk horizon). The upper 35 cm of this zone contains abundant carbonate nodules (Stage II morphology), 5–10 mm long.

The other soil series widely associated with the valley floors of the area, the Port series (Mobley and Brinlee, 1967), contrasts with the soil described above. Soils of the Port series are weakly developed, as are most soils developed in deposits of Holocene age. Characteristically, the Port soil is thick and dark colored. The profile of the Port loam examined in cutbanks along Canyon Creek consists of A/AB/Bk/C horizons and typically is leached to depths of 35–45 cm. The Port loam lacks a B horizon, but exhibits stage-II carbonate morphology in the form of abundant small nodules (5–12 mm long, 2–5 mm wide) and a perceptible whitening of the Bk horizon. Accumulation of this much secondary carbonate generally requires thousands of years. The Port soil is estimated to be at least several thousand years old, but substantially less than 10,000 yr. The soil is much more developed than the soil in fan alluvium (discussed later), which represents ~1,000 yr of pedogenesis, but it is younger than the sediment from the lower part of the Browns Creek alluvium (sample DIC-3179) that provided the 9,880 ± 160 yr age.

According to Mobley and Brinlee (1967, p. 53), buried soils are commonly found at depths of 75–150 cm in areas where the Port soils are developed. Unequivocal evidence of an unconformity in the upper part of the Browns Creek alluvium was not found, but a stratigraphic break exists that is nearly coincident with the bottom of the Port soil. This break was initially attributed to bioturbation, but it may be an unconformity. However, until better physical evidence of an unconformity is found, or until ^{14}C ages demonstrate its existence, this valley-floor alluvium will be treated as a single unit.

East Cache Alluvium

East Cache alluvium is the youngest unit and is present in relatively narrow bands along present-day streams (Figs. 2–4). It fills channels cut into the older valley-floor alluvial units, or through these units into bedrock (Figs. 5,6). Two terraces are cut into the East Cache alluvium in most places (Fig. 6). Along Browns Creek, the upper surface of the unit is ~3 m above stream level, and the two terraces are at 2 m and 1 m above stream level. The terraces along Canyon Creek are only a little higher (2.0–2.2 m and ~1.5 m), but are more uneven, because of a greater amount of flood erosion and deposition on them. These terraces appear to be mainly cut surfaces, rather than separate alluvial fills; even so, they mark times of stability between episodes of channel incision.

The East Cache alluvium is 1.2–3.5 m thick and calcareous; it ranges from clayey sand to mud composed of nearly equal amounts of sand, silt, and clay. Because of its high silt and clay content, the unit commonly maintains steep stream banks and is hard when dry. Stratification is generally absent to weak. Although the alluvium is calcareous, it does not contain accumulations of secondary $CaCO_3$.

Four ^{14}C ages indicate that the East Cache alluvium is latest Holocene in age (Table 1). Although the upper and lower age limits of this alluvium are not known precisely, I believe it was deposited between 800 and 100 yr ago. A large fragment of clean charcoal from near the middle of a 3-m-thick section along Canyon Creek had an age of 600 ± 50 yr (sample DIC-3161). Humus from a thin, buried A horizon within this alluvium on the west side of Browns Creek ~40 m downstream from the Meers fault provided an age of 470 ± 150 yr (sample W-5540). Charcoal and carbonized plant fragments in a cut-and-fill deposit along the present channel of Browns Creek had an age of 70 ± 150 yr (sample DIC-3165), and

colloidal organic matter from this deposit had a ^{14}C age of 310 ± 150 yr (sample W-5533).

Narrow stream channels have been incised into the East Cache alluvium to depths of ~3 m. Radiocarbon ages and historical data indicate that these channels were incised pior to 100 yr ago. The 70 ± 150 yr ^{14}C age cited above (sample DIC-3165) provides an imprecise minimum age for the time of incision. Also, East Cache Creek, the principal stream of the area, had incised its channel to depths of as much as 8 m before 1884, the date on the stone foundation of an abandoned bridge built across the channel at Fort Sill (Hall, 1978). Although dendrochronologic data were not collected, many large trees rooted in the bottoms and sides of channels cut in the East Cache alluvium appear to be 100 years or more old.

The soil formed in the East Cache alluvium consists of a weakly developed A/C profile. The A horizon is very dark gray (10YR 3/1, moist) to very dark grayish brown (10YR 3/2, dry), and is typically 16–18 cm thick. The C horizon is dark brown (7.5YR 4/4, moist) to brown (7.5YR 5/4, dry). This alluvium is unleached or is leached only in the upper 1–2 cm, and does not contain accumulations of secondary carbonate. Little or no A horizon has formed on the terraces, suggesting that they were cut well after the main body of alluvium was deposited. The weakly developed soil indicates an age for this unit that is consistent with that determined by radiocarbon dating.

FAULT-SCARP ALLUVIAL DEPOSITS

Deposits of sheetwash and fan alluvium are found locally on the downthrown side of the Meers fault. The fan alluvium was deposited where the fault displaced streams, and the sheetwash accumulated along the foot of the fault scarp in interstream areas. These deposits are of such limited extent and so widely scattered that it is difficult to characterize them as a unit. Nevertheless, they are important deposits for dating recent movement on the fault. Much of this alluvium is coeval with faulting, or closely postdates faulting. Where exposed, as along the larger streams of the area, the fault-scarp alluvial deposits can be related to other stratigraphic units that both predate and postdate faulting.

Sheetwash

Sheetwash, being the product of unconfined runoff, is generally not dissected by streams and, therefore, is generally not well exposed. However, it is well exposed in a cutbank where Browns Creek crosses the fault (Fig. 7). The sheetwash is dark colored and resembles a soil having an overthickened A horizon, but the dark color was inherited largely from soil eroded from the fault scarp, rather than from pedogenesis in place. Because the vertical component of displacement that formed the scarp was high-angle reverse movement, and most of the topographic offset was produced by warping, rather than by displacement that produced a free face (Crone and Luza, this volume), soil would have remained on most of the scarp initially. This soil was subsequently stripped as erosion beveled the warp, and a weakly developed A/C soil profile formed on the beveled surface.

The soil on the fault scarp in the cutbank along Browns Creek consists of an 18-cm-thick, unleached, calcareous A horizon over parent material (C horizon). A similar soil is formed in Browns Creek alluvium on the fault scarp near Canyon Creek (trench 1, Crone and Luza, this volume). At this locality, the thick, dark-colored Port loam has been stripped from the fault scarp and redeposited at the foot of the scarp. This sheetwash, like that along Browns Creek (Fig. 7), is dark colored and as much as 1 m thick.

Fault-Related Fan Alluvium

Small but morphologically distinct alluvial fans formed where the fault displaced small ephemeral streams and gullies; the best examples are in the Slick Hills (Fig. 8). Larger, but less distinct fans formed where the fault displaced perennial streams; the best examples are on Canyon Creek and Browns Creek. The small fans remain essentially undissected, because the drainage areas are small and runoff is seasonal. However, the fans along the larger streams were incised in late Holocene time and younger alluvium was deposited in channels in the fans (Figs. 2,3; Fig. 6, B–B′). The stratigraphic relations in exposures along the larger streams show that the fan alluvium was deposited in response to movement on the Meers fault.

The principal evidence linking the deposition of the fan alluvium to faulting includes (1) the location and shape of the deposits of fan alluvium and (2) the presence of large, angular clasts of bedrock in the fan alluvium on Browns Creek. Fan alluvium is present only on the downthrown side of the fault, and it is thickest and has the widest lateral extent at the fault. It is at least 1.4 m thick near the fault along both Canyon Creek and Browns Creek, and was presumably as wide as the pre-fault valley floor at each of these localities. The limits of fan alluvium are difficult to distinguish, except in stream cuts, because the fans grade gradually into the surrounding landscape. Along Browns Creek, the fan alluvium extended at least 180 m down-valley from the fault, and along Canyon Creek it extended at least 500–600 m down-valley.

Deposits like the fan alluvium were not observed anywhere else in either of the drainage basins studied. If deposits like the fan alluvium were present elsewhere, it is unlikely that they would not be noticed, because the fan alluvium is conspicuous. It differs sharply in texture from the underlying pre-fault valley fill, and the pale-brown to brown color of the fan alluvium contrasts with the nearly black color of the buried soil in the underlying Browns Creek alluvium. The buried soil is commonly ~75 cm thick and difficult to overlook. The fan alluvium is mostly sand and gravel that includes large cobbles and, in places, boulders. In contrast, the underlying valley fill, in both study areas, is chiefly silty clay and clayey silt.

Figure 7. Dark-gray sheetwash overlies Porter Hill alluvium (light-colored sediment) on the downthrown side of the Meers fault along Browns Creek.

Figure 8. View to north of Meers fault displacing Post Oak Conglomerate. Ephemeral streams are incised on the upthrown side of the fault (upper part of photo) and terminate in small, undissected alluvial fans deposited on the downthrown side of the fault. (Photograph by D. B. Slemmons).

The large, angular clasts of gray sandstone in the fan alluvium along Browns Creek are as anomalous as the buried soil underlying the fan alluvium. Most of the fan alluvium is pebbly sand derived from incision of alluvium on the upthrown side of the fault. The sandstone clasts compose <5% of the deposit, but are conspicuous because of their size and angularity. Most of the sandstone clasts are 15–25 cm across, but one is a boulder measuring 85 × 33 × 25 cm (Fig. 9). This boulder is particularly anomalous in a small, low-relief drainage basin where the bedrock is chiefly shale.

The sandstone boulder links the fan alluvium to movement on the Meers fault. Similar gray-sandstone fragments were not observed in the older alluvial units along Browns Creek, and this rock type does not crop out on the valley sides. However, gray sandstone is exposed on the upthrown side of the fault and in places along the stream channel for ~200 m upstream from the fault. This is the obvious source for the sandstone clasts, but the rock was not exposed until movement on the Meers fault caused Browns Creek to incise its channel on the upthrown side of the fault. Hence, the fan alluvium on Browns Creek clearly postdates faulting. The size of the sandstone boulder and its position near the surface of the fan (Fig. 9) suggest that deposition of the fan alluvium closely postdates faulting. Incision of the valley-fill alluvium on the upthrown side of the fault probably occurred soon after faulting, because the unconsolidated alluvium would have eroded easily. The only time that stream gradient and discharge were probably sufficient to transport a nearly 1-m-long boulder a distance of 30 m was shortly after faulting had produced the 5-m-high warp in the landscape.

Newly uplifted landscapes tend to be modified quickly. Morisawa (1975) described several examples of the immediacy of modification, including the adjustment of streams to fault-induced knickpoints. Knickpoints on perennial streams in the vicinity of Hebgen Lake, Montana, formed by faulting during the 1959 Hebgen Lake earthquake were eliminated in a period of less than a year to a few years. The drainage basins of the Montana streams are comparable in size to those of Canyon Creek and Browns Creek, although the relief within the Montana basins is somewhat greater. Also, the heights of the Montana fault scarps, about 3–6 m, were similar to the Meers fault scarp. However, the scarps across the Montana streams were formed in much coarser material than the scarps across Canyon Creek and Browns Creek. The former were in boulder gravels that contained many 1-m-long boulders.

It is unlikely that the rate of fault-scarp modification along Canyon Creek and Browns Creek differed much from that along the Montana streams. If anything, modification in the Meers area was probably faster, because the finer-grained alluvial fills would have been less resistant to erosion. Hence, regrading of stream channels across the Meers fault and deposition of the fan alluvium on the downthrown side of the fault was probably completed in less than a decade. Therefore, the ^{14}C ages of materials collected from the surface buried by the fan alluvium are believed to closely date the time of faulting.

Movement on the Meers fault produced a sharp knickpoint in stream channels that crossed the fault. Streams responded to the disruption by regrading their channels across the knickpoint. Upstream from the fault, the adjustment was by degradation, and stream incision is pronounced on the edge of the upthrown block all along the surface trace of the fault. Downstream from the fault, adjustment was by aggradation, and the fan alluvium is the product of this adjustment. Along the larger streams, Canyon Creek and Browns Creek, channel incision upstream

from the fault penetrated the valley fill and exposed bedrock (Fig. 5, B–B′; Fig. 6, A–A′). Downstream from the fault, fan alluvium buried the alluvium on the valley floor (Fig. 6, B–B′).

LATE HOLOCENE MOVEMENT ON THE MEERS FAULT

The Meers fault has crosscutting relations with valley-fill alluvium and terrace deposits of at least five ages, ranging from early or middle Pleistocene to late Holocene (Fig. 10). It displaces all but the East Cache alluvium, the youngest alluvial unit, which was deposited 800–100 yr ago. Soil humus, charcoal, and carbonized wood from surfaces buried by fault-related fan alluvium provide maximum ^{14}C ages for the fan alluvium and closely date the time of faulting (Fig. 11). Similar materials from the East Cache alluvium, which is unfaulted and truncates the fault-related fan alluvium, provide a minimum age for the fan alluvium and, thus, a minimum date for faulting.

Two ^{14}C ages of charcoal from the Canyon Creek area indicate that movement on the Meers fault occurred after 1,280 ± 140 yr ago (sample DIC-3167), but before 600 ± 50 yr ago (sample DIC-3161). Faulting is thought to have occurred nearer to the older limit than to the younger limit, because deposition of fan alluvium probably began soon after the streams were displaced by faulting, and was probably complete within a matter of years. Two ^{14}C ages of soil that was buried by fault-related fan alluvium on Browns Creek provided similar limiting dates. Soil humus concentrated from the uppermost part of the buried soil provided ^{14}C ages of 1,740 ± 200 yr (sample W-5543) and 1,360 ± 100 yr (sample DIC-3169). The older age is from a site on the east side of Browns Creek ~25 m downstream from the fault, and the younger age is from a site on the west side of Browns Creek ~120 m southwest of the fault.

The agreement between the charcoal ages and the soil-humus ages is particularly good, considering that the latter represent averages (mean residence times) for humus formed over the range of time that the soil was at the surface. Soil-humus ages are minimum ages for the beginning of soil formation, and maximum ages for the time of burial. Generally, the longer the soil was at the surface, the more imprecise the soil-humus ages. Humus is stable with respect to biological and chemical attack and tends to survive for hundreds to thousands of years, depending on the environment (Paul and others, 1964; Campbell and others, 1967; Sharpenseel and others, 1968; Gerasimov, 1971). The turnover time of humus (the time between formation and disappearance) tends to be hundreds of years in forest soils and thousands of years in grassland soils. The mean residence time of the organic matter in the thin A horizon buried in East Cache alluvium (470 ± 150 yr; sample W-5540) is probably not much different than the date of burial, because the soil was at the surface for only a short time. On the other hand, the soil buried by fault-related fan alluvium contained humus that probably had an average age of at least a few centuries at the time of burial.

Figure 9. Angular, nearly 1-m-long boulder of Permian sandstone, locally derived from bedrock on the upthrown side of the fault (to left of photo), embedded in the upper part of 1.4-m section of fault-related fan alluvium along Browns Creek.

Although charcoal is capable of providing more precise ^{14}C ages than soil humus, charcoal in fluvial deposits is also capable of being recycled from older to younger deposits, thus providing erroneous ages for the younger deposits (Blong and Gillespie, 1978). Therefore, it is desirable to have cross-checks on ^{14}C ages for fluvial deposits—either more than one charcoal age per alluvial unit, or age determinations for more than one kind of sample. In this study, the reasonably close agreement between the ^{14}C ages of charcoal and the ^{14}C ages of soil humus provides the desired cross-check.

The differing degrees of soil development in the various alluvial deposits provide additional checks on the reliability of the ^{14}C dating. The ages of the alluvial deposits, estimated on the basis of relative soil development, are consistent with the ^{14}C ages. The soil in the East Cache alluvium is weakly developed. It consists of a 16- to 18-cm-thick A horizon overlying a C horizon of unaltered, calcareous alluvium that does not contain accumulations of secondary carbonate. This weak soil development is consistent with ^{14}C ages that place deposition of the East Cache alluvium between 800 and 100 yr ago. Little or no soil is present on the terraces cut in the East Cache alluvium.

The soil formed on the slope of the fault scarp is similar to that in the East Cache alluvium, and the soil formed in the fault-related fan alluvium is only slightly more developed. The soil formed in the fan alluvium has a slightly thicker, darker A horizon than that in the East Cache alluvium, and in addition it has an AC horizon. Also, the soil in the fan alluvium is leached to depths of 8 cm, as opposed to the 0–2 cm of leaching found in the soil in East Cache

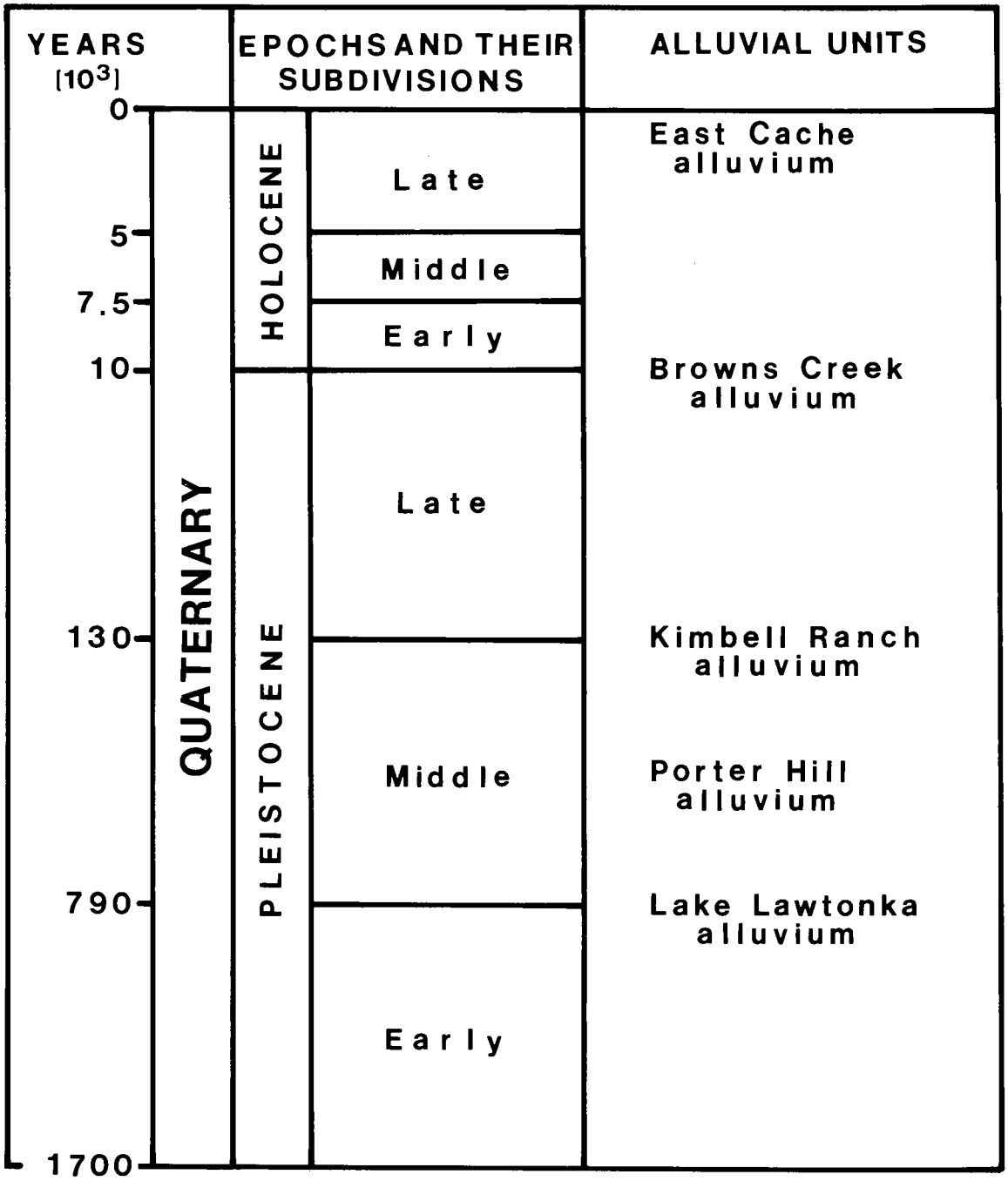

Figure 10. Time-stratigraphic relations and estimated ages of Quaternary alluvial units along the Meers fault.

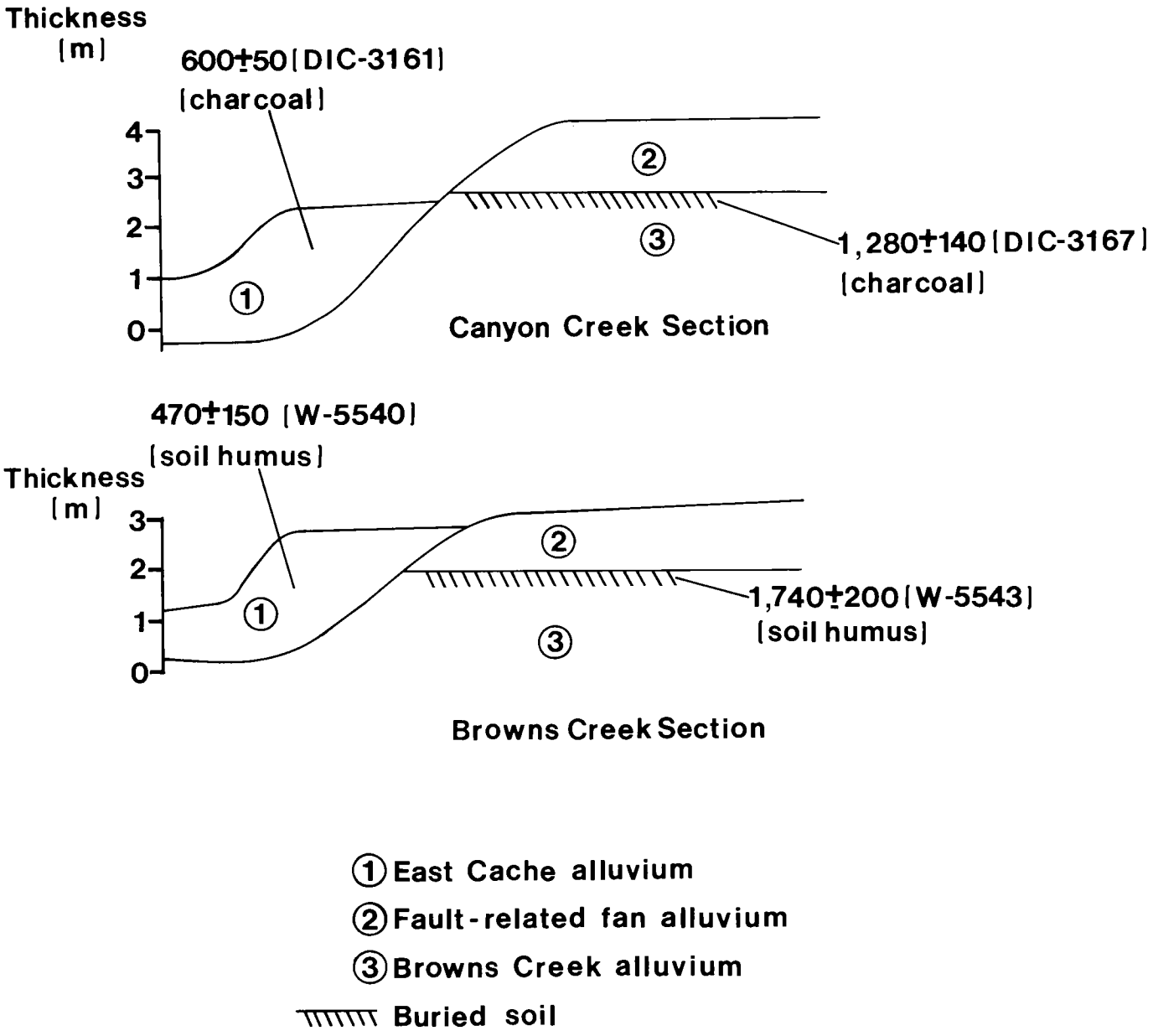

Figure 11. Schematic diagrams showing stratigraphic relations and ^{14}C ages that provide limiting dates for the time of recent movement on the Meers fault.

alluvium. The soil in sheetwash at the foot of the fault scarp has an exceptionally thick A horizon, but otherwise is weakly developed. Depth of leaching in all of these soils is minimal, secondary carbonate has not accumulated in any of them, and none has a B horizon. This indicates that the deposits and landforms with which they are associated are all geologically young and of similar age, which supports the conclusion that faulting closely preceded deposition of the East Cache alluvium. In contrast, the soils formed in Browns Creek alluvium, described earlier, are much more developed, suggesting that faulting occurred long after deposition of this alluvium.

ACKNOWLEDGMENTS

I thank the Oklahoma Geological Survey for logistical support and the invitation to undertake this study. Special thanks are due Kenneth V. Luza of the Oklahoma Geological Survey, for introducing me to the geology of the Meers area and for help and encouragement in the field and the office during the course of this work. Lester Brown and Charlie Bob Oliver were especially helpful in providing access to their properties. Anthony J. Crone, Kenneth V. Luza, and Alan R. Nelson reviewed this manuscript and provided several thoughtful suggestions.

Oklahoma Geological Survey Guidebook 24, 1986

HOLOCENE DEFORMATION ASSOCIATED WITH THE MEERS FAULT, SOUTHWESTERN OKLAHOMA

Anthony J. Crone and Kenneth V. Luza

INTRODUCTION

The southern Midcontinent has been widely regarded as part of the tectonically stable central interior of the United States, with no well-documented evidence of Quaternary faulting (Howard and others, 1978). The dispersed seismicity in the region can be spatially related to specific geologic structures only in a general way (Nuttli, 1979; Algermissen and others, 1982; D. W. Gordon, personal communication, 1985). As a result, seismic source zones in the Midcontinent have been defined primarily on the basis of historic earthquake-epicenter locations (P. C. Thenhaus, personal communication, 1985); the geologic and geophysical data presently available have been of limited value in identifying seismogenic structures.

Recent mapping in southwestern Oklahoma has identified a prominent scarp in Quaternary alluvium along part of the Meers fault. The scarp displaces youthful deposits, indicating that the fault may have generated large earthquakes in the geologically recent past (Donovan and others, 1983; Gilbert, 1983a,b; Slemmons and others, 1985) and that it is probably capable of doing so in the future. The presence of a possible major seismogenic fault in southwestern Oklahoma raises serious questions about the presumed tectonic stability and the potential for damaging earthquakes in the entire southern Midcontinent. Assessing the earthquake threat posed by the Meers fault requires an understanding of the characteristics and history of the recent displacements that have created the scarp.

In connection with activities performed under contract NRC 04-82-006-01 to study the seismicity in the vicinity of the Nemaha ridge in Oklahoma, a project was initiated in March 1984 to evaluate the evidence of Quaternary movement on the Meers fault. An important part of the study included excavating two trenches across the Meers fault scarp.

TRENCHING STUDIES

The stratigraphy in two trenches excavated across the scarp near Canyon Creek (Fig. 1) in March 1985 documents the near-surface deformation associated with the scarp and provides information about the recency and recurrence of earthquakes associated with the fault. In this paper we describe the stratigraphy in the trenches and the history of faulting recorded by the stratigraphy. Radiocarbon ages of selected samples from the trenches constrain the age of the latest surface-faulting event to the late Holocene.

The trenches were located in the SW¼SW¼ sec. 24, T4N, R13W, Comanche County, Oklahoma. The Meers fault is marked by a prominent, linear, down-to-the-south scarp that strikes N. 64° W. in this area. The trenches were oriented perpendicular to the strike of the fault scarp and were located so they could be excavated in Quaternary deposits of two different ages. Trench 1 was excavated in Holocene deposits, the youngest deposits known to be displaced by the fault, whereas trench 2 was excavated in deposits of Pleistocene age. By determining the amount of slip in deposits of different ages, we can identify recurrent movement and, with appropriate age information on the deposits, estimate recurrence intervals and long-term slip rates.

Trench 1

Trench 1, 22 m long and ~2.5 m deep, was ~150 m east-southeast of Canyon Creek, a major drainage in the area. The scarp here is 2.4 m high, with a maximum slope angle of 9°20′. The faulted deposits exposed in the trench are part of the Browns Creek alluvium, believed to be latest Pleistocene to middle Holocene in age (Madole, this volume). In Canyon Creek and other nearby drainages, the Holocene East Cache alluvium (Madole, this volume) is not faulted. About 30 m east of the trench, a small ephemeral stream has incised a shallow gulley into the scarp (Fig. 2).

At the bottom of the trench, weathered Hennessey Group shale of Permian age was exposed on both sides of the fault (Figs. 3,4). Near-surface weathering has obliterated all primary bedding in the soft, plastic, red, slightly silty shale. The Browns Creek alluvium rests on the shale. The lower part of the alluvium is a generally fining-upward sequence of interfingering and lenticular sands, silts, clays, and pebble–cobble gravels that grade upward into a massive clayey silt.

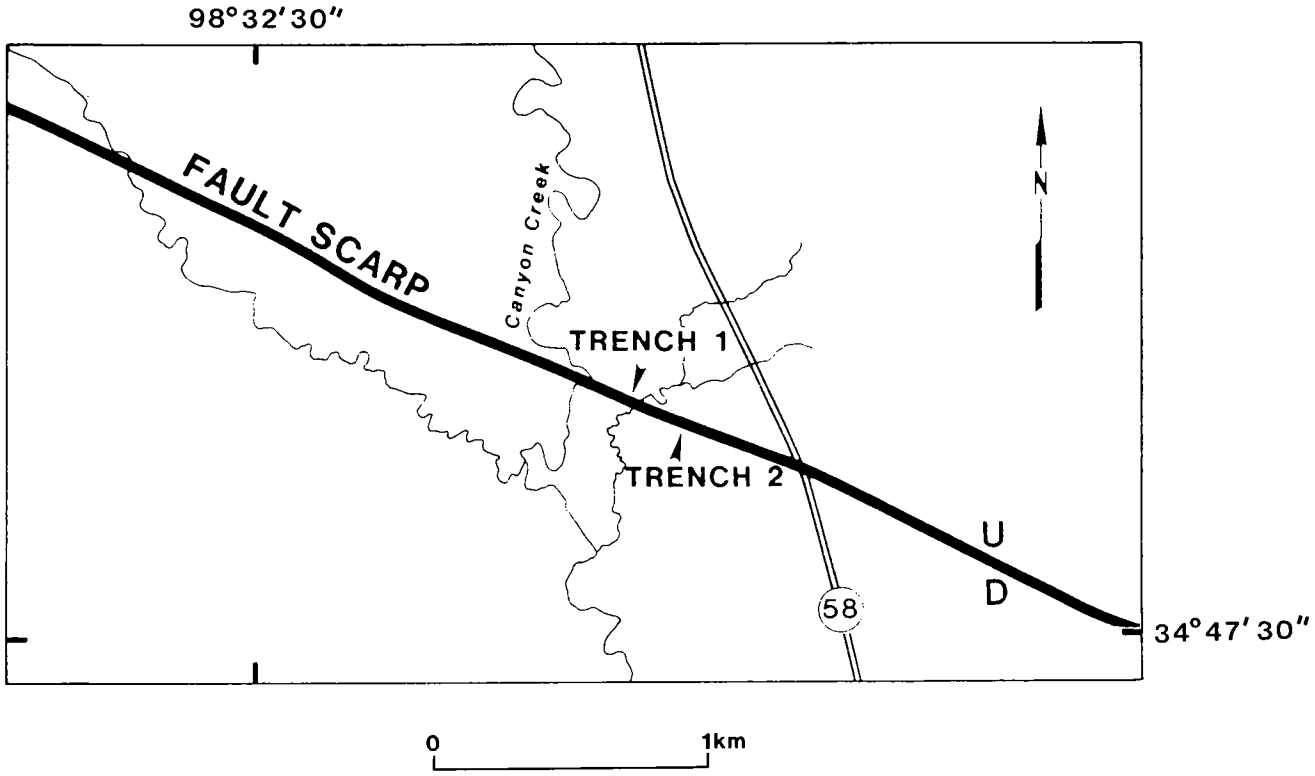

Figure 1. Location of trenches across the Meers fault, Comanche County, Oklahoma.

A weak soil with a simple A/C profile has formed in the calcareous, clayey silt on the stable surface of the upthrown block. The brown to dark-brown A horizon is noncalcareous, massive, sandy silt. Calcium carbonate leached from the A horizon has started to accumulate in the C horizon in the underlying clayey silt.

Following deposition of the Browns Creek alluvium and formation of an A horizon, the scarp formed and warped the alluvium into a monocline. Tension cracks and small-displacement faults (discussed below) developed near the crest of the monocline. After the scarp and faults formed, the nearby ephemeral stream flowed along the base of the scarp, eroded the A horizon and the massive clayey silt from the downthrown side of the fault, and deposited a sequence of interbedded fine gravel, sand, silt, and clay (not shown on Fig. 3). An organic-rich, clayey silt at the base of this sequence has a ^{14}C age of 1,730 ± 55 yr (sample DIC-3266). These fluvial deposits are overlain by a dark-brown, overthickened A horizon. The overthickened A horizon is mostly a colluvium of soil material stripped from the upper part of the scarp and moved down the slope, where it has accumulated.

Nearly all of the deformation in trench 1 is the product of flexing and warping; there is only minor brittle deformation (cracking and displacement on faults). The actual displacement on faults accounts for only 8–13% of the total deformation in the trench. The faulting is expressed as a reverse fault and a normal fault near the midpoint of the scarp (Figs. 3,4). The total stratigraphic throw along the length of the trench is 2.7–2.8 m. This is a minimum value, because the fluvial gravels on the downthrown side still have a tectonically induced SW dip where they continue below the bottom of the trench.

The most significant fault in the trench is the reverse fault, although it produced only 0.1 m of throw on the top of the Hennessey shale (coordinates in Fig. 3; 11.5 m horizontal, −0.5 m vertical). This fault strikes N. 59° W. and dips 49° NE, which is compatible with the regional strike of N. 64° W. for the scarp. The narrow zone of deformed sediments associated with this fault near the bottom of the trench becomes wider upward. A distinctive feature of this zone is a fingerlike pod of A horizon that extends downward through the massive silt and into the underlying gravel a distance of 1.15 m below the base of the soil horizon from which it was derived. Organic material from this pod of A horizon in the fault zone (Fig. 3; 12.2 m, 0.15 m) has a ^{14}C age of 1,660 ± 50 yr (sample DIC-3180). Similar to the A-horizon material, a pod of the massive silt extends ~0.8 m downward through the gravel and into the shale below. Beneath the silt in the fault zone, a small pod of gravel in the shale (11.3 m, −0.5 m) is down-dropped at least 0.40 m and is isolated from its source. Thus, the entire stratigraphic section of Browns Creek alluvium is elongated downward in the deformed zone associated with this small fault.

Drag associated with displacement on the small fault cannot explain the downward movement of the

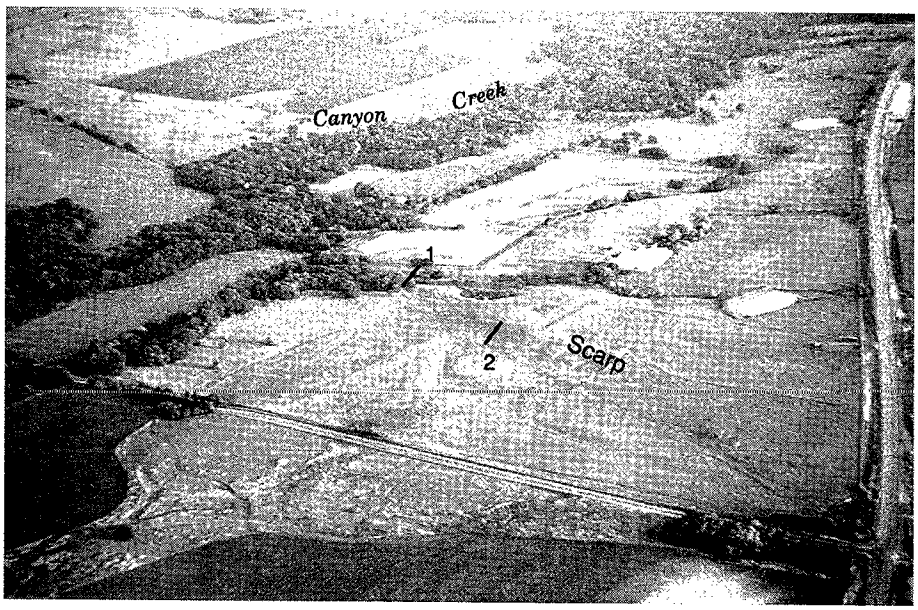

Figure 2. Aerial view of the Meers fault, looking north-northwest, showing trench locations (numbered lines, as labeled in Fig. 1). State Highway 58 on the right. Photograph by D. B. Slemmons, 1983.

sediments in this deformed zone. The dip-slip displacement on the small fault is only ~0.1 m (as shown by the displacement of the top of the shale), as compared to the downdip movement of the overlying sediments, 0.40 m for the gravel to 1.15 m for the A horizon. The dip-slip movement on the fault is insufficient to produce the observed amount of downdip movement of the sediments.

The best explanation for the observed relationships is that a block of Browns Creek alluvium collapsed into an open crack. The crack, which was narrower at depth, originally dipped ~60–70° NE. This dip was estimated by restoring the warped beds in the alluvium to horizontal and measuring the attitude of the crack. During the early phases of deformation, a tension crack formed in the alluvium near the crest of the monocline. As soon as the crack formed, a sliver of the alluvium from one wall collapsed into the opening. This collapse displaced the alluvial units more than the top of the shale. As warping of the monocline progressed, the originally near-vertical crack gradually rotated to a less-steep attitude. The small amount of reverse slip on this fault may be a result of near-surface compressional forces related to formation of the monocline.

Several pieces of evidence support this collapse interpretation. The extremely sharp contacts and the absence of slickensides or severe disruption of the sediments at the edges of the deformed zone suggest limited differential movement at these boundaries. Furthermore, the sharp contacts between the stratigraphic units within the deformed zone indicate very little internal shearing. The relatively undeformed succession of stratigraphic units in the deformed zone is also consistent with the collapse interpretation. Finally, the original attitude of the fissure is nearly perpendicular to the bedding in the alluvium, as might be expected for an extensional crack.

The other significant fault in this trench is a small normal fault that also probably formed in response to tension near the crest of the monocline. The near-vertical, down-to-the-south fault displaces the tops of both the shale (11.0 m; −0.25 m) and the gravel (10.9 m; 0.4 m) about 0.1 m vertically (Fig. 3). The position of this fault on the upthrown block of the reverse fault suggests that it is a secondary feature. An open fissure that extended down into the upper part of the gravel was filled with A-horizon material.

The small, triangular pod of gravel in the shale (11.2 m; −0.5 m) between the two faults probably formed by gravel collapsing into an open tension crack. Projecting the top of the shale across the crack indicates no vertical displacement. Furthermore, a narrow finger of A-horizon material (11.3 m; 0.5 m) directly above the pod probably filled the upper part of this crack (Fig. 3); the crack does not vertically displace the contact between the fluvial sands and gravels and the overlying clayey silts.

Trench 2

Trench 2, ~200 m east-southeast of trench 1, is 19 m long. There the scarp is 3.4 m high, with a maximum slope of 9°00′. On the upthrown side of the scarp, the trench exposed ~2.5 m of Porter Hill alluvium (R. F. Madole, personal communication, 1986) on weathered Hennessey shale. The lower part of the alluvium is a sequence of fluvial pebble–cobble gravels (Fig. 5). The gravels are capped by as much as 60 cm of silty sand and sandy silt that may contain a large component of loess. These fine-grained deposits may be much younger than the underlying gravels. A soil with an argillic (clay-rich) B horizon as much as 1

m thick has formed in the alluvium on the stable surface on the upthrown side of the fault. This soil and the position of the alluvium in the landscape (Madole, this volume) both suggest that the Porter Hill alluvium is much older than the alluvium in trench 1. The Porter Hill alluvium is believed to be middle to upper Pleistocene, but the time of deposition has not yet been determined.

In this trench, Hennessey shale was exposed only on the upthrown side of the fault (not shown in Fig. 5); a high water table and ground water seeping from the shale–gravel contact prevented deepening the trench to bedrock on the downthrown side. Immediately upslope from the fault, a rounded boulder of dolomite ~1 m in diameter rests on the shale (Fig. 5; 8.4 m, −0.75 m). During deposition of the gravel, the shale downslope from the boulder was scoured and backfilled with gravel.

The gravels in the lower part of the Porter Hill alluvium are divided into three units on the basis of the amount of matrix. In ascending order, the units are a pebble–cobble gravel, a clay-enriched gravel, and a clay-plugged gravel. Typically, the contacts between the units are gradational and, in places, difficult to map because of the coarse texture of the gravels.

On the upthrown side of the fault, the gravels are overlain by silty sand and sandy silt in which a soil with an A horizon and an argillic B horizon has formed. The dark-brown to dark-reddish-brown A horizon is noncalcareous, massive, silty sand, with abundant roots and a few cobbles as large as 20 cm. The dark-red to reddish-brown B horizon is noncalcareous, clayey sand, with a few cobbles as large as 15 cm. Cobbles are more abundant in the lower third of the B horizon. The B horizon has a massive to blocky structure and abundant clay that coats the sand grains.

The B horizon thins toward the fault zone and could not be identified downslope from the 10.1-m horizontal position (Fig. 5); downslope from this position to a point above the fault zone (12.5 m; 0.5 m), an A horizon rests directly on the clay-plugged gravel or gravel in the fault zone. The original A horizon and the B horizon found on the upthrown side of the fault were probably eroded in this area (between 10.1 m, 0.9 m and 12.5 m, 0.5 m) after the scarp formed. The A horizon that now rests directly on the gravels is mainly redeposited A-horizon material eroded from the upper part of the scarp.

On the downthrown side of the fault, the clay-plugged gravel is overlain by a 1.2-m-thick sequence of interstratified silty and clayey sands and sandy silt. The clayey sand directly above the gravel and the overlying sandy silt are interpreted respectively as a buried argillic B horizon and a buried A horizon, formed in silty and sandy alluvium (Fig. 5). The dark-reddish-brown B horizon is noncalcareous, has a massive to blocky structure, and contains a few pebbles and cobbles as large as 12 cm. Clay fills most of the pores in the B horizon and coats most of the sand grains. The noncalcareous, sandy silt of the A horizon

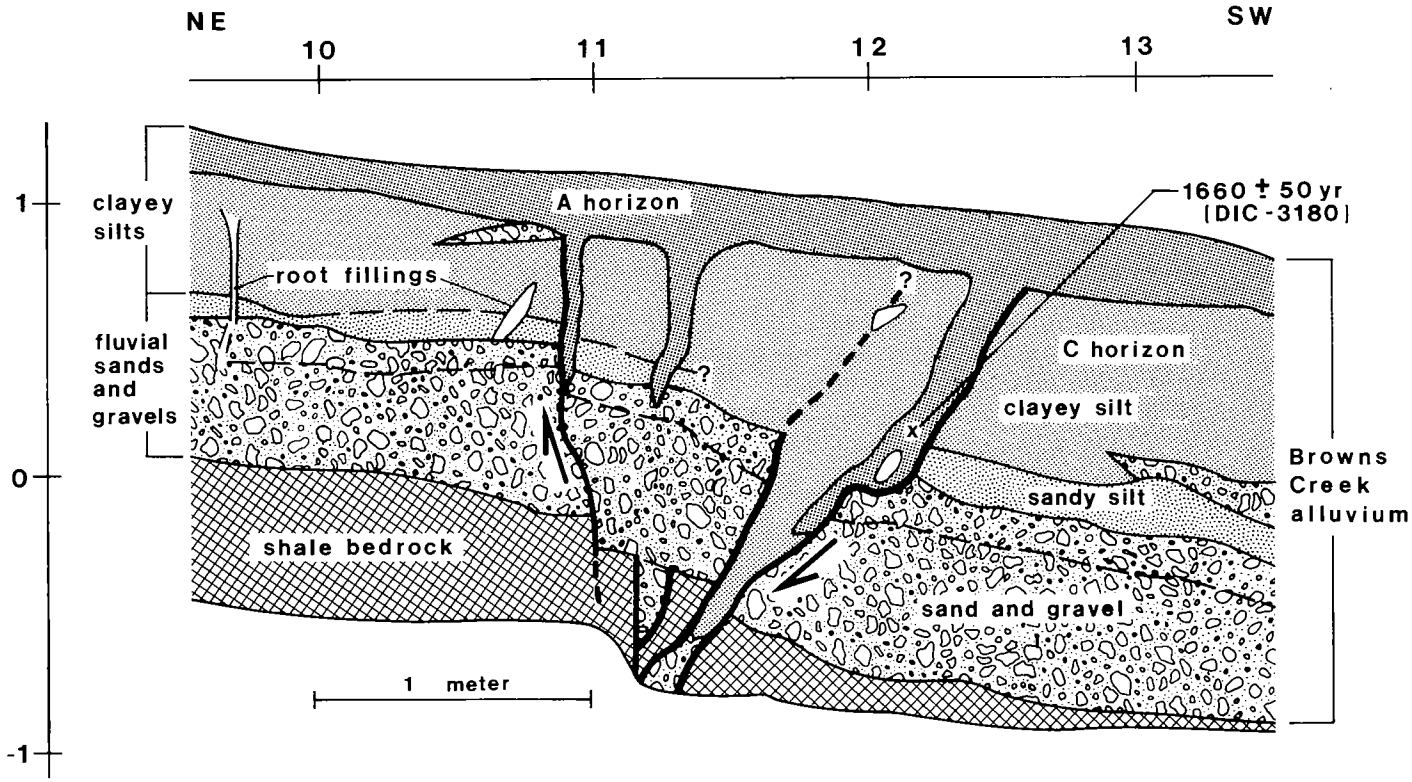

Figure 3. Part of the log of trench 1, showing stratigraphic relations near the main fault, and location of ^{14}C age sample. Heavy lines are faults and edges of cracks recognized by abrupt changes in the stratigraphy (dashed where inferred). Arrows show general sense of displacement across the main fault zone. Fine lines are stratigraphic contacts (dashed where subtle).

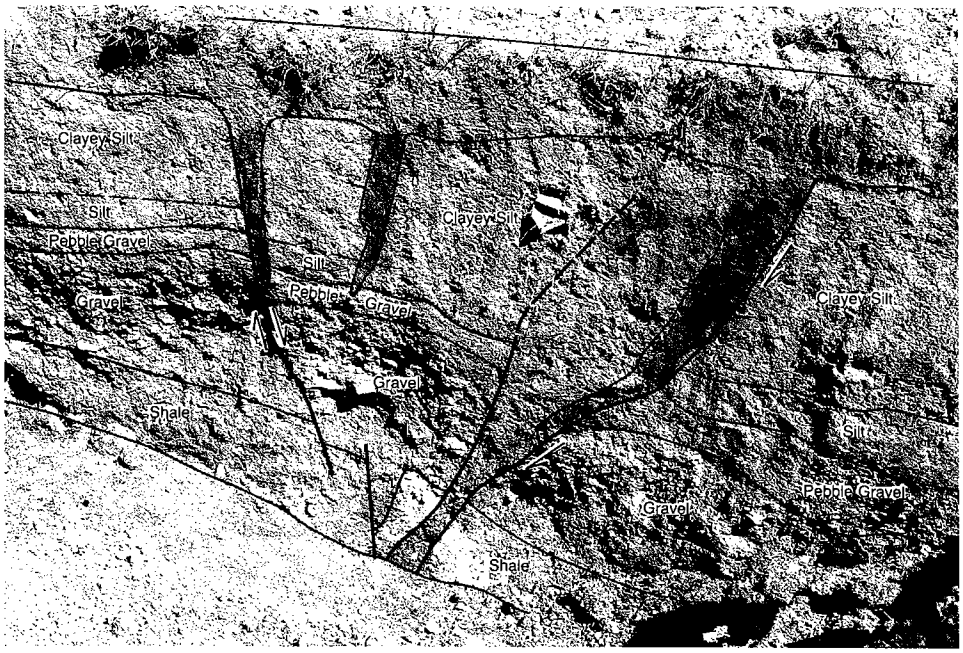

Figure 4. Photograph of fault zone in trench 1, looking east.

has a massive to granular structure, contains a few 1- to 2-cm pebbles and has less clay than the underlying B horizon. Generally, the sand grains are not coated with clay. The slightly greater content of organic matter in the dark-reddish-brown A horizon gives it a slightly darker color than the B horizon. Organic matter from the buried A horizon near the 17-m horizontal position (not shown in Fig. 5) has a ^{14}C age of 1,360 ± 50 yr (sample DIC-3183). The top of this buried soil defines the pre-faulting ground surface which was buried by colluvium derived from erosion of the scarp.

Adjacent to the fault zone, two small blocks of the buried A and buried B horizons overlie the buried A horizon (Fig. 5). These blocks are probably intact fragments of the buried soil that were dislocated by the surface faulting. As the newly formed scarp eroded, the blocks fell onto the pre-faulting ground surface and were subsequently buried by colluvium. In color and texture, these blocks are identical to the corresponding units of the buried soil from which they were derived.

A modern (post-faulting) soil composed of an A and a C horizon is forming in the colluvium that has accumulated on the downthrown side of the fault (Fig. 5). The modern C horizon is dark-reddish-brown, noncalcareous, clayey sand with massive to blocky structure; it contains a few pebbles as large as 1.5 cm. Clay coatings on the sand grains are abundant. The C horizon is only ~5 cm thick at the fault zone (near the 12.5-m horizontal position), but is >40 cm thick within a short distance downslope (near the 14-m horizontal position). This abrupt increase in thickness marks the approximate location of the free face of the fault scarp. Upslope from the free face, erosion stripped sediment from the upthrown side of the fault; downslope, colluvium accumulated and buried the pre-faulting ground surface on the downthrown side.

A fault zone with a reverse sense of slip vertically displaces the gravel units in the trench. The fault zone strikes N. 64° W. (identical to the regional strike of the scarp) and dips 56° NE. Differential shearing in the fault zone has mixed the pebble–cobble gravels into a poorly sorted, matrix-supported gravel. The shearing also reoriented a few elongate rhyolite clasts such that their long axes are subparallel to the boundaries of the fault zone. We could not identify discrete slip planes or find features that showed net slip directions in the coarse gravels.

The boundaries of the fault zone are subtle and generally difficult to identify, except where the pebble–cobble gravel on the upthrown block bounds the fault zone. At this boundary, the crude stratification in the pebble–cobble gravel ends and the clayey texture of the fault-zone gravel is obviously different from the texture of the pebble–cobble gravel.

The clay-plugged and clay-enriched gravels are exposed on both sides of the fault zone and can be used to measure the stratigraphic throw. The throw across the fault zone is only 0.6–1.0 m, compared to the total stratigraphic throw of 3.2–3.3 m along the length of the trench. The stratigraphic throw is probably a minimum value, because the gravels are still slightly warped where they extend beyond the southwest end of the trench. However, a profile of the scarp indicates a surface offset of 3.0 m and a scarp height of 3.4 m (as defined by Bucknam and Anderson, 1979). The surface offset approximates the net throw on the scarp and suggests that the stratigraphic throw is a good

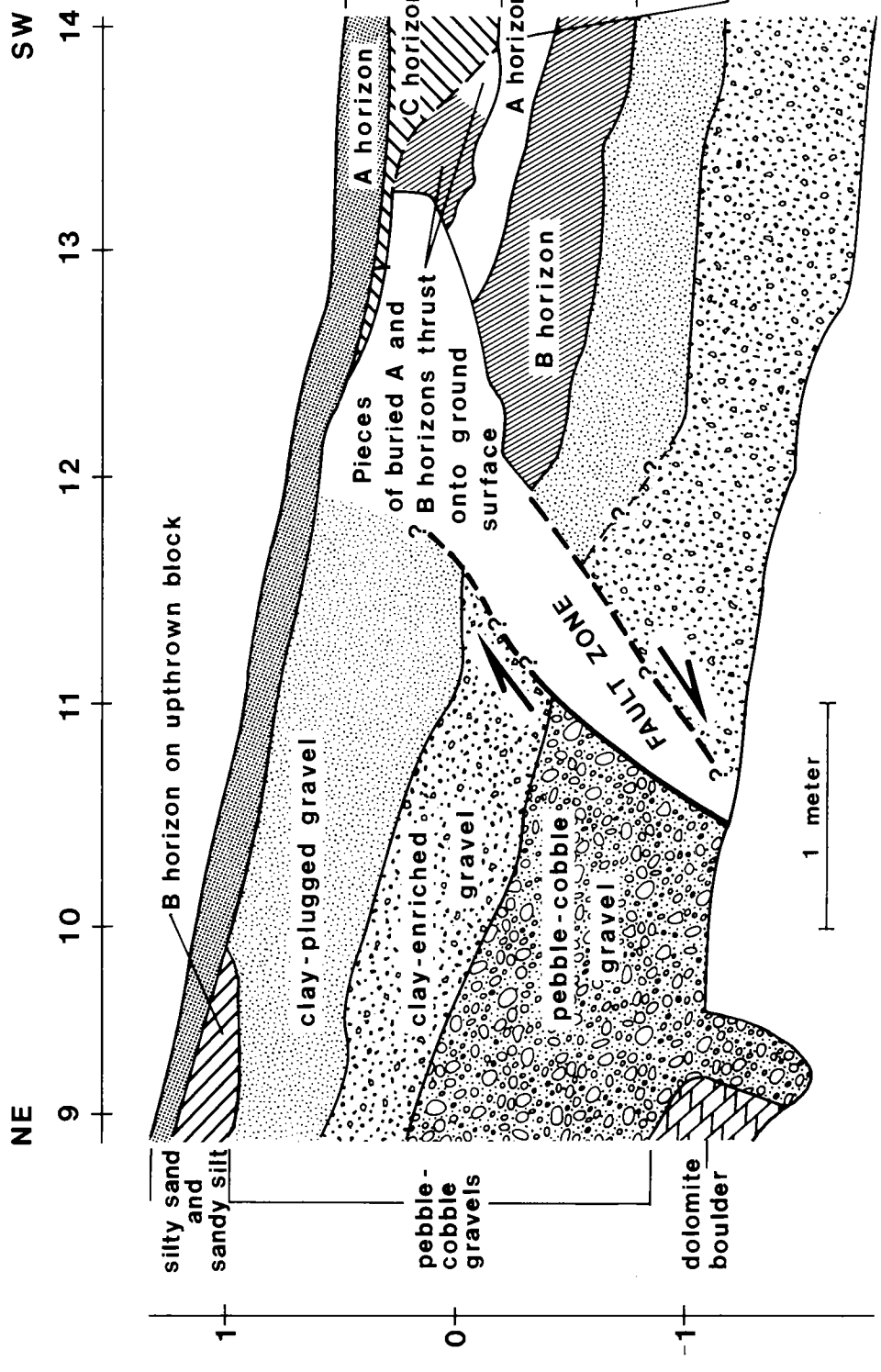

Figure 5. Part of the log of trench 2, showing stratigraphic relations near the main fault. Heavy lines are edges of a fault zone (dashed and queried where subtle); arrows show sense of displacement across the zone. Fine lines are stratigraphic contacts (dashed where subtle, queried where uncertain).

estimate of the net throw. Thus, from the stratigraphic data and the scarp profile, we estimate the net throw to be slightly more than 3 m.

The difference between the net throw (~3 m) and the throw across the fault zone (0.6–1.0 m) is the amount of deformation caused by warping. In this trench, only about one-quarter of the relief on the scarp results from displacement on the fault zone. Thus, in trench 2, as in trench 1, much of the relief on the scarp is the product of warping.

DISCUSSION

The two trenches provide important information about the age and characteristics of the deformation associated with the Meers fault scarp. In both trenches, the dominant mode of deformation is warping and flexing of the alluvium. Brittle deformation expressed as discrete faults accounts for about one-tenth of the total deformation in trench 1, and for about one-quarter of the total in trench 2. The difference in the amount of brittle deformation in the two trenches maybe related to the degree of induration of the sediments at each site. The soft, porous, completely unconsolidated Browns Creek alluvium in trench 1 deformed as an incompetent, plastic material. The high clay content in Porter Hill alluvium in trench 2 partially indurated the gravels and as a result the gravels behaved more competently and deformed in a more brittle fashion.

The surface faulting that formed the scarp on this part of the Meers fault is late Holocene in age. The ^{14}C ages on three samples of soil-derived humus from both trenches are between 1,730 ± 55 yr and 1,360 ± 50 yr. The stratigraphic position of these samples indicates that the ages closely approximate the time of surface faulting. The age of the faulting from our trenching study is consistent with the age determined from regional Quaternary stratigraphic studies (Madole and Rubin, 1985; Madole, this volume).

The stratigraphy in the trenches and scarp profiles suggests that the net tectonic throw at both trench sites is ~3 m. Post-faulting erosion, backfilling, and gradational stratigraphic contacts introduce uncertainty into the net throw measured at the trench sites, but, considering these uncertainties, the values of net throw at both sites are very similar. The similar amounts of throw and the stratigraphy at each site show that the alluvium in each trench was deformed by one surface-faulting event. Thus, major surface faulting has occurred only once since deposition of the gravel in trench 2. Although poorly constrained, the age of these gravels is thought to be middle to late Pleistocene. This implies a lengthy recurrence interval (tens of thousands of years) for surface faulting on this part of the Meers fault.

This conclusion assumes that the sense and amount of slip on the fault is consistent during succeeding events. An event with mainly lateral slip could be difficult to detect in the gravels in trench 2. An undetected event not evidenced in the gravels would reduce the inferred recurrence interval.

Long-term slip rates computed from the available data have large uncertainties, and therefore seem to be of limited value in characterizing the rate of strain accumulation on the fault. Without reliable information on the timing of successive events, the amount of any lateral slip, and the age of the Porter Hill alluvium, calculated slip rates are at best general estimates. Using 125,000 yr for the age of the Porter Hill alluvium and 3.0 m for the net slip, the resulting slip rate is 0.02 mm/yr. If the age of the alluvium is older, the slip rate will be less; if the net slip is larger because of lateral slip, the slip rate will be greater. In spite of the uncertainties, this slip rate is consistent with the slip rates expected in intraplate environments.

ACKNOWLEDGMENTS

This study was supported in part by U.S. Nuclear Regulatory Commission contract NRC 04-82-006-01 to the Oklahoma Geological Survey. We thank David Kimbell and Charlie Bob Oliver for their cooperation and permission to excavate the trenches on the Kimbell Ranch, and Douglas Lemley for his assistance in logging the trenches. Discussions with Robert C. Bucknam and reviews and suggestions by Richard F. Madole and Steven F. Personius have improved this manuscript.

Oklahoma Geological Survey Guidebook 24, 1986

BARITE TRAVERTINE AT ZODLETONE MOUNTAIN IN THE SLICK HILLS, SOUTHWESTERN OKLAHOMA

Paul Younger, R. Nowell Donovan, and Arthur W. Hounslow

INTRODUCTION

Barite precipitation at the surface of the Earth is an uncommon phenomenon, known from only four locations worldwide: at Hokuto, Taiwan; and Akita, Japan (Ishizu, 1915); near Hotchkiss, Colorado (Headden, 1905; Cadigan and others, 1976; Younger, 1986); and at Zodletone Mountain in southern Oklahoma. Here we describe the last-named occurrence, which is a spring-related deposit of Recent age located on the north side of the mountain (Fig. 1; see also Stop 3, this volume, map of Zodletone Mountain). We use the term "travertine" in a broad sense to include any surficial deposit, whether or not it has a phreatic or vadose character, and whether or not its precipitation has been influenced by (or "templated" by) vegetation.

THE MODERN SPRING

The spring is on the southern perimeter of the Anadarko basin, close to the northern edge of the frontal fault zone of the Wichita Mountains uplift. Cambrian sediments of the Arbuckle Group (specifically, the Fort Sill and lower Signal Mountain Formations) are the closest exposed bedrock.

Many other springs are associated with the Arbuckle Group in southern Oklahoma, but most of these occur in relatively simple hydrogeological settings where the Arbuckle Group forms outliers with suitable aquifer properties, the springs emerging around the edges of the outliers at geological contacts. Such springs are to be found in the Slick Hills (Havens, 1983) and the Arbuckle Mountains (Fairchild, 1984), where they are involved in the precipitation of calcite travertines (Emig, 1917). However, the quality of the spring water at Zodletone Mountain (Table 1) precludes the possibility that it originated as recharge into the limestone on Zodletone Mountain. Furthermore, the water is unlike that of any other spring water in Oklahoma (Havens, 1983). At present, the water is at the saturation level for barite.

The modern spring (Fig. 1) is enclosed by crumbling concrete walls which record an attempt to develop the area as a health spa. The surroundings are barren, resembling an industrial-waste site, and the astringent smell of hydrogen sulfide pervades the air (Zodletone is a corruption of an Indian term for "stinking mountain"). The spring water bubbles continually, and its orifice is lined with purple sulfur bacteria (Chromatiaceae). The spring feeds a tiny stream, which after a short course tumbles into and contaminates Saddle Mountain Creek. This stream is actively depositing calcite and barite as a coating around vegetation.

The soil profile around the spring has been greatly altered by reduction; soil in contact with the water is black, passing upward and outward through a gray horizon which contains alunogen (a white aluminum sulfate) and in places native sulfur and blades of selenitic gypsum. The latter are as much as 1.25 in. (3 cm) in length and may show chiasmatic twinning. The gray zone gradually passes into the normal (oxidized) red-brown soil profile.

Clearly, at one time more springs were active in the area; several drainage depressions as much as 35 ft (~10 m) from the active spring record drainage into Saddle Mountain Creek from extinct orifices. The gray soil in some of these depressions contains the unconsolidated remains of plant roots and stems which are coated by white barite.

Farther to the northwest (Fig.1) are several exposures of indurated travertine which mineralogically are either barite-cemented calcareous travertine or wholly barite travertine.

BARITE TRAVERTINE

In the field, the barite travertine shows varying degrees of induration and is associated with variable amounts of organic detritus, calcareous travertine, and detrital siliciclastics. As a result, a spectrum of textures from unconsolidated, sponge-like masses to solid rock with porosities of ~20% is found.

Thin-section studies of various travertine varieties reveal stunning mineralogical textures. In the unconsolidated travertine, barite occurs as isopachous coatings (typically 0.1–0.2 mm thick) on the inner and outer surfaces of tubules (Fig. 2). In the more-indurated deposits, various textures indicative of both vadose and phreatic conditions are found (Younger and others, 1985), including pendant and isopachous crystal growths (Figs. 3–5). Some cavities show drusy growth, and many crystals show growth lines delineated by lines of inclusions of organic matter and micrite (Fig. 6). Similar textures are also

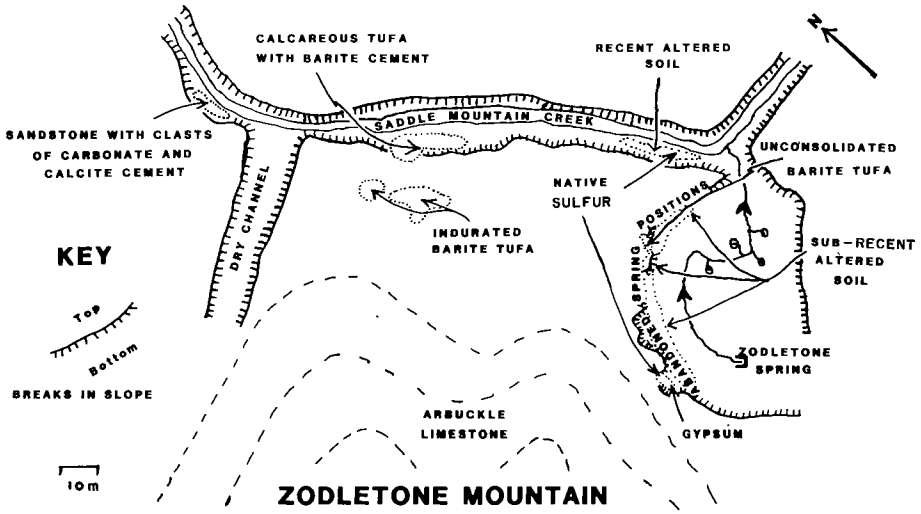

Figure 1. Location of barite deposits at Zodletone Mountain.

TABLE 1.—CHEMICAL ANALYSES OF ZODLETONE SPRING WATER

Constituent (mg/L) or property	DMZW-1	Sample ZT-1	Havens (1983)
Ba	43.5	35.0	—
Ca	273.5	296.0	—
Fe	1.1	—	—
K	28.6	—	—
Li	1.1	—	—
Mg	149.0	144.0	—
Na	2,500.0	2,550.0	2,900.0*
SiO_2	10.9	—	—
Sr	12.4	—	—
Cl	4,910.0	8,800.0	5,000.0
SO_4	70.4	55.0	90.0
HCO_3	—	481.0	270.0
CO_3	—	0.0	0.0
NO_3 (N)	—	3.0	—
TDS	8,001.0	9,926.0	9,160.0
Hardness (Ca, Mg)	—	—	1,300.0
pH	7.4	7.7	8.2
Conductivity (μS)	>10,000.0	15,040.0	14,800.0
Temperature (°C)	22	22	22

Notes: DMZW-1, sampled by Mrs. C. Patterson, Geology Department, Oklahoma State University, 12 July 1984; ZT-1, sampled by Paul Younger, Geology Department, Oklahoma State University, and by Agronomy Water and Soil Testing Laboratory, Oklahoma State University, 30 April 1985.
*Na + K.

found in the calcareous tufa and travertine (which in general, although not exclusively, predates the barite).

The longest and finest barite crystals, up to 6 mm across, are associated with the wholly barite travertine (Fig. 7). Most of the rock is composed of barite euhedra arranged in well-defined laminae. Characteristic features include lamellar twinning, plumose habit, and a distinctive chevron zonation (Fig. 8).

The chevron zonation is an unusual form of crystal growth produced by the expansion of the {110} form faces. In the normal growth of barite crystals (Fig. 9), faces of the {011} form dominate over the {110} form faces. However, in the Zodletone barite the {011} form faces have atrophied, resulting in the spectacular chevron form (Fig. 10). Similar changes in habit during the growth of barite crystals have been documented by Seager and Davidson (1952), but the cause of such habit changes is as yet unexplained.

TRACE-ELEMENT ANALYSIS

Three samples showing progressive barite induration were examined under X-ray fluorescence by M. L. Salmon at the Fluo-X-Spec. Laboratory, Denver, Colorado. The results (Table 2) show that as induration increases the content of heavy metals falls. This may be due to the progressive elimination of unaltered organic matter, which not only accommodates such ions as Ni and Co as substitutes for Mg in chlorophyll but also detains a wide variety of elements by surface adsorption. In the more-indurated samples ("mature barite travertine"), only divalent ions compatible with the barite lattice are present. All three samples are conspicuously radioactive, possibly because of the decay of radioactive strontium and/or lead.

WHAT IS THE SOURCE OF THE BARIUM?

Barium migrates from the mantle into the near-surface geochemical cycle by incorporation in K-feldspars, biotite, and other K-rich igneous minerals. Barium can substitute for potassium in such minerals, and may even form a Ba-feldspar (celsian) in solid solution with orthoclase (Rhodes, 1969).

In the Wichita Mountains igneous province, there are several alkalic rocks with high K-feldspar contents. Among these, the Carlton Rhyolite Group contains as much as 4,251 ppm Ba (Gilbert, 1982, p. 15). Weathering of such rocks under neutral or alkaline conditions would have produced montmorillonite–illite clay assemblages, whereas acidic conditions would have favored kaolinite formation (Russell and Allison, 1985). The type of clay produced is of importance to the barium cycle, because at neutral pH montmorillonite adsorbs Ba at ~70 meq/100 g of clay, whereas kaolinite will only bind ~10 meq/100 g of clay (Grim, 1968).

Within the context of the southern Oklahoma area, kaolinite production would have been favored by the humid environments of Mississippian and Pennsylvanian times, whereas montmorillonite–illite formation would have taken place during the early Paleozoic (in terrain that was a biological desert, devoid of humic acids) and under the arid conditions that prevailed in Permian times. In quantitative terms, the Permian probably was the most significant in terms of barium production. Contact of the montmorillonite with the evaporative Permian seas led to the widespread precipitation of barite as the Ba^{2+} and SO_4^{2-} ions met. Ham and Merritt (1944) noted that the far-famed barite roses of central Oklahoma occur in a zone roughly parallel to the Permian coastline. We suggest that barium which escaped "rosetting" during early diagenesis was subsequently released into deep saline ground waters in the Anadarko basin (bearing in mind that barite is 200% more soluble at 1,000 atm than it is at 1 atm). Barite was later precipitated when sulfate was encountered, or when the solubility of barite dropped as a result of brine migration to the surface.

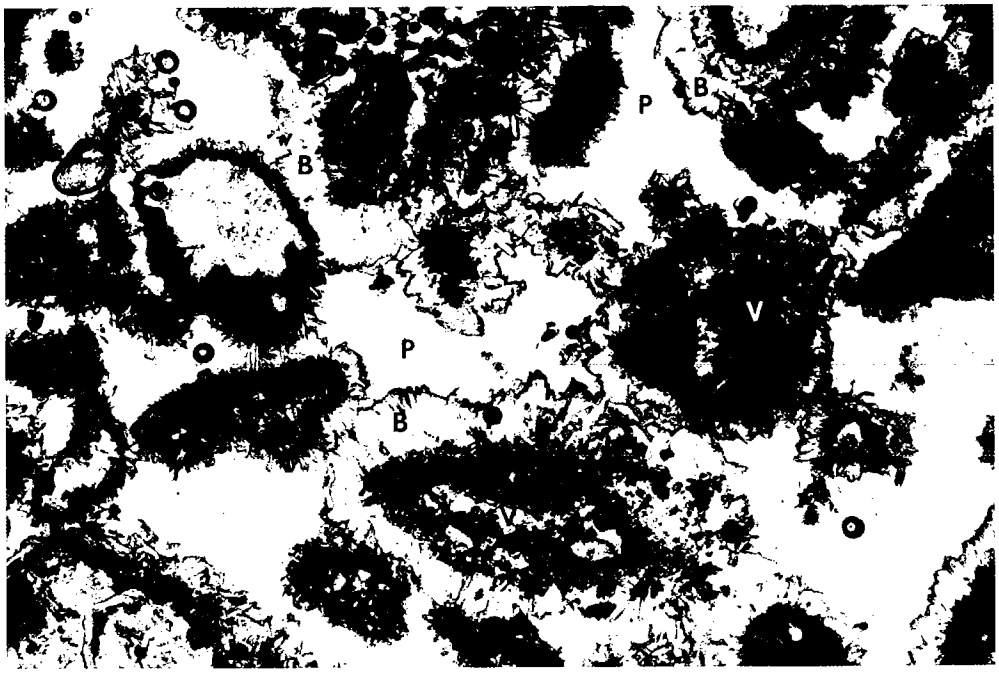

Figure 2. Isopachous fringe of euhedral barite (B) around calcareous travertine and vegetable matter (V); P = porosity. Field of view 10 mm across; ordinary light.

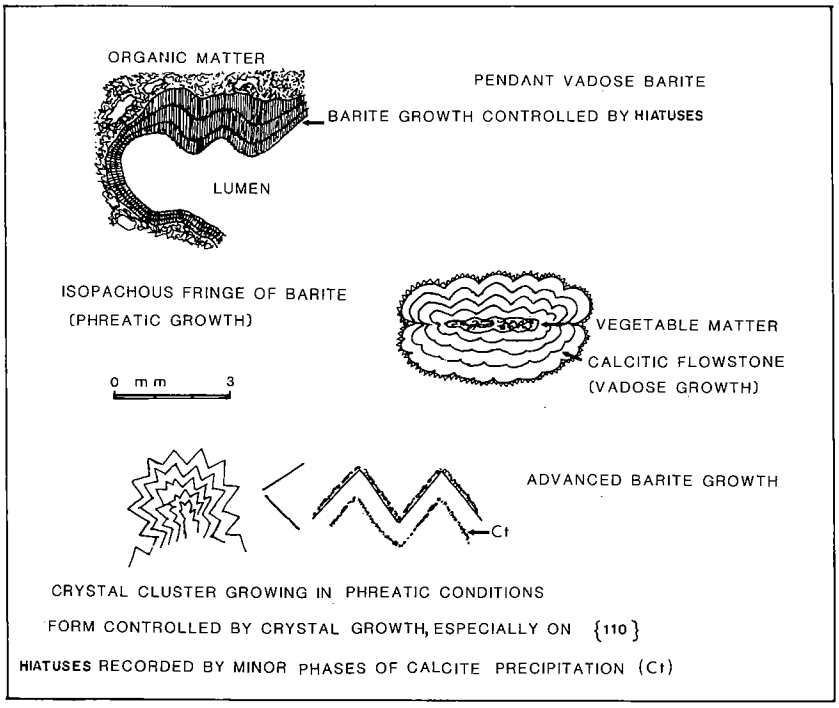

Figure 3. The principal barite textures.

Figure 4. Vadose barite (B) on vadose calcite (C). Note clear growth lines in the barite. Field of view 5 mm across, crossed polars.

Figure 5. Pendant (P), vadose (B), and isopachous (I) barite growing on calcareous travertine (C). Field of view 3 mm across; crossed polars.

Figure 6. Detail of euhedral barite cluster, showing organic matter and/or calcite delineating growth limits of crystals. The reason for the periodic cessations in barite growth is unclear (perhaps fluctuations in spring-water temperature). Field of view 0.75 mm across; ordinary light.

Figure 7. Cluster of barite crystals in mature barite travertine. Good crystal terminations indicate phreatic conditions during growth. Field of view 5 mm across; crossed polars.

Figure 8. Chevron zoning in euhedral barite, caused by the dominant growth of {110} at the expense of {011}. Field of view 0.1 mm across; crossed polars.

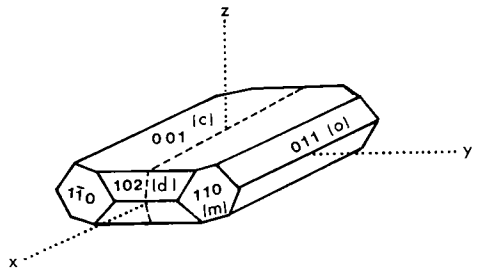

Figure 9. Generalized view of a simple barite crystal, showing possible forms.

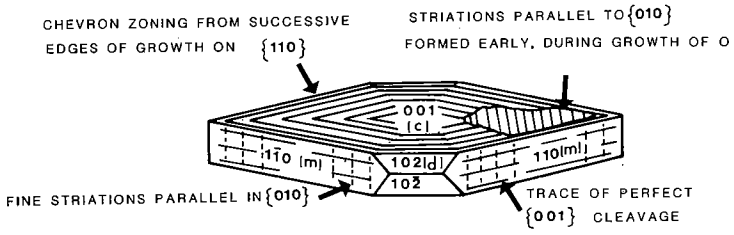

Figure 10. Mature barite crystal from Zodletone Mountain, showing relationship of forms to appearance.

WHAT IS THE MECHANISM OF BARITE PRECIPITATION?

Thermodynamic calculations demonstrate that the Zodletone Spring water is saturated with respect to barite and that precipitation is apparently inorganic. Any decrease in barite precipitation by comparison with the older, more-indurated deposits is probably due to the sulfate reduction performed by purple sulfur bacteria (Chromatiaceae).

According to the Sulin Oilfield Water Classification, the Zodletone water is a chloride–calcium type, chloride group, sodium sub-group class S1S2 (Table 3). Waters of this type are typical of deep, stagnant subsurface brines, most commonly associated with hydrocarbon occurrences (Collins, 1975). This result is important, as it suggests that the Zodletone water is an oil-field brine. The closest analyzed brines from the deep Anadarko basin, from four wells near Hobart in Kiowa County (Dwight's Energy Data, Charles Dunn, personal communication, 1984), show ionic concentrations which are an order of magnitude greater than those of the Zodletone water (with the exception of HCO_3^-). However, as the relative proportions of the components are similar (Table 4), we suggest that the Zodletone water is a deep oil-field brine diluted by contact with a near-surface ground water containing some bicarbonate and sulfate (supplying these ions to waters which were previously deficient in them). This latter ground water may well have passed through both Permian and Arbuckle Group strata. The reduction in Ba content from 104 mg/L in the subsurface brines to 43 mg/L at the surface suggests that subsurface precipitation of barite may be occurring.

Zodletone Mountain is located spatially above the Anadarko basin, as suggested by COCORP data (Brewer, 1982). It seems likely that the underlying reverse faults and associated fractures provide an escape route whereby deep-seated brines confined at depth can rise under a potentiometric head to contaminate the surface aquifer. (It is likely that any hydrocarbons in the immediate subsurface will already have escaped ahead of the water.)

TABLE 3.—SULIN CLASSIFICATION PARAMETERS FOR ZODLETONE SPRING WATER

Parameter	Value
*r*Na	10.96
*s*Na	39.66
*r*Ca	1.46
*s*Ca	5.27
*r*Cl	13.85
*s*Cl	50.10
$r SO_4$	0.15
$s SO_4$	0.53
*r*Mg	1.23
*s*Mg	4.44
Total *r*	27.64
*s*Na/*s*Cl	0.79
(*s*Na − *s*Cl)/$s SO_4$	−19.70
(*s*Cl − *s*Na)/*s*Mg	2.35
Palmer values:	
a	39.66
b	9.71
d	50.63

Explanation: *r* values = [ion] in (meq/L)/10; *s* values = *r* for each ion/total *r* (i.e., the sum of all the *r* values); meq/L, milliequivalents per liter = (mg/L of ion × valence of ion)/RAM of ion; Palmer values: a = *s*Na, b = *s*Ca + *s*Mg, d = *s*Cl + $s SO_4$.

TABLE 2.–SEMIQUANTITATIVE XRF SCAN FOR ELEMENTS WITH ATOMIC NUMBERS >21 FOR ZODLETONE MOUNTAIN SAMPLES

Sample	Elements present	Approximate concentrations (ppm)
Unconsolidated barite travertine	Cu	150
	Zn	19
	Pb	380
	Fe	710
	Co	44
	Ni	18
	Ba	300,000
	Sr	8,000
	Ti	490
	Cm	190
Barite-cemented calcareous tufa	Cu	88
	Zn	19
	Pb	330
	Fe	710
	Ba	310,000
	Sr	7,900
Mature barite travertine	Pb	670
	Fe	360
	Ba	350,000
	Sr	5,000

Note: If an element is not listed above, it means either (1) that it has an atomic number <21 and was not checked for, or (2) that it was not present at a concentration above the detection limit.

AN ECONOMIC CAVEAT

The presence of barium in the local Anadarko brines suggests that sulfate-bearing water should not be used during secondary recovery in adjacent oil fields, lest barite-scale precipitation occur. This is known to happen in other parts of the Anadarko basin (Cowan and Weintritt, 1976), further suggesting that Zodletone Spring water is a modified Anadarko-basin brine.

A broader economic question is whether or not this barite reflects subsurface development of a Mississippi Valley-type lead–zinc ore deposit. Sphalerite is known from the Arbuckle Mountains, and fluorite has been found on Bally Mountain, 3 mi southeast of Zodletone Mountain (Kelly Cloyd, personal communication, 1986). It is pertinent that Dozy (1970) postulated a genetic relationship between oil-field

TABLE 4.—KIOWA COUNTY OIL-FIELD BRINES COMPARED WITH ZODLETONE SPRING WATER

Sample	Depth (m)	Constituent (mg/L)					
		Ca	Ba	Na	Cl	HCO_3	Mg
Zodletone	0	273	43	2,500	4,910	270	149
35009819	539	9,285	2	64,000	123,090	61	2,405
35009820	532	11,312	104	60,928	122,080	41	2,788
35007461	532	10,100	93	54,400	109,000	37	2,150
35007462	538	8,780	2	57,200	110,000	55	2,150

brines and Mississippi Valley-type mineralizing fluids.

ACKNOWLEDGMENTS

We are grateful to Mr. Don Trobe, who owns the site, for his continued support. Curtis Ditzell originally mapped Zodletone, and we are grateful to him for use of his map. Younger acknowledges the award of a Harkness Fellowship, and Donovan is grateful for the support of the Oklahoma Geological Survey and Sun Co.

FIELD-TRIP STOP DESCRIPTIONS

"The one that died."—Stromatolites in the Cool Creek Formation showing turbinate columnar form. The one on the left has fallen, perhaps as a result of a storm. In its fall it clearly illustrates that the stromatolites in this colony formed distinctive relief on the Ordovician sea bed.

STOP 1
GEOLOGIC HIGHLIGHTS IN THE BLUE CREEK CANYON AREA

R. Nowell Donovan, Deborah A. Ragland, Mary B. Rafalowski, Kathy Collins, Tekleab Tsegay, David McConnell, David (Max) Marchini, Weldon Beauchamp, and David J. Sanderson

THE SETTING

Blue Creek Canyon is about 15 mi north-northwest of Lawton in southwestern Oklahoma (T4N, R13W). State Highway 58 runs through the canyon.

The entire area described here is part of the Kimbell Ranch, owned by Mr. and Mrs. David Kimbell of Wichita Falls. The ranch house is situated at the south end of the canyon and is managed by Charlie Bob and Dixie Oliver. Both the Olivers and the Kimbells have greatly encouraged the visits of geologists, and we are most grateful for their interest.

Descriptions are given here as a series of walks which start ~0.5 mi (~800 m) north of the ranch house at Red Hill (a small hill of Carlton Rhyolite Group capped by Post Oak Conglomerate, immediately west of Highway 58). The specific locations are keyed to sites located on Figure 1. These sites are A1–A15, B1–B3, and C1–C4. Some of this material has already been presented (Donovan and others, 1982,1984). However, we have revised and expanded our understanding of the area, incorporating much that is new.

GEOLOGIC THEMES

The relatively small area around Blue Creek Canyon contains a remarkable number and variety of interesting sites. Exposure quality, for this part of the world, is very good to excellent.

In general terms, the exposures illustrate several aspects of the development of the southern Oklahoma aulacogen. These are (1) the initial rift-related igneous activity; (2) early sedimentation in a basin with a decaying thermal imprint; (3) late Paleozoic deformation; and (4) burial of the resulting Permian relief.

Specific themes are keyed as follows:

1) The unconformity between the Carlton Rhyolite Group and the Timbered Hills Group: sites A4, A6, A12, A13, C1, C2, C5;

2) Sedimentary features of the Arbuckle Group: sites A3, A7, B1, B2;

3) The Blue Creek Canyon fault: sites A5, A7, A8, A9;

4) Other aspects of Pennsylvanian deformation: sites A2, A3, A10, A11, B3, C3, C4;

5) The Post Oak Conglomerate: sites A1, A14, A15, C5.

GEOLOGIC OVERVIEW OF THE AREA

The oldest rocks in the area are part of the Cambrian Carlton Rhyolite Group. The lavas were intruded by a number of diabase dikes, gently tilted, and cut by a number of N–S faults before they were reduced to a range of low hills by Late Cambrian (Franconian) time. The subsequent marine transgression (Fig. 2) was initially siliciclastic in character (Reagan Sandstone), but eventually a highly productive carbonate "factory" developed (Honey Creek Limestone). By this time, the rhyolite land surface had become an archipelago of small, rocky islands. These islands were buried by the time deposition of the Arbuckle Group commenced. The Arbuckle Group is >5,500 ft (1,680 m) thick in the southern Oklahoma aulacogen and is one of the world's great platform carbonate sequences. Succeeding (unexposed) lower Paleozoic rocks (Simpson Group, Viola Group, Sylvan Shale, and Hunton Group) were deposited before deformation began in Late Mississippian time.

This deformation, which concluded in Early Permian time, resulted in dismemberment of the aulacogen into a series of NW-trending basins (e.g., Anadarko, Hollis, and Ardmore) and uplifts (e.g., Wichita, Arbuckle, and Criner Hills).

In a regional context, the area forms part of the WNW-trending Wichita Mountains frontal fault zone, which constitutes the hinge between the Anadarko basin (to the north) and the Wichita uplift. The zone was the locus for Pennsylvanian tectonism during the late-deformation stage of the development of the southern Oklahoma aulacogen (Donovan, 1982; Gilbert and Donovan, 1984). This deformation was essentially transpressive, with left-lateral mo-

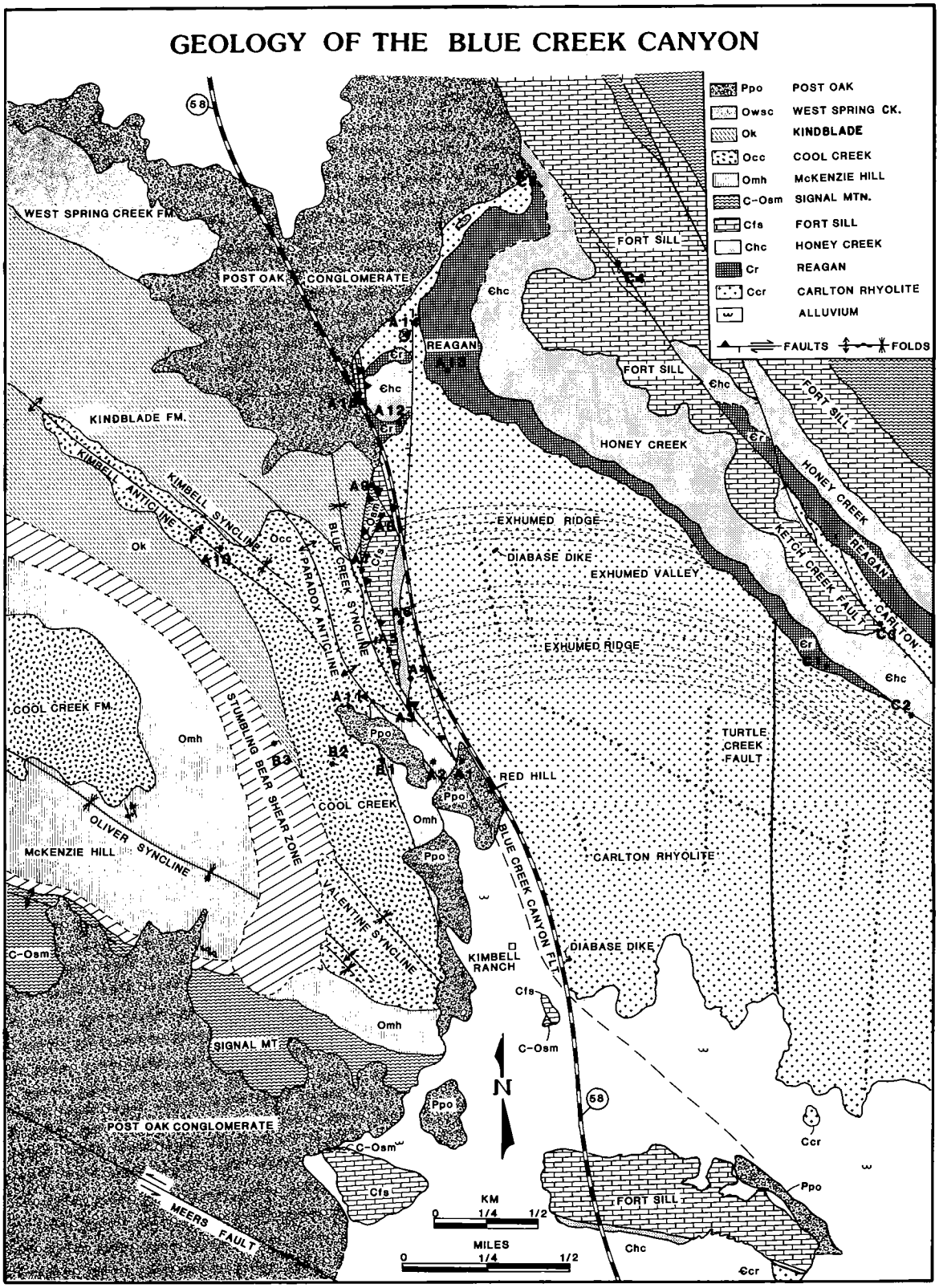

Figure 1. Geologic map of Blue Creek Canyon, showing sites discussed in text. (We are grateful to Diana Schaefer for drafting this map.)

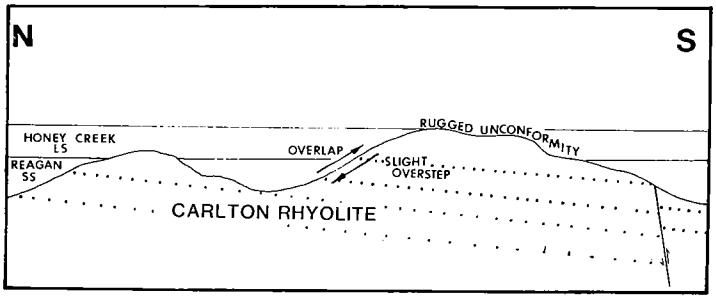

Figure 2. Stratigraphic relationships between the Carlton Rhyolite Group and the Timbered Hills Group (from Rafalowski, 1984).

tion along the length of the zone (McConnell, 1983; Beauchamp, 1983; Marchini, 1986). The zone is broken up into a number of blocks bounded by major faults.

The Blue Creek Canyon fault is the only one of these major structures whose Pennsylvanian character can be examined at the surface. It is an oblique high-angle reverse/left-lateral structure, trending N. 10° W. in the canyon area. It has a stratigraphic downthrow to the west which decreases northward from 2,400 ft (730 m) to 1,800 ft (550 m) along the length of the canyon (this variation in downthrow is not regionally significant, but simply reflects fold geometry in the western "footwall" block).

The N-trending segment of the fault exposed in the canyon is anomalous in trend. To the north and south, the fault bends until it is almost parallel with the regional WNW trend. Similar anomalous fault trends are common in the areas of both the Wichita Mountains and Arbuckle Mountains. Such segments may have utilized an early N–S fracture trend which is pre-Reagan Sandstone, post-Carlton Rhyolite Group. The Blue Creek Canyon example in its anomalous section appears to constitute a compressional bend.

The major faults in the frontal zone define blocks which have undergone differing amounts of deformation. In the present instance, the Blue Creek Canyon fault separates the Blue Creek "horst," to the east, from the Lawtonka "graben" (terminology of Harlton, 1972). The "horst" is a relatively undisturbed terrane dominated by moderate homoclinal NE dips. The "graben" on the other hand has been subjected to a "squeeze play" between the "horst" (to the NE) and the Wichita Mountains (to the SW across the Meers fault). The result is a structural mayhem of refolded reverse faults, rotated en echelon folds, and brittle shears, which together record intense left-lateral transpression and constitute the most intensely deformed terrane exposed in either the Wichitas or the Arbuckles (Donovan, 1982; Beauchamp, 1983; McConnell, 1983; Marchini, 1986).

In the small segment of the Lawtonka "graben" exposed in Blue Creek Canyon, the dominating structures are a group of four major folds which trend WNW and plunge consistently WNW. These folds are the Blue Creek syncline, the Paradox anticline, and the Kimbell fold pair. The latter folds have a lopsided "rabbit-ear" relationship to the structurally lower Paradox fold. A fifth large fold, the Blue Creek anticline, is in the "hanging-wall" block east of the Blue Creek Canyon fault. A feature of interest is that the Carlton Rhyolite Group is quite clearly involved in the folding.

Farther to the west is the enigmatic Stumbling Bear shear zone, a region of intensely deformed rock across which there is a stratigraphic discontinuity of as much as 2,200 ft (670 m). This structure has recently been interpreted as a transpressed thrust (Marchini, 1986).

As deformation concluded, the surfaces of the uplift areas were sculpted by erosion into irregular hills which were subsequently buried by Permian sediments. At present these hills are in various stages of exhumation from beneath the Permian cover. In general terms, the Permian rocks are conglomerates close to the old hills (Post Oak Conglomerate facies), but fine outward into the ancient valleys and basins.

SITE DESCRIPTIONS A1–A15

Site A1: Post Oak Conglomerate

The Permian Post Oak Conglomerate unconformably overlies the Carlton Rhyolite Group at the eastern end of Red Hill, whereas at the western end of the hill it overlies the McKenzie Hill Formation of the Arbuckle Group. Fracturing in the rhyolite is probably due to the Blue Creek Canyon fault, which can be projected to pass under Red Hill near the road (thus accounting for the differing unconformable relationships at either end of the hill; see Donovan and others, 1982). The conglomerate bears a light fracture pattern hinting at some slight post-Permian movement on the fault. The Permian deposit is a breccia-conglomerate consisting of pebble-sized clasts crudely bedded in layers derived either from west of the canyon (in which case the clasts are Ordovician limestone) or from east of the canyon (in which case the clasts are rhyolite or Cambrian limestone) (Donovan and others, 1982). The top of the hill is a good vantage point for viewing the Ordovician terrane; the conspicuous anticline in the foreground is the Paradox anticline.

Site A2: Paradox Anticline

After one crosses Blue Creek, the Paradox anticline can be examined in detail. The lithology here is the upper, cherty part of the McKenzie Hill Formation (Donovan and Ragland, this volume). Like other major folds in the area, the Paradox anticline is a complex, N-plunging fold of variable tightness (30–130°) and with fairly sharply defined axes. All the large folds in the area are basically parallel (class I; Ramsay, 1967), and as a result their axial traces are displaced by layer-parallel slippage in a number of places. One of these slippage décollements occurs on the eastern limb of the anticline between sites A2 and A3, where a group of small-scale drag folds showing

asymmetry and locally developed cleavage is confined to a layer ~20 ft (~6 m) thick between undisturbed beds in the McKenzie Hill Formation.

Site A3: Base of the Cool Creek Formation and the Blue Creek Syncline

Here a gully marks the position of the Thatcher Creek Member (Ragland and Donovan, 1985a), a quartz-rich, cross-bedded limestone which marks the base of the Cool Creek Formation. This member is a critical stratigraphic marker in unraveling the complexities of the Lawtonka "graben," maintaining its character over many miles of outcrop; here it can be followed around the axis of the Blue Creek syncline. The Blue Creek Canyon fault runs through the trees to the east, and as the fault is approached the beds become overturned by as much as 30°.

Site A4: Unconformity Between the Carlton Rhyolite Group and the Honey Creek Limestone

The Reagan Sandstone is missing at this unconformity; outcrops along the length of the canyon (e.g., at site A6) indicate that this area was an island until late in the history of the Honey Creek Limestone. The exposure is interesting in that a stabilized shell bank consisting of orthid-brachiopod valves formed above the thin basal breccia (Fig.3). Small calcite–hematite stromatolites are also present; the section has been interpreted as a sheltered coastline deposit (Donovan and Rafalowski, 1984).

Site A5: Blue Creek Canyon Fault Trace

A short distance above the unconformity at Site A4, the Honey Creek Limestone passes up into the

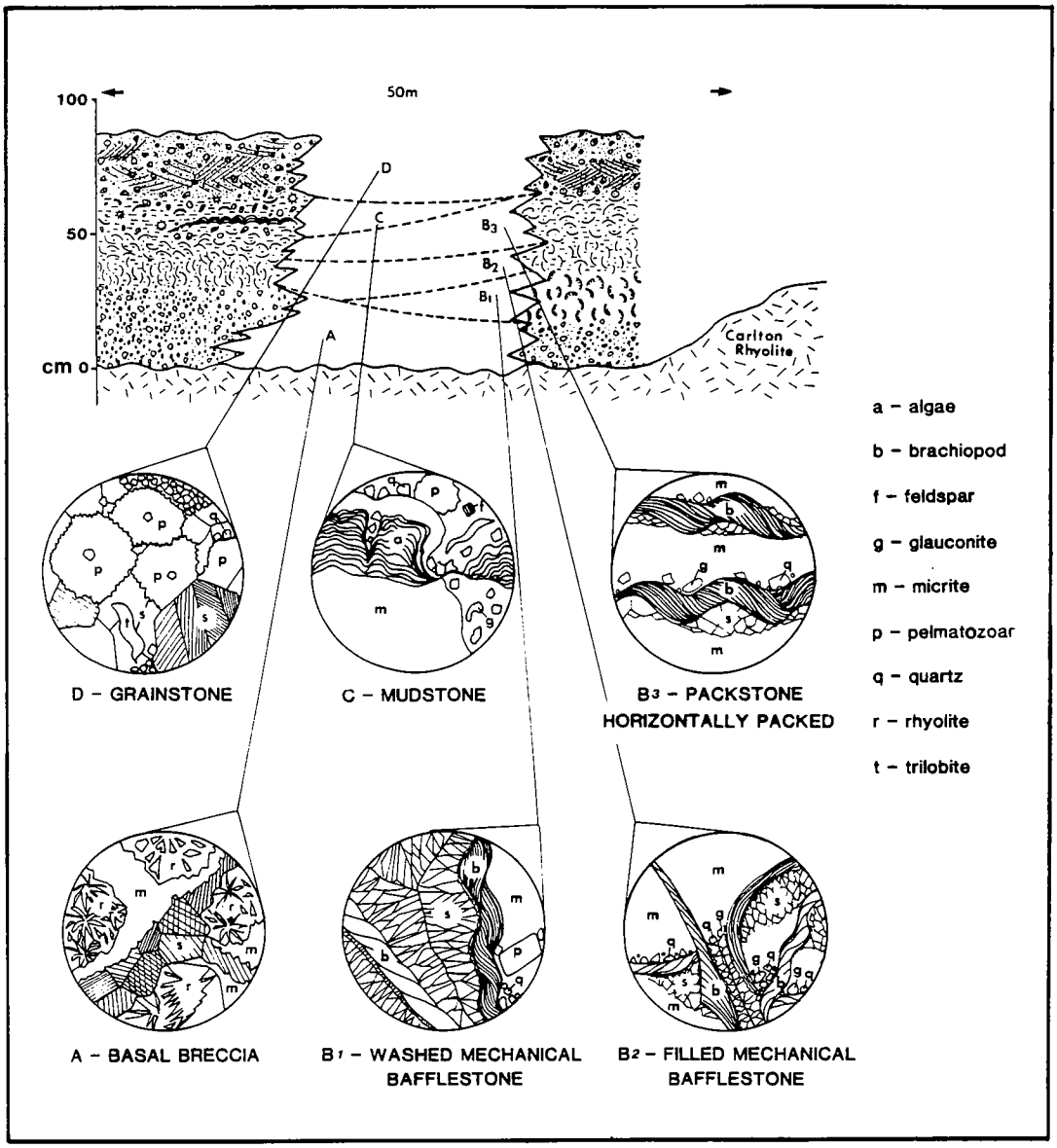

Figure 3. Field relationships and petrography of the basal Honey Creek Limestone at site A4. Note in particular the mechanical bafflestone produced by the stacking of orthid-brachiopod valves by wave action. Two varieties of bafflestones occur, one infilled by lime mud and other detritus (B2) and the other (B1) infilled by radiaxial fibrous calcite(s) (from Rafalowski, 1984).

Fort Sill Limestone, the lowest formation of the Arbuckle Group (a general description of these rocks is given by Donovan and Ragland, this volume). To the west, the Fort Sill outcrop is truncated by the Blue Creek Canyon fault trace. This trace is a conspicuous linear depression. The fault plane dips to the east at a high angle, indicating a reverse element of movement. In addition, prominent phacoidal shearing suggests a left-lateral component of motion.

Site A6: Unconformity Between the Carlton Rhyolite Group and the Honey Creek Limestone Revisited

The unconformity is well exposed at a small prospect pit (Fig. 4). The unconformity is most irregular and appears to be a wave-cut platform with numerous fissures and pedestals, which was covered by a detrital, coarse-grained carbonate sand composed mostly of broken primitive echinoids. This exposure has been interpreted as an exposed shoreline setting on the windward side of an island jutting from the Honey Creek sea (Fig. 5) (Donovan and Rafalowski, 1984).

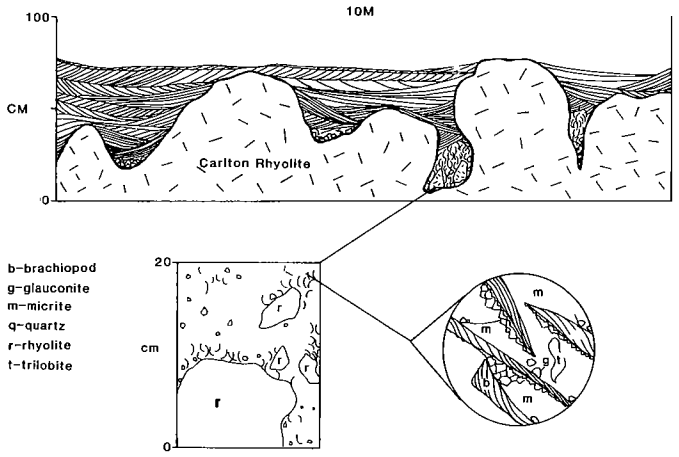

Figure 4. Irregular unconformity between the Carlton Rhyolite Group and the Honey Creek Limestone at site A6. Insets show petrographic details of sediments trapped between wave-cut pedestals (from Rafalowski, 1984).

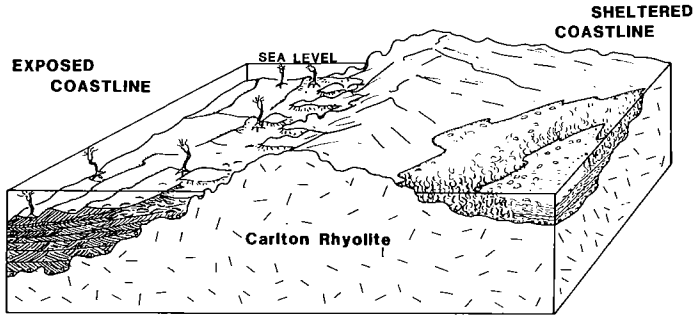

Figure 5. Environmental interpretation of the unconformity between the Carlton Rhyolite Group and the Honey Creek Limestone. Site A4 is interpreted as recording a sheltered coastline, whereas site A6 is regarded as recording an exposed coastline (from Rafalowski, 1984).

Site A7: Contact between the Fort Sill Limestone and the Signal Mountain Formation, and Minor Hanging-Wall Faults

Here the uppermost, massive member of the Fort Sill Limestone is overlain by the thin-bedded and more poorly exposed Signal Mountain Formation. This contact affords perhaps the most emphatic expression of a formation boundary in the Arbuckle Group. Feinstein (1981) has suggested that the sharpness of this contact reflects adjustment faulting during development of the initial aulacogen basin. By contrast, the Cambrian–Ordovician boundary, which is ~330 ft (~100 m) above the base of the Signal Mountain Formation (Stitt, 1978), is lithologically undistinguished.

The Fort Sill–Signal Mountain contact has been displaced by a number of small E–W faults downthrown to the south.

Site A8: Resolution of Space Problems within the Blue Creek Canyon Fault Zone

From Site A7, it is instructive to follow the strike of the Signal Mountain Formation in a northeastly direction. It will be clear that a major space problem is created by a change in strike (from N to NE); as a result, the Signal Mountain Formation appears to be on a collision course with the Carlton Rhyolite Group. However, at Site A8 a major N-trending fault cuts the section and emplaces a thin sliver of upper Fort Sill Limestone between the Signal Mountain and the rhyolite. A second fault between the Fort Sill and the rhyolite can be inferred to run more or less beneath the existing road (Fig. 1). The pond next to the road is fed by springs emerging from the latter fault plane.

Site A9: A Fault Conjunction

The fault at Site A8 can easily be traced northward into an old quarry excavated when the road through the canyon was made. The quarry was excavated into the Signal Mountain limestone in a zone which was crushed between the Blue Creek Canyon fault (to the west) and the "pond" fault. The hanging wall of the latter fault is exposed on the eastern wall of the quarry and shows oblique slickensides and gouging suggestive of left-lateral transpression. Left-lateral shear phacoids are exposed on the floor of the quarry. A left-lateral sense of drag is shown by the beds in the quarry (Fig. 6).

Site A10: The Four Major Folds

From this point, a walk of 0.5 mi (~800 m) west to the top of the hill on the horizon crosses all four of the major folds in the area (Fig. 1). The most photogenic of these folds is the Kimbell anticline at the top of the hill. It is interesting to note how the axes of the folds swing to a more northwesterly orientation as they emerge from the canyon area.

The view from the hilltop (Kimbell Mountain) is an impressive one. To the west lies the contorted terrane

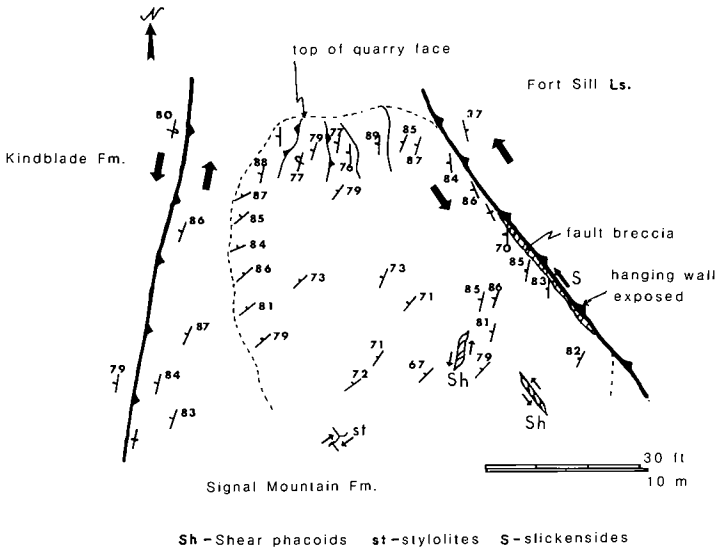

Figure 6. Sketch map of relationships in the quarry at site A9. Note the sense of left-lateral drag in the Signal Mountain sediments.

of the Lawtonka "graben"; to the north is the valley eroded along the Blue Creek Canyon fault where it resumes its northwesterly trend; to the east lies the Blue Creek "horst," where the Cambrian Timbered Hills Group unconformably overlies the Carlton Rhyolite Group (the conspicuous peak is Ring Top Mountain); to the south the igneous Wichita Mountains rise across the Meers Valley.

Site A11: The Paradox Anticline Revisited

Red Hill can easily be seen from the top of the hill at A10. The recommended return route is along the axis of the Kimbell anticline until this fold merges into the western limb of the Paradox anticline. The space problems of parallel-fold geometry are clearly apparent on this walk—nowhere more so than at site A11, where the Paradox anticline is spectacularly well exposed. The paradox here is provided by an interplay of plunge and hill slope which results in the fold having the convincing appearance of a syncline with a very tight axis. Sitting astride this axis and looking generally northward is a good situation for reflecting on the geometries of the four major folds in the area. Because of a consistent plunge to the north, their form can be studied through a stratigraphic thickness of ~3,000 ft (~900 m).

Site A12: Unconformity Between the Carlton Rhyolite Group and the Reagan Sandstone

This site lies at the north end of the canyon to the east of the road. In this area, flow-banded Carlton rhyolite is well exposed. Above the rhyolite lies the Reagan Sandstone, which here comprises a 5-ft-thick (1.5-m-thick) basal conglomerate consisting of pebbles of rhyolite cemented by hematite. Above this is a 2-ft (60-cm) lithic sandstone, followed by ~8 ft (~2.4 m) of highly glauconitic, cross-bedded greensand which is interbedded with a thin rhyolite-pebble conglomerate. Throughout the Slick Hills, the greensand is everywhere the top unit of the Reagan, consisting of as much as 55% of fine-sand-sized pellets of glauconite, plus quartz, rhyolite, and broken phosphatic shells of inarticulate brachiopods—all either set in a matrix of iron-rich illite or (toward the top) cemented by calcite.

The passage from the Reagan into the Honey Creek Limestone (marked by the incoming of lenses of cross-bedded, coarse grainstones) is located in a prospect pit a few yards to the northeast.

Site A13: A Second Exposure of Reagan

Crossing an obvious fault-controlled gully to the northeast, we can examine a somewhat thicker exposure of Reagan. The basal facies is a very coarse-grained lithic sandstone, overlain by a coarse-grained, cross-bedded (sets as much as 2 ft, or 60 cm, thick) quartz arenite, some shale (mostly covered) and the upper greensand unit. This sequence is 60 ft (18 m) thick and passes up into a full sequence of Honey Creek Limestone on the slopes of Ring Top Mountain to the east.

Site A14: Post Oak Boulder Conglomerate

This site features an enigmatic exposure of Post Oak Conglomerate consisting of angular boulders of the Fort Sill Limestone as much as 20 ft (6 m) in diameter. The deposit, which rests unconformably on the Carlton Rhyolite Group, is one of a number of similar deposits in the Slick Hills, all of which seem to be related to nearby fault scarps (Donovan, 1984)—in this case the Blue Creek Canyon fault.

Site A15: Post Oak Pebble Conglomerates and the Permian Sculpting of Blue Creek Canyon

Along Highway 58 at the north end of the canyon are several exposures of the Post Oak Conglomerate (Donovan, 1982). One of the more interesting of these deposits, located in a ditch to the east of the road, shows Post Oak Conglomerate composed of diverse types of locally derived clasts as much as 2 ft (60 cm) in diameter, resting on an irregular surface of Fort Sill Limestone. The relationships here suggest that Blue Creek Canyon was first sculpted in Permian times. Pebble imbrication hints that drainage at this spot was to the north (not south, as now). Of particular interest are the coarsely crystalline, fibrous calcite cements in the conglomerate close to or on the unconformity. These cements are coatings as much as 2 in. (5 cm) thick which record initial vadose conditions (i.e., flowstone precipitation), followed by phreatic crystal growth, suggesting that the water table gradually rose through a highly porous gravel.

SITE DESCRIPTIONS B1–B3

Site B1: Contact Between the McKenzie Hill and Cool Creek Formations

Northwest of Red Hill (Fig. 1), in the valley of Thatcher Creek, are impressive cliffs carved in the boundstones and associated sediments which form the top part of the McKenzie Hill Formation. A band rich in the brachiopod *Finkelnbergia* is present but difficult to find. More obvious are siliceous sponges and a variety of cherts, including burrow fills and nodules. Above the McKenzie Hill, where the valley widens and runs parallel to strike, is the type locality (sec. 11, T4N, R13W) of the Thatcher Creek Member (Ragland and Donovan, 1985a). This multistoried unit is composed mainly of limestone and detrital quartz in varying amounts; it ranges in thickness from 12 ft (3.7 m) to 16 ft (5 m). The member weathers to a characteristic gully that can be traced throughout the Slick Hills and the Arbuckle Mountains.

Site B2: Algal Boundstones

Above site B1, the Cool Creek Formation is well exposed and full of interest, particularly on the left-hand (southern) side of the valley, ~330 ft (~100 m) above the base of the formation, where an extensive algal-boundstone complex terminates (see Ragland and Donovan, this volume, particularly fig. 2). This complex can be traced over half a mile (1 km) to the north. The 20-ft-high (6-m-high) bioherm terminates abruptly against laminated mudstones and intraformational conglomerates. The mudstones and intraformational conglomerates show compactional draping around the end of the buildup. Approximately 10 ft (~3 m) to the south, the laminated sediment interfingers with algal mat, possibly suggesting that a shoreline lay in that direction.

Site B3: The Stumbling Bear Thrust and Shear Zone

Westward from Site B2, the Cool Creek passes upward into the Kindblade Formation. The sequence is homoclinal, being disturbed only slightly by minor folding and fracturing. This conformity is abruptly terminated at Site B3, the Stumbling Bear shear zone. The boundary of the shear zone (the Stumbling Bear thrust; Marchini, 1986) emplaces rocks of the Signal Mountain Formation against the Kindblade, indicating a stratigraphic discontinuity of ~2,000 ft (~600 m). Within the 600-yd-wide (550-m-wide) shear zone, rocks of the Signal Mountain and McKenzie Hill Formations have been greatly distorted in what is probably the most structurally complex terrane exposed in Oklahoma. Well developed throughout the zone are broken, disharmonic, and sheared folds; small faults; left-lateral, en echelon solution arrays (Fig. 7) with associated Riedel fractures (McCoss and Donovan, this volume); and pervasive pressure-solution cleavage. The intensity of deformation gradually decreases to the west across a smaller

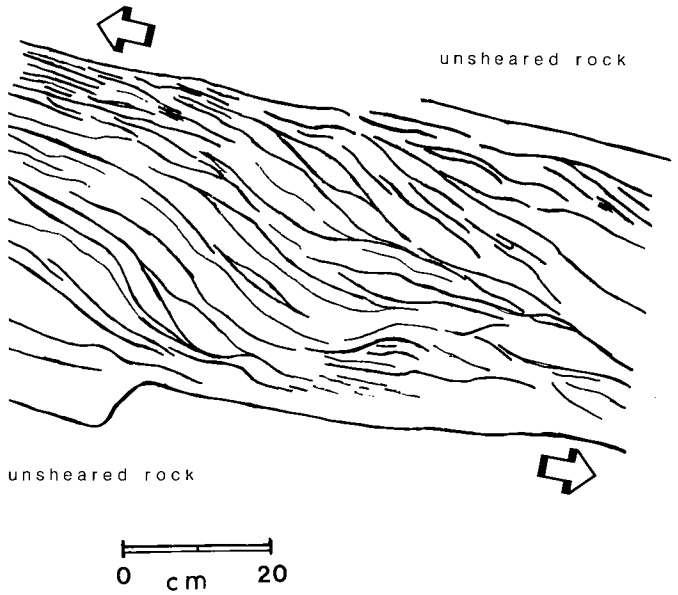

Figure 7. Field sketch of a left-lateral, en echelon pressure-solution array in the Stumbling Bear shear zone.

thrust into relatively undeformed McKenzie Hill rocks. Marchini (1986) has interpreted the whole complex at site B3 as a flat in a left-lateral transpressed thrust, climbing to the northwest with a generally steep trajectory. If this is the case, then the smaller thrust which forms the southwest boundary of the shear zone is the roof of a duplex.

SITE DESCRIPTIONS C1–C5

Site C1: The Reagan Sandstone

To the east of Highway 58, the Carlton Rhyolite Group is well exposed as a series of low hills. Beyond the rhyolite hills lies a strike-parallel valley which closes to the north and south and is eroded in the Reagan Sandstone. There are several good exposures of sandstones in the valley, particularly at site C1, where a tan-colored, lenticular quartz arenite displays medium-scale cross-bedding, reactivation surfaces, and a fine display of *Skolithos* trace fossils (Fig. 8). Some herringbone cross-bedding is present in subjacent sandstones (Tsegay, 1983). The whole sequence appears to record a storm-tide interplay in a shallow-marine environment.

Site C2: Overlap of the Reagan Sandstone

The closure of the valley to the southeast of site C1 is an expression of buried Cambrian relief, which is best appreciated by walking the rhyolite–sediment unconformity to site C2. From a maximum thickness of 120 ft (37 m), the Reagan gradually thins until it is completely overlapped by the Honey Creek Limestone. Among many interesting features are (1) an ankerite band at the contact of the Honey Creek and Reagan (Cloyd and others, this volume), and (2) wedges of rhyolite conglomerate and breccia shed

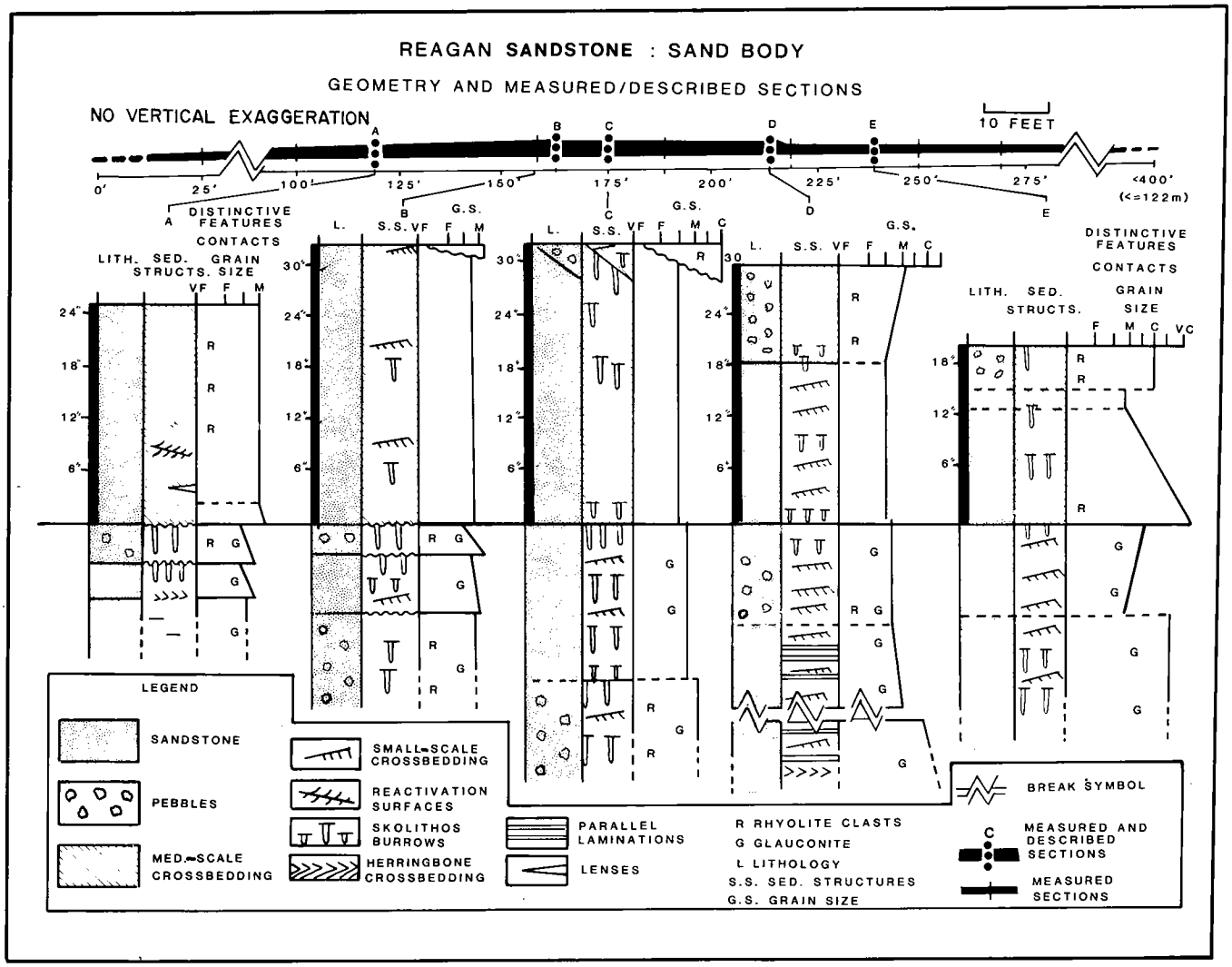

Figure 8. Log of a characteristic lenticular sandstone body in the Reagan Sandstone. (We are grateful to Diana Schaefer for drafting this diagram).

from the rhyolite island as it was gradually overlapped (Donovan, 1984).

Site C3: The Ketch Creek Fault

The view east from site C2 is across the valley of Ketch Creek, which is eroded along a fault with a stratigraphic downthrow of 500 ft (150 m) to the west at this point, decreasing to zero to the north-northwest. The fault bifurcates and gradually passes into a number of small fractures and west-facing monoclines when traced to the north. The dip of the fault plane wavers on both sides of vertical, but is mostly steep and to the west. The precise significance of the fault is uncertain; on balance, the structure appears to be a normal fault with some evidence of left-lateral shear displacement.

Site C4: A Walk Along the Ketch Creek Fault

The Ketch Creek fault can easily be traced as a geomorphic lineament to the north. Springs utilize the fault plane at two sites where the Carlton Rhyolite Group is faulted against the Fort Sill Limestone. While most of the fault-related deformation (including some tight folding) is located in the downthrown (western) block, the stratigraphic disparity is reduced by the gradual appearance of younger beds in the eastern block. The view to the northeast encompasses almost 4,500 ft (1,350 m) of unbroken Arbuckle Group carbonates dipping 20–30° NE.

Site C5: Double Unconformity—Carlton Rhyolite Group, Reagan Sandstone, and Post Oak Conglomerate

The final stop on this walk is a spectacular double unconformity involving (1) the Reagan Sandstone–Carlton Rhyolite Group relationship, and (2) the Post Oak Conglomerate and lower Paleozoic sequence. The latter unconformity is especially impressive: One side of a steep-sided Permian valley is clearly exposed, and the Post Oak clasts markedly fine upward and outward from the unconformity.

STOP 2
GEOLOGIC HIGHLIGHTS OF THE BALLY MOUNTAIN AREA

R. Nowell Donovan, Deborah A. Ragland, Kelly Cloyd, Steve Bridges, and R. E. (Tim) Denison

THE SETTING

The Bally Mountain Range is located in eastern Kiowa County, in southwestern Oklahoma (R14W, T6N). The principal landowners in the area are Mr. W. Hodges and Mr. D. Leatherbury; we are grateful to them for permission to visit the sites listed.

Bally Mountain itself is the type section of the Carlton Rhyolite Group; a thickness of 3,600 ft (1,100 m) can be inspected (Ham and others, 1964). The rhyolite lies unconformably beneath the sandstones and limestones of the Timbered Hills Group, which in turn underlies the Arbuckle Group. The sediments form modest hills north and west of Bally Mountain. The top (West Spring Creek) formation in the Arbuckle Group was almost completely eroded in Permian times; otherwise, the area offers the most complete and easily accessible exposure of the group in Oklahoma. Counting the rhyolite, Bally Mountain displays an apparently complete section of ~9,000 ft (2,750 m) of lower Paleozoic rocks. The Bally Mountain Range is part of a Permian landscape which is being exhumed in this part of Oklahoma. Permian pediments, conglomerates, and karst fills in the limestones help to confirm that these are ancient hills formed of ancient rocks—not modern hills formed of ancient rock.

In this communication we develop a number of geological themes which are keyed to locations shown in Figure 1.

THE CARLTON RHYOLITE GROUP (SITE A1)

The Carlton Rhyolite Group is part of an enormous acidic igneous complex of Cambrian age (~525 m.y.) which formed during the initiation of the southern Oklahoma aulacogen. The total volume of magma was enormous—perhaps 6,000 mi^3 (25,000 km^3) (Gilbert, *in* Gilbert and Donovan, 1982). The rhyolites are the extrusive equivalent of the Wichita Granite Group, the two rock groups having virtually identical chemistry. The maximum known thickness of rhyolite is ≥4,500 ft (1,370 m), and the volcanic rocks are believed to occupy an area of 17,000 mi^2 (44,000 km^2) in southern Oklahoma.

Ham and others (1964) located the type section of the Carlton Rhyolite Group on Bally Mountain, where a mostly unbroken, easily accessible succession of 3,600 ft (~1,100 m) of flows, welded tuffs, water-laid tuffs, and flow breccias is displayed. Some flows are spherulitic, others are ignimbrites and show flow banding, while most are massive and essentially featureless.

UNCONFORMITY BETWEEN THE CARLTON RHYOLITE GROUP AND TIMBERED HILLS GROUP (SITE B1)

By Late Cambrian time (after an interval of perhaps 15 m.y. or less), the rhyolites had weathered to a range of low hills. This topography was gradually transgressed during Franconian time; the initial deposits were siliciclastics (Reagan Sandstone); subsequently, the Honey Creek Limestone formed. At this later period, the higher parts of the rhyolite topography formed an archipelago (Donovan, 1982; Donovan, *in* Gilbert and Donovan, 1984). A superb example of a Franconian "island" can be seen at site B1; not only is the Reagan absent but a good part of the Honey Creek is missing too. Approximately 200 ft (~60 m) of stratigraphic overlap occurs at this site.

The unconformity is not as profound as that at the base of the Paleozoic transgression over much of the United States. The time span represented by the unconformity is short, the topographic relief is modest, and there is only a mild angular unconformity (~5°) between igneous and overlying sedimentary layers. The brevity of the time span is a reflection of the setting of the unconformity within the aulacogen.

THE TIMBERED HILLS GROUP (SITE C1)

The Reagan Sandstone at site C1 consists of a basal breccia of rhyolite clasts, a few feet of tan-colored lithic sandstones, and a topmost unit of ~30 ft (~9 m) of dark-green glauconitic sandstone (in places glauconite constitutes 60% of the constituent grains). Over 200 ft (60 m) of the lower Reagan is absent (Tsegay, 1983); this is not surprising, in view of the proximity of Franconian "land" (site B1). The upward passage from Reagan into Honey Creek is marked by

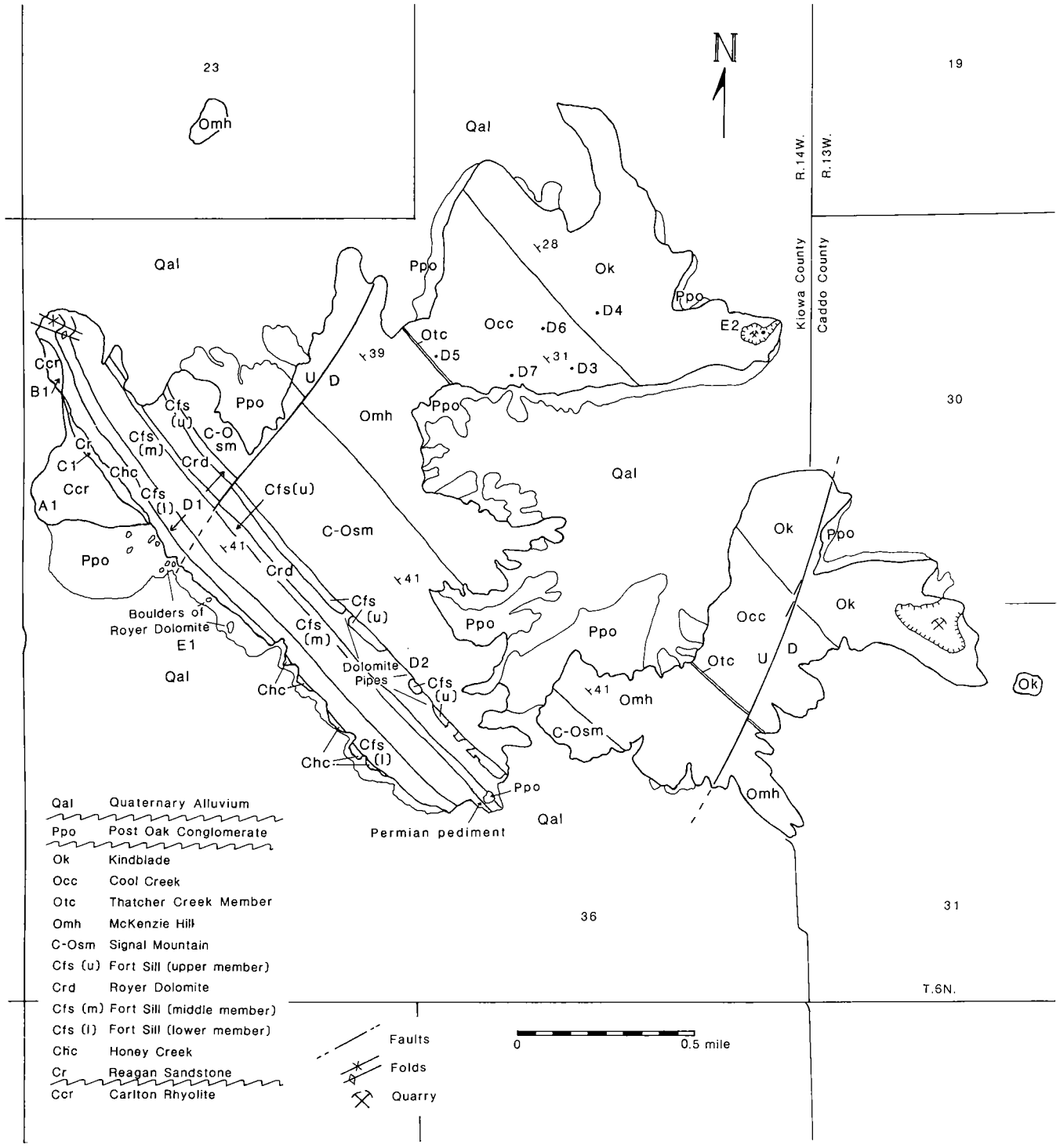

Figure 1. Geological map of the northeast part of the Bally Mountain Range. Sites A1–E2 are areas highlighted in text.

orange-weathering stringers and thin beds of ankerite (Cloyd and others, this volume). This orange-weathering zone is everywhere a distinctive feature at the contact between the two formations and appears to be a diagenetic product of the reaction between glauconite and carbonate-rich ground waters related to the overlying limestone. The Honey Creek is an impure, coarse-grained, cross-bedded, bioclastic limestone composed of vast amounts of broken pelmatozoans, subordinate robust-shelled trilobites, some brachiopods (including phosphatic inarticulate), and quartz and glauconite grains. It appears to have formed as a stacked series of tidally influenced sandbars (Rafalowski, 1984).

THE ARBUCKLE GROUP (SITES D1–D7)

About 4,000 ft (~1,200 m) of limestones assigned to the Arbuckle Group are well exposed in a continuous section which dips 25–45° NE. Various parts of this section have been described by workers from several areas in the Slick Hills (e.g., Barthelman, 1968; Brookby, 1969; Stitt, 1977; Donovan, 1982; Stitt, 1983; Ragland, 1983; Rafalowski, 1984; Ditzell, 1984). In addition, the sequence has been reviewed by Donovan and Ragland (this volume, in particular fig. 1).

Few locations so eloquently display the characteristic motifs of platform carbonate deposition. The seemingly endless tiers of "tombstones" remind us of the unique character and dimensions of the great Cambrian–Ordovician platform. Obviously, it is impossible to describe this great section in detail here; in this account we simply highlight some features of particular interest.

Site D1: The Fort Sill Limestone

The Fort Sill Limestone on Bally Mountain and adjacent Zodletone Mountain is divided into five informal members:

5) Massive algal boundstones (topmost);

4) A thick, stratabound dolomite (a replacement of massive algal boundstones);

3) Massive algal boundstones;

2) Alternations of lime mudstones with very thinly bedded dolomitic mudstones;

1) Thinly bedded limestones which are dominantly mudstones but contain important packstones and grainstones (some oolitic), plus a few horizons of stromatolites (basal).

Elsewhere in the Slick Hills, units (3), (4), and (5) are conjunct, as the dolomite is not developed. This dolomite is a coarsely crystalline deposit with some intracrystalline porosity; it is usually referred to as the "Royer dolomite," although Donovan and Ragland (this volume) have suggested the term "Bally Dolomite."

Site D2: Discordant Dolomite

For the most part, the Bally Dolomite maintains stratigraphic integrity, but toward the eastern end of the exposure discordant zones of complete dolomitization extend from the Royer to the top of the Fort Sill (and locally a small way into the overlying Signal Mountain Formation). Some of the boundaries of these zones appear to coincide with NE-trending joints; the dolomite is particularly coarse-grained and contains vugs lined by baroque crystals. Some illitic clay is present. This discordant dolomite differs texturally from the underlying stratabound dolomite. Similar discordant dolomites occur in other parts of the Slick Hills. In each case they are associated with a preexisting stratabound dolomite, and we suggest that they record the passage of warm, dolomite-saturated fluids through existing fractures. Given the structural setting, these fluids probably originated in the Anadarko basin (Donovan, this volume).

Site D3: Intraformational Conglomerates

The dominant lithologies in the Arbuckle Group are clastic limestones, ranging from intraformational conglomerates through grainstones and packstones to wackestones and mudstones. Intraformational conglomerates are a common lithology, forming perhaps 10% of the entire sequence; those in the Signal Mountain and Cool Creek Formations are particularly well exposed.

The textural immaturity of many of these limestones suggests a storm-affected environment. A constant interplay among fair-weather deposition, hardground cementation, and storm-induced erosion is suggested by the fact that lime-mud intraclasts are the commonest allochem (followed by peloids, fossil trash, and ooids).

Site D4: Grainstone Shoals

Ooids are developed best (but not exclusively) in the Cool Creek and Kindblade Formations, where they form the dominant constituent in cross-bedded grainstones (which presumably record migrating ooid shoals). Fine-sand-sized quartz and lime-mud intraclasts are common nuclei for ooid growth. Also, uncoated quartz grains are present in variable amounts in most grainstones. Some herringbone cross-bedding (Fig. 2) hints at slight tidal influences on the platform.

Site D5: Quartz–Carbonate Sandstones—The Thatcher Facies

Detrital quartz is conspicuous in the Arbuckle Group from the base of the Cool Creek Formation (Thatcher Creek Member of Ragland and Donovan, 1985) and at several higher horizons, including the base of the West Spring Creek Formation. All these units are similar in that they consist of laterally persistent, cross-bedded quartz–carbonate sandstones (Fig. 3) which occupy small, erosive-based channels.

Site D6: Stromatolites

Algal boundstones are found throughout the group; those in the Cool Creek Formation are particularly fine (Ragland and Donovan, this volume). One extremely well-exposed algal reef is composed of colonies of nonbranching columnar members that radiate, forming a "sunburst" pattern in cross-profile (Fig. 4). The internal structure of this unit is intermediate between stromatolitic and thrombolitic. In other words, the well-defined laminations characteristic of true stromatolites are not well developed (if at all), suggesting that the reef grew in the subtidal zone. Ooids (most of which are at least partially silicified) are the dominant intracolumn grains, suggesting that the reef developed in reasonably well-agitated water.

Site D7: Dolomite and "Cauliflower" Cherts

This site is described by Cloyd and others elsewhere in this volume (see particularly their fig. 2). Abundant "cauliflower" cherts are present; these contain minute inclusions of anhydrite and celestite. In addition, small pseudomorphs of chert (after gypsum?) are found. Two varieties of dolomite are present: the earliest is a stratabound dolomicrite (possibly of evaporative origin), and the second is a discordant dolosparite similar to that seen at site D2.

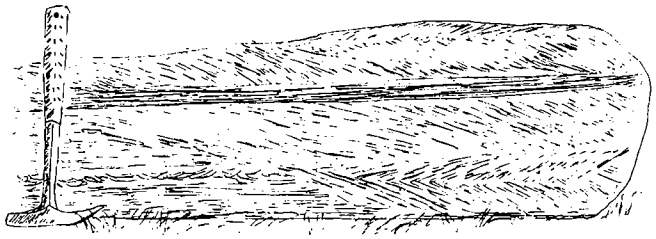

Figure 2. Field sketch of a quartz-rich, oolitic grainstone marked by bipolar herringbone cross-bedding (Kindblade Formation).

THE PERMIAN IMPRINT ON BALLY MOUNTAIN (SITES E1 AND E2)

Site E1: Permian Landforms

A double, or overlapping, unconformity is found throughout the Slick Hills. Not only does the Reagan Sandstone onlap the Carlton Rhyolite Group, it and the succeeding formations are onlapped by the Permian Post Oak Conglomerate facies.

As noted, the Bally Mountain Range is an exhumed Permian hill complex surrounded by its own detritus (the Post Oak Conglomerate). Two aspects of the Permian imprint are particularly interesting close to the ridge (Raggedy Mountain) formed by the Bally (Royer) Dolomite. First, at the southwest edge of the hill, house-sized boulders of dolomite clearly have tumbled from the outcrop on the hill above. Some of these boulders may have fallen recently, but at least two of them are embedded in the calcrete which cemented the Post Oak Conglomerate. These huge boulders may represent sporadic rock falls; on the other hand, they may record a seismic effect similar to that documented in the nearby Permian of the Meers Valley (Donovan, 1984; Collins, 1985; Bridges, 1985). Second, at the southeast edge of the dolomite ridge a small deposit of Post Oak sits on what appears to be a Permian pediment sloping gently upward to Raggedy Mountain.

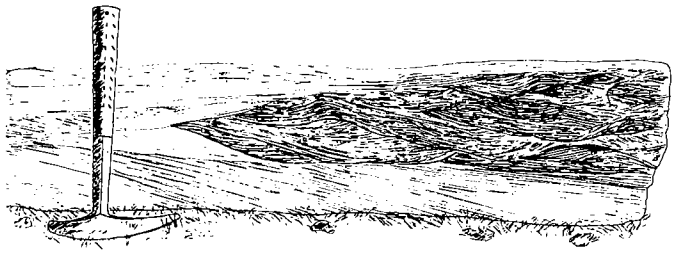

Figure 3. Field sketch of a calcareous quartz arenite, illustrating complex trough and planar cross-bedding characterized by abundant reactivation surfaces (Kindblade Formation).

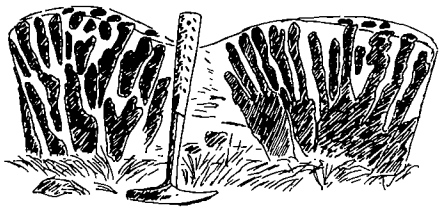

Figure 4. Field sketch of a "sunburst" algal reef in the Cool Creek Formation. Laterally continuous unit composed of dendritic and columnar members. Internal texture is intermediate between stromatolite and thrombolite.

Site E2: A Permian Cave System

A compelling Permian feature is located in a quarry near the northeast end of the Bally Mountain Range. The quarried rock is the Kindblade Formation, but the geologic interest in the quarry centers on the Permian karst fissures which follow fractures in the limestones. These fissures are securely dated by an abundant (although fragmented) fossil vertebrate fauna documented by Simpson (1979). The vertebrates are mixed with laminated green clays and poorly sorted detritus (chert and limestone pebbles) derived from the Kindblade Formation. Associated karst deposits, which are older than the vertebrate-bearing detritus, include phreatic and vadose calcite-spar textures, flowstone, cave pearls, and horizontally interlaminated beds of clay and travertine which show some soft-sediment deformation (Bridges, 1985). The most intriguing feature of the travertine is that many of the fibrous calcite crystals contain numerous inclusions of hydrocarbon (Donovan, this volume). This would appear to date a phase of hydrocarbon migration through these beds in Permian (specifically Leonardian) time.

SUMMARY

The geology of the Bally Mountain Range records in a single, conveniently accessible exposure several aspects of the development of the southern Oklahoma aulacogen:

1) The initial Cambrian igneous phase, as manifested by the Carlton Rhyolite Group;

2) Deposition of platform carbonates in a Cambrian–Ordovician subsidence phase associated with a decreasing geothermal gradient;

3) Pennsylvanian deformation, which in this area has produced gentle homoclinal tilting toward the northeast;

4) Permian sculpting of the resulting topography; and

5) Hydrocarbon migration during Permian time.

STOP 3
GEOLOGIC HIGHLIGHTS AT ZODLETONE ("STINKING MOUNTAIN")

R. Nowell Donovan and Curtis Ditzell

THE SETTING

Zodletone Mountain (SW¼SW¼ sec. 9, T6N, R14W) is a 250-ft-high (76-m-high) eminence in Kiowa County in southern Oklahoma; it is the northernmost member of the Slick Hills Range and rises 1,649 ft (500 m) above sea level. The mountain is the property of Mr. Dan Trobe, who lives a mile to the east of the mountain. We are grateful to Mr. Trobe for permission to visit the site.

GEOLOGIC THEMES: BARITE TRAVERTINE

There are two geologic themes of unusual interest at Zodletone Mountain: the Cambrian sedimentary sequence, and the modern barite-depositing spring on the north edge of the mountain (Fig. 1). The barite travertine which has formed in the spring area is a rare type of deposit, known elsewhere in the world at only three sites. Only at Zodletone has barite been shown to be actively precipitating. The deposit is described in the paper by Younger and others in this volume.

GEOLOGIC THEMES: LOWER PALEOZOIC SECTION

Zodletone Mountain is an exhumed Permian landform, covered in places by a thin veneer of Permian detritus—the Post Oak Conglomerate facies. Some of this detritus obscures the unconformity between the Reagan Sandstone and the underlying Carlton Rhyolite Group, which forms the bulk of Zodletone Mountain (Fig. 1). Otherwise, the Cambrian sediments are well exposed on two spurs that run northward from the main (rhyolite) hill mass.

The Cambrian sedimentary sequence includes the Timbered Hills Group, comprising the Reagan Sandstone and Honey Creek Limestone and the Cambrian part of the Arbuckle Group (the Fort Sill and lower Signal Mountain Formations) (Tsegay, 1983; Ditzell, 1984; Rafalowski, 1984). A generalized log for this succession is given by Donovan and Ragland elsewhere in this volume.

THE TIMBERED HILLS GROUP

At Zodletone, the Timbered Hills Group is beautifully exposed; in particular, the Reagan Sandstone is noteworthy for the geometry of its sandstones and their trace fossils. The Reagan is thicker than on adjacent Bally Mountain (Stop 2, this volume); good-quality exposures are present on both spurs of the mountain (Figs. 2,3).

Both Reagan sections are dominated by quartz-rich sandstones of medium to coarse grain. The more-basal sandstones contain numerous rhyolite grains and are cemented by quartz and hematite. The upper sandstones are glauconitic and cemented by quartz and calcite; they contain abundant broken phosphatic brachiopod shells and (more rarely) phosphate nodules (Tsegay, 1983).

Sandstone geometries are mostly lenticular and dominated by trough cross-bedding in sets as much as 5 ft (1.5 m) thick. The overall paleocurrent distribution is bipolar, with opposed but unequal modes oriented NNW and SSE, suggesting a general tidal influence. However, the thicker lenticular sandstones appear to have migrated to the SSE, perhaps because storm action enhanced tidal movement. The most impressive of these sandstones is located on the eastern outcrop.

Apart from phosphatic brachiopods, the Reagan has yielded few body fossils. However, it does display a fine array of trace fossils, particularly the vertical burrows of the *Skolithos* ichnofacies, including *Arenicolites*. In general, trace fossils are more abundant in the tan-colored sandstones than in the highly glauconitic greensands, perhaps because the latter formed in a less-oxygenated setting. Such trace fossils as do occur in the glauconitic sandstones tend to have a horizontal character.

The trace fossils of the western exposure are particularly fine and include one spectacular piece of cross-bedding where successive reactivation surfaces in the set are defined by burrows oriented normal to the cross-set laminae (Fig. 4). This arrangement indicates an episodic origin for this cross-bed. When eventually stabilized, the unit was colonized by a final group of *Skolithos* organisms, which grew larger than the earlier inhabitants of the migrating cross-bed.

The overlying Honey Creek Limestone consists of a mixed quartz, glauconite, and pelmatozoan grainstone complex characterized by bipolar cross-bedding with orientations similar to those in the underlying

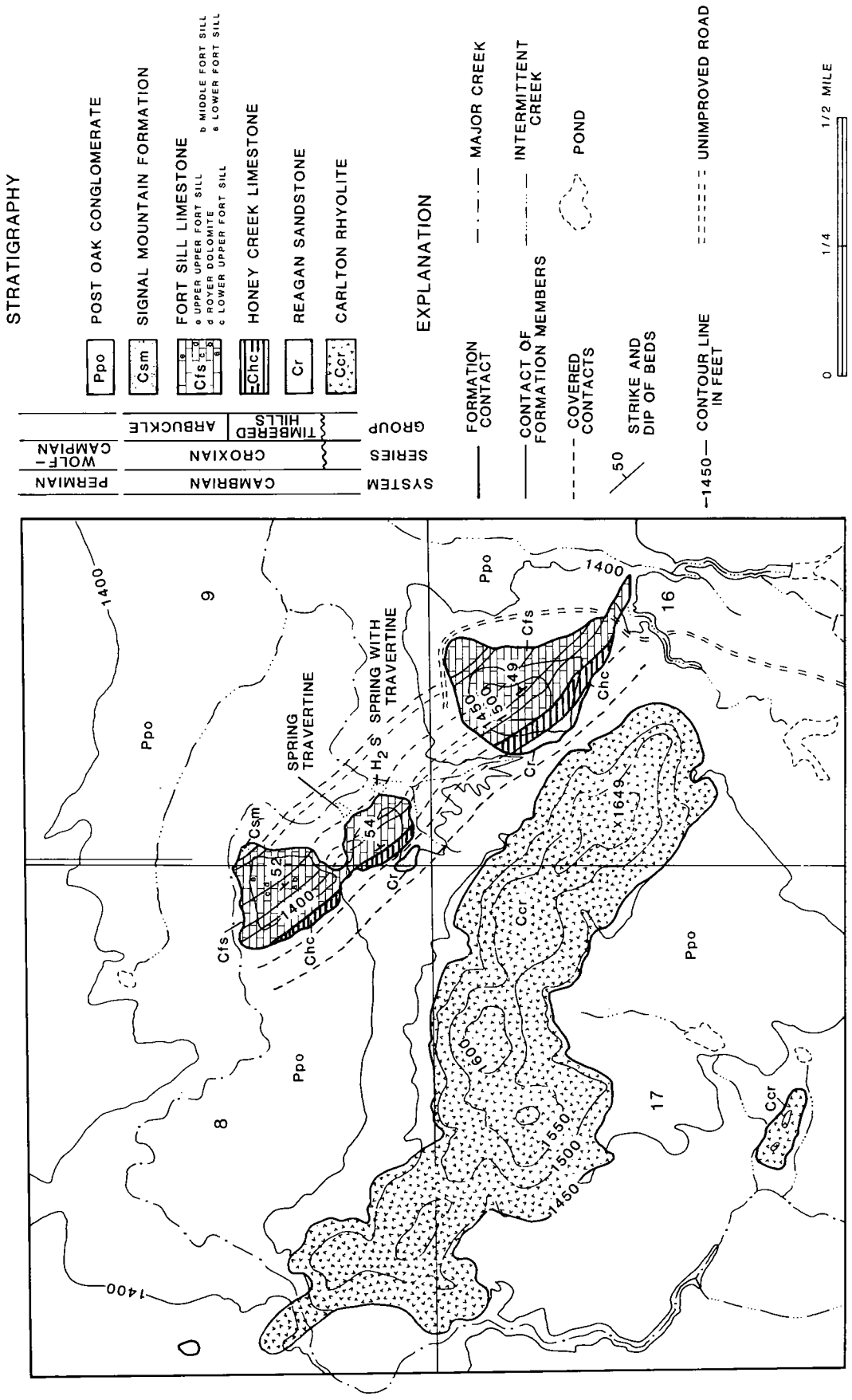

Figure 1. General geology of Zodletone Mountain, T6N, R14W, Kiowa County (from Ditzell, 1984).

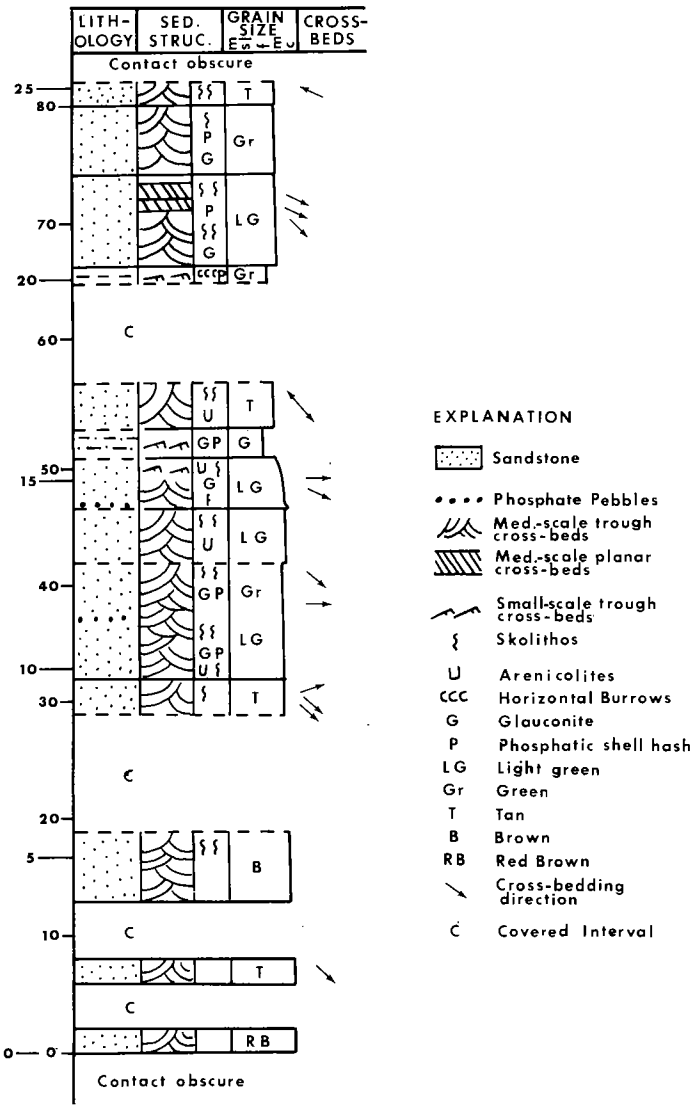

Figure 2. Log of Reagan Sandstone exposed on the west spur of Zodletone Mountain.

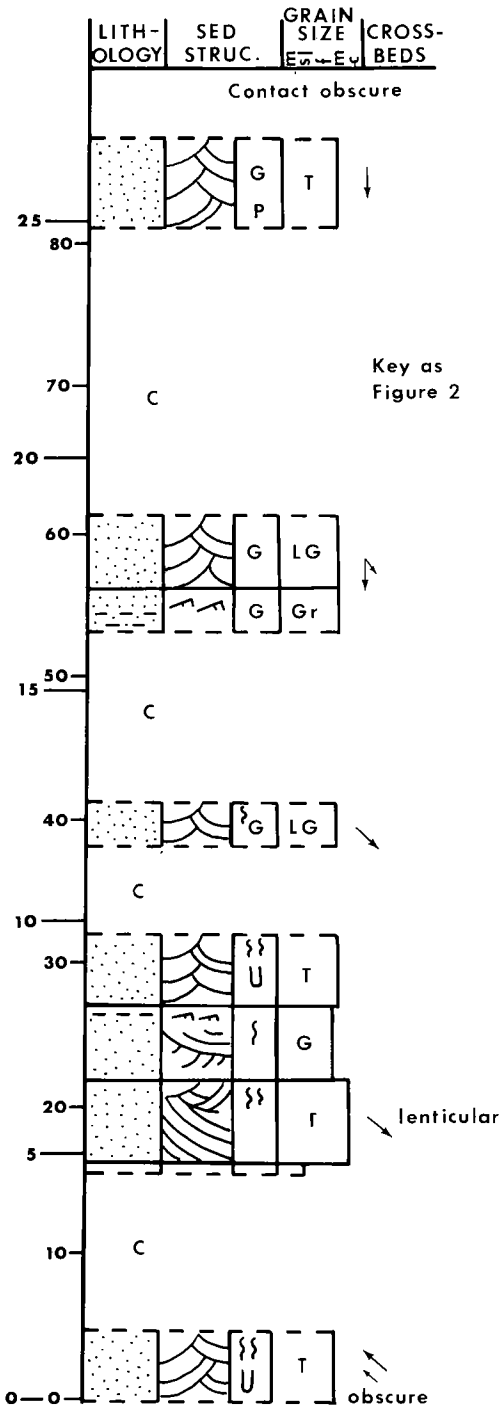

Figure 3. Log of Reagan Sandstone exposed on the east spur of Zodletone Mountain.

Figure 4. A single cross-bedding set from the western outcrops of the Reagan Formation. Note how *Skolithos* burrows are oriented normal to cross-bedding, indicating that successive surfaces were colonized by small individuals. This indicates that the cross-bed is punctuated by numerous hiatiuses, and that in a sense each cross-bed is a reactivation surface. Once completely constructed, the top surface was then colonized by larger individuals.

Reagan (Rafalowski, 1984). However, the cross-beds are smaller (sets ~6 in., or ~15 cm) and are more uniform in size. They appear to have formed as small, tidally influenced, lunate dunes, rather than as the complex sandbars found in the Reagan. Details of sediment organization are difficult to interpret in some cases because of the great amount of pressure solution to which the carbonates have been subjected.

The Arbuckle Group is similar to the section seen on adjacent Bally Mountain in that it displays a five-fold division of the Fort Sill Limestone, including a thick, stratabound dolomite at the same general level as the Royer in the Arbuckle Mountains. This bed has been termed the "Bally Dolomite" (Stop 2, this volume).

On both hill spurs at Zodletone, the lowest beds of the Signal Mountain Formation are exposed. The contact with the underlying Fort Sill is sharp; some glauconite and a good deal of ferroan dolomite characterize the lowest 10 ft of the Signal Mountain (Ditzell, 1984).

SUMMARY

Two themes connected to the evolution of the southern Oklahoma aulacogen can be developed at Zodletone. The first of these is the Franconian transgression across the Carlton Rhyolite Group land surface; the Zodletone outcrops record a complex tide–storm interplay of sand migration. The setting was initially dominated by siliciclastic-sediment production, but gradually became one of the world's greatest recorded carbonate "factories." The second theme relates the structure of the Wichita uplift frontal fault zone to the upward migration of brine from the Anadarko basin. At Zodletone, this brine has produced one of only four known barite-travertine deposits.

STOP 4
GEOLOGY OF THE COOK CREEK ROAD CUT

R. Nowell Donovan, Deborah A. Ragland, and Diana Schaefer

THE SETTING

Unlike the Arbuckle Mountains, the Slick Hills lack the impact of Interstate Highway construction. There are few modern road cuts through the Hills, and of these the most instructive is the Cook Creek road cut on State Highway 19, about 10 mi (16 km) west of Apache. Permian karst features in this road cut have been described by Donovan (1982) and are updated here, but the principal purpose of this communication is to describe a short section of the Ordovician Kindblade Formation (Arbuckle Group) in detail.

PERMIAN PALEOKARST

The Cook Creek road cut cuts through a spur of a hill which forms part of the Blue Creek horst (Donovan, this volume). The exposed rocks are in the upper part of the Kindblade Formation. Small caves decorated with a variety of vadose flowstones occur all along the road cut. These caves are preferentially developed along the N–S mode of an orthogonal joint set (Fig. 1). In 1982 Donovan suggested that these caves were of Permian age, noting that the hill spur was a Permian landform, exhumed from beneath Post Oak Conglomerate, and that the N–S karst trend accords well with paleodrainage directions in the conglomerate. Since 1982 a single bone fragment, similar to those found in cave deposits of undoubted Permian age, has been found. In addition, some of the flowstones contain inclusions of liquid hydrocarbon similar to those found on Bally Mountain (Stop 2, this volume).

THE KINDBLADE FORMATION

The Blue Creek horst displays an unbroken section of the Arbuckle Group of ~4,500 ft (~1,400 m) in length. Detailed examination of sedimentary aspects of this sequence is a monumental task. Characteristic complexity is shown by the 65 ft (20 m) of strata exposed in the road cut. In our logging of this section (Fig. 2), we have attempted to establish an empirical data base (Table 1) in order to quantify depositional processes on the great Cambrian–Ordovician Arbuckle platform.

There are some weaknesses in the data:

1) Part of the section is dolomitized to an extent that the original sediment is obscured;

2) Exposure in the lower part of the section is not particularly clean;

3) There is probably a degree of operator variance in classifying the various mud-supported textures;

4) Hardgrounds are not always easy to spot (many are more apparent in thin section than outcrop); and

5) Anastomosing stylolites have removed a considerable part of the section.

In general terms, algal boundstones are probably underrepresented in the sequence by comparison with other sections in the Kindblade.

The Primary Lithologies

A gradational sequence of lithologies quantitatively dominates the section. This spectrum shows gradual variations of grain size from intraformational conglomerate to mudstone, and gradual variations in textural cleanliness from well-worked grainstones and intraformational conglomerates to completely mud-supported fabrics. Allochems are variable mixtures of intraclasts, ooids, peloids, and bioclastic grains. Only oolitic grainstones show a compositional integrity which is unadulterated by other types of grains.

Primary sedimentary structures seem to indicate a low-key environment; the largest observed cross-bed set (in an oolitic grainstone) is only 4 in. (10 cm) thick. Bed thicknesses are remarkably similar, regardless of lithology; the whole sequence (apart from boundstones) is built of a series of small-scale accumulations of sediment, some of which was well-washed, but most of which was poorly sorted and mixed with lime mud. Many of the bed boundaries are hardgrounds (indicating penecontemporaneous cementation); others are obscured by stylolites. In environmental terms, the sequence can be explained by reference to the "platform triangle" (Donovan, this volume), whereby deposition in very shallow wa-

ter above and below fair-weather wave base was followed by rapid cementation and subsequent rip-up by storms (forming the intraclasts which are the commonest allochem in the sequence). There are few evidences of supratidal cementation (some subaqueous shrinkage cracks; Donovan and Foster, 1972), and none of the evaporitic connections noted in the Cool Creek Formation by Cloyd and others (this volume).

Dolomite in the Section

Fine-grained, stratigraphically concordant dolomite is found in several regularly spaced zones as much as 4 ft (1.2 m) thick. This dolomite (a micrite) rarely replaces the entire primary texture, but forms a small-scale irregular pattern of connected dolomite around isolated patches of limestone ("leopard-skin" texture; Fig. 3). This pattern may record variations in permeability (related to partial lithification) which were encountered by dolomitizing fluids. The absence of an evaporative connection, the apparent pre-lithification, penecontemporaneous aspect of much of the dolomite, and the stratigraphic concordance suggest that the dolomite formed under the auspices of the ground-water-mixing mode. The regular spacing of dolomite zones in the sequence (Fig. 2) may indicate a regular (cyclic) oscillation in relationships between sea water and meteoric ground water due to variations in sea level. It is of interest and perhaps supportive of the interpretation that a thin zone of chert nodules occurs above each dolomite occurrence—and the chert itself may also be of a ground-water-mixing origin.

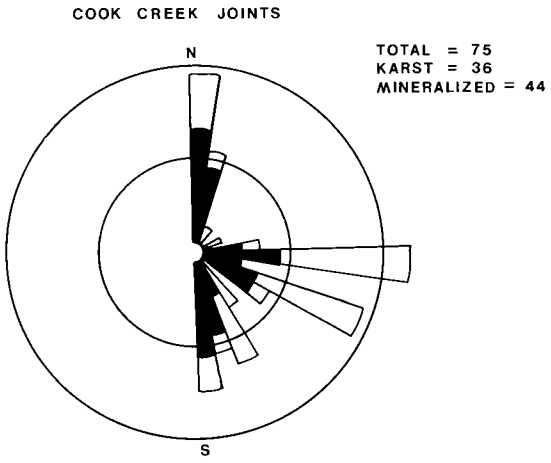

Figure 1. Rose diagram illustrating orientation of vertical joints in the Cook Creek road cut. The largest caves are associated with the N–S joint mode. Karst joints shown in black.

Platform Carbonate Cannibalism

A simple comparison of modern short-term rates of carbonate production with likely rates of subsidence during deposition of the Kindblade in the aulacogen shows the former to be greatly in excess of the latter (Donovan, this volume). In other words, the platform could produce sediment faster than it could be trapped by burial. Three lines of evidence show how this problem was resolved. Multiple intersecting hardgrounds (Fig. 4) illustrate that in the short term the sequence was continuously reworked and redistributed across the platform. Second, karstic weathering surfaces (Fig. 5) suggest periodic removal of carbonate by dissolution during periods of subaerial exposure. Third, a large number of bedding-parallel stylolites (Fig. 6) evidence a considerable amount of post-lithification carbonate removal. Assuming that stylolite amplitude relates directly to the amount of solution on the stylolite surface, the data in Table 1 indicate that about 23% of the section may have been removed by pressure solution. In a sense, the sequence back-stripped autonomously.

TABLE 1.—SEDIMENTARY PARAMETERS RELATED TO THE COOK CREEK CARBONATE SECTION*

Lithology	No. of Beds	Avg. thickness of bed (in., cm)	Percent of primary lithology	
Intraformational conglomerate	34	2.7 (6.9)	14.0	
Grainstone	26	3.4 (8.5)	13.5	] 31.0
Oolitic grainstone	37	3.0 (7.8)	17.5	
Packstone	44	2.5 (6.4)	17.0	
Wackestone	28	2.2 (5.6)	9.5	
Mudstone	47	2.5 (6.4)	18.0	
Algal boundstones	4	16.5 (42.0)	10.0	

*Primary lithology detectable in 88% of sequence; remaining 12% too heavily dolomitized.
Notes: 121 hardgrounds detected; 2 karst surfaces detected; through 312 in. (792 cm), 306 stylolites were found, with an average maximum amplitude of 0.25 in. (6 mm).

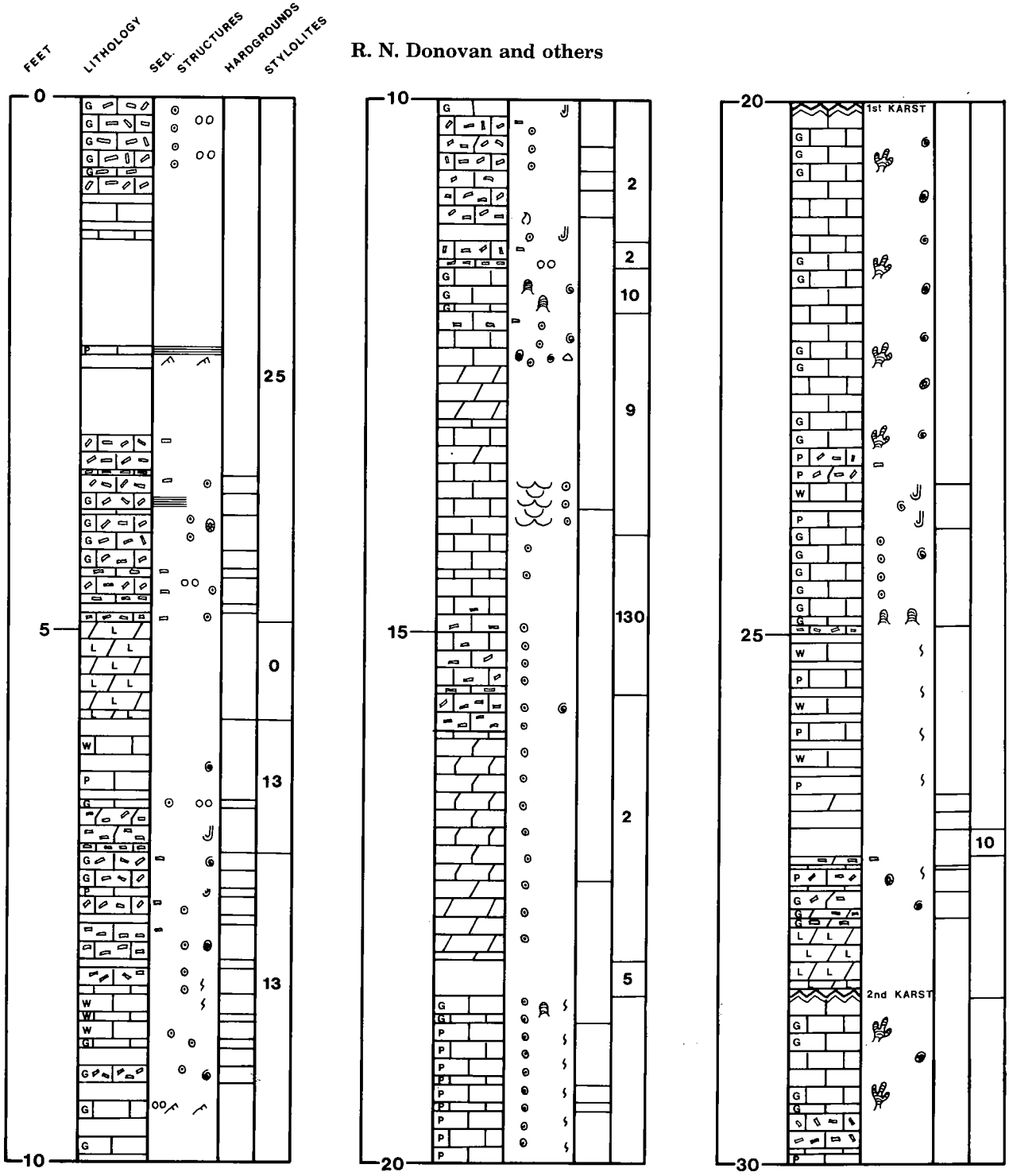

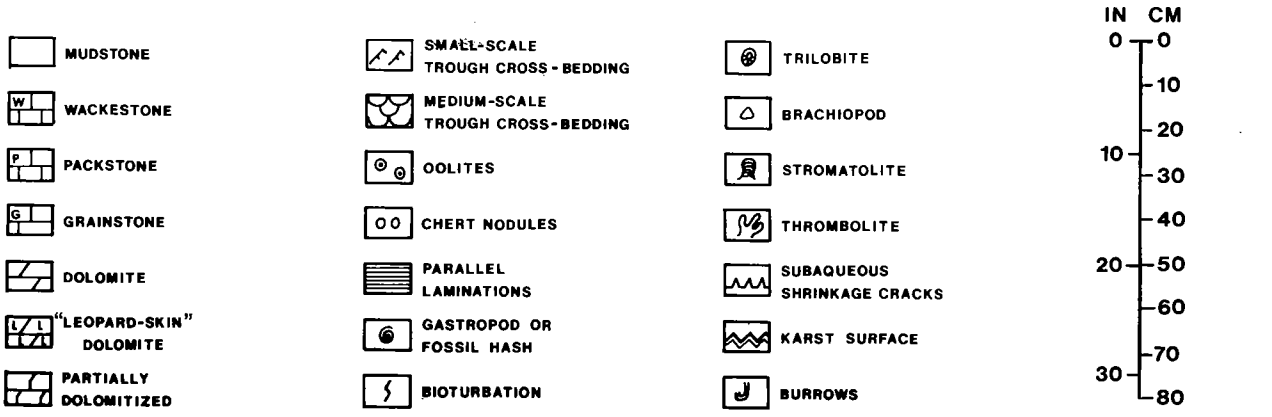

Figure 2. Log of the Kindblade Formation in the Cook Creek road cut.

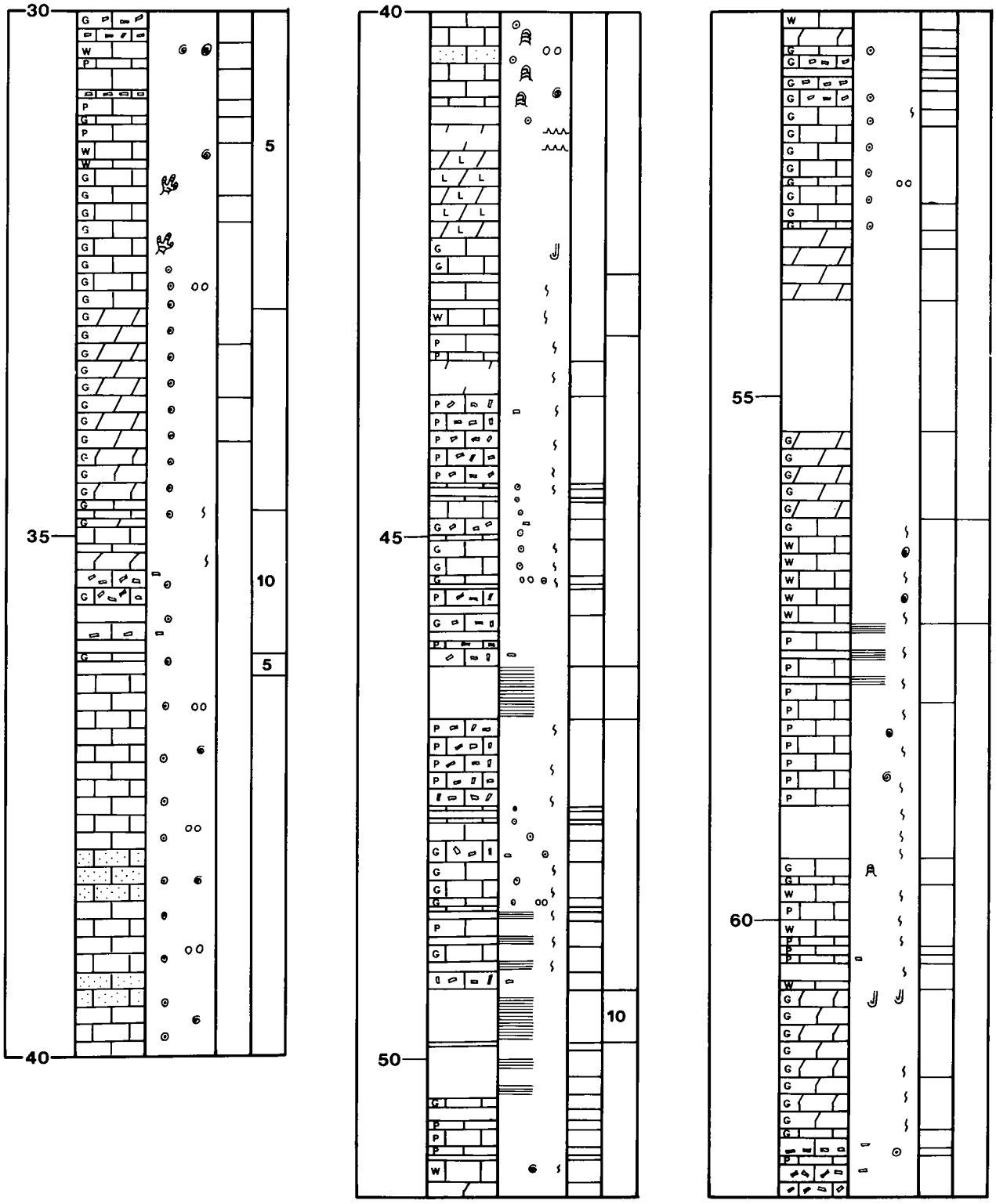

TOTAL SECTION - 61'10"

Figure 3. Zone of partial dolomitization, illustrating typical "leopard skin" dolomite texture (dolomite appears lighter than calcite). Note zone of cherts (S) above dolomite.

Figure 4. Characteristic hardground (H) developed between an oolitic grainstone (O) and a mudstone-wackestone sequence (M) containing several visually less impressive hardgrounds.

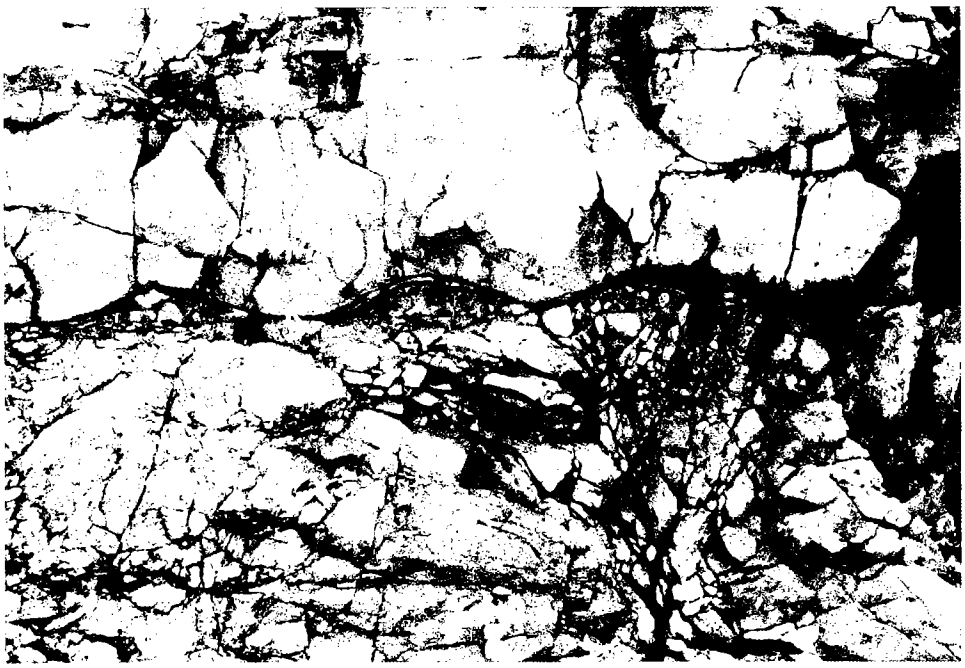

Figure 5. One of two scalloped karstic surfaces (K) occurring in the outcrop. Maximum relief on the surface is 5 in. (13 cm).

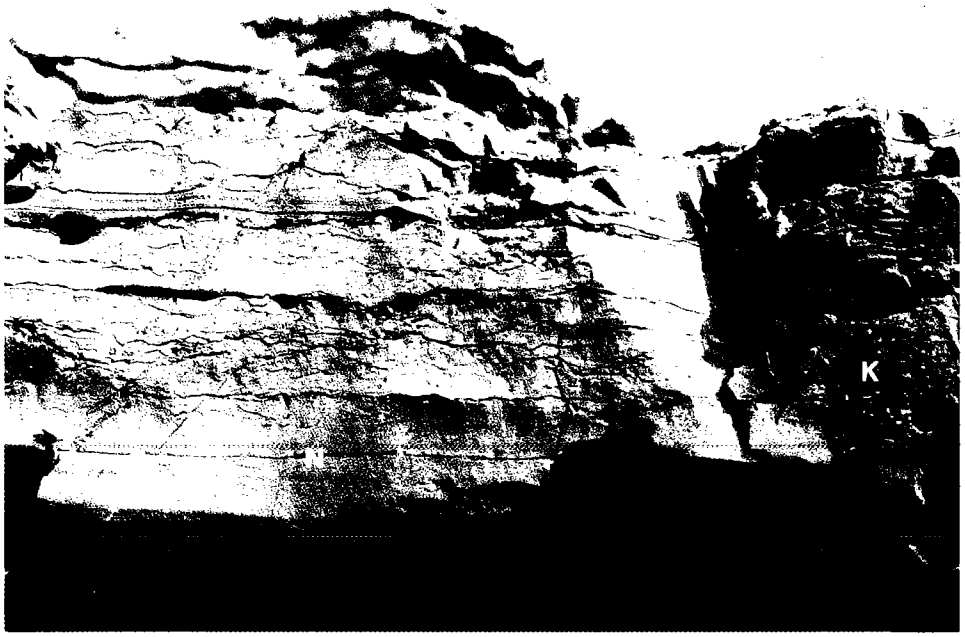

Figure 6. Line-mudstone–wackestone sequence containing multiple stylolites. Note that some bed boundaries (e.g., B) are stylolitized and some are not (N), and that many stylolites do not relate to boundaries. To right of pencil is a Permian karst fill (K).

STOP 5
THE MEERS FAULT: MODEST FINALE FOR A HOARY GIANT?

R. Nowell Donovan

INTRODUCTION

On the north side of the Meers Valley, the gentle contours of the southern Slick Hills are disturbed by a compellingly constant lineament which runs a straight course for 16 mi (26 km). For the most part, this lineament severs Recent deposits which lie atop Permian Post Oak Conglomerate or Hennessey Group shale. However, along one short stretch, Ordovician Arbuckle Group rocks (McKenzie Hill Formation) are present north of the lineament.

This feature has recently been interpreted (Donovan and others, 1983; Gilbert, 1983a) as a record of modern rejuvenation of the Meers fault—a distant echo of a time-honored past. The ancient fault is a major structure which constituted the southwest boundary of the frontal fault zone between the Wichita uplift and the Anadarko basin as these structures developed in Pennsylvanian time. The late Paleozoic displacement is difficult to quantify accurately, but probably involved at least 10,000 ft (3,000 m) of vertical separation, plus an unknown amount of left-lateral displacement. The more recent movement is much more modest, involving a downthrow to the south which has a maximum displacement of ~20 ft (6 m) and a left-lateral displacement of similar dimensions.

The Recent movement represents a reversal of the vertical sense of Paleozoic displacement. Furthermore, the younger fault plane is either vertical or dips to the north at angles of as much as 70° (indicating high-angle reverse motion). The sense of this dip is opposite that suggested by COCORP deep subsurface data (Brewer and others, 1983). It is worth noting that linkage of the COCORP structure to the surface trace is not easy.

The Recent activity of the fault has led to a great deal of scientific investigation over the last few years. Some of the results of these investigations are presented elsewhere in this volume. In this contribution an evocative section of the fault and related features are described. This "Oliver section" is located on the Kimbell Ranch; I am grateful to Mr. Kimbell and to his manager, Charlie Bob Oliver, for permission to investigate the site.

As an addendum, an interesting Post Oak Conglomerate outcrop located within a fault-rejuvenation gorge is described. It demonstrates the character of the Permian alluvial fans which debouched from the Slick Hills.

GEOMORPHIC EVIDENCES OF RECENT FAULT MOVEMENT

Quaternary rejuvenation of the Meers fault was initially suspected on geomorphic evidence (Fig. 1). For example, the fault line is constant in its throw, regardless of the resistance to weathering exhibited by the materials it cuts. In addition, recent drainage patterns have been interrupted, as evidenced by:

1) The sediment ponding of northward-draining tributaries;

2) Displacement of river terraces;

3) Rejuvenation of streams crossing the fault scarp (with resultant knickpoints developed upstream); and

4) Gullying developed along the fault scarp, with resulting drainage piracy.

All these features are admirably developed within the Oliver section (Fig. 1). In addition, a constant amount of left-lateral offset of sediment ponds is clearly apparent.

FRACTURE PATTERNS RELATED TO THE FAULT

Recently the Oklahoma Geological Survey has trenched the fault where it cuts the Post Oak Conglomerate (Fig. 1, point Y). Mr. Oliver has allowed this trench to remain open for inspection: It shows one principal and two or three minor lines of displacement which are essentially vertical and contain some silica-rich, tan-colored infill. Near-horizontal slickensides are visible on some pebbles.

All along its trace in the Post Oak terrain, the fault is associated with a large number of fractures. Major modes of distribution of these fractures (Fig. 2) are interpreted as Riedel (R, R_1) shear fractures developed in response to a left-lateral sense of shear on

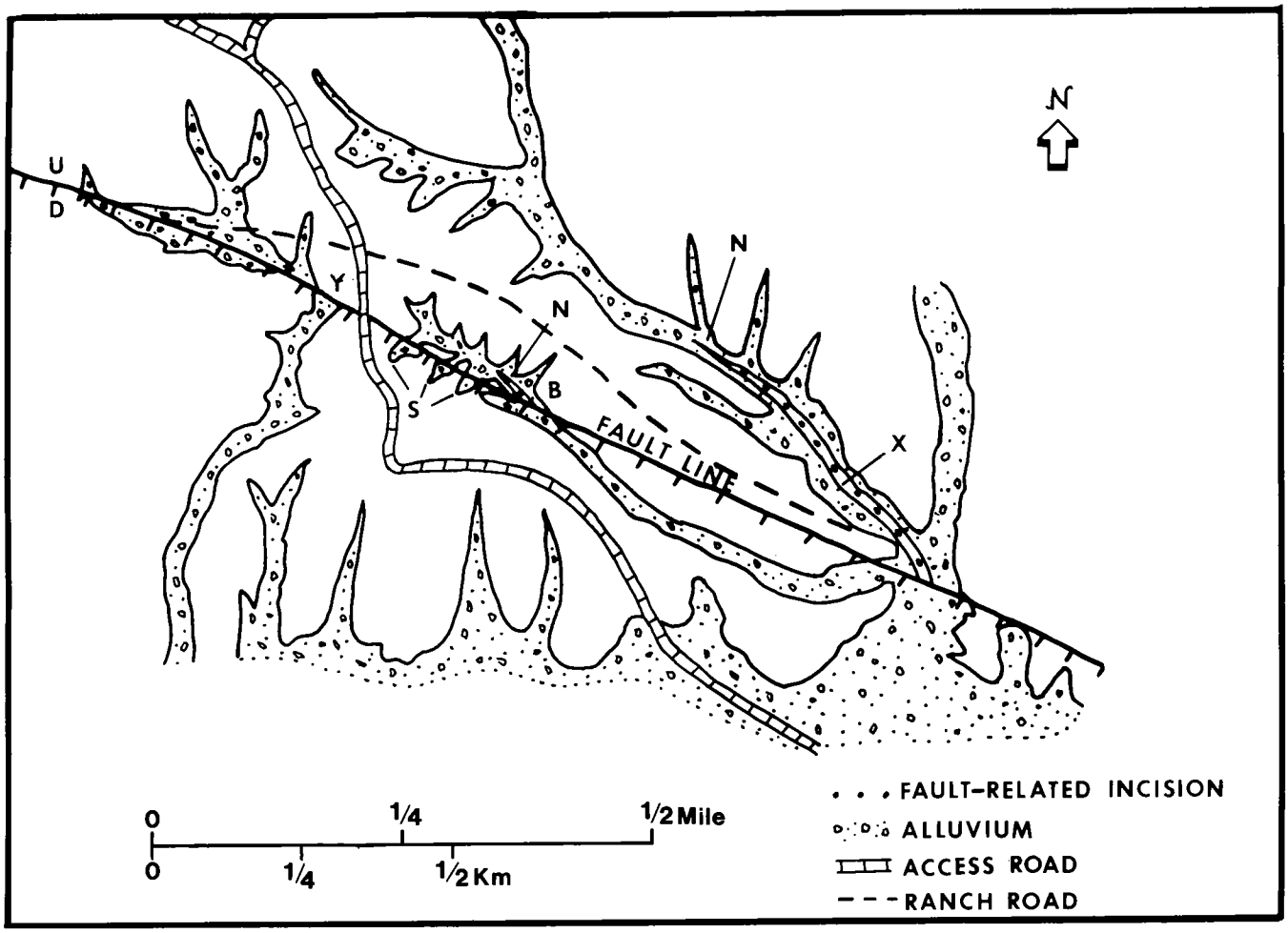

Figure 1. The "Oliver section" of the Meers fault. S = sediment-entrapment ponds formed where the fault scarp has impeded drainage; N = fault-related knickpoints; B = recent gullying along fault trace; X = Post Oak Conglomerate exposures represented in Figure 3; Y = excavation site on fault scarp.

the main fault. Individual pebbles showing both left-lateral (R) and right-lateral (R_1) displacement can be found along the Oliver section. Few tensional fractures are present, presumably because deformation has been essentially transpressive.

THE POST OAK CONGLOMERATE

The Post Oak Conglomerate cut by the Meers fault is a well-indurated limestone-pebble conglomerate consisting of subangular to subrounded (solution-modified) pebbles of the local Arbuckle Group rocks. The facies has been interpreted as the deposits of small alluvial fans debouching from the adjacent Slick Hills (Gilbert and Donovan, 1984). An interesting section is exposed in the fault-related rejuvenation gorge shown (Fig. 1, point X). At this point, a sharply defined channel is incised into earlier conglomerates.

By comparison to Permian sedimentation in the Anadarko basin, the rate of sediment entrapment in the Meers Valley was very low, as the valley was not an area of pronounced subsidence. Some evidence in

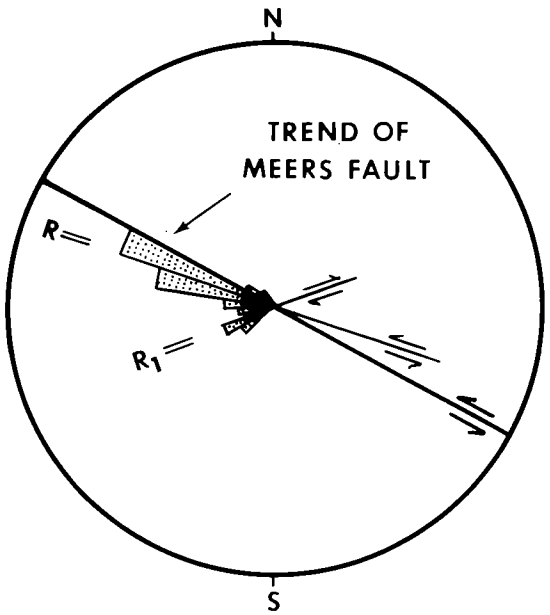

Figure 2. Fracture pattern affecting the Post Oak Conglomerate adjacent to the Meers fault. R and R_1 = Riedel fractures.

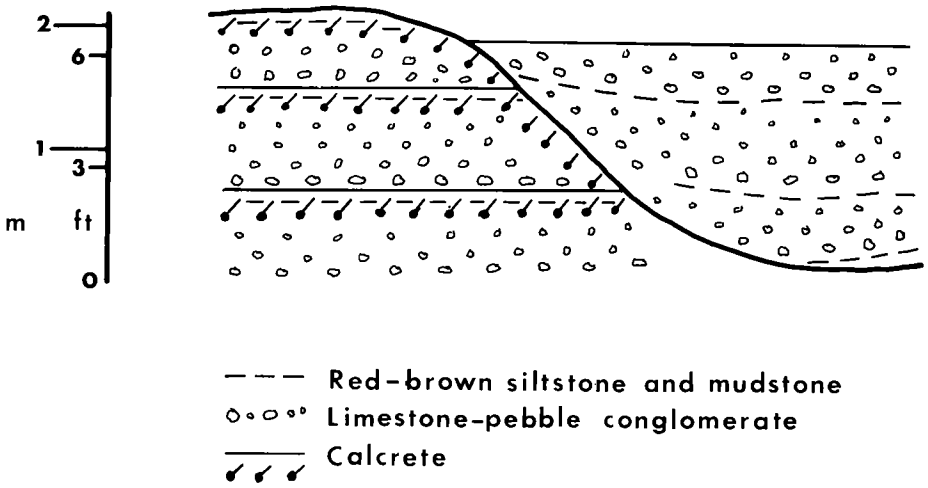

Figure 3. Diagrammatic field sketch of a Post Oak Conglomerate exposure (Fig. 1, point X) near the "Oliver section." Vegetation omitted.

support of this hypothesis is the close spacing of calcareous pedocals (calcretes) in the Post Oak Conglomerate. Calcretes in the area have been described by Gilbert and Donovan (1982), Collins (1985), and Bridges (1985). These authors have noted that calcretes require a stable geomorphic setting which persists for thousands of years in order to form. The close spacing of calcretes in Post Oak sequences indicates slow, episodic sedimentation, punctuated by frequent periods of nondeposition and soil development.

The section illustrated in Figure 3 gives some idea of the episodic nature of sedimentation in the conglomerate (both pre- and post-channel incision). Red-brown mudstones and siltstones demarcate pauses in sedimentation; calcretes formed when these pauses were of sufficient duration and the climate was favorable for their development (i.e., semiarid). Episodic sedimentation on alluvial fans may be of either climatic or tectonic origin. In the Meers Valley, both mechanisms may have been operative (Gilbert and Donovan, 1984). The channel cut represents an avulsion event. The stratified nature of the infill suggests that originally the channel was simply a sediment-supply corridor (located above the fan intersection point), which was subsequently clogged with sediment. It is pertinent that the upper slopes of this channel were calcreted before being overlain by sediment.

COLLECTED REFERENCES

Aitken, J. D., 1967, Classification and environmental significance of cryptalgal limestones and dolomites, with illustrations from the Cambrian and Ordovician of southwestern Alberta: Journal of Sedimentary Petrology, v. 37, p. 1163–1178.

Algermissen, S. T.; Perkins, D. M.; Thenhaus, P. C.; Hanson, S. L.; and Bender, B. L., 1982, Probabilistic estimates of maximum acceleration and velocity in rock in the contiguous United States: U.S. Geological Survey Open-File Report 82-1033, 99 p.

Babaei, A., 1980, The structural geology of part of the Limestone Hills in the Wichita Mountains, Caddo and Comanche Counties, Oklahoma: Oklahoma State University unpublished M.S. thesis, 63 p.

Barthelman, W. B., 1968, Upper Arbuckle (Ordovician) outcrops in the Unap Mountain–Saddle Mountain area, northeastern Wichita Mountains, Oklahoma: University of Oklahoma unpublished M.S. thesis, 65 p.

Beauchamp, W. H., 1983, The structural geology of the southern Slick Hills, Oklahoma: Oklahoma State University unpublished M.S. thesis, 119 p.

Birkeland, P. W., 1984, Soils and geomorphology: Oxford University Press, New York, 372 p.

Blong, R. J.; and Gillespie, R., 1978, Fluvially transported charcoal gives erroneous ^{14}C ages for recent deposits: Nature, v. 271, p. 739–741.

Bonilla, M. G.; Mark, R. K.; and Lienkaemper, J. J., 1984, Statistical relations among earthquake magnitude, surface rupture length, and surface fault displacement: Seismological Society of America Bulletin, v. 74, p. 2379–2411.

Brewer, J. A., 1982, Study of southern Oklahoma aulacogen, using COCORP deep seismic-reflection profiles, *in* Gilbert, M. C.; and Donovan, R. N. (eds.), Geology of the eastern Wichita Mountains, southwestern Oklahoma: Oklahoma Geological Survey Guidebook 21, p. 31–39.

Brewer, J. A.; Good, R.; Oliver, J. E.; Brown, L. D.; and Kaufman, S., 1983, COCORP profiling across the southern Oklahoma aulacogen: overthrusting of the Wichita Mountains: Geology, v. 11, p. 109–114.

Bridges, S. D., 1985, Mapping, stratigraphy, and tectonic implications of Lower Permian strata, eastern Wichita Mountains, Oklahoma: Oklahoma State University unpublished M.S. thesis, 129 p.

Brookby, H. E., 1969, Upper Arbuckle (Ordovician) outcrops in Richards Spur–Kindblade Ranch area, northeastern Wichita Mountains, Oklahoma: University of Oklahoma unpublished M.S. thesis, 73 p.

Brown, W. G., 1984, Washita Valley Fault system: a new look at an old fault, *in* Borger, J. G., III (ed.), Technical proceedings of the American Association of Petroleum Geologists, Mid-Continent Section, 1981 regional meeting: Oklahoma City Geological Society, p. 68–80.

Bucknam, R. C.; and Anderson, R. E., 1979, Estimation of fault-scarp ages from a scarp-height-slope-angle relationship: Geology, v. 7, p. 11–14.

Budnick, R. T., 1983, Recurrent motion on Precambrian-age basement faults, Palo Duro Basin, Texas Panhandle [abstract]: American Association of Petroleum Geologists Bulletin, v. 67, p. 433.

Butler, G. P.; Kendall, G. St. C.; and Harris, P. M., 1983, Recent evaporites from the Abu Dhabi coastal flats, Persian Gulf: Shale Shaker, v. 83, p. 44–69.

Butler, K. R., 1980, A structural analysis of the Cambrio–Ordovician strata on the north flank of the Wichita Mountains, Oklahoma [abstract]: Geological Society of America, Abstracts with Programs, v. 12, p. 2.

Cadigan, R. A.; Felmlee, J. K.; and Rosholt, J. N., 1976, Radioactive mineral springs in Delta County, Colorado: U.S. Geological Survey Open-File Report 76-223, 39 p.

Campbell, C. A.; Paul, E. A.; Rennie, D. A.; and McCallum, K. J., 1967, Applicability of the carbon-dating method of analysis to soil humus studies: Soil Science, v. 104, p. 217–224.

Cardott, B. J.; and Lambert, M. W., 1985, Thermal maturation by vitrinite reflectance of Woodford Shale, Anadarko basin, Oklahoma: American Association of Petroleum Geologists Bulletin, v. 69, p. 1982–1998.

Chowns, J. M.; and Elkins, J. E., 1974, The origin of quartz geodes and cauliflower cherts through silicification of anhydrite nodules: Journal of Sedimentary Petrology, v. 44, p. 885–903.

Collins, A. G., 1975, The geochemistry of oilfield waters, *v. 1 of* Developments in petroleum science: Elsevier, Amsterdam, 496 p.

Collins, K., 1985, The evolution of the Meers Valley in the Wichita Mountains, Oklahoma: Oklahoma State University unpublished M.S. thesis, 128 p.

Condie, K. C., 1982, Plate-tectonics model for Proterozoic continental accretion in the southwestern United States: Geology, v. 10, p. 37–42.

Cowan, J. C.; and Weintritt, D. J., 1976, Water-formed scale deposits: Gulf Publishing Co., Houston, 569 p.

Davies, P. J.; Butler, B.; and Ferguson, J., 1978, The formation of ooids: Sedimentology, v. 25, p. 703–730.

Decker, C. E., 1939, Two Lower Paleozoic groups, Arbuckle and Wichita Mountains, Oklahoma: Geological Society of America Bulletin, v. 50, p. 1311–1322.

Ditzell, C., 1984, The sedimentary geology of the Cambro–Ordovician Signal Mountain Formation as exposed in the Wichita Mountains of southwestern Oklahoma: Oklahoma State University unpublished M.S. thesis, 165 p.

Donovan, R. N., 1982a, Geology of Blue Creek Canyon, Wichita Mountains area, *in* Gilbert, M. C.; and Donovan, R. N. (eds.), Geology of the eastern Wichita Mountains, southwestern Oklahoma: Oklahoma Geological Survey Guidebook 21, p. 65–77.

——— 1982b, Stop 11—Highway 19 area, *in* Gilbert, M. C.; and Donovan, R. N. (eds.), Geology of the eastern Wichita Mountains, southwestern Oklahoma: Oklahoma Geological Survey Guidebook 21, p. 154–155.

——— 1984, The geology of the Blue Creek Canyon area, *in* Gilbert, M. C.; and Donovan, R. N. (eds.), Recent developments in the Wichita Mountains: Geological Society of America Guidebook for Field Trip No. 1, South-Central Section, 18th annual meeting, p. 40–101.

Donovan, R. N.; and Foster, R. J., 1972, Subaqueous shrinkage cracks from the Caithness Flagstone Series (Middle Devonian) of northeast Scotland: Journal of Sedimentary Petrology, v. 42, p. 309–317.

Donovan, R. N.; and Rafalowski, M. B., 1984, The anatomy of an early Cambrian shell bank in the Honey Creek Formation, southwestern Oklahoma [abstract]: Geological Society of America, Abstracts with Programs, v. 16, p. 82.

Donovan, R. N.; Babaei, A.; and Sanderson, D. J., 1982, Stop 10—Blue Creek Canyon, *in* Gilbert, M. C.; and Donovan, R. N. (eds.), Geology of the eastern Wichita Mountains, southwestern Oklahoma: Oklahoma Geological Survey Guidebook 21, p. 148–153.

Donovan, R. N.; Sanderson, D. J.; and Marchini, D., 1982, An analysis of structures resulting from left-lateral strike-slip movement between the Wichita Mountains

and Anadarko Basin, southwestern Oklahoma [abstract]: Geological Society of America, Abstracts with Programs, v. 14, p. 476.

Donovan, R. N.; Beauchamp, W.; Ferraro, T.; Lojeck, C.; McConnell, D.; Munsil, M.; Ragland, D. A.; Sweet, R.; and Taylor, D., 1983, Subsidence rates in Oklahoma during the Paleozoic: Shale Shaker, v. 33, p. 86–88.

Donovan, R. N.; Gilbert, M. C.; Luza, K. V.; Marchini, David; and Sanderson, David, 1983, Possible Quaternary movement on the Meers fault, southwestern Oklahoma: Oklahoma Geology Notes, v. 43, p. 124–133.

Dozy, J. J., 1970, A geological model for the genesis of lead–zinc areas of the Mississippi Valley, U.S.A.: Transactions Institute of Mining and Metallurgy, Section B, Applied Earth Sciences, 79 p.

Emig, W. H., 1917, Travertine deposits of Oklahoma: Oklahoma Geological Survey Bulletin 29, 76 p.

Fairchild, R. W., 1984, Springs in the Arbuckle Mountain area, south-central Oklahoma: Oklahoma Geology Notes, v. 44, p. 4–11.

Feinstein, S., 1981, Subsidence and thermal history of southern Oklahoma aulacogen: implications for petroleum exploration: American Association of Petroleum Geologists Bulletin, v. 65, p. 2521–2533.

Folk, R. L.; and Pittman, J. S., 1971, Length-slow chalcedony: a new testament for vanished evaporites: Journal of Sedimentary Petrology, v. 41, p. 1045–1058.

Gebelein, C. D., 1969, Distribution, morphology, and accretion rate of recent subtidal algal stromatolites, Bermuda: Journal of Sedimentary Petrology, v. 39, p. 49–69.

Gerasimov, I. P., 1971, Nature and originality of paleosols, *in* Yaalon, D. H. (ed.), Paleopedology origin, nature and dating of paleosols: Israel University Press, Jerusalem, p. 15–27.

Gilbert, M. C., 1982, Geologic setting of the eastern Wichita Mountains, with a brief discussion of unresolved problems, *in* Gilbert, M. C.; and Donovan, R. N. (eds.), Geology of the eastern Wichita Mountains, southwestern Oklahoma: Oklahoma Geological Survey Guidebook 21, p. 1–30.

——— 1983a, The Meers fault of southwestern Oklahoma—evidence for possible strong Quaternary seismicity in the midcontinent [abstract]: EOS, v. 64, p. 313.

——— 1983b, Timing and chemistry of igneous events associated with the southern Oklahoma aulacogen: Tectonophysics, v. 94, p. 439–455.

——— 1983c, The Meers fault—unusual aspects and possible tectonic consequences [abstract]: Geological Society of America, Abstracts with Programs, v. 15, p. 1.

——— 1984, Geological setting of the southern Oklahoma aulacogen, *in* Gilbert, M. C.; and Donovan, R. N. (eds.), Recent developments in the Wichita Mountains: Geological Society of America Guidebook for Field Trip No. 1, South-Central Section, 18th annual meeting, p. 1–40.

——— (ed.), 1986, Petrology of the Cambrian Wichita Mountains igneous suite: Oklahoma Geological Survey Guidebook 23.

Gilbert, M. C.; and Donovan, R. N. (eds.), 1982, Geology of the eastern Wichita Mountains, southwestern Oklahoma: Oklahoma Geological Survey Guidebook 21, 160 p.

——— 1984, Recent developments in the Wichita Mountains: Geological Society of America Guidebook for Field Trip No. 1, South-Central Section, 18th annual meeting, 101 p.

Gile, L. H.; Peterson, F. F.; and Grossman, R. B., 1966, Morphological and genetic sequences of carbonate accumulation in desert soils: Soil Science, v. 101, p. 347–360.

Gordon, D. W.; and Dewey, J. W., 1985, The Wichita–Ouachita seismic zone—southern Oklahoma seismicity in a regional context: Earthquake Notes, v. 55, p. 2.

Gregg, J. M.; and Sibley, D. F., 1984, Epigenetic dolomitization and the origin of xenotopic dolomite texture: Journal of Sedimentary Petrology, v. 56, p. 908–931.

Grim, R. E., 1968, Clay mineralogy [2nd ed.]: McGraw-Hill, New York, 596 p.

Haar, L. A.; Fletcher, J. B.; and Mueller, C. S., 1984, The 1982 Enola, Arkansas, swarm and scaling of ground motion in the eastern U.S.: Seismological Society of America Bulletin, v. 74, p. 2463–2482.

Habicht, J. K. A., 1979, Paleoclimate, paleomagnetism, and continental drift: American Association of Petroleum Geologists, Studies in Geology 9, 31 p.

Hall, S. A., 1978, Geology of archaeological sites at Fort Sill, Oklahoma, *in* Ferring, C. R. (ed.), An archaeological reconnaissance of Fort Sill, Oklahoma: Contributions of the Museum of the Great Plains No. 6, Lawton, p. 57–70.

Ham, W. E., 1956, Resume of the geology of the Wichita Mountains, Oklahoma, *in* Chase, G. W.; Frederickson, E. A.; and Ham, W. E. (eds.), Petroleum geology of southern Oklahoma: American Association of Petroleum Geologists, Tulsa, p. 36–55.

Ham, W. E.; and Merritt, C. A., 1944, Barite in Oklahoma: Oklahoma Geological Survey Circular 23, 42 p.

Ham, W. E.; Denison, R. E.; and Merritt, C. A., 1964, Basement rocks and structural evolution of southern Oklahoma: Oklahoma Geological Survey Bulletin 95, 302 p.

Harlton, B. H., 1951, Faults in the sedimentary part of Wichita Mountains of Oklahoma: American Association of Petroleum Geologists Bulletin, v. 35, p. 988–999.

——— 1963, Frontal Wichita fault system of southwestern Oklahoma: American Association of Petroleum Geologists Bulletin, v. 47, p. 1552–1580.

——— 1972, Faulted fold belts of southern Anadarko basin adjacent to frontal Wichitas: American Association of Petroleum Geologists Bulletin, v. 56, p. 1544–1551.

Havens, J. S., 1983, Reconnaissance of ground water in vicinity of Wichita Mountains, southwestern Oklahoma: Oklahoma Geological Survey Circular 85, 13 p.

Headden, W. P., 1905, The Doughty Springs, a group of radium bearing springs on the North Fork of the Gunnison River, Delta County, Colorado: Colorado Scientific Society Proceedings, v. 8, p. 1–30.

Hofmann, H. J., 1969, Attributes of stromatolites: Geological Survey of Canada Paper 69-39, 58 p.

Howard, K. A.; Aaron, J. M.; Brabb, E. E.; Brock, M. R.; Gower, H. D.; Hunt, S. J.; Milton, D. J.; Muehlberger, W. R.; Nakata, J. K.; Plafker, G.; Prowell, D. C.; Wallace, R. E.; and Witkind, I. J., 1978, Preliminary map of young faults in the United States as a guide to possible fault activity: U.S. Geological Survey Miscellaneous Field Studies Map MF-916, 2 sheets, scales 1:5,000,000 and 1:7,500,000.

Ishizu, R., 1915, The mineral springs of Japan, part 1 [specially edited for the Panama–Pacific International Exposition, San Francisco]: Imperial Hygienic Laboratory, Tokyo, 94 p.

Jaanusson, Valdar, 1984, What is so special about the Ordovician?, *in* Bruton, D. L. (ed.), Aspects of the Ordovician system: Universitetsforlaget, Oslo, p. 1–3.

James, N. P., 1984, Introduction to carbonate facies models, *in* Walker, R. G. (ed.), Facies models: Geological Association of Canada, Geoscience Canada Reprint Series 1, p. 209–211.

Kanamori, H., 1983, Magnitude scale and quantification of

earthquakes: Tectonophysics, v. 93, p. 185–199.
Kanamori, H.; and Allen, C., 1985, Earthquake repeat time and average stress-drop, *in* Das, S.; Boatwright, J.; and Scholz, C. (eds.), Earthquake source mechanics, *v. 6 of* Fifth Maurice Ewing Series: American Geophysical Union, Washington, D.C.
Lade, P. V.; and Cole, D. A., Jr., 1984, Ground rupture zones in alluvium over dip-slip faults, *in* Hardcastle, J. H. (ed.), Proceedings of the 21st Annual Engineering Geology and Soils Engineering Symposium: University of Idaho, Moscow, Idaho, p. 29–44.
Larson, E. E.; Patterson, P. E.; Curtis, G.; Drake, R.; and Mutschler, F. E., 1985, Petrologic, paleomagnetic, and structural evidence of a Paleozoic rift system in Oklahoma, New Mexico, Colorado, and Utah: Geological Society of America Bulletin, v. 96, p. 1364–1372.
Lawson, J. E., Jr.; DuBois, R. L.; Foster, P. H.; and Luza, K. V., 1979, Earthquake map of Oklahoma: Oklahoma Geological Survey Map GM-19, scale 1:750,000.
Logan, B. W., 1961, Cryptozoan and associate stromatolites from the Recent, Shark Bay, western Australia: Journal of Geology, v. 69, p. 517–533.
Logan, B. W.; Rezak, R.; and Ginsberg, R. N., 1964, Classification and environmental significance of algal stromatolites: Journal of Geology, v. 72, p. 68–83.
Machette, M. N., 1985, Calcic soils of the southwestern United States, *in* Weide, D. (ed.), Soils and Quaternary geology of the southwestern United States: Geological Society of America Special Paper 203, p. 1–21.
Madole, R. F.; and Rubin, Meyer, 1985, Holocene movement on the Meers fault, southwest Oklahoma: Earthquake Notes, v. 55, p. 1–2.
Madole, R. F.; Crone, A. J.; and Luza, K. V., 1985, Investigation of the Meers fault, southwestern Oklahoma: preliminary results: Report to U.S. Nuclear Regulatory Commission under contract no. NRC 04-82-006-01.
Marchini, W. R. D., 1986, Transpression: an application to the Slick Hills, southwest Oklahoma: Queen's University of Belfast, Northern Ireland, unpublished Ph.D. thesis, 286 p.
McConnell, D., 1983, The mapping and interpretation of the structure of the northern Slick Hills, southwest Oklahoma: Oklahoma State University unpublished M.S. thesis, 131 p.
McCoss, A. M. [in press], Simple constructions for deformation in transpression-transtension zones: Journal of Structural Geology.
McCracken, Earl, 1955, Correlation of insoluble residue zones of upper Arbuckle of Missouri and southern Kansas: American Association of Petroleum Geologists Bulletin, v. 39, p. 47–59.
McGookey, D. A.; and Budnick, R. T., 1983, Tectonic history and influence on sedimentation of rhomb horsts and grabens associated with Amarillo Uplift, Texas Panhandle [abstract]: American Association of Petroleum Geologists Bulletin, v. 67, p. 511.
McLean, R.; and Stearns, D. W., 1983, Fault analysis in Wichita Mountains [abstract]: American Association of Petroleum Geologists Bulletin, v. 67, p. 511–512.
McLenzie, D., 1978, Some remarks on the development of sedimentary basins: Earth and Planetary Science Letters, v. 40, p. 25–32.
Milanovsky, E. E., 1981, Aulacogens of ancient platforms: problems of their origin and tectonic development: Tectonophysics, v. 73, p. 213–248.
Mobley, H. L.; and Brinlee, R. C., 1967, Soil survey of Comanche County, Oklahoma: U.S. Department of Agriculture, Soil Conservation Service.
Morgan, K. M.; Koger, D. G.; Lambert, D. D.; and Wilhelm, S. J., 1985, Recent advancements in the resolution of Landsat imagery for geologic mapping: Oil and Gas Journal, v. 83, p. 66–67.
Morisawa, Marie, 1975, Tectonics and geomorphic models, *in* Melhorn, W. N.; and Flemal, R. C. (eds.), Theories of landform development: Sixth Annual Geomorphology Symposia Series, Binghamton, New York, p. 199–216.
Nelson, H. F.; Brown, C. W.; and Brineman, J. H., 1962, Skeletal limestone classification: classification of carbonate rocks—a symposium: American Association of Petroleum Geologists Memoir 1, p. 224–252.
North American Commission on Stratigraphic Nomenclature, 1983, North American stratigraphic code: American Association of Petroleum Geologists Bulletin, v. 67, p. 841–875.
Nuttli, O. W., 1979, Seismicity of the central United States, *in* Hatheway, A. W.; and McClure, C. R., Jr. (eds.), Geology in the siting of nuclear power plants: Geological Society of America, Reviews in Engineering Geology, v. 4, p. 67–93.
O'Leary, D. W.; Friedman, J. D.; and Pohn, H. A., 1976, Lineament, linear, lineation: some proposed new standards for old terms: Geological Society of America Bulletin, v. 87, p. 1463–1469.
Paul, E. A.; Campbell, C. A.; Rennie, D. A.; and McCallum, K. J., 1964, Investigations of the dynamics of soil humus utilizing carbon dating techniques: Transactions of the Eighth International Congress of Soil Science, Bucharest, p. 201–208.
Peterson, M. N. A.; and Von der Borch, C. C., 1965, Chert: modern inorganic deposition in a carbonate precipitation locality: Science, v. 149, p. 1501–1503.
Powell, B. N.; and Phelps, D. W., 1977, Igneous cumulates of the Wichita province and their tectonic implications: Geology, v. 5, p. 52–56.
Pratt, B. R.; and James, N. P., 1982, Cryptalgal–metazoan bioherms of Early Ordovician age in the St. George Group, western Newfoundland: Sedimentology, v. 29, p. 543–569.
Radke, B. M.; and Mathis, R. L., 1980, On the formation and occurrence of saddle dolomites: Journal of Sedimentary Petrology, v. 50, p. 1149–1169.
Rafalowski, M. B., 1984, Sedimentary geology of the late Cambrian Honey Creek and Fort Sill Formations as exposed in the Slick Hills of southwestern Oklahoma: Oklahoma State University unpublished M.S. thesis, 147 p.
Ragland, D. A., 1983, Sedimentary geology of the Ordovician Cool Creek Formation as it is exposed in the Wichita Mountains of southwestern Oklahoma: Oklahoma State University unpublished M.S. thesis, 170 p.
——— 1984, Silica in the Ordovician Cool Creek Formation as seen in southwestern Oklahoma [abstract]: Oklahoma Geology Notes, v. 44, p. 103.
Ragland, D. A.; and Donovan, R. N., 1985a, The Thatcher Creek member: basal unit of the Cool Creek Formation in southern Oklahoma: Oklahoma Geology Notes, v. 45, p. 84–91.
——— 1985b, The Cool Creek Formation (Ordovician) at Turner Falls in the Arbuckle Mountains of southern Oklahoma: Oklahoma Geology Notes, v. 45, p. 132–148.
Ragland, D. A.; Donovan, R. N.; and Rafalowski, M. B., 1985, Cryptalgal boundstone morphologies in the Timbered Hills and Arbuckle Group Limestones of Oklahoma [abstract]: Oklahoma Geology Notes, v. 45, p. 217–218.
Ramsay, J. G., 1967, Folding and fracturing of rocks:

McGraw-Hill, New York, 560 p.
Rhodes, J. M., 1969, On the chemistry of potassium feldspars in granitic rocks: Chemical Geology, v. 4, p. 373–392.
Riggs, R. M., 1957, Thrust faulting along the Wichita Mountain front: Shale Shaker, v. 10, p. 7–11.
Russell, M. J.; and Allison, I., 1985, Agalmatolite and the maturity of sandstones of the Appin and Argyll groups and Eriboll Sandstone: Scottish Journal of Geology, v. 21, p. 113–122.
Sabins, F. F., Jr., 1978, Remote sensing: principles and interpretation: W. H. Freeman, San Francisco, 426 p.
St. John, J. W., Jr.; and Eby, D. E., 1978, Peritidal carbonates and evidence for vanished evaporites in the Lower Ordovician Cool Creek Formation, Arbuckle Mountains, Oklahoma: Gulf Coast Association Geological Societies Transactions, v. 28, pt. 2, p. 589–599.
Sanderson, D. J.; and Donovan, R. N., 1974, The vertical packing of shells and stones on some recent beaches: Journal of Sedimentary Petrology, v. 44, p. 680–688.
Sanderson, D. J.; and Marchini, W. R. D., 1984, Transpression: Journal of Structural Geology, v. 6, p. 449–458.
Schatski, N. S., 1946, The Great Donets Basin and the Wichita system—comparative tectonics of ancient platforms: SSSR Akad. Nauk. Izv., Geology Series No. 1, p. 5–62.
Scholz, C. H.; Aviles, C. A.; and Wesnousky, S. G., 1986, Scaling differences between large interplate and intraplate earthquakes: Seismological Society of America Bulletin, v. 76, p. 65–70.
Seager, A. F.; and Davidson, W. F., 1952, Changes in habit during growth of baryte crystals from the north of England: Mineralogical Magazine, v. 29, p. 885–894.
Seismological Society of America, 1985, Meers fault symposium, 80th annual meeting [abstract]: Earthquake Notes, v. 55, p. 1–3.
Sharpenseel, H. W.; Ronzani, C.; and Pietig, F., 1968, Comparative age determination on different humic matter fractions, *in* Isotopes and radiation in soil organic matter studies: International Atomic Energy Agency, Vienna, p. 67–73.
Shinn, E. A., 1983, Tidal flat, *in* Scholle, P. A.; Bebout, D. G.; and Moore, C. H. (eds.), Carbonate depositional environments: American Association of Petroleum Geologists Memoir 33, p. 171–210.
Siedlecka, A., 1972, Length-slow chalcedony and relics of sulfates—evidence of evaporitic environments in the Upper Carboniferous and Permian beds of Bear Island, Svalbard: Journal of Sedimentary Petrology, v. 42, p. 812–816.
Simpson, L. C., 1979, Upper Gearyan and Lower Leonardian terrestrial vertebrate faunas of Oklahoma: Oklahoma Geology Notes, v. 39, p. 3–21.
Slemmons, D. B., 1982, Determination of design earthquake magnitudes for microzonation: Proceedings of the Third International Earthquake Microzonation Conference, Seattle, Washington, p. 119–130.
Slemmons, D. B.; Ramelli, A. R.; and Brocoum, S. J., 1985, Earthquake potential of the Meers fault, Oklahoma: Earthquake Notes, v. 55, p. 1.
Stitt, J. H., 1977, Late Cambrian and earliest Ordovician trilobites, Wichita Mountains area, Oklahoma: Oklahoma Geological Survey Bulletin 124, 79 p.
——— 1983, Trilobites, biostratigraphy, and lithostratigraphy of the McKenzie Hill Limestone (Lower Ordovician), Wichita and Arbuckle Mountains, Oklahoma: Oklahoma Geological Survey Bulletin 134, 55 p.
Stone and Webster Engineering Corp., 1983, Areal geological characterization report for the Palo Duro and Dalhart Basins, Texas: U.S. Department of Energy, DOE/CH/10140-1.
Suess, E.; and Futterer, D., 1972, Aragonitic ooids: experimental precipitation from seawater in the presence of humic acid: Sedimentology, v. 19, p. 129–139.
Thatcher, W., 1975, Strain accumulation and release mechanism of the 1906 San Francisco earthquake: Journal of Geophysical Research, v. 80, p. 4862–4872.
Tilford, N. R.; and Westen, D. P., 1985, The Meers fault in southwestern Oklahoma: implications of the sense of recent movement [abstract]: Association of Engineering Geologists, Abstracts and Program, 28th annual meeting, p. 77.
Toomey, D. F.; and Nitecki, M. H., 1979, Organic buildups in the Lower Ordovician (Canadian) of Texas and Oklahoma: Fieldiana, Geology, New Series No. 2, 181 p.
Tsegay, T., 1983, Sedimentary geology of the Reagan Formation (Upper Cambrian) of the Blue Creek Canyon, Slick Hills, southwest Oklahoma: Oklahoma State University unpublished M.S. thesis, 95 p.
Wickham, J.; Roeder, D.; and Briggs, G., 1976, Plate tectonics model for the Ouachita foldbelt: Geology, v. 4, p. 173–176.
Wilson, J. L., 1975, Carbonate facies in geologic history: Springer-Verlag, New York, 471 p.
Windley, B. F., 1977, The evolving continents: John Wiley and Sons, New York, 385 p.
Younger, P. L., 1986, Barite travertine in southwestern Oklahoma and west-central Colorado: Oklahoma State University unpublished M.S. thesis, 175 p.
Younger, P. L.; Patterson, C.; Donovan, R. N.; and Hounslow, A. W., 1985, Barite tufa from Zodletone Mountain, southwestern Oklahoma [abstract]: Geological Society of America, Abstracts with Programs, v. 17, p. 198.
Zoback, M. L.; and Zoback, M. D., 1980, State of stress in the conterminous U.S.: Journal of Geophysical Research, v. 85, no. B11, p. 6113–6156.

STRATIGRAPHY OF THE SLICK HILLS

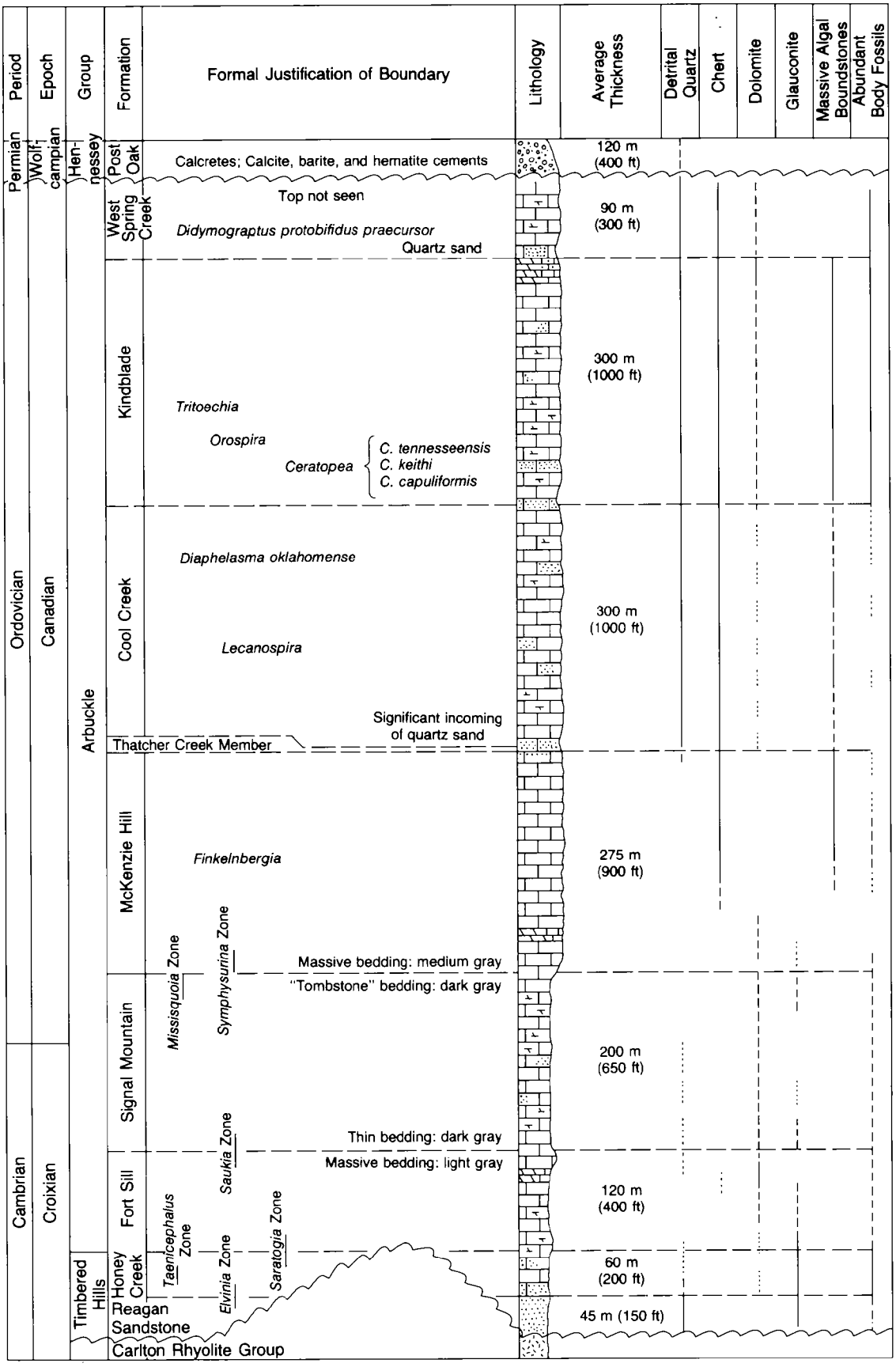

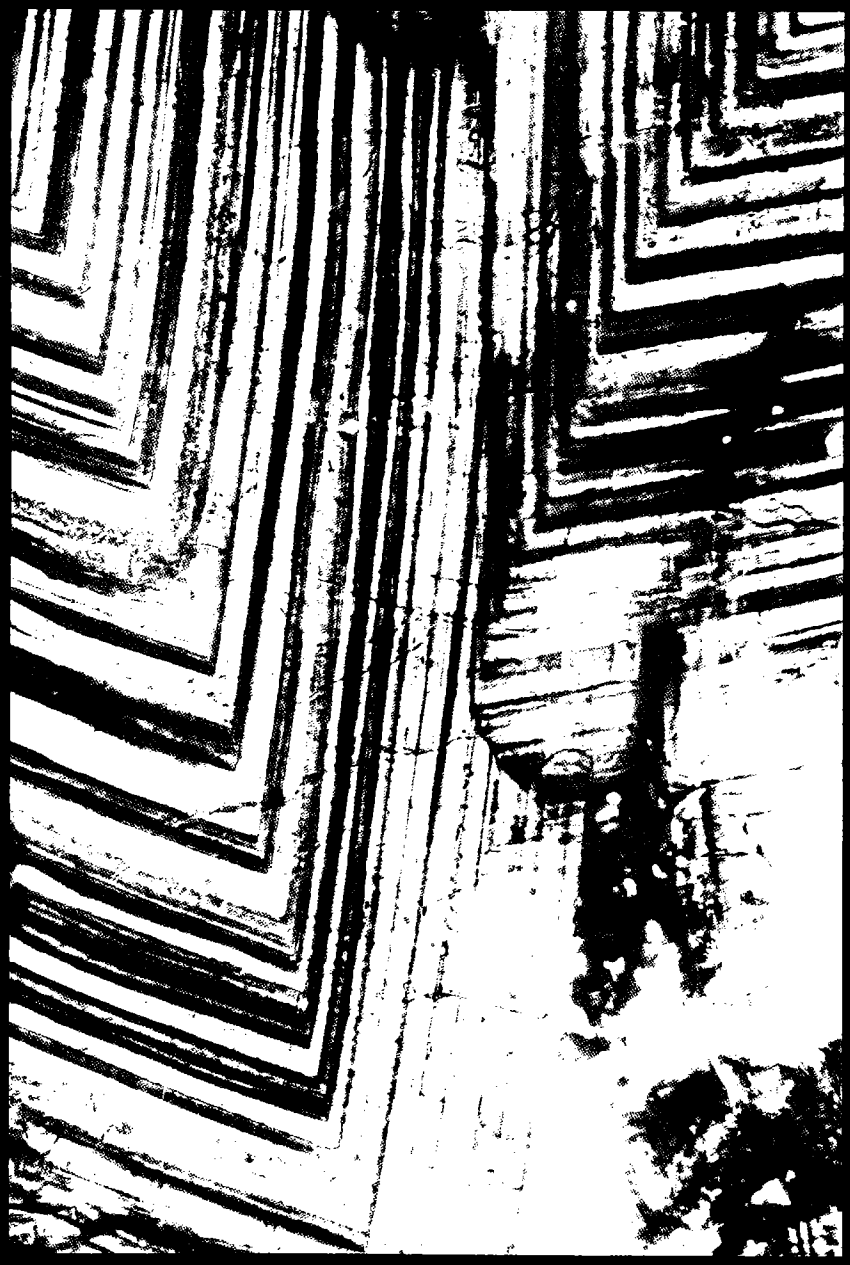

OKLAHOMA GEOLOGICAL SURVEY
1908